Modulation of Oscillatory Activity in the Cortico-Subthalamic Pathway by Electrical Stimulation in Rodents and Humans.

by

Eszter Kormann

Brasenose College

A thesis submitted to the University of Oxford
in fulfilment of requirements for the degree of
Doctor of Philosophy



University of Oxford,
Brain Network Dynamics Unit,
Department of Pharmacology
October, 2018

Declaration

I, Eszter Kormann, confirm that the work presented in this thesis is my own. Where information has been derived from other sources, I confirm that this has been indicated in the thesis.

Signed:……

Date:……..……

Dedication

Mamának, Szesze

Dedicated to my Grandmother, with love

Acknowledgements

I would like to thank Dr. Andrew Sharott for taking me as his first official student for Sharott lab. I cannot express the gratitude for the wonderful supervision that was a great balance between allowing me to explore my ideas and but supporting me through the difficulties as well as discoveries. My time under your supervision has been invaluable. I would also like to thank Prof Peter Brown for his co-supervision and Prof Pete Magill for his provisional supervision, which he constantly tried to cancel, but thankfully never managed. Thanks for Prof Peter Somogyi for making it possible to start my first year at Oxford. Thanks to Dr. Christian Moll for his collaboration and support with the patient project. Thanks for Clarendon Fund and Brasenose College for financially supporting this work.

Special thanks to Abbey. Without her insight and substantial analytical work, this thesis would have not come to fruition. She is a wonderful supervisor and friend, and I hope I can sometimes make up for the many hours of patient Matlab tutoring she invested in me.

To all members and associates of the Sharott lab and BNDU: I have never been in a more accepting working environment and I am grateful to be a part of a team of good scientists and good humans. BNDU was my second home for the past five years. I am particularly grateful to Farid, Eduardo, Magdalena, Colin, Hayriye, Rahul, Nat, Jennifer and all the members of the animal facility nad admin staff for their professional support as well as their friendship.

To all of my friends: thanks for providing me with a feeling of home in Oxford. To Szabi, whom I never would have survived first year without, but will never forgive that he wasn't here for my entire stay at Oxford. To Eddie, Jovana, Florence, Huma, Olga, Abhilasha, Virginia, Nada, Vilija, Andreas, Allan, Mina, Franziska: your friendship is the most invaluable thing I gained at Oxford. To all of you: I am counting on many new adventures. Thanks to OUPLC and associates for introducing me to more effective stress management techniques.

To Dom: thanks for empowering me and making me feel warm with your love and for supporting me through the hardest times of my write up.

Finally, I would like to say thanks to my family, in particular my grandparents and siblings. I am grateful for raising me a headstrong, diligent and independent woman, who knows no fear of limitations. I cannot express the gratitude I feel for the unconditional love and support and their unselfishness to let me go and explore. Thank you for the phone calls when you shared my success and also when you lifted me up and encouraged me when things were not going so well. I hope you forgive me for the time I spent away and you know that it was all for you.

Abstract

Parkinson's disease (PD) is a debilitating motor disorder characterized by degeneration of dopaminergic cells in the Basal Ganglia (BG). This loss of dopaminergic neurons gives rise to abnormal synchronization of neuronal activity in the beta frequency range (around 20 Hz) across the cortico-basal ganglia network in parkinsonian humans and animals. Interestingly, in tremor patients the phase of ongoing peripheral oscillation can be exploited with electrical 'phase interference', whereby cortical stimulation on specific phases of the tremor dampens both the pathological neuronal activity and resulting symptoms. Computational modelling suggests that the amplitude of beta oscillations could be modulated by applying stimulation at a specific phase. Such a strategy would allow selective targeting of the oscillation, with relatively little effect on other activity parameters. Harnessing the phase of a pathological neural activity, therefore, may be a promising way to increase the specificity and efficacy of stimulation protocols for deep brain stimulation (DBS) treatment of motor disorders. The principal aim of this study was to examine the 1) effect of stimulation phase-in supressing and amplifying the amplitude of the ongoing pathological beta oscillations of the motor cortex and subthalamic nucleus (STN); and 2) investigate the phase relationship between and the power of ongoing beta oscillations in these brain areas. Complimentary experiments were carried out in PD patients undergoing microelectrode mapping for the implantation of DBS electrodes as well as in the 6-OHDA hemi-lesioned rat model of PD. In awake PD patients displaying beta oscillations we recorded cortical EEG, STN LFP as well as multiunit activity from the STN. The data obtained from these human intraoperative recordings revealed that electrical stimulation arriving on consecutive cycles of a specific phase of the subthalamic oscillation can suppress its amplitude and coupling to cortex. Additionally, combining data recorded from Parkinsonian rats and awake PD patients we demonstrate that the amplitude of beta oscillations in the cortex and the STN ramp up when these assemblies were at their most common phase alignment ("preferred phase"). Our data suggests that phase-dependent stimulation could thus be a valuable strategy for treating brain diseases and probing the function of oscillations in the healthy brain. These results provide further evidence that periods of particular phase alignments between nodes of the cortical-basal ganglia circuit can lead to amplification of oscillations at the same frequency.

List of Abbreviations

6-OHDA – 6-Hydroxydopamine

AC-PC Line – Anterior Commissure - Posterior Commissure Line

AP – Action Potential

BG – Basal Ganglia

BUA – Background Unit Activity

CTC – Communication Trough Coherence

CTX – Cortex,

Cz – Central Midline

DBS – Deep Brain Stimulation

ECoG – Electrocorticography

EEG – Electroencephalography

EMG – Electromyography

EPSP – Excitatory Post-Synaptic Potential

FDR – False Discovery Rate

Foxp2 – Forkhead Box Protein P2

Fz – Frontal Midline

GA – Global Activation

GABA – Gamma-Aminobutyric Acid IPSP

Gpe – Globus Pallidus Externa

Gpi – Globus Pallidus Interna

H_2 – Field H_2 Of Forel,

IC – Internal Capsule,

IFC – Inferior Frontal Cortex

L-DOPA – Levodopa

LFP – Local Field Potential

M1 – Primary Motor Cortex

MPTP – 1-Methyl-4-Phenyl-1,2,3,6-Tetrahydropyridine

NB – Neurobiotin

P3/4 – Left/Right Parietal

PAC – Phase-Amplitude Coupling

PD – Parkinson's Disease

PMd/v – Dorsal/Ventral Premotor Area

PPN – Pedunculopontine Nucleus

PSI – Phase Stability Index

PSTH – Peri Stimulus Time Histogram

Pz – Posterior Midline

Ra. Prl. – Prelemniscal Radiation

RF – Reticular Formation

SD – Standard Deviation

Snc – Substantia Nigra Pars Compacta

Snc – Substantia Nigra Pars Compacta,

Snr – Substantia Nigra Pars Reticulate

STN – Subthalamic Nucleus

STR – Striatum

SWA – Slow Wave Activity

THA – Thalamus,

UPDRS – Unified Parkinson's Disease Rating Scale

Z.i – Zona Incerta

Publications

Research carried out by the DPhil candidate contributed to the following publications, but not included in this thesis

Garas, F. N., **Kormann**, E., Shah, R. S., Vinciati, F., Smith, Y., Magill, P. J., & Sharott, A. (2018). Structural and molecular heterogeneity of calretinin-expressing interneurons in the rodent and primate striatum. *J Comp Neurol, 526*(5), 877-898. doi:10.1002/cne.24373

Garas, F. N., Shah, R. S., **Kormann**, E., Doig, N. M., Vinciati, F., Nakamura, K. C., Dorst, M. C., Smith, Y., Magill, P. J., & Sharott, A. (2016). Secretagogin expression delineates functionally-specialized populations of striatal parvalbumin-containing interneurons. *Elife, 5*. doi:10.7554/eLife.16088

Publications included in this thesis

Kormman*, E., Holt*, A., Gulberti, A., Pötter-Nerger, M., McNamara, C., Cagnan, H., Little, S., Köppen, J. A., Buhmann, C., Westphal, M.,Gerloff, C., Brown, P., Engel, A., Hamel, W., Moll, C. & Sharott, A. (2019). Phase-Dependent Suppression of Beta Oscillations in Parkinson's Disease Patients. *J Neurosci, 39*(6), 1119-1134. doi:10.1523/JNEUROSCI.1913-18.2018

Table of Contents

Declaration **1**

Dedication **0**

Acknowledgements **0**

Abstract **0**

List of Abbreviations **0**

Publications **0**

Table of Contents **0**

Chapter I General Introduction **0**

1.1. Basal ganglia 0

1.1.1. Circuit overview of the anatomy and functional connectivity: the Albin/DeLong model 0

1.1.2. Additions to the Albin/Delong model 1

1.1.3. Theories of basal ganglia function 3

1.2. Subthalamic Nucleus 8

1.2.1. Anatomy and functional connectivity 8

1.2.2. STN Electrophysiology 13

1.2.3. STN Function 14

1.3. Parkinson's disease 18

1.3.1. Symptoms and main therapeutic approaches 18

1.3.2. Animal models for Parkinson's disease 19

1.3.3. Consequences of DA depletion on the basal ganglia physiology 20

1.4. Oscillations in Neuronal Processing 23
1.4.1. Oscillations across different coding levels 23
1.4.2. Role of oscillations in healthy coding 26
1.4.3. Oscillations involving the Subthalamic Nucleus 29
1.5. Beta oscillations 35
1.5.1. Description, clinical relevance 35
1.5.2. Role of beta oscillations in (losing) motor control 36
1.6. Therapeutic Brain Stimulation 43
1.6.1. Deep Brain Stimulation 43
1.6.2. DBS actions 47
1.6.3. Motivation behind optimization approaches: side effects and efficacy 51
1.7. Summary of main aims and findings 57
Chapter II Human Intraoperative Recording and Stimulating Setup 61
2.1. Introduction 61
2.1.1. Challenges of optimizing parameter settings for continuous stimulation 61
2.1.2. Assessment of the modulatory effect of continuous stimulation on evoked responses of the STN and its afferents 65
2.2 Aims 66
2.3. Methods 67
2.3.1. Ethics and patient selection. 67
2.3.2. Surgical procedures 68
2.3.3. Electrophysiological recording. 69
2.3.4. Electrical stimulation of the dorsal STN area. 71
2.3.5. Analytical methods 73

2.4. Results 76
2.4.1. Experimental setup to ensure stimulation artefact is kept to a minimum. 76
2.4.2 Off –line approach to remove residual stimulation artefact: Kalman filter. 78
2.4.3. Beta frequency stimulation does not corrupt the oscillatory profile or the baseline firing properties of the STN. 79
2.4.4. Recovery of action potentials and firing rate changes of the STN neurons 81
2.4.5. Beta frequency stimulation is effective in modulating the spiking pattern of the STN activity. 84
2.4.6. Beta frequency stimulation is effective in modulating the activity of the cortex 89
2.5. Discussion 91
2.5.1. Stimulation does not impose adverse effect or induce gross changes in the network state or the local activity of the STN 91
2.5.2. Stimulation is effective in modulating the local activity of the STN and its outputs 92

Chapter III Phase-dependent suppression of beta oscillations in Parkinson's disease patients 95

3.1. Introduction 95
3.1.1. Role of pathological oscillation in Parkinson's disease 95
3.1.2. Deep Brain Stimulation as an efficient but suboptimal therapeutic option 96
3.1.3. Phase dependent approaches to stimulation 96
3.1.4. Electrophysiological Output Measures of Phase-Dependent Modulation 98
3.2. Aims 100
3.3. Methods 101

3.3.1. Acquiring signals for analysis 101

3.3.2. Stimulation protocol 101

3.3.3. Instantaneous phase and amplitude estimation. 104

3.3.5. Instantaneous effects of stimulus phase. 104

3.3.3. Cumulative effects of stimulus phase 104

3.3.6. Surrogate data. 105

3.3.7. Calculation of the Background Unit Activity 107

3.3.8. Phase Synchrony Index 107

3.4. Results 108

3.4.1. Phase-dependent modulation of beta amplitude 108

3.4.2. Increased phase-specificity enhances cumulative phase-dependent suppression of beta amplitude 115

3.4.3. Phase-dependent suppression of beta amplitude was dependent on stimulation amplitude 119

3.4.4. Phase dependent suppression of oscillatory STN output 121

3.4.5. Phase dependent suppression led to decreased synchronization 123

3.5. Discussion 125

3.5.1. Phase dependent amplitude suppression relies on consecutive pulses 125

3.5.3. Implications for therapy 127

3.6. Conclusions 129

Chapter IV Phase alignment dependent modulation of the amplitude of beta oscillation in Parkinson's Disease 130

4. 1. Introduction 130

4.1.1. Communication Through Coherence 130

4.1.2. Pathological coherence in PD 130

4.2. Aims 132
4.3. Methods 132
4.3.1. Rat dataset 132

4.3.2. Unilateral 6-hydroxydopamine hemi-lesion 133

4.3.3. *In vivo* electrophysiological recording and juxtacellular labelling. 135

4.3.4. Electrical stimulation of the motor cortex. 141

4.3.5. Histology and imaging. 142

4.3.6. Selection of activated state for analysis. 145

4.3.7. Human dataset 148

4.3.1. Data Analysis 150

4. 4. Results 152
4.4.1. Characterizing preferred phase alignment between cortex and STN in rats. ... 152

4.4.2. Effect of beta frequency stimulation in 6-OHDA hemilesioned rodents 163

4.4.3. Establishing the effect of preferred and non-preferred phase alignment in PD patients 171

4.5 Discussion 176
4.5.1. There is preferred phase alignment between the cortex and the subthalamic nucleus of parkinsonian animals and PD patients 176

4.5.2. Defining the time course of amplitude and synchronisation of pathological beta oscillations 176

4.5.3. Relevance of preferred phase and non-preferred phase to amplitude modulation of beta oscillations. 177

4.5.4. Beta frequency stimulation of cortex disrupts the distribution of preferred and non-preferred phase synchronized periods. 179

Chapter V Discussion 180

5.1. General summary of the results 180

5.2. Similarities and differences in recording from parkinsonian animals versus Parkinson's disease patients 180

5.3. General implications to pathological and healthy oscillations 185

5.4. Limitations 189

5.5. Suggestions for closed-loop applications 190

Supplementary Tables 194

References 204

Chapter I General Introduction

1.1. Basal ganglia

1.1.1. Circuit overview of the anatomy and functional connectivity: the Albin/DeLong model

The basal ganglia are a collection of nuclei on situated deep in the forebrain, forming one of the brainstem-thalamo-cortical loops (**Fig 1.1.**). The majority of structures of the BG utilise GABA as their neurotransmitter, and form parallel, connected inhibitory nodes under the control of excitatory inputs from the cortex and the thalamus. Apart from the two main glutamatergic inputs, the sole excitatory element of the BG is the subthalamic nucleus (STN). The other counterparts are: the striatum (STR), the internal and the external segment (or entopeduncular nucleus in rodents) of the globus pallidus (GPi/GPe) and the substantia nigra pars reticulata (SNr).

The classic model to encompass the routes for information flow within the BG was laid out by Albin and DeLong (Albin et al., 1989; DeLong, 1990). According to this model, cortical inputs to the striatum are separated into two pathways for information flow through the basal ganglia. Striatal medium spiny neurons (MSNs) in the "direct" pathway send axons directly to the basal ganglia output nuclei, which form GABAergic synapses. The net effect of the direct pathway is to inhibit the output nuclei and disinhibit the brainstem and thalamic targets. MSNs in the polysynaptic "indirect" pathway inhibit neurons in the GPe, which disinhibit excitatory neurons in the STN, which in turn project to the output nuclei. The overall effect of the indirect pathway is therefore to increase the activity of neurons in the output nuclei, inhibiting their thalamic and brainstem targets. Depending on the balance between the direct vs indirect pathway activation, this will either exert further inhibition or disinhibit of the outputs. The main organising principle of the BG is, as opposed to laminar

structures such as the cortex, that there are many nodes of inhibitory feedforward and feedback connections projecting to small excitatory nodes. A key feature of the network is that striatal neurons are mostly quiescent at rest, whereas the activity of the intermediate and output nuclei is mostly tonic or irregular, high frequency firing (Wilson & Groves, 1981). Cortical, excitatory input to striatal neurons thus leads to transient excitation of neurons in the direct and indirect pathways, leading to cascades of inhibition and disinhibition in downstream structures. The phasic inhibition (arising from the indirect pathway) exerting excitatory control over the outputs is considered to be anti-kinetic. Contrarily the disinhibition (arising from the direct pathway), that displays inhibition on the outputs, is supposedly pro-kinetic.

The main neuromodulator in the BG is dopamine (DA). Dopaminergic projections arise from the substantia nigra pars compacta (SNc) and acts on D1 or D2 receptors, which are expressed on neurons of the direct and indirect pathways respectively (Smith et al., 1998). The distinction between D1 or D2 receptor expression patterns gives rise to a molecular classification for MSNs subtypes which tallies with the Albin and DeLong model. Activation of D1 receptors leads to increased activity in direct pathway neurons, whereas activation of D2 receptors leads to decreased activity of indirect pathway neurons (Albin et al., 1989; DeLong, 1990). Dopaminergic SNc input thus regulates the balance between the direct and the indirect pathway, with increased dopaminergic input favouring activity in the direct pathway and vice versa. Thus, the net outcome of DA presence is excitatory to the BG target structures, and as such, ‘pro-kinetic’.

1.1.2. Additions to the Albin/Delong model

There have been several important additions to the Albin/Delong framework based on the discovery of additional anatomical connections. The so-called “hyperdirect” pathway is a monosynaptic projection from the cortex to the STN and is the only excitatory route through

which the cortex can directly influence the BG computation (Nambu et al., 2000). Alongside the vast cortical projection (discussed above), the BG receives input from several thalamic nuclei. Excitatory afferents to the striatum derive from intralaminar nuclei, the centromedian and parafascicular nodes, the mediodorsal, ventrolateral nuclei of the thalamus (Parent & Hazrati, 1995a). The STN is known to send direct efferents to the thalamus and the striatum, and connected to the pontine nuclei (Lanciego et al., 2012;Bostan & Strick, 2010). In addition to the nigrostriatal pathway, the ventral tegmental area (VTA) also sends dopaminergic innervation to the ventral striatum (or nucleus accumbens). Furthermore, some of these neurons co-release inhibitory and excitatory transmitters too (Stuber et al., 2010; Tritsch & Sabatini, 2012). Apart from the canonical targets, vast bi-directional projections to and from the brainstem (the mesencephalic locomotor region including the pedunculopontine nucleus; the superior colliculus) was recently explored (Martinez-Gonzalez et al., 2011; Martinez-Gonzalez et al., 2011; Benarroch, 2013; Hikosaka, 2007; Redgrave et al., 2010)

The STN participates several pathways: it is a station for the indirect pathway, acts as an input station (cortex) and provides feedback due to its reciprocal connections with the striatum and the GPe. GPe is not only a recipient of the striatal inhibition and subthalamic excitation, but also sends projections back to these structures and the output stations. There are two distinct types of pallidal projection neurons: the first ones form the indirect pathway by providing inhibition of the downstream structures (prototypical neurons, GP-TI); the other type provides massive, net-like GABAergic and enkephalinergic innervation to the striatal MSNs and some of the interneurons. These latter type is referred to as arkypallidal neurons (GP-TA; Mallet et al., 2012). In addition to inputs from the direct and indirect pathways, neurons in the SNr and GPi, are also influenced by excitatory inputs from the thalamus (Deschenes et al., 1996) and cholinergic modulatory input from the PPN (Edley &

Graybiel, 1983). Additionally, downstream topography is preserved throughout the BG, especially regarding the pattern of cortical and thalamic projections onto the striatum and the STN (Parent & Hazrati, 1995b,Flaherty & Graybiel, 1991). These parallel routes are not completely segregated, which potentially allows for the integration of limbic/motor and associative information of functionally segregated circuits (Nelson & Kreitzer, 2014).

1.1.3. Theories of basal ganglia function

Establishing a model that encompasses the healthy and diseased anatomical and physiological connections that occur dynamically in different behavioural control is challenging. All three models I highlight here were established to explain how BG participates in advising the cortex on the execution or termination of movement initiation. They all address to certain complexity the selective and adaptive nature of motor control. Additionally, most of these models base their assumptions on the observations in patients and experimental animals with hypo- or hyperkinetic movement disorders.

Rate model

The theoretical framework summarising the functional implications of the Albin/Delong model is often referred to as the 'Rate model'. The Rate model's advantage that it provides straightforward and testable predictions for understanding movement control and the loss of it in disease conditions. It is called 'Rate', because its assumptions and predictions are based on describing the monotonic changes in the balance of the net outcome of the firing rates between the direct and the indirect pathways. Regardless of the obvious shortfalls of anatomical detail in macro and micro-circuitry of the Albin/Delong framework, the Rate model successfully predicted some of the electrophysiological phenomena observed in motor disorders related to BG dysfunction in patients and animal models for the disease (pro and contra evidence summarised here: Nelson & Kreitzer, 2014). In patients, hypokinesia (a feature of Parkinson's disease (PD), discussed in detail below) correlates with increased

firing rate in the STN and the GPi (Benazzouz et al., 2002;Levy et al., 2001) and reducing the firing rate is also known to correlate with symptomatic relief (Levy et al., 2001). Some, but not all animal models mimicking hypokinetic conditions also show changes firing rates predicted by the framework (Filion et al., 1991; Bergman et al., 1994). Selective experimental manipulation (ablation, optogenetic silencing and/ or stimulation) of the striatal D1 or D2 receptors,, mimicking the imbalanced net activity between the indirect and direct pathways, induced hypo- or hyperkinetic behaviours in line with the predictions of the rate model in a series of studies (Drago et al., 1998; Durieux et al., 2009; Durieux et al., 2012;Gradinaru et al., 2009; Hikida et al., 2010; Kravitz et al., 2010).

Despite of its merits, the rate model falls short on delivering explanation for several experimental observations, including: **1)** GPi lesion ameliorates both hypo- and hyperkinetic symptoms (Bergman et al., 1994); **2)** some studies found both pathway to be pro-kinetic to a certain extent, and inhibition of both pathway causes delayed initiation (Cui et al., 2013;O'Hare et al., 2016; Tecuapetla et al., 2016); **3)** the direct pathway has projections to the GPe (Chang, Wilson & Kitai, 1981; Fujiyama et al., 2016); **4)** firing rate changes associated with changes in motor behaviour are not consistent or minor in the striatum and the GP and some cortical neurons increase their firing to indirect pathway activation (Wichmann & DeLong, 1999, Eusebio et al., 2009,Litvak et al., 2011;Oldenburg & Sabatini, 2015a); **5)** some of the optogenetic studies provide implicative evidence for the Rate model, but doesn't prove that movement initiation/ inhibition depends on such balance (Gradinaru et al., 2009; Kravitz et al., 2010).

Action selection

The rate model is powerful when it comes to making assumptions of over-practiced motor programs when the outcome of the computation is a simple and pre-wired, however fails to explain for the automatic choice included in selection of certain motor programs. Mink

(1996) hypothesised that the BG is acting as a brake on the autonomously running motor programs. This model has two, enduring ideas. The first one is that BG operates on an activation/ selection-based-disinhibition of competing motor programs, supressing the unwanted actions while removing inhibition from desired movement patterns. In other words, adaptive behaviour is achieved by selecting certain motor programs via removing inhibition from the neurons involved in the stream needed for that action to be executed. This idea corresponds to the fairly segregated topographic organisation of the basal ganglia and influenced viewing the structure of the information flow as 'channels' (Romanelli et al., 2005). A study by Blenkinsop et al. (2017) highlights that action selection is an emergent property of a network that is organised in segregated as channels that explains for the pattern of a characteristic multiphasic evoked potential by movement/ cortical input (see in detail below). Additionally, it has been shown that the ratio of the inhibited-to-activated GPi neurons is significantly lower in the primate model of Parkinson's disease, indicating that hyperkinesia results from activation of the output nuclei that is not specific to the requirements for a focal action selection (Boraud et al., 2000).

The action selection model, using the concept of lateral inhibition, addresses that movement control is a dynamic process. It has been hypothesised that the inhibition exerted locally by the axon collateral network of the medium spiny neurons in the striatum can create a dynamic and input dependent spatiotemporal firing patterns between striatal domains (Wickens & Arbuthnott, 1993; Wickens & Oorshcot, 2000). The number of striatal domains resembles the number of GPi neurons, therefore the structure of inhibition is hypothetically preserved downstream. The lateral inhibition is further enhanced by the action of the GABAergic interneurons in the striatum, and putatively aids to fine tune and make the activity pattern of these neurons more focused (Koos & Tepper, 1999). The action selection model overcomes the conflict that firing rate changes are minor and direct and indirect

pathway activation can coexist. The action selection model, however, does not take into account that **1)** local, intra-node inhibition from axon collaterals is small (Jaeger et al., 1994) or coming from interneurons, **2)** doesn't fully explain for why decorrelation is the basic state of the cortico-BG network (Raz et al., 2000), **3)** doesn't explain how information flow from the cortex is subject to huge amount convergence, whereas the structure of the information is preserved (similarly to file compression on computers, Zheng & Wilson, 2002).

Dimensionality reduction models

The action selection model presupposes that information arriving in a refined and highly organised manner from almost the entire cortical mantle, thalamus and brainstem; and it is largely restructured within the recurrent loops of the BG. A theory that focuses on the vast amount of downstream convergence is the dimensionality reduction model (Bar-Gad et al., 2000; Bar-Gad et al., 2003b). The advantage of this model is that it can explain how multiple dimensions for parallel information streams operate by the utilisation of Hebbian and anti-Hebbian reinforcement learning rules. It is based on the assumption that the activity of the output nuclei represents the compressed version of the cortical activity, and becomes highly correlated only after the exposure to novel input. Correlated neural activity, on the other hand, activates lateral inhibition, which causes inter-nucleus decorrelation. The dynamical rearrangement between correlated and non-correlated states signals saliency, which is imposed on the output stations by the corticostriatal input. This provides a mechanism for compressed state updates to influence the cortical decisions on action selection, based on the highly divergent input information.

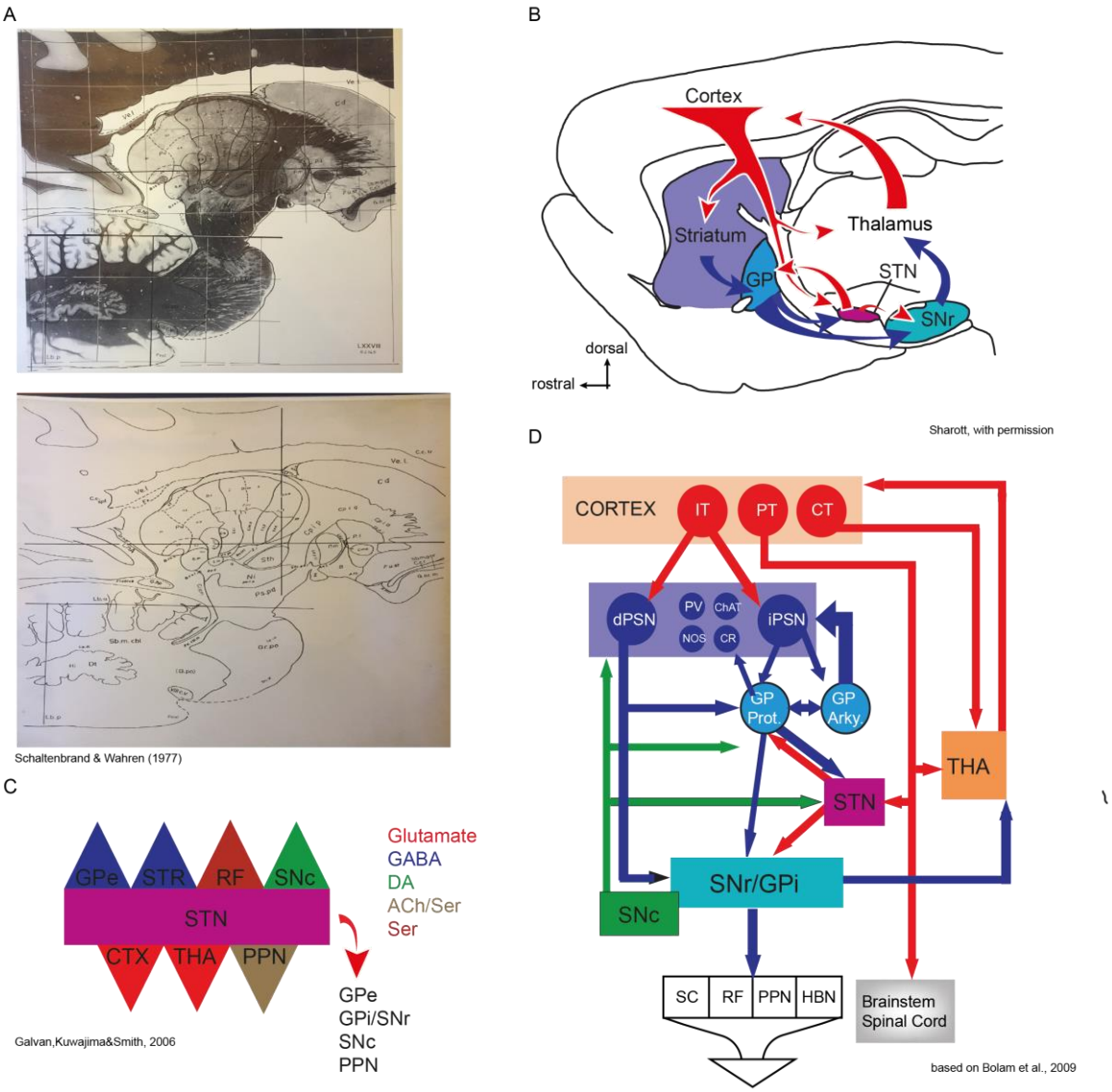


Figure 1.1. The basal ganglia connectivity in humans. A) Most composite nuclei of the human Basal Ganglia displayed on a horizontal plane image and outline taken from the Schaltenbrand & Wahren (1977) Human Brain Atlas. **B)** Connectivity outline of cortico- basal ganglia – thalamocortical circuitry in the rodent. Red arrows denote excitatory and blue arrows denote inhibitory connections. **C)** The subthalamic nucleus receives vast and diverse modulatory connections and relays information to many parts of the Basal Ganglia. GPe: globus pallidus externa, GPi: Globus Pallidus interna, STR: striatum, RF: reticular formation, SNc: substantia nigra pars compacta, CTX: cortex, THA: thalamus, PPN: pedunculopontine nucleus. **D)** Connections between the major input and output structures (cortex, thalamus and brainstem) and the component nuclei of the Basal Ganglia in respect to some of the major cell types. Thalamocortical information is processed via distributed and parallel routes.

1.2. Subthalamic Nucleus

1.2.1.Anatomy and functional connectivity

The subthalamic nucleus (STN) is a densely packed, biconvex (lens shaped) structure surrounded by the thalamus, the substantia nigra and the internal capsule (Yelnik & Percheron, 1979; Parent et al., 2000; Oorschot, 1996. The borders of the STN can be delineated by the expression of the forkhead homeobox protein 2 transcription factor (FoxP2, Campbell et al., 2009), which is widely expressed in STN neurons but not in surrounding structures. The dendritic arborisation in the STN of the rodents extends to the surrounding areas, such as the zona incerta. This is not the case in primates (Afsharpour, 1985a,; Rafols & Fox, 1976). Historically, STN is the sole glutamatergic member of the BG, however it has recently been shown that dopaminergic axons in the accumbens and cholinergic striatal interneurons can release glutamate as well (Tecuapetla et al., 2010; Nelson et al., 2014).

Anatomy and physiology of the STN neurons

In contrast to other basal ganglia structures, cell types are not defined in the STN, although there is evidence, albeit limited, for heterogeneity. It has recently been implied that nicotinic receptor subunit expression might define subsets of STN neurons (Xiao et al., 2015). Additionally, anatomical studies suggest that neuronal population can be distinguished based on the existence of local axon collaterals (Kita et al., 1983). STN neurons have on average 7 dendrites that thin out distal to the soma (Afsharpour, 1985a; Sato et al., 2000;Yelnik & Percheron, 1979). The dendritic tree of STN neurons roughly follows the shape of the nucleus, the longest dendrites can roughly be as long as the border of the nucleus running parallel to them. The dendritic tree can cover up to 2/3 of the nuclei and can spam to the cerebral peduncle in rodents (Kita et al., 1983). This feature implies large

computational capacity for converging input. Interestingly, STN neurons are 'spiny', although these dendritic spines are sparse (Bevan et al., 1995).

Their intrinsic membrane properties predispose subthalamic neurons to generate most of their spiking activity autonomously, discharging in the absence of synaptic input (Bevan & Wilson, 1999). *In vitro*, STN neurons display a set of features that predispose them to exhibit persistent tonic activity that is hypersensitive to synaptic input (Wilson, 2015). STN neurons display a scoop-shaped and regular voltage pattern that is defined by the push and pull of three main currents that makes up their bursty extracellular firing pattern. Additional ion channel mechanisms shape the switch from burst to single-spike mode (Bevan & Wilson, 1999). In slices, STN neurons tend to display rhythmic tonic activity (between 5-40 Hz), but are able to fire at significantly higher frequencies (Nakanishi et al., 1987). Above 40 Hz, STN neurons are twice as sensitive to input as at lower frequencies (Bevan & Wilson, 1999). Triggered by membrane hyperpolarisation, a subset of STN neurons are also capable of firing rebound bursts (Beurrier et al., 1999).

Prominent ion channels underlying the action potential (AP) generation are the voltage-gated Na channels, allowing for a persistent, slowly inactivating, 'resurgent' sodium currents (Surmeier et al., 2005;Do & Bean, 2004; Mercer et al., 2007). These Na channels are activated by voltages lower than those observed in non-autonomously firing neurons and assists the prompt repeated firing after the decay of the voltage (Do & Bean, 2003, 2004). AP is generated when this sodium influx overrides the Ca-activated potassium current at ~ 45 mV (Bevan & Wilson, 1999). The gradual depolarisation starts immediately after an AP was fired. The autonomous firing properties of these neurons are further aided by the medium and fast lag repolarisation by voltage-dependent (medium) K^+ and small conductance Ca^{2+}+ dependent K^+ (fast) channels, that forces quick recovery onto the membrane (Hallworth et al., 2003).

STN connectivity

STN is in a unique position due to its extensive connectivity with almost every up- and downstream stations within the cortico-thalamic basal ganglia loops.

Inputs and intrinsic organisation. The main intra-basal ganglia input is provided by both segments of the dorsal pallidum (Canteras et al., 1990; Hamani et al., 2004; Carpenter et al., 1981). STN has a firm and well-studied functional connectivity with the GPe (GP in rodents, Parent & Hazrati, 1995). The GP projects to STN in a rostrocaudal topographic organisation and efferents are arranged in a laminar structure that runs parallel to the medullary lamina. The inhibitory input from the GPe is organised in a celltype-specific manner[1] as well. Two main celltypes have been described in the GPe: the parvalbumin expressing arkypallidal neurons that contact downstream structures of the BG and the preproenkephalin expressing prototypic neurons that contact the striatum solely (Mallet et al., 2012). These celltypes are markedly important in understanding the functional connectivity between the STN and the GPe due to their distinct firing pattern and differential phase-alignment in regards to the STN (Bogacz et al., 2016). Arkypallidal neurons do not send axons to STN, with synapses being formed solely with prototypic GP neurons (Mallet et al., 2012; Abdi et al., 2015). PV-expressing GPe (prototypic) projections are known to be evenly distributed within the STN, Lhx6 –GPe projections were targeting the edges of the nucleus (Mastro et al., 2014). The anatomical and physiological nature of this projection is set out to hinder highly correlated activity between the two nuclei (Baufreton & Bevan, 2008). Firstly, the GPe contacts the STN sparsely and in a highly selective manner: strikingly, single GPe neurons contact very small number of STN neurons, with multiple synaptic contacts that are dispersedly clustered within the STN (Baufreton et al., 2009).

[1] Here I am going to refer to the cell-types by their prominent molecular marker

Secondly, presynaptic GPe input imposes short term depression on the STN neurons, which causes tonic and desynchronised activity between the two nucleus (Atherton et al., 2013).

STN receives excitatory inputs from many areas of the cortex. These connections are crucial, because this is the only direct, monosynaptic excitatory pathway from the executive structures that reaches the non-striatal basal ganglia directly (Mathai & Smith, 2011). The cortical input also provides a basis for an attempt to divide STN into the classic intrinsic organisation pattern segregating motor, associative and limbic parts (Alexander et al., 1990). Accordingly, STN receives input from motor areas (M1, SMA, PMd PMv) and the frontal eye field (Canteras et al., 1990; Matsumura et al., 1992; Nambu et al., 2002, **Fig 1.2.**). The motor cortical pathways are highly segregated (Inase et al., 1999) Additionally, 'limbic' cortical afferents reach the STN from the orbitofrontal cortex and 'associative' connections from cingulate, somatosensory, and insular cortex (Hamani et al., 2004, **Fig. 1.2.**). Inputs arriving from mostly layer V of the motor cortex reach the STN dorsally and laterally, whereas associative and limbic regions innervate the medial part (Afsharpour, 1985b,Monakow et al., 1978). The 'pyramidal' corticofugal neurons of the lateral and medial agranular cortex contact several stations of the thalamus, basal ganglia and the brainstem along with the STN (Kita & Kita, 2012). However, the boundaries of the tripartite classification are less clear in the light of modern functional anatomy studies, although there is converging evidence for the existence of functional subdivisions in primates and humans (Brunenberg et al., 2012; Accolla et al., 2016b;Alkemade et al., 2015). A perhaps more relevant organising principle is the complex somatotopic organisation within the nucleus (Monakow et al., 1978, Nambu et al., 1996; Nambu et al., 1997,Rodriguez-Oroz et al., 2001, **Fig 1.2.**). Interestingly, some of the calcium-binding proteins show clear zones of distribution: calretinin being ventromedially and parvalbumin being dorsolaterally expressed (Fortin & Parent, 1996; Augood et al., 1999).Topographically organised thalamic

input is arriving mostly from the parafuscicular division to the proximal dendrites of the STN spines as opposed to the cortical synapses, that innervate the distal dendrites (Bevan & Bolam, 1995). Both thalamic and cortical synapses operate via postsynaptic AMPAR and NMDAR action (Chu et al., 2015; Mouroux et al., 1995).Last, but not least, the brainstem provides rich neuro-modulatory input. In particular, the dopaminergic input from the substantia nigra pars compacta is topographically organised and vulnerable to neurodegeneration in PD (Cragg et al., 2004;Hassani et al., 1996; François et al., 2000, **Fig. 1.1. C**). Additionally, the role of glutaminergic and cholinergic innervation from the PPN (Clarke et al., 1997;Flores et al., 1996) and serotoninergic innervation from the raphe is yet to be explored (Lavoie & Parent, 1990; Parent et al., 2010).

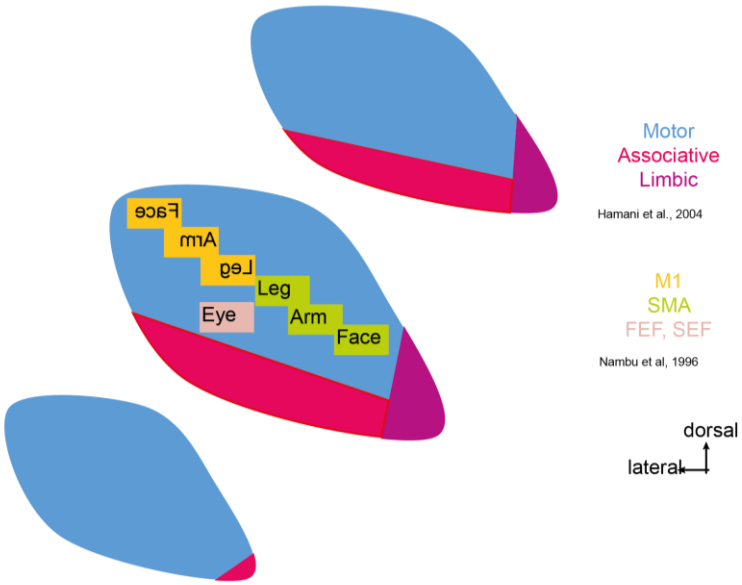


Figure 1.2. Cortical somatotopy represented in the microcircuitry of the STN. Tripartite organisation (limbic, associative and motor) and highly organised somatotopic representation is due to the strictly arranged cortical input to the STN in non-human primates and humans (Hamani et al., 2004). The M1 maps information of the hind limb, forelimb, orofacial in a lateral to medial order (Nambu et al., 1996). The SMA projection follows that arrangement, but in an inverse order. The frontal (FEF) and supplementary (SEF) eye fields are projecting to the ventral parts of the STN.

Outputs. Majority of STN axons contact all three extra-striatal stations of the basal ganglia, with a minority of GPe/SNr, GPi and GPe only branches (Sato et al., 2000 , **Fig. 1.1. C**). The main efferent connection of the STN is the GPe: it contacts large number of neurons in a heterogeneous and sparse distribution in the GPe and receives major inhibitory feedback to its glutamatergic activation (Baufreton et al., 2009; Fonnum et al., 1978; Oertel & Mugnaini, 1984). Along with contacting the dendritic shafts in both components of the SNr, STN sends sparse *en passant* synapses to the striatum (Parent & Hazrati, 1995b). STN reaches all of its contact structures via glutamatergic connections and asymmetric synapses, using AMPAR and NDMAR (Bevan et al., 1994). Interestingly, STN is not only reciprocally connected to the GPe but also sends extensive efferents to the superficial layers (II/ III, IV) of the cortex, making both the indirect and hyperdirect connection mutual and subject to integration via reciprocal feedback (Degos et al., 2008). Interestingly, reciprocity underlies highly coherent activity with the cortex, whereas the connection with the GPe is distinctly uncorrelated (Bevan et al., 2002;Bar-Gad et al., 2003a). Lastly, via a previously largely overlooked connection STN also projects back the substantia nigra pars compacta and innervates masses of dopamine neurons causing short-latency excitation of the SNc (Watabe-Uchida et al., 2012).

1.2.2.STN Electrophysiology

Tri-phasic response to cortical stimulation

It has been shown that reciprocal connections of the STN and GPe form an autonomously firing, ‘pacemaking’ loop (Plenz & Kital, 1999). As part of the indirect pathway, this uncorrelated but coordinated action of STN-GPe loop funnels irregular rhythmicity onto the output nucleus. Additional to the prompt (2.5 ms) and direct excitation exerted by the hyperdirect pathway, converging input from the striatal direct and STN-GPe indirect pathway will shape a characteristic multiphasic evoked potential by single cortical stimulus

(Fujimoto & Kita, 1993; Maurice et al., 1998;Magill et al., 2001, Urbain et al., 2000). The direct pathway triggers a medium lag inhibition, which may or may not be followed by a long latency excitation caused by the striatal inhibition of the GPe that causes disinhibition of the STN. The existence of the third component is due to the indirect pathway action, and will dictate whether the cortical input triggers movement promoting or inhibiting decision from the BG (Blenkinsop et al., 2017).[2] The characteristic of this cortical evoked potential will be discussed in detail in Chapter II and IV.

1.2.3. STN Function

Motor function, action selection and switching between actions

Early observations of STN lesions implicated the involvement of STN in motor function, as selective damage to the nucleus was reported to induce 'hemiballismus' and chorea, which was confined to the contralateral side in case of an unilateral lesion in human patients, whereas dyskinesia was observed with experimentally induced lesions in monkeys (Carpenter, 1955; Hamada & DeLong, 1992; Lee & Marsden, 1994). Micro-stimulation in healthy monkeys, on the other hand, does not seem to trigger movement, which is implicative of its involvement in subtle motor control functions or shaping response inhibition (Wichmann et al., 1994a).

Pioneering studies related STN single cell activity in behaving monkeys to movement parameters and described a complex relationship with movement amplitude, peak velocity and direction (Georgopoulos et al., 1983). STN motor function was also linked not only to active but also proprioceptive and passive joint movements in descriptive studies on behaving and sleeping monkeys (DeLong et al., 1985; Wichmann et al., 1994b). Additionally, a highly somatotopical organisation was revealed within the nucleus that

[2] A computational model based on segregated channels can explain for the presence of the indirect pathway response, thus the action selection

follows the pattern of the cortical input (Nambu et al., 1996). It has also been shown that activity of pairs of STN neurons are uncorrelated during moving or when limbs are being moved (Wichmann et al., 1994a). Due to its connection to cortical areas responsible for eye movement control (frontal eye field, supplementary eye field), an extensive line of research was carried out on the involvement of the ventral STN in the timing and control of saccadic and intentional eye movements (Matsumura et al., 1992; Huerta & Kaas, 1990). The timing of modulation related to voluntary and saccadic movement (as compared to single joint EMG activity or oculomotor activity) shows a sustained, relatively large latency range pre- and postmovement. Furthermore, STN activity can be elicited by 1) sensory-guided movement (visual, auditory), 2) the attentional/memory-related tasks involving action (Schlag & Schlag-Rey, 1987;Goldberg & Bruce, 1985); 3) motion-related passive proprioception, even motor imagery (Wichmann et al., 1994b; Kühn et al., 2006). This versatility and flexibility in timing, and indistinctiveness in triggering modalities further reaffirms the STN's involvement in regulatory movement control and sensory-motor integration rather than just initiation.

STN population activity was repeatedly demonstrated to be involved in coding for motor effort in a series of studies carried out using imaging techniques and extracellular LFP recordings in PD patients (Spraker et al., 2010;Vaillancourt et al., 2007;). In particular, Tan et al. (2016) demonstrated that temporal features of the gripping force and the vigour can be captured by beta and gamma oscillations, and that the combination of the two is powerful in predicting gripping force. To this date, not a lot of studies have been focusing on single neuron coding for motor effort and vigour. Patil et al. (2004) showed that the firing of large population of STN neurons were modulated by the gripping force and can be used for designing simple BMIs. Lipski et al. (2017) showed various stereotypical responses a single STN neuron can elicit in preparation and during grip force production and revealed that

motor coding in this task depends on the phase synchronisation between the cortex and the STN.

STN is known to be involved not only in scaling, but also in switching between motor programs. Study by Isoda and Hikosaka (2008) attempted to describe the direction of information flow during the switch from non-intentional to volitional saccades. It was shown that STN neurons play an important role in the switch, inhibiting the unwanted motor pattern by mirroring the activity of the supplementary eye field and putatively sending a rapid and direct excitatory signal to the SNr, which exerts inhibitory effect on the cortex. Furthermore, a subset of neurons was involved in facilitating the instructed action, but majority of the STN neurons were related to the inhibition of the undesired movement pattern.

Response inhibition

In agreement with the STN being involved in the suppression of unwanted action, a series of studies focused on the role of STN in response inhibition. Studies investigating the role of the STN in stop-signal reaction time measures were able to address the competition between stop and go in response inhibition (Logan et al., 1984). Eagle et al. (2008) found that lesions of the STN causes reduced accuracy in the timing of such responses. A functional imaging study indicated that STN plays a role in the suppression of the thalamocortical output during the 'go' response, moreover, the tractography used in this study revealed the involvement of the hyperdirect pathway in forming such response (Aron & Poldrack, 2006). Evidence for the causative involvement of the STN in forming the stop/pause response has recently been shown by an optogenetic study in mice (Fife et al., 2017). This study demonstrated that STN excitation interrupts licking behaviour and, furthermore, acute inactivation attenuates the interruptive effect of surprise in this task.

Conflict, decision making and impulsivity

In line with the STN's involvement in inhibitory control, impulsivity is one of the main affective side-effects of high-frequency deep brain stimulation in patients (Temel et al., 2005; Frank et al., 2007). A prominent feature of impulsivity is the inability, or reduced capability, to abstain from actions in high-conflict situations. High frequency stimulation of the STN results in a prominent error-pattern in the performance of PD patients, who display significantly shorter reaction times with higher incidence of error. This result implies that STN is involved in the accuracy of the decision by putting a brake on the behaviour (Frank et al., 2007). Single unit recordings from microelectrodes in PD patients undergoing DBS surgery have provided direct evidence for STN neurons coding for decision making parameters, with neurons showing increased firing rates during high conflict trials (Zaghloul et al., 2012). Furthermore, Zavala et al., 2015 showed that, in an action-selection task involving conflict, while some STN neurons show classic, movement-related increases in their firing rate (late cells), others are modulated by the cue (early cells). The firing rate of these early cells remain elevated during high conflict trials and seem to be modulated by STN oscillations. STN is also involved in pathological gambling in human patients and rat models for this condition (Rosa et al., 2013; Jahanshahi, 2013, Aleksandrova et al., 2013).

Reward

Given its reciprocal connections to the motivation-related ventral stream (see above), it is not surprising that the STN participates in shaping reward-related responses. Baunez and colleagues carried out a series of studies using STN lesioned animals performing a reward related operant task. It has been established that STN participates in coding for the anticipation of the reward and workload associated to and the nature of the expected reward (Baunez et al., 2002; Baunez et al., 2005; Baunez et al., 1995; Eagle et al., 2008; Lardeux & Baunez, 2008; Lardeux et al., 2009).

1.3. Parkinson's disease

1.3.1. Symptoms and main therapeutic approaches

Parkinson's disease (PD) is the second most common neurodegenerative and the most common motor disorder, affecting mostly the elderly population (Nolden et al., 2014). The aetiology of the disease is unclear, heredity factors can only be identified in a small portion of the cases (Fahn & Sulzer, 2004). It has long been established that PD can be characterised by a progressive loss of TH-expressing striatal axons combined with the loss of somato-dendritic TH expression in the SNc. However, symptoms only become apparent when cell death exceeds approximately 80% (Ehringer & Hornykiewicz, 1960; Brooks, 2004). While it was first characterised as the tremulous disease, PD has 4 main symptoms. Alongside tremor, patients display rigidity, slowness of movement (bradykinesia) and gait disturbances (Connolly & Lang, 2014). One symptom group is generally more dominant, which helps choosing the appropriate drug therapy (Connolly & Lang, 2014). Dopamine replacement-based medication can be highly effective, but is often limited by severe motor (dyskinesias) and non-motor side effects (depression, impulsive behaviour) and partial efficacy (motor fluctuations, Obeso et al., 2000). The main types of PD medications are levodopa and DA receptor agonists, MAOBIs (DA breakdown inhibitor), anticholinergics and NMDA receptor blockers (for review see: Connolly & Lang, 2014). After a couple of years (especially early-onset patients) develop remittance periods, when the medication is no longer effective. Off-periods can be alleviated by introducing changes into medication tactics (increasing, fractionating, introducing different drugs). Patients who initially responded well to dopamine replacement therapies but having stubborn refractory symptoms and long off-periods can be considered for ablative or deep brain stimulation (DBS) surgery (Benabid et al., 2009; see the details below).

1.3.2. Animal models for Parkinson's disease

Uniquely, the electrophysiological correlates of Parkinson's disease can be investigated in humans due to the possibility of microelectrode recordings from the surgical targets of DBS. Invasive recordings from the diseased human brain provided valuable pathological insight, albeit confounded by the inflexibility of the recording location, duration of such recordings and the lack of healthy controls. In order to overcome these limitations, *in vivo* animal models based on toxicity or transgenic manipulation have been established (Schober, 2004). The choice of model largely depends on the specific objectives of the research question: some models reproduce certain features of PD better than others (Blandini & Armentero, 2012). With the availability of genetically modified rodent strains, there are now many excellent models or neurodegeneration available (Chesselet et al., 2008; Gispert et al., 2009). Here I am going to focus on the classic, toxicity-based models: the lesions using MPTP and 6-OHDA. Both animal models are efficient in replicating DA depletion, have good clinical predictive validity, and are associated physiological changes. In terms of delivery, MPTP can be delivered systemically, whereas 6-OHDA requires local administration. Classic studies with MPTP were done on non-human primates, but in can be used in mice and other species, although rodents seem to be less sensitive to the toxin. 6-OHDA, on the other hand, is most commonly used in rodents. Due the severity of symptoms induced by bilateral lesion, 6-OHDA is usually injected to only one side of the brain, which can then be utilised for semi-sided behavioural testing (e.g. apomorphine-induced rotations or stepping test, Schwarting & Huston, 1996b; Olsson et al., 1995). An intact side also provides control for histology. Both models share the downside of not reproducing the progressive nature of the disease faithfully, although there MPTP can be gradually administered over longer periods (Przedborski & Vila, 2001). Both models respond to levodopa treatment and recreate some aspects of the symptomatology of the motor dysfunction, however tremor is not usually

observed after 6-OHDA treatment. Both the MPTP and 6-OHDA model of PD therefore provides an excellent test-bed to examine pathophysiological changes by recording and manipulating neuronal activity, and Parkinsonian symptoms.

1.3.3.Consequences of DA depletion on the basal ganglia physiology

Dopamine depletion causes and profound disturbance within the thalamocortical basal ganglia loops that can be characterised by marked changes in the firing rate, pattern and network-level oscillations across the basal ganglia.

Rate changes

Changes in the firing rates of neurons in many nodes of basal ganglia has been demonstrated in PD patients and animal models of the disease (Filion et al., 1991;Wichmann et al., 1994a, 1994b; Bergman et al., 1994; Hassani et al., 1996; Schneider & Rothblat, 1996, Escola et al., 2003,Bergman et al., 1990; Aziz et al., 1991;Wichmann & DeLong, 1999; Walter & Vitek, 2004, Boraud et al., 1998; Soares et al., 2004). Some of these changes are in line with the classic Albin/DeLong model, however there are also several inconsistencies (Bar-Gad & Bergman, 2001). In a hypokinetic condition, a significant increase in the firing rate of output structures (SNr / GPi) and the STN, and a decrease of activity in GPe would be the core prediction of the Rate model (Alexander et al., 1986;Bergman et al., 1994). Presumably the decreased inhibition from GPe results in the over activity of GPi, which then exerts exaggerated inhibition on the thalamus, impeding the initiation of motor command. Ultimately, some of these changes are inflicted by the computational output of the striatum. Accordingly, there are wide-spread changes in synaptic plasticity and firing properties of the MSNs in the striatum (Kreitzer & Malenka, 2008). For example, direct-pathway MSNs display lower firing rate after dopamine depletion (Mallet et al., 2006). Even tough, these changes in the firing rates are remarkably inconsistent (see discussion about the

Albin/Delong model above, Wichmann & DeLong, 1999; Eusebio et al., 2009;Litvak et al., 2011; Oldenburg & Sabatini, 2015b). Applying the Albin/DeLong model to predictions about the rate changes would mean that the 'anti-kinetic' indirect pathway is dominating the communication by inhibiting the motor programs and hindering the activation of the 'pro-kinetic' direct pathway (Mink, 2003; Nambu, 2008). This result is promoted by basic findings and translational observations. The selective optogenetic activation of the D1 vs D2 receptors replicated the predictions from the Albin/DeLong model (Kravitz et al., 2010). Moreover, lesioning overactive nodes results in motor improvement of PD (Bergman et al., 1990).

Interpretation of the rate model is not straightforward in the light of the study by Boraud et al., 2000, who found that the rate change in the GPi was only prominent in the receptive field changes of the neurons, as coding for a passive movement became less selective to a single joint. Some clinical findings also seem to be contradictory to the Albin/DeLong model: lesioning the GPi improve motor symptoms, and lesions of the thalamus or the GPe does not result in experimentally induced symptoms of PD (Obeso et al., 2000; Soares et al., 2004).

Pattern changes

Along with the firing changes, some nodes of the BG display enhanced oscillatory activity in their spike trains. This is particularly prominent in the increase of bursting activity in the pallidum, entopeduncular nucleus (or GPi) and the STN (Filion et al., 1991; Bergman et al, 1994; Raz et al., 2000, Ruskin et al., 1999). The bursting activity of single neurons markedly decreases after the combination of dopamine depletion with cortical ablation, which suggest that in anaesthetised rodents, cortical input is crucial in driving the patterned activity of the GPe and STN (Magill et al., 2001). In human PD patients, STN spike trains display coherent and coordinated bursting in the absence of movement or anti-parkinsonian medication (Levy

et al., 2002). Tai et al. (2011) have recently shown that blockade of T-type Ca^{2+} currents, that considerably contribute to the burst activity of STN neurons alleviate motor deficits in the 6-OHDA model for Parkinson's disease. Furthermore, this group has also demonstrated that an unconventional, low-frequency stimulation therapy, that is normally ineffective for DBS patients, can be made therapeutic by lengthening the depolarising pulse and decreasing the availability of those channels.

Oscillatory changes

A robust finding across patients and animal models is that activity gets more rhythmic and coordinated within and between the nodes of BG in PD. The oscillatory changes on the level of a single neuron can happen in lower frequency ranges, that resembles the mean frequency of the peripheral tremor (below or around 10 Hz), and at faster bands around 20-25 Hz in parkinsonian rodents and human patients (10 Hz in Parkinsonian primates) that the literature refers to as 'beta band oscillation' (Brown & Marsden, 1999).

Example for exaggerated tremor frequency oscillation, is that the otherwise remarkably uncorrelated GP neurons get robustly synchronised in MPTP-treated non-human primates which effect is reversible with L-DOPA treatment (Raz et al., 2000, Bar-Gad et al., 2003a). GPe cells in MPTP-treated vervet monkeys display tremor-frequency bursts (Raz et al., 200). Tremor-related, movement sensitive unit activity was also found in the STN of PD patients, however it was not the dominant discharge pattern of the nucleus, irregular and tonic neurons formed the vast majority of recorded cells (Rodriguez-Oroz et al., 2001).

In the STN, units readily display oscillatory activity with a higher prominent frequency component at the beta (20-25 Hz) range (Levy et al., 2001). Intriguingly, despite being a major input and output to the BG, there are not that many studies focusing on the activity patterns of single units in the motor cortex (Li et al., 2012). It has been established that –in line with what has been observed with other structures –motor cortical units oscillate

without pronounced rate-change (Goldberg et al., 2002; Goldberg et al., 2004; Pasquereau & Turner, 2011). Furthermore, oscillatory coupling between STN neurons and the locking of STN neurons to the LFP was shown in by many studies (Kuhn et al., 2005; Weinberger et al., 2006a; Mallet et al., 2008;Moran et al., 2012). The engagement of local and global population in beta band oscillation and synchronisation during PD coding will be discussed further above.

1.4. Oscillations in Neuronal Processing

1.4.1.Oscillations across different coding levels

Strictly speaking, an oscillation is a periodic deviation from the mean (Gatev et al., 2006). Periodic fluctuations emerge on all functional level of healthy and diseased neuronal networks (Buzsaki & Draguhn, 2004). Despite being ubiquitous property of neuronal activity, it has been challenging to provide evidence for the role of neuronal oscillations role in information coding. This is due to the basic problem of investigating the role for a phenomenon that is supposedly exert their influence top-down: the acid-test of significance would be to eliminate oscillations, but no other components of neuronal communication. Since oscillatory activity is generated as an emergent property of the temporal relationship between ion channel openings, membrane potential fluctuations, spike time relations, getting rid of the oscillations would entail depleting its generators. There is, however, converging evidence spamming from recurring membrane potential fluctuations to large scale recordings, and interactions between the different levels of neuronal organisation that supports the functional role for oscillations. Here I will focus on the role of oscillations in healthy and diseased thalamocortical-basal ganglia loops, highlighting the patterned and oscillatory interactions in which the subthalamic nucleus engages.

Activity-features of neural elements can be captured across different levels of spatial magnification, but conventionally neuroscientific scope is clustered between the two

extremes of studying large population of summated activity and the extra/intracellular activity of a single cell (Moran & Bar-Gad, 2010). The extremities of these two approaches suffer from the trade-off between having great spatial resolution reflecting the organisation versus having sufficient number of observations bearing implications of function. To overcome these limitations, some studies have investigated the correlative relationship between the two (Logothetis, 2002; Bartho et al., 2004).

Extracellular recording

Extracellular recordings acquired by microelectrodes are used to collect action potential (AP) or 'unit' traces from the close vicinity of the recording tip (Buzsaki et al., 2012). Extracellular recordings reflect shorter time windows (as action potentials decay faster) and spams across low spatial resolution (couple of hundreds of micrometres; Henze et al., 2000. The signal acquired this way consists mainly of spiking activity, but can also contain postsynaptic potentials (Mitzdorf, 1985) and membrane potential changes (Moran & Bar-Gad, 2010; Pedemonte et al., 1998). The shape and size of the AP will be dependent on the recording distance and the placement of the electrode relative to the neuron's ultrastructure, intrinsic properties of the membrane and anatomical features of the neuron (Henze et al., 2000; Gold et al., 2006; Buzsaki et al., 2012). Generally speaking, the shape of the AP is less sensitive to the placement of the electrode, hence it is commonly used to decide whether a particular waveform picked up by the electrode potentially belongs to the same neuron (Quiroga, 2007). The procedure when a stable and separable waveform-train is assigned to a single neuron and converted into a point-process is referred to as spike sorting (Lewicki, 1998). In some cases, the waveforms are not dissimilar enough to definitively distinguish between putative single neurons. In this case, the channel is extracted as a multi-unit (Tankus et al., 2009).

Electroencephalography, Electrocorticography, Local Field Potentials

The first ever recorded electrical trace was in fact rhythmic and reflected a summated activity of many different neuronal elements (Berger, 1929). Electroencephalography (EEG) is acquired by electrodes placed on the skull surface and reflects not only the membrane potential fluctuations and the participating ionic currents summated over centimetres, but also the neuronal architecture of the cortex. Electrocorticogram (ECoG) signal is identical in principal to the EEG, but the signal-to-noise ratio is improved by placing the recording electrode in contact with the dura. This is possible with grids of multiple electrodes or ball electrodes placed over the burr hole in patients undergoing surgery, and by small screws fixed onto the scull of experimental animals. The cortex is a layered structure which lends itself to create potential changes between the parallel surfaces of many principal neurons creating electrical sinks and sources (Eccles, 1951). The synaptic currents along the dendrites of pyramidal cells create positive and negative deflections in the EEG (Kandel et al., 2000;Baker et al., 1997;Creutzfeldt et al., 1966;Donoghue et al., 1998;Frost, 1968; Mitzdorf 1985;Steriade, 2000).

Both LFP and EEG detects signals from larger areas and incorporates a summation of activity over a broader time window, indicating that the underlying mechanisms represented are slower processes, such as membrane potential fluctuations (Logothetis, 2002, Moran & Bar-Gad, 2010). The signal composition of the LFP reflects subthreshold membrane, rather than action potential related changes, both linkedto ion channel permeability (Eccles, 1951). Even though LFPs were primarily studied in laminar structures (cortex, hippocampus), fact that LFP can be recorded from electrodes placed directly into the neural tissue enabled the acquisition of population activity from non-laminar structures. In particular, in the STN, which is a structure densely packed with large axons aligned along a primary axis in an elliptical fashion parallel to the rostro-caudal border of the nucleus, a

sink and source summation, similar to what has been observed in the cortex, is possible (Brown & Williams, 2005). However, in most composite nuclei of the BG, LFP is more likely to reflect the in- and output balance within the macro-circuit rather than the sink and source differences within structure (Moran & Bar-Gad, 2010). The BG LFPs can capture simultaneous changes in local population activity, as there is evidence for the correlation between LFP fluctuations and 1) synchronous membrane potential changes (Goto & O'Donnell, 2001) and 2) stimulation induced firing rate changes (Magill et al., 2004b). In fact, the importance of the LFP in BG research assumes that the signal is a sum of the *synchronous* activation of a given structures neural elements (Kuhn et al., 2005; Goldberg et al., 2004; Brown & Williams, 2005).

Background Unit Activity

The so-called background unit activity, a signal that can be extracted from microelectrode recordings by high-pass filtering and spike removal, offers a solution to bridge the gap between the good spatial and temporal resolution (Moran & Bar-Gad, 2010). The calculation of the BUA entails rectification, spike-removal and high-pass filtering. This method has shown to reflect the coordinated activity of a small neuronal ensemble, rather than only a handful of neurons. BUA has proven to be useful to investigate oscillatory relations within the BG, especially regarding disease states (Moran et al., 2008b).

1.4.2. Role of oscillations in healthy coding

Oscillations can be described in terms of neural events being adjusted to a common time frame. Persistent time locking can happen between oscillating and non-oscillating events, between ion channels, neurons, small assemblies and larger neural populations. Time locking can also happen between different levels of coding such as a single neuron can be locked to the activity produced by a large population of cells. The main question of studying the function of oscillations is how synchronous activity of different elements is utilised by

the brain. Here I will focus on two frameworks: that periodic patterns of activity can create a 'background' for patterned input (from other structures or from the external world), laid out by Wilson (2015) and the communication through coherence (CTC) theory (Fries, 2005). A recurring idea regarding the function of oscillations is that it creates a reference frame, in relation to which neuronal events can gain context. The context is created by having a blank canvas on which activity time locked to the input is meaningful. One example for this in the BG is how mostly quiescent striatal neurons code for movement by an abrupt increase in their firing (Kimura et al., 1984). This is a suitable conceptual framework for understanding healthy and diseased oscillatory coding on the level of extracellular spiking in the basal ganglia.

In the cortex, healthy oscillations have proven to be underlying complex cognitive mechanisms such as feature binding and attention (Engel et al., 1991; van Wijk et al., 2012). The problem of feature binding refers to the paradox of experiencing objects as one 'gestalt' (i.e. objects) while neurons are coding for the elements of the whole (i.e. colours, contours). It has been suggested that neural computation overcomes the 'binding' problem by temporally coordinating the activity of different inputs carrying information about the same gestalt by providing a neural 'master clock' (Singer & Gray, 1995). The phase relationship in which inputs reach the target will select what elements belong to the same percept (Fries et al., 1997). The more generalised theory called communication by coherence, put forward by Pascal Fries, (Cannon et al., 2014; Fries, 2005; Fries et al., 2008) is more applicable to both motor and sensory coding. According this theory, the success of the communication between two oscillators will depend a coherent and specific phase relationship between the input and the receiver. More specifically, in case of successful communication transfer, input spikes reach the receiver in its most excitable phase. These more common 'preferred phase alignment scenarios' provide a temporal frame during the input has a maximal effect on the

receiver, hence the communication is efficient. Naturally, non-preferred scenarios occur when communication is prohibited, and crosstalk with other connected structures are preferred. The dynamic balance between these two phase alignment scenarios is essential for coding information. This framework ties in well with the overarching question of how synchronous large-scale activity is correlated with health and disease within the basal ganglia (Cagnan et al., 2013a; Cagnan et al., 2015).

This thesis is particularly focused on the functional implications of oscillatory synchrony in a single frequency band, but this is admittedly an oversimplified view of neuronal processing (Brittain & Brown, 2014). A power spectrum of a given electrophysiological signal usually contains peaks at multiple frequencies and it has been established that neurons can adjust their firing to multiple rhythms. Moreover, cross-frequency coupling has a functional relevance and partial correlation can show functional relevance to multiple oscillatory components (Moran et al., 2008; Chen et al., 2010;Lopez-Azcarate et al., 2010, Oswal et al., 2013, Tan et al., 2016).

As it will be revealed in the upcoming section in relation to Parkinson's disease, maximum synchrony does not necessarily lead to maximum network performance (Cagnan et al., 2013a). Information theory can help to understand this relationship (Barlow, 1961; Hanslmayr et al., 2012). From the point of view of entropy, it is plausible that overly-exaggerated synchrony will cause sub-optimal information flow by cramming the communication with fuelling only one type of interaction with the highest power (Brittain & Brown, 2014). In high synchrony, novelty arising from changing environmental demands or cross talk with not highly synchronised other structures are not promoted, hence the flexibility of the system is impeded. Intermittent periods of high synchrony might be favourable to code for the boundaries of a sensory or a motor event (stop and go; what features belong together, Kuhn et al., 2004;Frank, 2006;Aron, 2007). High synchrony might

also subserve decision making semantic categorisation or during selection between motor programs (Hanslmayr et al., 2009; Kuhn et al., 2004). A healthy system is presumably primed for but not constantly stucked at high synchrony stages.

1.4.3. Oscillations involving the Subthalamic Nucleus

Ionic currents to create autonomous clock-like firing in the STN

Unlike many neurons in the forebrain, that fire as the result of integrating the synaptic input, some of the BG downstream structures and upstream interneurons display autonomous firing properties (Goldberg et al., 2009;Maurice et al., 2004; Atherton & Bevan, 2005;Bevan et al., 2006; Chan et al., 2004). The spontaneous pacemaker activity is present in slice-preparations, in the absence of synaptic input (Plenz & Kital, 1999;Kita & Kitai, 1991). This section discusses the ionic currents that contributes to the membrane-level oscillations that create a sustained and regular tonic activity. These features are similar in the extrastriatal BG, but here I will focus on the ion channel mechanisms shaping the autonomous spiking of the STN. The fine-tuned interplay between the constant sodium, and the re-sensitising potassium currents creates a membrane milieu that predisposes STN neurons to fire highly regulated and tonic AP trains. In other words, STN neurons, like some other cell types of the basal ganglia are set up to have no resting membrane potential and be able to display stable pacemaker activity.

Discussing the subcellular-level mechanisms are crucial in understanding how neuronal oscillations evolve in native and pathological conditions for several reasons. The high frequency autonomous firing disposition creates a ‘blank’ background, upon which the main inputs inhibitory (GPe) and excitatory (thalamus and motor cortex) can impose context-dependent firing patterns. In addition, autonomous spiking can play a role in decoupling interconnected nodes of the basal ganglia by providing periodically occurring temporal reference for postsynaptic activity, that will dictate the net outcome of the synaptic input

(Baufreton et al., 2005; Bevan et al., 2002, McIver et al., 2018). Autonomous activity likely counteracts enhanced synaptic patterning, which is known to promote abnormal network states in the extrastriatal BG (McIver et al., 2018).

STN neurons display irregular and patterned activity

Neurons that have no actual resting membrane potential tend to integrate synaptic input in terms of likelihood (Wilson, 2015). The excitatory and inhibitory inputs will move the timings of the action potentials forward or backward. Various sources of incoming information will result in an irregular firing pattern, which is further enhanced by the act that STN has vast convergence, that means receiving a large set of asynchronous and weak inputs. In line with these assumptions, STN neurons rarely display perfectly timed tonic activity *in vivo*. In quiet wakefulness, STN neurons display high frequency tonic and irregular firing patterns, which readily switch to burst mode (Matsumura et al., 1992; Overton & Greenfield, 1995; Wichmann et al. 1994; Bergman, 1998). STN neurons show little to no correlation in their cross-correlogram within the nucleus and with other nodes of BG (Wichmann et al., 1994, Mallet et al., 2008). The wide range of activity patterns showcased by these neurons regardless of a relatively steady firing rate supports that if the firing of STN neurons gets highly regular, it implies dysfunctional over-coordination between its inputs.

What shapes the irregularity of the firing pattern? The patterning of the firing rate comes from within and outside of the BG. Within the basal ganglia, the most important connection stems from the GPe, which forms a reciprocal disinhibition loop (discussed above). Additionally, upstream source via the motor cortex that can reach the STN via inhibitory connections of the indirect pathway and direct excitation (hyperdirect pathway, as discussed above).

In vitro, Plenz & Kitai's (1999) landmark study showed that deprived from its main upstream inputs, the GPe and STN forms a pacemaking loop. Conversely, correlated rhythmic activity is not observed in native preparations (Loucif et al., 2005). Nevertheless, it has been shown that the GPe can readily pattern autonomous STN membrane oscillations in an amplitude- and pattern specific manner (Bevan et al., 1998). Large IPSPs elicit synchronised activity, small IPSP leads to temporarily deactivate and phase reset in the membrane potential of STN neurons. Trains of different IPSPs can, however, elicit a range of responses in the STN. Furthermore, electrical simulation can evoke large IPSPs can reset and synchronise STN neurons (Baufreton et al., 2005). These studies emphasise that the GABA-mediated inhibitory connection from the GPe imposes phasic patterning rather than tonic transmission modes onto the STN (Bevan et al., 2006).

Information about the excitatory (cortical and thalamic) input is less understood *in vitro.* A single EPSP can speed up the generation of the AP compared to the autonomous firing, but this effect depends on the precise timing of the postsynaptic input, middle-phase EPSPs being more effective (Farries & Wilson, 2012). In line with the weak and asynchronous 'patterning' framework, glutamatergic EPSPs evoked by 20 Hz stimulation elicit weak phase locking in the STN. Intriguingly, this patterning can be amplified by imposing synthetic feedback inhibition (presuming preceding activity from the GPe, Nakanishi et al., 1987; Baufreton et al., 2005). Moreover, it has been shown that synaptic integration is complex and non-linear in case of frequent or large EPSPs that cannot be explained for with what has been observed with a single and regular EPSP (Farries et al., 2010; Farries & Wilson, 2012).

The relationship between the STN and its inputs is affected by the presence of dopamine. Dopamine acts as an attenuator: in the presence of DA both IPSPs and EPSPs are reduced compared to dopamine-depleted animals (Bevan et al., 2002). The effect size of the

postsynaptic currents can be restored by D2 receptor agonists (Shen & Johnson, 2000; Zhu et al., 2002). The fact that D2 receptor activation reduced GABAergic transmission more readily than the EPSPs implies that DA loss has a potentially larger effect on mediating the GPe-STN than the CTX- STN connection. These findings have been reviewed by Terman et al. (2002) computational work concluding that weakened pallidal inhibition can led to the emergence of oscillations by switching irregular to rhythmic relationship. Another interesting conclusion of the model is that these structures are not predisposed to generate a tightly coordinated activity under physiological conditions, but irregular activities readily emerge. More recently, McIver and colleagues (2018) have shown that increased D2 SPN activity led to the reduction of autonomous firing in dopamine depleted rodents. Furthermore, the decorrelation from the motor cortex, that is characteristic of STN neurons in intact circuits, was promoted by the chemogenetic restoration of autonomous firing in these neurons.

The complexity of synaptic integration implies that STN neurons are executing dynamic, rapid and highly adaptive computations that will largely rely on the amplitude, phase and relationship between different synaptic inputs (Bevan, 2017). These phase-specific interactions between the timing of the synaptic input and the postsynaptic activity cycle will likely achieve network level effects on the dynamic decoupling that is characteristic of healthy, and lost in diseased states of the cortico-BG network.

STN neurons are sensitive to input and have a tendency to be modulated by upstream network oscillations

STN is the only extra-striatal node of the basal ganglia that receives direct excitatory cortical input (Nambu et al., 2000). Early *in vitro* studies show that STN is extremely sensitive to excitatory input, small changes in excitatory synaptic input can not only change the firing rate of the neurons, but also switch their discharge mode from single spike to burst mode

(Kitai & Kita, 1987). *In vivo* STN neurons fire 10-25 Hz and their discharge pattern alternates between single spike mode, highly regular tonic firing and burst mode (Beurrier et al., 2000; Beurrier et al., 1999;Wigmore & Lacey, 2000; Urbain et al., 2000). During passive movements in non-human primates, some dorsal STN neurons (30-50%) are modulated by contralateral joint movements: most of the responsive neurons increase their firing rate, but some of them display multiphasic and complex responses (Wichman et al., 1994). This finding is supported by microelectrode recordings in the human (discussed in detail below, for example Lipski et al., 2017). The fact that not all STN neurons modulate their firing and the responses are not reflecting 1-1 motor coding implies that the STN shapes but not dictates the movement command of the basal ganglia triggered by the cortical and thalamic activation. (Kitai & Deniau, 1981; Matsumara et al., 1992; Fujimoto & Kita, 1993; Wichmann et al., 1994; Mouroux et al., 1995).

Changes in the firing pattern of STN neurons is heavily dependent on the cortical state of the animal (Magill et al., 2000; ; Urbain et al., 2000). Urethane/ketamine anaesthesia in rodents to investigate the firing of STN neurons and their relation to network activity (Magill et al., 2000). Slow wave activity (SWA) and global activation (GA) closely resemble forebrain activity in the sleeping and awake brain, respectively (Magill et al., 2000). During slow oscillations, the continuous large amplitude ~1 Hz waves are superimposed with a waxing-and-waning “spindles” (7-12 Hz) appearing on the top of the slow waves (Steriade et al., 1993). Under these conditions, STN units are entrained by the cortical SWA and spindles (Magill et al., 2004b). The capricious change in SWA or sensory stimulation can lead to intermittent periods of GA (Magill et al., 2000). GA in control animals is mostly dominated by higher amplitude oscillations that influence the firing of STN neurons only weakly (Magill et al., 2006; Magill et al., 2004b). Rhythmic cortical activity imposes patterned activity not only onto the STN, but also onto the STN-GP loop, as coupling of the

two structures is only present during SWA, but not GA. Cortical ablation diminishes the low-frequency oscillatory discharge pattern in STN neurons (Magill et al., 2001). This further supports the fact that the STN- GP network does not reinforce emergent oscillatory activity in the absence of patterned input. In healthy animals, STN firing promotes irregularity as the cortical inputs get more complex during the awake state (Urbain et al., 2002).

Intriguingly, the cortical influence is largely modulated by the presence of dopamine. In dopamine-depleted animals, regardless of cortical ablation, some of the low frequency oscillatory activity is preserved: 6-OHDA hemilesioned animals seems to display oscillatory activity more readily and more similar to what has been observed in slice preparations (Magill et al., 2001). This proves that in the absence of DA promotes regularity even in the absence of the cortical drive.

Coordinated population activity in the hyperdirect pathway

In vivo, healthy animals STN doesn't display characteristic network oscillations, only ones that are related to the sleep cycle and ultra-slow rhythms (Ruskin et al., 1999). This is not surprising in the light of what has previously been described: the nucleus comprises of an anatomically homogenous population of neurons that show little to no correlated activity, sparsely connected to its pattern-generating counterparts (Bevan et al., 2002). In this section I discuss the oscillatory relationship between the local activity of the STN and its main upstream output, the cortex.

The simplest way to measure oscillatory interactions between structures is to calculate the coherence between the two signals (Brillinger, 1981). Coherence depicts a linear, frequency-domain relationship between the phase and amplitude without considering the directionality of the relationship (Sharott et al., 2005). To observe high coherence at a given frequency component, one has to assume temporal locking (phase coupling) with fixed amplitude ratios

between the two oscillatory structures (Magill et al., 2004). As it has already been discussed on the topic of the spiking activity, STN LFP is robustly coherent with cortical activity (especially in comparison with the GP), mirroring SWA, spindle and GA activation with short time lags and reversed polarity in the anaesthetised rat (Magill et al., 2004). Furthermore, this relationship seems to be dictated by the cortex (Sharott et al., 2005). During SWA, STN LFP contain mostly ~ 1 Hz and 10-14 Hz ('spindle range') components. As opposed to SWA that provides highly patterned input, higher arousal states, such as paradoxical sleep or awake state, result in a less focal frequency distribution of the STN LFP.

There is limited evidence that oscillations contribute to healthy motor coding. STN LFP recordings of PD patients who underwent DBS surgery imply that transient changes in beta frequency oscillations might play a role in movement control (Lalo et al., 2007). In particular, the appearance of a beta frequency (14-35 Hz) component is supposedly 'akinetic': movement initiation cues are signalled by the desynchronization in the beta band, whereas the cessation of the movement correlates with beta rebound (Parkes et al., 2006). Although the significance of beta desynchronization and post-movement rebound in healthy motor coding is not confirmed, it highlights the fact that dynamic and transient network desynchronization is necessary for movement initiation, which is in line with the assumptions of the CTC theory (Kuhn et al., 2004; Williams et al., 2002).

1.5. Beta oscillations

1.5.1. Description, clinical relevance

Oscillatory changes are prominent features of the cortico-basal ganglia network in movement disorders. One particularly prominent feature of cortico-basal ganglia circuits in PD is the emergence of pathologically exaggerated beta oscillations (12-35 Hz) observed in patients and rodents with a Parkinsonian phenotype (Brown & Marsden, 1999, Sharott et al.,

2005, Mallet et al., 2008). It has been demonstrated that an overwhelming proportion of patients with PD who have undergone DBS surgery displays STN beta oscillations recorded from the externalised electrode tips otherwise used for stimulation (Little et al., 2013). Peter Brown's work was pioneering in describing the role of beta oscillation in PD and, at the same time, attempting to relate this pathological phenomenon to healthy oscillatory coding.

1.5.2. Role of beta oscillations in (losing) motor control

As it has been previously discussed, establishing causality between the functional role for oscillations in health or disease is increasingly challenging. However, there is mounting evidence that is suggestive of such relationship between the emergence of excessive synchrony in beta range and the Parkinsonian state.

Firstly, dynamics of beta synchronisation is related to movement control. Since its first mention by Jasper and Andrews (1938), it has been documented by several groups that beta activity is anti-kinetic, at least in relation to voluntary (but not postural) movement. Transient synchronisation measured at and between the nodes of the cortex and STN ranging between (13–30 Hz) is repeatedly associated with preparation for the execution of the movement and inhibiting action immediately following movement (Lalo et al., 2007, Parkes et al., 2006;Leventhal et al., 2012; Jenkinson & Brown, 2011). In line with this effect, beta desynchronization can be observed during voluntary action (Kuhn et al., 2004, Doyle et al., 2005; Devos et al., 2006). Furthermore, cortical stimulation at these frequencies are known to exert anti-kinetic effects (Joundi et al., 2012; Pogosyan et al., 2010).

It is also noteworthy that beta desynchronization does not follow a somatotopic arrangement and that the timing of rebound is not precisely following movement onset in trial-by-trial comparisons (Feingold et al., 2015b; Crone et al., 1998). Conversely, some studies found that the role of beta in explaining for the variance in the vigour and timing of

a manual grip task is only partially sufficient to predict the course of the movement, as higher and lower frequency components were also necessary to explain for the features of movement dynamics (Tan et al., 2013). Gamma band oscillations, for example, are known to have the exact opposite relationship with movement initiation, gamma activity synchronises during the movement and gamma frequency stimulation promotes force production (Crone et al., 1998; Cheyne et al., 2008; Pfurtscheller et al., 2003; Joundi et al., 2012).

Secondly, beta oscillations readily emerge in Parkinsonian phenotypes in different animal models for the disease. In this section, I will discuss studies on the 6-OHDA lesioned rats and the MPTP treated primates (models discussed above). The animal models provide an insight the dynamics and potential mechanism for excessive oscillations. Furthermore, these experiments make it possible to record such activities from many nodes (even those stations that are not conventional targets for DBS, thus not available for electrophysiological investigations in human patients) and many levels (single neurons, field potentials) of the cortico-basal ganglia system.

In MPTP-treated animals, oscillations emerge at frequencies between 4 and 15 Hz (Bergman et al., 1994; Wichmann et al., 1994b; Raz et al., 2001; Raz et al., 2000; Heimer et al., 2002). Intriguingly, the increase in firing rate alone in this model does not produce Parkinsonism alone, which is contradictory to the predictions of the Rate model (Soares et al., 2004). Even though MPTP lesioned non-human primate model is considered to be the most faithful reproduction of the symptoms that has been observed with PD patients, the 6-OHDA rodent model is nonetheless important test-bed to electrophysiological phenomena associated with PD. Beta oscillations in 6-OHDA lesioned rodents resemble more closely to the spectral properties of the human oscillations (Sharott et al., 2005; Mallet et al., 2008a;Bronte-Stewart et al., 2009;Kühn et al., 2009). Interestingly, beta oscillations only

appear a couple of weeks after successful dopamine depletion, which suggests compensatory, network level mechanisms. To date, transgenic models for PD in mouse such as PARKIN-KO and alpha-synuclein mutation have no documented effect on over-excessive synchronisation.

Thirdly, the amplitude of beta oscillations correlates with symptoms and the severity and progression of the disease. The amplitude of beta oscillations reduces with a wide range of therapeutic methods, including dopamine agonists and DBS and much lower during the so called off periods. It has been shown in patients that the amplitude of the beta oscillations correlates with the clinical akinesia and rigidity scores, and that L-DOPA treatment induces suppression in beta power, that also correlates with the reduction in the same symptoms (Little & Brown, 2012; Little et al., 2012). In patients with higher rigidity scores, an increased proportion of single units are known to oscillate at beta frequencies, which suggests a mechanistic relationship (Sharott et al., 2014a). More recently it has been shown that on-line fluctuations in beta power can be exploited to gain an insight of the severity of clinical symptoms between patients (Chen et al., 2010; Little & Brown, 2012; Little et al., 2012).

In MPTP-treated monkeys, high frequency DBS causes comparable effects by reducing the amplitude of ~ 10 Hz oscillations. Furthermore, this modulation is known to correlate with symptomatic relief (Hashimoto et al., 2003;Meissner et al., 2005;Xu et al., 2008;Johnson et al., 2009;McCairn & Turner, 2009). In 6-OHDA hemilesioned rats, a conventional motor test, the apomorphine induced rotation revealed similar effects to that of non-human primates and PD patients. The dopamine agonist apomorhpine decreased the power and the synchrony of beta oscillations by the time the animal starts to rotate (Sharott et al., 2005). Frequency-related changes were shown in this model too: the centre frequency of the beta coherence is not stable over time, as it was ramping up after the hemi-lesion took place. This finding is complimentary to what has been observed in in the cortex and striatum

of healthy rats, but in a higher frequency range following administration of dopaminergic drugs (Berke, 2009).

Additionally, the amplitude of the beta oscillation seems to be ubiquitous in the network and affect oscillatory connections. Beta oscillations readily emerge in almost all stations of the motor (dorsal) stream of the cortico-basal ganglia-thalamocortical loop (Levy et al., 2001; Stein & Bar-Gad, 2013; Zaidel et al., 2010). In line with the existing functional division throughout the nodes of BG, single neuron beta oscillations are more prominent in the dorsal stream (Moran et al., 2008b, Zaidel et al., 2010). It is notable, however, that there is less available data suggesting oscillatory activity of single neurons in the thalamus (Guehl et al., 2003;Pessiglione et al., 2005) and the SNr, whereas the mean frequency of single neuron oscillations varies significantly between species compared to what has been observed with human patients (Stein & Bar-Gad, 2013).

As it has been discussed in previous sections, the activity of BG nodes, with some exceptions, is highly uncorrelated in healthy animals. In PD patients and animals with PD phenotypes, however, network coupling enhances to a pathological extent across many stations and many computational levels for processing. In the STN, spike trains showing rhythmic activity in beta range, but not in the tremor-band show phase locking to the local activity of the STN ensemble they are surrounded by (measured by the metric called background unit activity, see above) in patients and in non-human primates (Moran & Bar-Gad, 2010; Moran et al., 2008a).

Importantly for this thesis, oscillatory interactions between the STN and the motor cortex get pathologically exaggerated in PD. As it has been established in previous sections, STN neurons are particularly sensitive to cortical input. This connection is pathologically pronounced in DA depleted states (Magill et al., 2001). Furthermore, the enhanced

oscillatory relationship can be captured in the magnitude and stability of phase relation between the local activity of the STN and the motor cortical EEG (Marsden et al., 2001;Williams et al., 2002; Kuhn et al., 2004;Fogelson et al., 2006;Lalo et al., 2008 Sharott et al., 2005, **Fig 1.3. A**). Most prominent oscillatory coupling occurs in alpha and high beta band after overnight withdrawal of L-DOPA in patients (Folgelson et al., 2006). It has been demonstrated in patients that strong oscillatory coupling at 10-30 Hz occurs between the STN and the motor related areas of the cortex, which is particularly prominent over the midline indicating the involvement of supplementary rather than primary motor areas (Mardsen et al., 2000; Williams et al., 2002). Moreover, the most consistent coherence with midline EEG was also recorded with the macro contact that shown the highest effectiveness in terms of clinical response (Mardsen et al., 2000). In terms of directionality of the effect, it has been established in a series of studies that the EEG is phase-led STN LFP by around 20 ms (Mardsen et al., 2000; Williams et al., 2003, Lalo et al., 2008,Litvak et al., 2010a). Lalo and colleagues (2008) demonstrated the dynamics of this coupling as the function of movement and L-DOPA medication. The cortico-STN coupling is reportedly bidirectional and asymmetric; as cortex drives the STN more prominently during rest, however, dopamine-medication related changes were more prominent in gamma band. Additionally, the heightened coherence between M1 and the STN can be diminished by the administration of anti-parkinsonian medication (Hirschmann et al., 2013). Sharott and colleagues (2018) observed oscillatory coupling between STN units and different areas of the cortex in relation to movement (**Fig 1.3. B**). In line with previous studies (Lalo et al., 2008), cortico-subthalamic desynchronization measured in single unit activity reduced during movement, but to varying extent. The size of the effect was mostly dependent on whether the locking was calculated from cortical areas involved in mostly the execution versus the planning of movement. A large proportion of units remained synchronised to the SMA, whereas the

most of the oscillatory coupling in beta range between the STN and the M1 was reduced as expected.

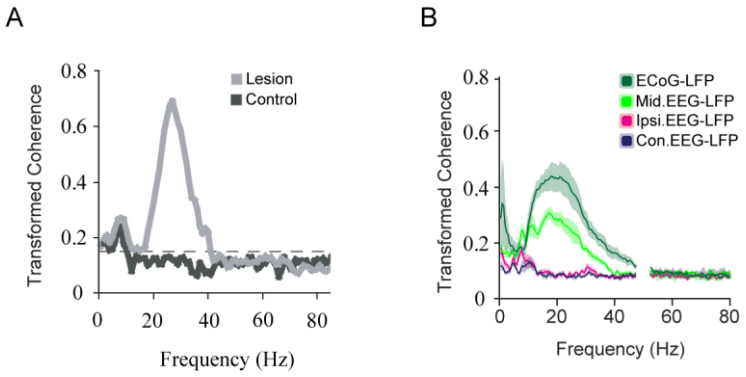


Figure 1.3. Corticosubthalamic coherence in beta range is elevated in Parkinsonian animals and PD patients. A) Mean transformed coherence values between the STN and the ECoG of healthy (dark grey line) and 6-OHDA hemilesioned animals (light grey line). Peak is between 20 and 35 Hz for the 10 lesioned animals (adopted with permission from Sharott et al., 2005). **B)** Mean transformed coherence between the STN and cortical signals of human PD patients display a peak in the same range as in the parkinsonian rats. Note that the peak coherence has a prominent anatomical distribution, was significantly larger for the as the ECoG and midline-EEG pairs display a more robust peak than the ipsilateral and contralateral pairs (ECoG: n = 7; EEG channels: n = 9, Kruskal-Wallis, p = 0.000008, post-hoc Dunn's tests). Adopted from Sharott (2018) with permission

Exaggerated coherence can be recorded from 6-OHDA hemilesioned rat experiments too (Magill et al., 2001; Sharott et al., 2005; Mallet et al., 2008b, Degos et al., 2008). Sharott (2005) and Mallet (2008) characterised the coherence between the motor cortex and the STN and established that in the 6-OHDA hemilesioned model displays beta coherence around 20 Hz, and seems to be subject to movement-related and chronic changes, and appears to be unaffected by the acute administration of D1/D2 antagonists implying plasticity mechanisms (**Fig 1.3. A**). Additionally, it has been shown that the motor symptoms precede the excessive beta synchronisation in case of unilateral versus bilateral lesions (Degos et al., 2008). Furthermore, mutual information coded by STN neuronal ensembles increased, which

indicated lower information coding capacity during these periods of high oscillatory coupling (Mallet et al., 2008b).

Dissecting the specific role of phase and amplitude in the dynamics of the exaggerated coherence is still under investigation. The peak coherence measured between the cortex and the STN increases progressively while the power is supressed during apomorphine-induced rotations and spontaneous movement (Sharott et al., 2005). Lipski et al. (2017) showed that the synchrony between the firing of the STN neurons and the cortical activity is correlated with grip force production in a phase-specific manner. It is also known that the amplitude of the oscillating neurons in the STN is highly synchronised with the phase of fast (gamma) oscillations in the M1. Pathological phase-amplitude coupling (PAC) appears to be specific to PD as it was not observed in dystonia patients (Shimamoto et al., 2013).

In terms of heightened oscillatory connection between different nodes, beta coherence was also captured between the motor cortex and the SNr of awake and behaving dopamine depleted rats (Brazhnik et al., 2012). Interhemispheric coupling of the STN LFPs in lower and higher beta bands has also been demonstrated (de Solages et al., 2010). In terms of the cortex, units display higher coherence between neurons and with the LFP (Li et al., 2012). Inter-regional cortical coherence has been demonstrated in the 6-OHDA lesioned models well as in patients (Degos et al., 2008; Silberstein et al., 2005). In patients, the degree of this coupling was correlated with clinical improvement, and that levodopa or high frequency stimulation reduced such coupling, which effect also scaled with symptom severity scores (Silberstein et al., 2005). Heightened coherence appears in relation to peripheral activity too. Hirschmann et al. (2013) showed strong coherence between the muscle activity and M1 as well as STN, both of which correlated negatively with rigidity

experienced during OFF-states, indicating the clinical relevance of beta coupling between the cortex, STN and the periphery.

1.6. Therapeutic Brain Stimulation

1.6.1.Deep Brain Stimulation

Although there is no cure for PD, and motor symptoms inevitably worsen as the disease advances, there are many effective ways to alleviate symptoms and to slow disease progression. Two mainstay approach includes pharmacological (DA or gene-expression related) and surgical (ablation or electrical stimulation) treatment options. Even though Levodopa and other drugs affecting dopaminergic transmission are considered the first line of treatment for PD, long-term administration eventually leads to dyskinesias and prolonged periods of impaired (OFF state) versus asymptomatic periods (ON state, Obeso et al., 2000). In patients who are fit, have no history of dementia, fragile circulation or mood disorders and have previously been responding to dopaminergic medication, deep brain stimulation (DBS) is a viable treatment option.

Ablative surgeries have undeniable benefits for patients too, pallidotomy (Baron et al., 1996;Lang et al., 1997;Vitek, 2002) and subthalatomy (Guridi & Lozano, 1997;Bergman et al., 1990;Alvarez et al., 2001) is known to alleviate dyskinesia and symptoms mostly associated with rigidity; whereas the selective lesioning of the motor thalamus, particularly the ventralis intermedius (VIM) is known to be effective for tremor-related symptoms (Tasker, 1990). Albeit these procedures are not without side-effects or risks (Hariz, 2002; Moro et al., 2002). Lesioning, particularly bilaterally, is known to cause many unwanted side-effects (for e.g. hemiballismus in case of subthalamtomy), but more importantly, due to its irreversible nature, there is no room for corrections or evaluative adjustments based on symptom severity and individual recovery-profile (Vidaković et al., 1994; Moro et al., 2002). In 1987, Benabid and colleagues reported that high frequency stimulation of the VIM

produced comparable symptomatic relief in tremor patients with 'mild and regressive' symptoms (Benabid et al., 1987). Interestingly, the authors settled on 100-130 Hz, (still used as the stimulation frequency for conventional DBS settings) because the programmable stimulator's frequency rate was limited to that range. Ever since, DBS is an approved (1997) and successful (over 100000 patients underwent surgery) treatment option for movement disorders including essential tremor, dyskinesia and PD; and more recently to certain mood-related and psychiatric conditions (depression, anorexia nervosa, Hariz et al., 2013).

Procedure, efficacy

After careful patient selection and choosing the surgical target, patients undergo – in most cases bilateral – implantation of the stimulating leads attached to an internal pulse generator (Moro et al., 2002). The surgical procedure can be performed while patients are awake, and some groups aid target localisation by microelectrode recording and mapping of the region of interest during test-stimulation. The programming of the stimulator is done remotely by the neurologist and takes place 2-4 weeks post implantation. More detailed discussion on the surgical procedure in Chapter II.

To this date, more than 100 000 patients have benefitted from DBS surgery (Fasano & Lozano, 2015). Overall, DBS offers a long-lasting improvement in the patient's symptoms, quality of life and functionality (Perestelo-Pérez et al., 2014;Schuepbach et al., 2013). To this date, direct evidence explaining the mechanism of DBS is lacking. However, a good framework should, in theory, be able to account for the following observations regarding DBS in movement disorders.

1) DBS causes similar effects to ablative surgery, which intriguingly means that DBS improves symptoms by disabling (inhibiting or disturbing) at least some of the downstream actions of the BG (Wichmann & DeLong, 2016).

2) Regardless of its disabling action, DBS does not inhibit new motor learning, on the contrary, it seems to facilitate it (Wilkinson et al., 2011; Van Wouwe et al., 2011). A study by Mure et al. (2012) found that sequence learning was improved by deep brain stimulation but not by levodopa infusion, furthermore, these effects were most pronounced in the SMA, in accordance with electrophysiological studies (Sharott et al 2018, Litvak et al., 2010a, see above) and Whitmer et al. (2012). Improvement of learning and memory performance was also reported in parkinsonian rats undergoing DBS (Hao et al., 2017).

3) The effect of DBS is frequency-specific: low frequency stimulation exaggerates rigidity and bradykinesia, whereas stimulating with more than 100 Hz it is an effective therapeutic option (Moro et al., 2002, Pogosyan et al., 2009; Wach et al., 2013, Pedrosa et al., 2014). Differential effects of the frequency of the stimulation was reported in an early study by Hassler (1979), who found that cats responded differently to low and high frequency pallidal stimulation, and that 20 Hz frequency stimulation could inhibit the attentional response to contralateral the contralateral side. Chen and colleagues (2007), for example, found significant slowing in a tapping task in case of 20-Hz stimulation as compared to 50 and 130 Hz. Conversely, in a study using a task with transcranial alternating current stimulation and implemented longer lags between stimulation and task, did not find more pronounced bradykinesia (Krause et al., 2014).

4) The placement of DBS electrodes is surprisingly forgiving. Even though there are specific considerations in choosing a target over another. Specifically, VIM stimulation works well in tremor patients but not effective for patients with rigidity (Hyam et al., 2015). On the other hand, both STN and GPi produces similar therapeutic outcomes (Fasano & Lozano, 2015;Odekerken et al., 2013;Sako et al., 2014;Weintraub et al., 2013). Additionally, slightly ‘off-target’ placement, like antidromically stimulating the cortex via exciting the fiber tracks

around the STN, is documented to have a great side-effect-to-efficacy ratio in some studies. Furthermore, this might even explain for some of the STN-specific actions of DBS (Devergnas & Wichmann, 2011;Li et al., 2012; Li et al., 2007;Hanajima et al., 2004; Kuriakose et al., 2010; Gradinaru et al., 2009).

5) Reduction of heightened synchrony is associated with symptom improvement. Several studies reported that high frequency DBS reduces the amplitude of the ongoing beta oscillations (Kühn et al., 2008;Ray et al., 2008 Wingeier et al., 2006;Eusebio et al., 2010). This might be another key mechanism of action, since the amplitude of beta oscillation is also reportedly associated to symptoms, as discussed above. DBS also reduces the pathologically exaggerated coherence within the nodes of the BG, but according to some studies, motor improvement only correlates with the reduced local synchrony in the STN (Oswal et al., 2016). This might be because the cortical power is shown to be reduced in a location-specific manner, over locations that are supposedly from the hyperdirect pathway, such as the SMA (Whitmer et al., 2012,Sharott et al., 2018b). Thus, the effect of DBS on the coherence between not functionally connected areas of the cortex and the STN would not give a reasonable/meaningful result. Additionally, a study looking at the acute effect of high frequency DBS found that beta oscillations remained unchanged, whereas lower frequency oscillation increased during the first application of DBS (Rossi et al., 2008). This, in line with literature on beta evolving as a compensatory mechanism (Mallet et al., 2008b) suggest that supressing beta oscillations might rely on a chronic or compensatory mechanism as well. The assumption that destroying overly exaggerated synchrony must rely on longer term network changes is further supported by the fact that longer DBS decreases beta oscillations for a longer time (Bronte-Stewart et al., 2009).

1.6.2. DBS actions

While the exact mechanism of action is still under debate, this section describes some of the theories concerning how DBS might exert its therapeutic effect.

Inhibition of targets

This theory explains for the observation that the effect of DBS was compared to, in fact, developed from ablative surgical methods (see point 1) in previous section). There is an assumption that DBS works via inhibiting the neural elements of the pathologically overactive downstream structures via inhibiting the high frequency firing and removing the hyperexcitation from the BG outputs, which also tallies with the assumptions of the Rate model (Benazzouz et al., 2000;Chiken & Nambu, 2016). Neural activity can, in theory, be decreased by the effect of a depolarisation block in the vicinity of the recording electrode (Beurrier et al., 2001); activating or inhibiting the synaptic output (Dostrovsky et al., 2000;Anderson et al., 2006); or interfering with the balance of neurotransmitters (Llinás et al., 2002).

Indeed, some studies found decreased firing rate of the target structures ((Dostrovsky et al., 2000; Filali et al., 2004;Meissner et al., 2005). For example, Beurrier and colleagues (2001) found that extracellular application of very high frequency stimulation in slices causes a long lasting (~ 6 mins) inhibition of the tonic firing in the STN. This mechanism was explained by the almost complete blockade of the persistent sodium current, and partially affected the Ca^{2+}-mediated post-hyperpolarization. Contradictory to these findings, several studies found that glutamate levels are actually increased during high frequency stimulation (HFS), and furthermore, output stations can be excited by the high frequency stimulation (Windels et al., 2000; Hashimoto et al., 2003). Additionally, Do and Bean (2003) found that the average firing rate was higher during HFS, silencing being an exception rather than a rule.

Some modelling studies drew attention to the paradox that concomitant inhibition of the target and activation of the outputs can be explained by the fact that the differential effect of DBS on the soma versus the axons (McIntyre et al., 2004; Montgomery Jr et al., 2000;Vitek, 2002). This was recently supported by an optogenetic study in behaving mice (Gradinaru et al., 2009).

An elaboration to this theory suggest that changes in firing pattern, such as bursting, is important in the explanation for the symptoms, hence might be a key mechanism in explaining for DBS action (Bevan et al., 2006). Some studies suggested that disruption of pathological bursting restores efficient commination between structures, thus improves symptoms (Gale et al., 2009; Tai et al., 2011). In favour of this hypothesis, some reports provide evidence for the decreased bursting during DBS and its effect on modifying pathological burst transmission within the system (Hahn et al., 2008).

The rate model based explanation of DBS action however cannot account for the fact that HFS of GPi is also efficient, and other mechanisms related to DBS actions, such as the frequency-specificity and the disruption of the heightened synchrony.

Information lesion

The information theory suggests that the most important action of high frequency DBS is to exert a stimulation-locked, low-information content noise on the GPi. However, this is not the healthy pattern of the GPi, it still hinders the flow of pathological information content by forcing a constant and unvaried input (Agnesi et al., 2013;Dorval et al., 2008;Grill et al., 2004). This assumption largely relies on the finding that HF DBS of the GPi inhibits the healthy triphasic evoked response by the selective inhibition of the cell bodies (Chiken & Nambu, 2016;Nambu et al., 2000). The strength of this theory also lies in the fact that it can explain for the frequency-specificity of the stimulation, because low-frequency stimulation

is not capable to induce the high frequency tonic firing that is needed to induce an information lesion of the GPi (Dorval et al., 2010).

Some modifications of this theory ('selective filter') suggested that some of the sensorimotor related signalling is preserved, while pathological activity is filtered out during the modified transmission patterns induced by the DBS (Agnesi et al., 2013).

Decoupling

Many studies have found that DBS reduces the pathologically exaggerated synchrony within the therapeutic target nuclei and between the nodes of BG. In particular, the amplitude of beta oscillation significantly reduces after the application of HFS DBS (Meissner et al., 2005;Bronte-Stewart et al., 2009; Eusebio et al., 2011; McCairn & Turner, 2009). Moreover, this effect is known to correlate with symptomatic relief (Kühn et al., 2009).

One possible driver of this mechanism might be the antidromic activation of the motor cortex that is disruptive to the local cortical synchrony (Ashby et al., 2001a;Devergnas & Wichmann, 2011;Kuriakose et al., 2010; Li et al., 2014). In line with this observation, DBS is shown to reduce the overt coherence between the STN and the mesial premotor cortex (Oswal et al., 2016). In fact, another study concluded that in MPTP-treated monkeys, the amplitude of the beta oscillations reduce only slightly compared to the decoupling effect of stimulation (Moran et al., 2012). Another potential mechanism of action might be that DBS reduces the heightened phase-amplitude coupling between the cortex and the STN (de Hemptinne et al., 2013a,van Wijk et al., 2016; Voytek & Knight, 2015).

Brittain and Brown (2014) has recently attempted to tie the mechanism of the attenuation of the beta oscillations with theories of information coding. Revisiting Barlow's (1961) framework for entropy, the authors hypothesized that the overly exaggerated beta restricts coding space and decrease entropy by hindering the adaptation to novel circumstances

(Barlow, 1961). In healthy states, transient presence of beta synchrony proves to be useful in for e.g. action selection by inhibiting the unwanted or not anymore relevant programs (Kuhn et al., 2004; Brittain et al., 2012). This also tallies with the literature showing that motor learning improves during DBS. Unleashed beta oscillations, on the other hand, might impair the system's ability to form a flexible response shaped by the principles of rate coding. Decreased entropy might also underlie the observations that the motor cortex follows rate coding more efficiently after the beta synchrony has been destroyed, as the motor output neurons firing rate increases (Baker et al., 2001; Spinks et al., 2008). This actively upheld status quo will mean that synchrony-wise the system is being stuck in a loop: the disease state is maintained by the pathological oscillation itself (Tass & Majtanik, 2006). Additionally, regardless of its instantaneous symptomatic relief in PD (but not in other movement disorders) both DBS and beta oscillation rely on long term network changes, which seems to be in productive alliance: as the symptomatic relief that can be correlated to the reduced beta seems to be the case after long time application of the stimulation, and is not affected by the intermittent cessation in the stimulation (Trager et al., 2016).

Attractive as this theory sounds, there are certain limitations and inconsistent findings related to the role of desynchronization in DBS action. For example, Weinberger et al., 2006b reported a dissociation between symptomatic improvement and the reduction in beta, whilst other showed symptomatic improvement without a robust change in the power spectra (Foffani et al., 2006; Levy et al., 2001).

Summary

The most likely reason why the key mechanism behind DBS action has established is because it potentially exerts its effect via a combination of local and network level mechanisms, modifying coding on different timescales (Kringelbach et al., 2007). Moreover, findings presented here will heavily rely on the strengths and weaknesses of the

experimental model and recording/stimulation setup that has been implemented in the study, which varies largely in this field. Confusing as it sounds, an important thing to note is that regardless of the fact that many mechanisms might be in place that are captured better or worse by certain circumstances of the stimulating and recording, the main issue remains: what features can be harvested for optimisation of DBS?

1.6.3. Motivation behind optimization approaches: side effects and efficacy

Side effects

Despite of its success and good response rate, DBS like any other treatment option is not without pitfalls. Stimulation-induced side effects include dysarthria, reduced verbal fluency, and impairments in balance and gait (Baizabal-Carvallo et al., 2014;Benabid et al., 1991;Rodriguez-Oroz et al., 2005;Okun et al., 2005;Miocinovic et al., 2013;Ostrem et al., 2014).

Additionally, DBS is not yet universally effective for all patient groups (for eg. tremor - Deuschl & Elble, 2000) and not all the symptoms respond equally well to high frequency stimulation (for eg. gait, freezing –Moreau et al., 2008). Finally, the most invasive and exposed to infections part of the surgery is the subcutaneous placement of the IPS generator. The improvement of the battery life might in theory prolong the time between the reimplantation procedures (however this issue might be more easily helped by the development of wireless and rechargeable batteries (Lee et al., 2013). Some groups have proposed a closed-loop DBS (cDBS) approach similar to what has been long implemented with cardiac pacemakers, where the timing or the patterning of the stimulation largely relies on the ongoing state of some markers of the disease. This, in theory would serve the dual purpose. On one hand, closed loop approaches might be more energy-efficient and more efficacious (symptomatic relief: side-effect) simply because it is on-demand and tailored to

the patients individual needs (Eberle et al., 2011). On the other hand, establishing the most efficient stimulation protocol might uncover some of the mechanisms for DBS and PD.

Considerations for a closed loop approach: peripheral or central

The first variable to consider when it comes to cDBS is whether a peripheral or a central signal should be used (Meidahl et al., 2017 ;Little & Brown, 2012,Priori et al., 2013). In other words, a system could be designed on the close monitoring of certain symptoms or can be related more closely to the site of generation. An approach relying on peripheral biomarker might be easier to implement due to the robustness and less-transient nature of the signal. This is a particularly strong incentive in case of tremor. As demonstrated by some studies, tremor provides a reliable biomarker for implementing closed-loop approaches (Brittain et al., 2013;Cagnan et al., 2013a; Cagnan et al., 2014; Cagnan et al., 2017). Even though tremor characteristics can be differentiated between essential tremor and PD and are known to reflect certain aspects of the underlying motor system (Brittain et al., 2013). Arguably, regardless of the success of these approaches, a central biomarker is potentially more desirable (but see Yamamoto et al., 2013 using EMG; Baram, 2013 - using head-mounted accelometer). Firstly, a central signal is directly involved in the pathogenesis of the disease – it allows for a more selective targeting and potential prediction of certain features of the symptoms. Additionally, finding a central biomarker would mean that the system won't have to rely on recording each symptoms independently that could be quite challenging, especially in the case of PD, where the 4 cardinal symptoms are quite different in movement kinetics to each other. Finally, implementing a central biomarker is a "tidy solution", because it is fixed chronically implanted, the patient won't experience the inconvenience of having to personally take care of and be cautious with a device throughout engaging with different actions.

In terms of a central signal, there are still at least two options: should a device rely on local field potential or single unit recordings. Single units seem to be more obviously reflecting the local brain communication, and already have successfully been implemented in a closed loop study on monkeys by Rosin et al. (2011), where a single pulse or a short spike train recorded from the M1 or the GPi served as a feedback signal for fixed-lag stimulation of the GPi. Conversely, LFPs recordings seem to present a more viable candidate, because of their stability: single unit recordings are less reliable over a long period of time. Additionally, LFP recordings have wide availability in patients, whereas single units to this end cannot be recorded outside of the intraoperative test-stimulation that can be done with leads equipped with a micro-tip. Beta oscillations due to their 1) involvement in motor control, 2) correlation to symptomatic relief, 3) ubiquitous nature, 4) reproducibility in animal models and 5) the fact that the signals can be collected from the parts of the DBS setup that is already in place, seem to be an ideal candidate for a closed-loop biomarker.

Considerations for a closed loop approach: Cortex or STN

As discussed before, there are numerous surgical target possibilities might come in consideration for collecting beta signal, but generally speaking, two target locations have been focused on so far: the subthalamic nucleus and the (mesial/ supplementary motor) cortex.

Successful studies utilising cortical feedback signal include the aforementioned study on monkeys by Rosin et al. (2011). Using cortical signals in patients is a viable option, since surgical centres increasing implant subdural strips (ECoG) as a routine part of the procedure. Cortical recordings paired with cortical stimulation also bear the promise of not having to rely on invasive surgery at all (Wu et al., 2008). Removing the recording away from the close vicinity of the stimulation electrode means that the signal is confounded with much less stimulation artefacts (in case of STN stimulation), which implies a better signal-

to-noise ratio. Additionally, utilising a cortical signal that can be gained independently from the placement of the DBS lead would free up all contacts for possible stimulation without having to sacrifice any for recording. Independent placement might make a tremendous difference in cases of axonal/ white matter tract DBS approaches, where recording neuronal activity is less reliable (i.e. depression, tremor). Last, but not least, cortical signal is much larger in amplitude, hence easier to acquire.

Opposing to this view, supporters of the STN biomarker approach pointed out that the cortical beta signal is not particularly strong and that the clinical relevance of the cortical beta is much less researched (Little & Brown, 2012; Priori et al., 2013). This might be because EEG consists of the signal collected from large number of neuronal elements of the cortex, not all of which is functionally involved in the genesis of the beta signal. Additionally, subdural strips are challenging to navigate over the areas of the cortex that are functionally connected to the STN (mesial, SMA ;Oswal et al., 2012;Horn et al., 2017;Accolla et al., 2016a; Sharott et al., 2018c), and ECoG trajectories are hard to track. Even though beta is not pathologically elevated in the human cortex, Starr and colleagues have demonstrated that phase-amplitude coupling (PAC) is increased compared to other diseases and responsive to DBS (Shimamoto et al., 2013,De Hemptinne et al., 2013b; De Hemptinne et al., 2015). A closed loop approach relying on PAC, however, tracking the amplitude of high-frequency oscillations, which are a low amplitude signal. STN appears to be a better choice from the point of feasibility (biomarker derived from the contacts already in place for stimulation) and the fact that STN beta is well researched and seem to be robust over many years (Giannicola et al., 2012. STN beta, as discussed before is the best researched electrical fingerprint of the disease, as it not only correlates with the symptoms, but also is supressed by levodopa and DBS (nucleus may be a pathophysiological mechanism in Parkinson's disease (see above, Lopez-Azcarate et al., 2010).

Optimisation: Power or Phase

Optimisation algorithms based on a central oscillatory signal recorded from the STN can still vary in the pattern of stimulation. Closed loop stimulation was first pioneered merely by using the amplitude of the ongoing beta oscillations as a biomarker. Little et al. (2013) showed that in a double-blinded evaluation setup, patients showed just as much symptomatic relief when the stimulation was only delivered in the periods of high amplitude beta oscillations, but in this case, stimulator was on for less than half as long as with conventional approaches. A more recent analytical framework pointing out the importance of the long beta bursts in symptom severity, revealed that this effect was mostly due to cutting long beta bursts shorter (Tinkhauser et al., 2017a; Tinkhauser et al., 2017b). This effect was mirrored by a study conducted on non-human primate by Johnson et al. (2016) that found a power-based closed approach is more effective at reducing rigidity for being on for only for 50% of the time.

Another important assumption for implementing a closed loop approach is that it can overcome some of the therapy-induced side-effects by specifically tackling the clinically relevant periods and minimising the stimulation onset. This was indeed confirmed by a study focusing on speech related adverse effects (Little et al., 2016). Taking an individually fitted scalar, continuous time-control approach Rosa et al. (2015); Rosa et al. (2017) found that not only was the closed-loop system effective, but it also caused less side-effects by significantly reducing medication caused dyskinesias.

Amplitude-responsive systems are only one way to implement closed-loop approach. In the cardiac research, the timing of the stimulation is often determined by the application of the stimulation in a fashion that is periodically perturbing coupled oscillators (Winfree, 1967). Some cardiac pacemakers operate on the mathematical basis that hitting a specific phase of an ongoing oscillation can elicit selective amplitude changes, similarly to the swing

that will flaunt according to the specific point in time it has been pushed. One way to capture this is to calculate the ‘phase response curve’ that reveals how exactly the phase of an input, such as a stimulation pulse, affects (advances or delays) the phase of an oscillator (Wilson & Moehlis, 2014).

Experimental evidence of successful phase-dependent approaches has been twofold. Pseudo-phase tracking was implemented in a study applying same frequency stimulation, where the stimulation was naturally drifting in and out of phase with the ongoing tremor. Similar to what has been established with noise-cancelling headphones, an anti-phase stimulation reduced resting tremor up to 50% in PD. An aforementioned study by Rosin et al. (2011), showed that constant lag stimulation of the GPi is successful in alleviating MPTP-induced symptoms. Constant lag stimulation can be regarded a form of phase-specific stimulation given that the oscillation is stable. In this paper, delivering the stimulation with 80 ms lag was putatively superior because it phase-matched one cycle of the ongoing low frequency oscillation (12.5 Hz). A milestone in the implementation of an actual phase-tracking closed loop approach was reported by Cagnan et al. (2017)who showed that tremor phase-selective application of DBS alleviated tremor in 3 of the 5 tested essential tremor patients. Regardless of the small sample size and the acute recordings, this is a very promising tactic for closed loop implementation.

Regarding PD, an approach called ‘coordinated reset’ has been suggested by Tass et al. (2012). This approach suggests an essentially open-loop solution that does not use an electrophysiological biomarker, but rather operates on the basis of applying a stimulus pattern that favours decoupling. The idea is to destroy pathologically exaggerated synchronous activity based on multi-site recordings by aiming for driving out-of-phase interactions. To this date, a closed loop stimulation based on the stimulation phase in relation to the ongoing beta oscillation in PD has not been attempted.

1.7. Summary of main aims and findings

The overarching aim of this thesis was to explore pathological oscillations and oscillatory innervation in PD. More precisely, this thesis's main objective was to understand some of the underlying mechanisms of beta oscillations on different levels of neuronal processing and to compare some of these effects between experimental setups in rodents and humans by demonstrating basic and translational insights.

Study 1 (Chapter II) *Introduction/Novelty.* In the first study, my aim was to outline an intraoperative stimulation approach that enabled me to record various electrophysiological signals while implementing a continuous stimulation in PD patients undergoing DBS surgery. The frequency of the stimulation was matched to the ongoing oscillation. This approach is novel because it attempted to overcome the overshadowing and corruptive effect of the stimulation. Stimulating with high frequencies can result in amplifier saturation immediately after the electrical pulse and can make it difficult to record oscillatory activity and spikes. *Problem /question.* Recording at the site of the electrical stimulation therefore presents an analytical burden in subtracting the instantaneous effect of the stimulation in the vicinity of the stimulating electrode. Changing the stimulating parameters, on the other hand, necessitates that the modulation can be achieved without significantly corrupting the instantaneous phase and amplitude information. *Results*. Low frequency, low intensity bipolar biphasic stimulation allowed for the recovery of the signal after off-line artefact removal. Additionally, the stimulation did elicit physiologically tangible effects that is demonstrated by clear modulation of STN neuronal spiking and cortical evoked potentials. In summary, this study implemented a novel stimulation protocol at beta frequency that allowed for a modulatory but not enforcing control of the STN output and the cortex in awake human patients undergoing DBS surgery.

Study 2 (Chapter III) *Introduction/novelty.* Deep Brain Stimulation is a widely used and effective treatment option for PD patients. Optimising stimulation protocols has been the forefront of scientific interest in order to improve side-effects and overcome partial efficacy of DBS. Recent studies on similar movement disorders and animal models of PD have suggested that implementing closed loop approaches, where the onset of the stimulation is dictated by peripheral or central markers of symptom severity is effective in alleviating symptoms of the disease. *Problem/question.*To further improve DBS in patients, it may be necessary to account for the temporal dynamics of the ongoing pathological beta oscillations in order to selectively modulate their amplitude by controlling the timing of the stimulation. *Aims*. The main aim of this chapter was to establish whether the phase at which the electrical stimulation was delivered, relative to the underlying beta oscillation, could produce short latency effects on the amplitude of the pathological activity within the STN. Additionally, the chapter probes the parameters of the beta phase at which this modulation is the most prominent. *Results.* The results demonstrate that phase-dependent suppression or amplification of beta oscillations requires at least 2 or more cycles of the stimulation pulses consecutively arriving on a specific phase of the ongoing oscillation. Instantaneous phase-amplitude modulation of individual electrical stimuli (when the consecutive nature of the stimulation was not considered) could also be seen, but it was not significant compared to the surrogate data. The phase bins that led to maximum suppression or amplification was specific to each patient. These effects were easier to trigger when the overall beta power was low. In some cases, the precise frequency matching between the stimulation and the oscillation allowed for higher phase-resolution. These instances provided evidence for higher phase specificity leading to a larger effect size. The importance of consecutive phase-dependent stimulation was trialled not only using the STN LFP, but also on different output measures. For this purpose, the background unit activity (BUA, description above) was

chosen because it indicates the spiking activity (output) of the STN. Additionally, the phase stability index (PSI) was calculated to indicate the stability of the phase relation between the STN and the cortex. With these findings, I demonstrate that STN outputs can be supressed and amplified in a phase-dependent manner. Additionally, I also show that regardless of the fact that the amplitude of the cortical beta was unchanged, the phase alignment between the cortex and the STN is less stable during the suppressive phase bins. These findings provide a proof-of-principle framework for the potential optimisation of DBS by implementing the phase as an input to a closed-loop algorithm.

Study 3 (Chapter IV) *Introduction/Novelty.* The main aim of the last chapter was to address whether the amplification of beta oscillations in PD has the same underlying mechanisms that have been suggested for functional communication. An influential theory explaining healthy coding in terms of synchronization is the communication by coherence (CTC) framework put forward by Pascal Fries. According to this theory, the success of the communication between two oscillators will depend on a coherent and specific phase relationship between the input and the receiver. In the most frequently occurring, 'preferred' phase alignment the input has a maximal effect on the receiver, hence the communication is efficient. Naturally, non-preferred scenarios occur when communication is prohibited, and crosstalk with other connected structures are preferred. The dynamic balance between these two phase alignment scenarios is essential for coding information. *Main question.* In this chapter, I hypothesised that in PD, the dynamic element of the CTC is compromised. More precisely, I proposed that it is possible that the power of the pathological beta oscillation ramps up because efficient communication within the cortico-BG loops is pathologically enhanced by the system maintaining mostly the preferred phase alignment. *Aims.* The first specific aim was to show that there is a likely phase alignment between the two oscillating structures of the cortico-BG network in Parkinsonian rodents and PD patients. The second

objective was to interrogate whether preferred phase alignment is associated with an increase in amplitude over time in the cortex and the STN. And finally, I was interested to see whether this phase alignment can affect the firing properties of the STN neurons. *Results.* In 6-OHDA hemi-lesioned rats I found that the phase alignment between the STN and the cortex is not homogenously distributed: some phase alignments occur more often than others and the power of both signals is the highest at the most probable phase alignment. Based on these findings, recording epochs could be split into periods of preferred and non-preferred phase alignments. Albeit starting on a higher baseline, the power significantly increased by the 2nd cycle of preferred phase alignment, and stayed elevated. In comparison, during the non-preferred phase, the power of both the cortical and the STN activity slightly dropped then stayed around the baseline. Low frequency stimulation selectively modulated the phase-alignment dependent changes in the STN by diminishing the differences between the preferred and non-preferred alignment, but exerted no modulation on the cortical phase-alignment dependent modulation. Surprisingly, results were identical when the analytical framework was trialled on the data acquired from PD patients undergoing DBS. This study suggests that the CTC theory can be successfully applied in the understanding of the pathologically exaggerated beta oscillations. This work further suggests that coherence can be split into beta amplification favouring and non-favouring periods, and that synchronisation in the cortico-subthalamic loop precedes the power increase.

Chapter II Human Intraoperative Recording and Stimulating Setup

2.1. Introduction

Parkinson's disease patients undergoing deep brain stimulation surgery have not only benefitted from the therapeutic effects of the electrical stimulation, but also contributed to the understanding of the physiology of diseased basal ganglia networks (Engel et al., 2005). Target localisation during deep brain stimulation can be aided by microelectrode recordings assessed *in situ* by the neurophysiologist assisting the surgery. Microelectrode recordings are carried out by some neurosurgical teams in order to map the STN area (Guridi et al., 2000; Benabid et al., 2000; Benazzouz et al., 2000; Romanelli et al., 2005; Romanelli et al., 2004). The precise – often single cell – resolution of these recordings can also be used for experimental purposes utilising the short time window after the tips reached the target but prior to the implementation of the permanent electrodes. Microrecordings are often followed by high frequency stimulation via the different electrodes to pinpoint the trajectory with the maximising the therapeutic effect while minimising the side effects (Hamel et al., 2003; Seifried et al., 2012). This has also provided the opportunity to record local field potential and spike train recordings during electrical stimulation and behavioural tasks (Sauleau et al., 2005;Engel et al., 2005, Zaghloul et al., 2012).

2.1.1. Challenges of optimizing parameter settings for continuous stimulation

In this chapter I outline the development and optimisation of experimental and analytical strategies that enabled the investigation of the effect of stimulation timing relative to the ongoing pathological activity in PD patients discussed in the next chapter. Despite the

obvious constraints imposed by recording in the operating room, there are still many degrees of freedom when it comes to DBS stimulation parameters, including anatomical targeting, stimulation arrangement and stimulation intensity, as well as defining the analytical measures are necessary to assess whether the stimulation is modulatory (Kuncel & Grill, 2004).

Local stimulation makes it challenging to recover the time-domain features of an oscillation due to various different ways the signal can be corrupted. In general terms, an artefact on an electrical potential refers to deviations of any kind that are not physiological. In the case of this study, the main artefact originates from the electrical stimulation. It is challenging to remove an artefact stemming from continuous stimulation that is anatomically adjacent to the recording site due to its large amplitude and big corruptive effect. Bipolar stimulation with high (~ 100 Hz) frequency reportedly causes amplifier saturation during and continuing drift after the DBS pulse that can last up to milliseconds and can hinder the detectability of oscillatory activity and spikes (Carlson et al., 2010). Local stimulation can make the analysis of stimulation effects on the oscillation parameters difficult, in case the continuous and periodic stimulation is leading to large spectral peaks in the LFP. This effect has a potential to be imposed on the power spectra of the signal and hence to interfere with the assessment of the frequency components of interest (Syed et al., 2012). On the other hand, off-line approaches for stimulus artefact removal can more readily be utilised for stimulation triggered artefacts that occur periodically and with a relatively stable artefact waveform (Thut et al., 2005).

The aim of this study was to measure an interaction between the stimulation and ongoing oscillatory activity (see below). In this context, it is important to consider that certain stimulation parameters can silence ongoing spiking activity. Mid latency (few hundreds of milliseconds) silencing of STN firing by high frequency stimulation was

reported in patients undergoing DBS surgery (Welter et al., 2004; Filali et al., 2004) and rodents (Tai et al., 2003), Perhaps more surprisingly, stimulation at beta frequency can reduce STN firing by up to 80% (Milosevic et al., 2018). Under these conditions, any changes in the oscillatory content of the LFP, which can be primarily generated by synaptic potentials, may be rendered irrelevant if the output of the local neurons is quiescent. Other studies report no overall firing rate changes when implementing microelectrode stimulation, probably due to lower current densities (Carlson et al., 2010). Below I outline the main considerations choosing the stimulation parameters and artefact removal methods, and how they have been approached in previous work.

In terms of stimulation arrangement, monopolar and bipolar settings are feasible. The main difference between the monopolar and bipolar arrangement is the relative distance between the anode and cathode. In a monopolar configuration, this distance is relatively long, which translates to a larger current spread of the electrical potential. Bipolar configuration, however, creates less spread which makes it more likely to confine the stimulation to the target area (Ranck, 1975). The leading cause for eliciting unwanted symptoms is poor targeting, which implies that the target localisation has a huge importance in avoiding unwanted side-effects (Hariz, 2002). Bipolar setting provides a more confined spread, hence has the potential to be more limited to the area around the electrode (Volkmann et al., 2002). In terms of intensity used with different arrangements, relatively low (up to 3 V) amplitude stimulation seems equally effective delivered in both configurations, whereas higher amplitudes tend to cause more side effects in monopolar stimulation (Kuncel & Grill, 2004). Nevertheless, from the point of view of data acquisition, choosing between the two involves a trade-off between the ability to collect more data versus having a less corrupted signal. This is because the monopolar setup has the benefit to free

up more electrodes for recording and the bipolar setup allows for a potentially smaller electrical artefact.

Another adjustable parameter is the stimulation intensity. It is known that symptomatic relief correlates with an increase of stimulation amplitude up to 3 V at which symptomatic alleviation has been reported to plateau and adverse effects worsen (Moro et al., 2002). While higher stimulation intensities will lead to larger effect sizes, they will also generate larger stimulus artefacts. Stimulating with higher amplitudes does not only make it harder to remove the artefact but can also lead to monotonically dictating the activity of the STN or supressing it (Garcia et al., 2005). *In vitro* whole cell and *in vivo* mRNA hybridisation rodent studies conclude that when stimulation intensity is sufficiently high, spontaneous firing can be suspended by continuous high frequency stimulation. Under these conditions, the activity of recorded STN neurons can become entirely driven by the stimulation pulses (Garcia et al., 2003, Tai et al., 2011). Although the modulating effect of the stimulation seems to be the resulting from the interplay between the amplitude and frequency used: low frequencies (~ 20 Hz) are not capable to elicit such effect, regardless of using higher current intensity settings (Garcia et al., 2003). It is important to note that these short latency (> 1 ms) effects cannot be accurately assessed in patients due to the long shadowing effect of the electrical artefact.

In terms of pulse width, a therapeutic standard pulse ranges between 60–210 µs. In clinical practice, a relatively short length is recommended, since the pulse length is known to be directly related to the charge, which has to be kept to as short as possible in order to reduce chances of tissue damage (Kuncel & Grill, 2004). Stimulating with biphasic waveforms, while providing less focal delivery, is reported to impose lower chance of corrosion of the electrode and damaging the neuronal tissue since it has to be with a balanced charge (Pudenz et al., 1975,McIntyre & Grill, 2000).

Post hoc artefact removal approaches can be implemented in order to obtain an artefact-free signal while retaining as much information from the oscillation around the stimulus as possible. In terms of a removal algorithm, Morbidi et al. (2007) suggested the benefit of implementing the Kalman filter approach. The most straightforward off-line method proposes a subtraction of a template generated by simply averaging the signal tightly around the stimulation pulse. While being effective in removing the evoked component, template subtraction often fails to capture some segments of the electrical shift due to the heterogeneity of the artefacts. As opposed to average subtraction, Kalman filter has the potential to overcome the problem of a non-homogenous, complex and variable artefact such as TMS-induced contamination of an EEG trace (Morbidi et al., 2007). This is due to the Kalman methods recursive nature, which allows for adaptive corrections when replacing the corrupted epoch with the estimated signal.

2.1.2. Assessment of the modulatory effect of continuous stimulation on evoked responses of the STN and its afferents

Choosing the stimulation parameters carefully to ensure the artefact is kept to minimum on the other hand necessitates a means to assess whether the stimulation has a modulatory effect on the target structure. Physiological measures, such as single cell peristimulus time histograms (PSTHs) and cortical evoked potentials (cEPs) driven by the stimulation of the STN and its inputs provide a suitable criterion to establish whether our target signals display consistently time-locked changes.

STN neurons typically respond to afferent input with complex multiphasic responses that are result from the interaction of monosynaptic and reciprocal polysynaptic input with their intrinsic pacemaker-driven firing (Nambu et al., 2000; Magill et al., 2004a). ~1 Hz stimulation the frontal cortex of the rat and M1 of a monkey evoked a stereotypical cascade of changes in the firing rate of the STN neurons. In both species, the multiphasic response

could be characterized by an early, short latency excitation, a short inhibition (or robust reduction in firing) and a late excitation, followed by a long inhibition of the STN neurons. In the same way, electrical and transcranial magnetic stimulation of the STN while measuring cortical evoked potentials (cEP) is well documented in the literature (Ashby et al., 2001a;Baker et al., 2002, MacKinnon et al., 2005, Tisch et al., 2008). For instance, cEP resulting from 20 Hz bipolar stimulation of the STN were described in detail by Walker et al. (2012). This study was using therapeutic stimulation intensities (ranging between 3 and 4.4 mA, determined by the motor improvement of the contralateral arm). Briefly, three evoked peaks 1, 6 and 22 ms following stimulation were identified. Polarity was dependent on the anode- cathode reversal, but the 1 ms peak was relatively consistent across patients, intensities and the electrode setup. It has been hypothesised that 1 ms peak is the result of the antidromic whereas the 6 ms peak is more likely due to the ipsilateral orthodomic activation of the STN. The later peak occurring at 22 ms on the other hand reflects a polysynaptic activation of the pallidothalamic pathways (Kuriakose et al., 2010). Establishing the modulatory effect of stimulation with these measures is a prerequisite of a more complex analysis presented in the next chapter.

2.2 Aims

The aim of this chapter is to outline a novel intraoperative stimulation approach that enabled us to record various electrophysiological signals (spike trains of single neurons, local field potential and electroencephalograms) of the cortico-basal ganglia loops while implementing a continuous, same frequency local stimulation. Our objective was to achieve this without significantly corrupting the features of ongoing neural activity, especially the spectral properties (instantaneous phase and amplitude information) of the ongoing beta oscillation.

Here I demonstrate that the human DBS intraoperative setup that was optimised to implement an experimental protocol utilising beta frequency stimulation, while concurrently

gaining a clean signal for analysis. More precisely, I demonstrate that the stimulation allowed for the recovery of the instantaneous phase and amplitude properties of the oscillatory signals by showing that the spectral properties of the ongoing beta oscillation were unchanged following the successful off-line artefact removal. Furthermore, this chapter shows that, regardless of the low stimulation intensities, the stimulation had a modulatory effect on STN spiking activity and led to modulation of the cortical EEG.

2.3. Methods

2.3.1. Ethics and patient selection.

The experiments were conducted in agreement with the Code of Ethics of the World Medical Association (Declaration of Helsinki, 1967) and were approved by the local ethics committee. Recordings and concomitant beta frequency stimulation were made in ten patients (6 males, 4 females, average age: 62.1 years SD: 7.6 years) undergoing bilateral microelectrode-guided implantation of DBS electrodes in the STN. Patients were previously diagnosed with advanced idiopathic Parkinson's disease and gave their informed consent to participate. All patients met the selection criteria stated by the CAPSIT-PD committee (Defer et al., 1999). Clinical details are summarized in **Supplementary Table 2.1**. Motor symptoms and cognitive impairment were tested on and off) dopaminergic medication (after ~12 hs medication withdrawal by using the Unified Parkinson's Disease Rating Scale (UPDRS, Fahn, 1987) and the Mattis Dementia Rating Scale (Mattis, 1988). The inclusion of akinetic/rigid dominant patients were preferred in this study, because it has previously been shown that the amplitude of the beta oscillation correlates with this subset of symptoms (Kühn et al., 2009). Patients showed significant improvement of motor symptoms following levodopa intake (motor section (III) of the Unified Parkinson's Disease Rating Scale)

2.3.2. Surgical procedures

Patients were selected to undergo bilateral implantation of DBS electrodes into the STN. Surgeries were performed under local anaesthesia, so that the patients were awake during recording and stimulation. Participation in the study extended the surgical procedure by approximately 15-30 minutes. Every effort was made to keep additional time to a minimum, and stress level was continuously monitored using a visual analogue scale to ensure any prolongation had no effect on the patient's level of distress. Surgical procedures and targeting details have been previously described (Hamel et al., 2003; Sharott et al., 2014a). Prior to surgery patients stopped taking all anti-parkinsonian medication overnight in order to reduce the risk of intracerebral hematomas. Patients were head-fixed with an MRI-compatible Zamorano–Dujovny frame (Stryker Leibinger). Surgical planning of the electrode trajectories was based on fused images of CT and MRI scans acquired the day of surgery. This was done based on the high resolution images that were fused of the gadolinium-enhanced volumetric T1 MRI and T2-weighted spin echo MRI sequences and of the computerized tomography scan using a commercially available algorithm (iPlan; Brainlab). The stereotaxic targeting of STN was approximated based on the following coordinates: 11–13 mm lateral, 1–3 mm inferior, and 1–3 mm posterior to the midcommissural (AC-PC line) point. The trajectory was altered to avoid hitting major blood vessels, sulci, and ventricles. Based on the surgical planning, a burr hole was made on skull and the micromanipulator (used to advance the electrode) was mounted and stereotactic coordinates were applied. On demand, brief administration of low-dose and quickly reversible anaesthetic agents such as remifentanil or propofol were used. These agents do not have long lasting anaesthetic effect and dos not seem to influence microelectrode recording in the awake state (Machado et al., 2006). Nevertheless, administration of any kind of anaesthetic agents were stopped prior to the microelectrode mapping procedure.

2.3.3. Electrophysiological recording.

Microelectrode recordings (Alpha Omega Neuroprobe, AlphaOmega, Nazareth, Israel) were performed along three parallel tracks arranged in a concentric array (Neuro Omega, Alpha Omega, Nazareth, Israel). This arrangement is often referred to as 'BenGun', named after A.-L. Benabid who introduced it (**Fig. 2.1. A**, Benazzouz et al., 2002). Both unit activity and local field potentials (LFPs) were recorded from the microelectrode contact **Fig. 2.1. B**). Microelectrode recordings were performed using three stainless steel microelectrodes. The central electrode was aimed at the anatomically planned target and was separated by 2 mm from outer electrodes anteriorly in the parasagittal plane and laterally in the coronal plane. Unit activity was band pass filtered between 0.6 and 6 kHz, amplified (×20,000), and sampled at 44 kHz, while LFPs were band pass filtered between 0.00070 and 0.4 kHz and sampled at 1.375 kHz. Recordings were referenced to the uninsulated distal most part of the guide tube for that microelectrode (contact size of this macro tip ~1 mm, impedance <1 kΩ), located 3 mm above the micro tip. EEG was recorded from scalp electrodes (needle electrodes) placed approximately at positions Fz, Cz, Pz, P3, and P4 (international 10-20 system), referenced to the nose. Signals were amplified (x55,000), band-pass filtered between 0 and 0.3 kHz, and sampled at 1.375 kHz (**Fig. 2.1 B**). Recordings were initiated above the intercomissural level and were assessed by the physician's online assessment relying on the digital conversion and auditory output of the online spike sorting algorithm (alpha-omega system, in-built function). STN borders could be delineated based on elevated background activity levels (Moran et al., 2008b) and characteristic firing properties of STN neurons (Sharott et al., 2014a, **Fig. 2.1 B**). STN units could clearly be identified and distinguished from zona incerta on the superficial and substantia nigra on the deep border based on their high frequency, irregular and 'bursty' discharge pattern.

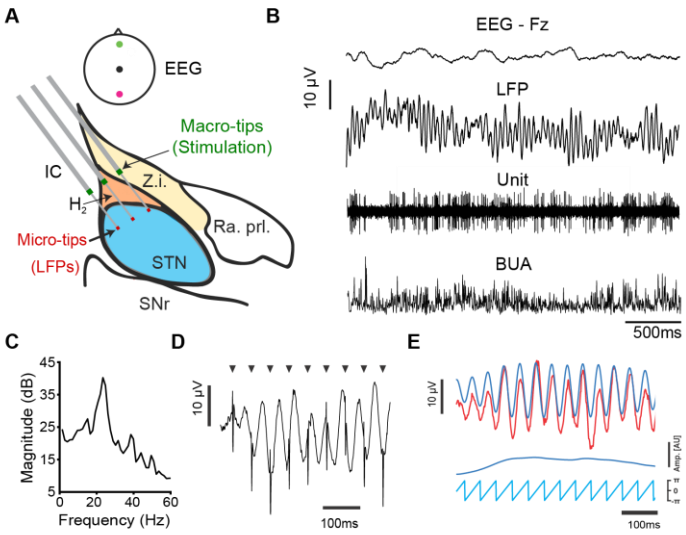


Figure 2.1. Corticosubthalamic recordings during beta frequency stimulation in PD patients. A) Schematic of the surgical setup shown on a sagittal view of the STN area, 11 mm lateral to the midline; modified from (Schaltenbrand and Bailey, 1959). Three microelectrodes were implanted along parallel tracks arranged in a concentric array. Stimulation was delivered through macro-tips located dorsal to the subthalamic nucleus while local field potentials were recorded from micro-tips within the subthalamic nucleus. Z.i.= zona incerta, IC = internal capsule, H_2 = field H_2 of Forel, Ra. Prl. = prelemniscal radiation, STN = subthalamic nucleus, SNr = substantia nigra pars reticulata. EEG was recorded from midline and frontal locations (Fz, Cz, and Pz). **B)** Examples of signals recorded and used: EEG, local field potentials, unit activity, and background unit activity (BUA, generated using the unit channel, discussed in detail in Chapter III). Example beta oscillation detected in the subthalamic local field potential recording. **C)** A peak around 23 Hz can be seen in the power spectrum (corrected for 1/f falloff). **C)** Bipolar, beta frequency stimulation (near peak beta frequency) was delivered through two macro-tips while local field potentials were recorded from the unstimulated micro-tip. **D)** The signal (red) was bandpass filtered (blue) ± 3 Hz around the peak beta frequency. The Hilbert transform was used to estimate instantaneous phase (light blue) and amplitude (dark blue) from the filtered signal.

2.3.4. Electrical stimulation of the dorsal STN area.

Anatomical arrangement of recording and stimulation. Electrical stimulation was delivered through the macroelectrode contacts using one (monopolar configuration, one patient) or two electrodes (bipolar configuration, n=19, number of recording positions) while the microelectrode recording contact was within the STN. This resulted in stimulation being applied to the area immediately dorsal to the STN while LFP signals and units were recorded by the microelectrode contact within the STN (**Fig. 2.2.**).

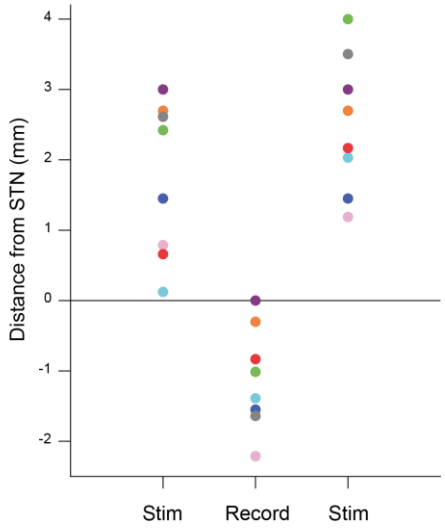


Figure 2.2. Distance of stimulation and recording contacts from the entrance to the subthalamic nucleus (STN). The dorsal STN border (set to zero) was defined for each patient based on physiological activity. For all 8 patients, both stimulation contacts were dorsal to the STN while all recording contacts were within the STN. Each patient colour is consistent with colours used in the next chapter (e.g. Fig 3.4.).

Frequency. Stimulation was applied at or near the peak beta frequency (matched frequency stimulation) to determine effects of stimulation timing on beta oscillation amplitude as discussed in the next chapter (Brittain et al., 2013; Cagnan et al., 2013a). When the time constraints of the surgery allowed for, an on-line power spectrum (Alpha-Omega) was used to acquire the average peak frequency of the baseline LFP signal. In these cases, stimulation frequency was adjusted to the peak frequency of the STN LFP (e.g. 25 Hz stimulation if the oscillation's average peak was around 25 Hz). If this was not possible, 20 Hz stimulation was applied. The average oscillation frequency was 19 ± 5 Hz, and the stimulation frequency was an average of 2.75 ± 1.75 Hz different from the peak beta frequency.

Stimulation waveform and configuration. In one patient, monopolar, monophasic stimulation (pulse width: 100 µsec amplitude: 0.25-1 mA, constant current, stimulation time: as permitted) was trialled. In the rest of the patients bipolar, biphasic, stimulation pulses (total pulse width: 200 µsec, 100 µsec initial phase negative, 100 µsec positive phase, amplitude: 0.25 – 2 mA, 3 mA in one case as shown below, constant current, stimulation time: 15-115 seconds, as permitted) was delivered. In all cases, stimulation did not result in motor evoked potentials, and patients were not aware of stimulation applied.

2.3.5. Analytical methods

Spike train processing. Spiking (single and multi-unit) activity was separated from background activity using standard spike sorting procedures post-hoc (Spike2 8.12 x64, Cambridge Electronic Design). A characteristic spike train of a single and a multi-unit recording is shown on **Fig. 2.6**. Spike sorting followed conventional methods. Microelectrode recordings with spiking content were chosen for sorting after the amplification of the signal as described above. A template wavemark was chosen by defining the peak-to-peak length and amplitude boundaries specific to the most prominent putative single unit. After setting the trigger levels, the recorded spikes were template-matched across the baseline and stimulated periods. Consecutively, the detected spike events were separated using principal component analysis and supervised clustering. Distinct clusters were isolated as single units whereas not clearly delineable, 'fuzzy' clusters were referred to as multi-units. Firing rates were during stimulation were compared to baseline rates by accounting for a 2.5 ms window during which spikes cannot be detected due to the stimulus artefact. [3]

[3] Spike extraction and sorting of extracellularly recorded action potentials refer to a multi-step process during which the activity of a single neuron recorded by a microelectrode is separated from the background noise, electrical artefact (movement or stimulation) and the spiking of other neurons. Generally speaking, the diameter, material and shape of the microelectrode will dictate the signal-to-noise ratio and influence how many neurons are being captured at one recording depth/stage/point. The aim of this process is to reliably isolate the activity of a single neuron so that it can be converted into an analogue binary signal (zeros and ones): a series of time stamps assigned to each spike.

Spike sorting utilises certain physiological principles of neural communication (Lewicki, 1998). For example, the refractory period of membrane excitability is at least 1 ms: if two spikes occur consecutively with shorter interspike interval, they likely don't belong to the same single neuron. Another important feature is that the waveform of the action potential originating from the same neuron is relatively stable in amplitude and shape. This characteristic waveform on the other hand is heavily influenced and can be distorted by both intrinsic properties and extrinsic factors. To name a few, brain-state dependent firing mode of each neuron might alter the amplitude of the waveform (cells displaying brain-state dependent 'burst-mode show decreasing amplitude and increasing interspike interval (Bunney, Walters, Roth, & Aghajanian, 1973), and the relative

distance of the tip from the location of the neuron, as well as the placement of the tip on the neuron (cell-body, axon, dendrite). Generally speaking, spike sorting is a highly heuristic and process that is prone to many types of systemic classification errors. The most common ones include the discovery of false positives, false negatives and false or double match (Izhar Bar-Gad, Ritov, Vaadia, & Bergman, 2001). Sorting is more difficult if the signal-to-noise ratio is low (high level of hash compared to the amplitude of the action potentials) or multiple spikes don't occur with a long enough time-lap allowing for clear distinction ('spike overlap problem'/ 'shadowing effect', Bar-Gad et al., 2001). A specific case of the shadowing effect is when the spikes are shadowed by an artefact (such as electrical stimulation). Automated spike sorting algorithms are commercially available and widely used, but for the reasons mentioned above, spike sorting is often refined by the supervision (visual inspection and manual verification) of the experimenter.

The basic workflow of establishing a likely correspondence of a series of action potentials to a single neuron follows similar steps, out of which can be carried out with varying complexity (Lewicki et al., 1998, (R. Q. Quiroga, Nadasdy, & Ben-Shaul, 2004),(Wood, Black, Vargas-Irwin, Fellows, & Donoghue, 2004). Following acquisition, waveforms have to be delineated from the background signal ('**detection'**). This is most simply done by setting a threshold for the height of spike (amplitude tresholding). Amplitudes that's 2 < SD higher than the baseline signal is likely to reflect deflections caused by spiking. Voltage threshold triggered spike detection is effective but often corrupted by artificial waxing-and-waning of the amplitude (for example the electrode movement triggered by breathing or cardiovascular palpations). Similarly, an amplitude threshold might be effective in separating the spikes from the background but won't be informative about whether each individual spike belongs to the same neuron in a spike train. For further isolation and classification, the shape of the action potential is useful to be considered ('**feature analysis**'). In order to subtract representative spike template, certain parameters reflecting the shape of the action potentials (such as the width) can be helpful. The more feature is taken into account the more refined the isolation will be, but the amplitude and peak-to-peak width is often used. A more refined approach to extract spike parameters include the implementation of principal component analysis before clustering. In this case, uncorrelated variables are extracted as components that and can further be used for clustering. Ideally, each component represents a neuron, although supervision is often required to decide how many clusters are actually representing distinct neurons. The output parameters of any of those methods then can be used to implement **clustering**. The goal of clustering is to assign spikes to putative neurons via grouping the subtracted features. Scatter plots of prominent parameters can be useful to visually inspect how similar action potentials are, and cluster boundaries can be defined manually after visual inspection ('**cluster cutting'**). Heuristic cluster separation approach can be improved by using algorithms such as K-means or Bayesian clustering – that can take in consideration the variation of parameters, components or templates is advised to aid this process. Higher accuracy can be achieved by using model spikes that serve as templates for the classification of action potentials ('**template matching'**, (Millecchia, McIntyre, & Research, 1978). Euclidian distance can then be calculated to assess how different spikes are from the model spike template.

Stimulus artefact removal. Data were analysed off-line using MATLAB (Mathworks, Natick, MA). A linear interpolation was used to remove the sharp electrical artefact in the analysed signal. To remove stimulus evoked artefacts seen in the LFP (**Fig. 2.3 C**) a Kalman filter approach was used for reasons outlined in the introduction (Morbidi et al., 2007). The Kalman filter is a recursive approach which predicts the current state of the system and uses noisy measurements as feedback to update the prediction at each sample point. Briefly, we assume the recorded LFP is a summation of the unstimulated signal and the stimulus artefact, which can be modelled before application of the algorithm. An autoregressive model was fit to a segment of unstimulated data and a transfer function model was fit to the average stimulus evoked artefact. The Kalman filter was then implemented and results used to estimate the artefact-free signal without phase distortion.

Spectral power analysis. Spectral power was used to evaluate overall effects of beta frequency stimulation on STN activity. Spectra were normalized to the total power between 5 – 45 Hz and expressed as percentage of total power (%). Power between 0-5 Hz and above 45 Hz was eliminated to avoid contamination by movement and noise. The Wilcoxon's signed rank test was used to evaluate statistical effects of stimulation on beta power. Non-parametric tests were used to avoid distribution assumptions given small sample sizes.

Cortical evoked responses. For cortical evoked responses, EEG signals were bandpass filtered between 0.001 kHz and 0.1 kHz, to remove the contribution of slow drifts and high frequency activity, and notch filtered between 0.049 and 0.051 kHz, to remove line noise. Evoked responses were then calculated by taking epochs off the midline EEG contacts (stimulus pulse to the next one), align to stimulus onset and average. The underlying assumption for these calculations is that the averaging will eliminate the noise and amplify the recurrent pattern of evoked responses (Walker et al., 2011).

2.4. Results

2.4.1. Experimental setup to ensure stimulation artefact is kept to a minimum.

The experimental approach presented in the next chapter required a stimulation protocol that could unequivocally modulate STN activity on the scale of several beta cycles, but not cause gross changes over timescales of seconds. To provide these conditions, we examined several stimulation parameters. To this end, we compared monopolar versus bipolar configurations (**Fig. 2.3**). The amplitude of the stimulation was also taken into consideration. A range of supra-threshold stimulation amplitudes were tested in order to optimise the stimulation effect but keep the size of the artefact minimal. For the purpose of this study we tried to find a stimulation amplitude that represents an optimal balance between exerting modulatory, but not enforcing effect. We kept the stimulation amplitude below what is used for typical DBS parameter settings in all cases (below 3 mA, Priori et al., 2006). In order to be able to account for amplitude dependent effects, in cases we trialled 3 different amplitudes ranging between 0.25 and 2 mA. The pulse width was kept the same between the different experimental protocols used. For this study, 100 ms length was used for monopolar stimulation. For the reasons discussed in the introduction, the monopolar stimulation was tested against a bipolar protocol, where biphasic initial negative waveform was used (100 ms pulse width for both negative and positive phases).

Monopolar stimulation on the two extremities of the amplitude settings used (0.25 and 3 mA) was delivered in one patient. This setting, regardless of the stimulation intensity used, resulted in a long and substantial DC offset on the two recording channels (data shown for 0.25 mA **Fig. 2.3 A**). In another patient, bipolar biphasic initial negative stimulation at 3 mA was trialled (**Fig. 2.3 B**). Interestingly, amplitude still had to be lowered in order to reduce the stimulation induced DC drift, as the LFP signal was significantly corrupted.

However, when the amplitude reduced to 0.25 mA, all the main properties of the LFP signal including the phase could be recovered (**Fig. 2.3 C**). All in all, utilising bipolar stimulation and significantly reducing the stimulation intensity allowed for a clean signal and a distinct artefact that was removed. For the rest of the experiments presented in this study, bipolar, biphasic stimulation between 0.25 and 1.5 mA was used.

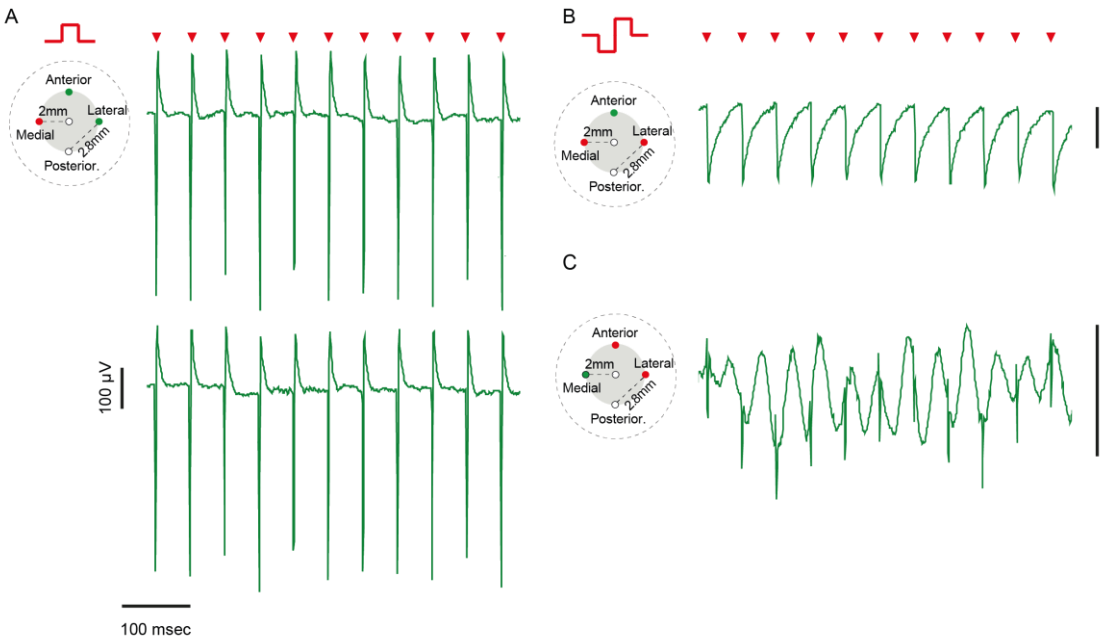


Figure 2.3. Demonstrating the magnitude of the artefact displayed on the STN LFP signals with different arrangements and parameter settings implemented for the continuous 20 Hz stimulation of the area dorsal to STN. A) Monopolar monophasic (pulse width: 100 µs) stimulation (medial contact is used for stimulating) leads to robust DC-offset on the two microelectrodes recording the STN LFP (anterior and lateral contacts). Stimulation amplitude: 0.25 µV. **B)** Bipolar, biphasic (initial negative waveform, each phase is 100 µs long, stimulation is delivered between the lateral and the medial contact) stimulation result in a robust electrical artefact using 3 µV stimulation intensity. **C)** Artefact is markedly reduced on the microelectrode used for LFP recording (medial) implementing 0.25 µV bipolar biphasic stimulation (delivered with the same setting as B, stimulating between the anterior and lateral contact).

2.4.2 Off –line approach to remove residual stimulation artefact: Kalman filter.

With implementing an off-line artefact removal approach, we attempted to delineate the signal from the artificial components for each stimulation trial. The artefact evoked by the stimulus is phase locked to the delivery of the stimulation, and remains similar in shape and amplitude throughout the trials, whereas the residual component is the information baring oscillatory signal. Hypothetically, the simplest approach to artefact removal is to take the voltage deflection over a window around each stimulation pulse, sum it across trials and then divide it by the number of trials (Thut et al., 2005). This will result in a single waveform that can be used to determine the time course and the polarity of a vector that can be used to replace the artefact. However, this residual signal would still be contaminated with the fluctuations introduced by the standard deviation of the average. This is especially pronounced on the edges of the window taken around the artefacts. In order to deal with this, we utilised a more refined approach to predict the 'edge zones'. After replacing the sharp peak introduced by the stimulation with a linear function, the Kalman filter approach was used to adaptively deal with the edges of the artefacts (**Fig. 2.4.**). These indicate the times when following the artificially introduced drift, the signal returns to baseline (Morbidi et al., 2007). This filter utilises an optimal estimation algorithm that predicts the parameter of interest (in this case, the signal returning to baseline after the stimulation-induced drift). This is done by applying a recursive approach similar to feedback control systems, where the discrepancy between the prediction and the measurement is used to upgrade the predictions of the model. In order to do so, we had to have a model for 'signal' and a model for the artificial components. The model for the artefact was made up by extracting the shape of the average artefact and fitting a transfer function model. In order to model the signal, an unstimulated portion of the data was taken and an autoregressive model was fitted which is

known to work efficiently on non-stationary signals such as EEG and LFP. The Kalman filter then compared the two models and output was used to obtain a continuous signal from which the phase information can be subtracted.

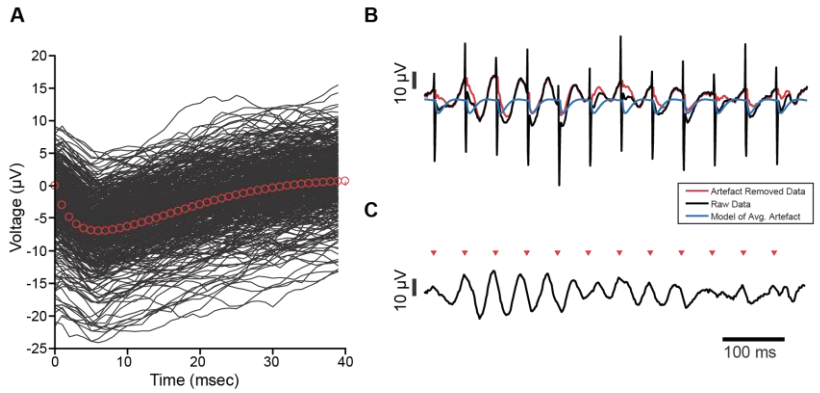


Figure 2.4. A Kalman filter approach was used to remove stimulus evoked artefacts from local field potential recordings. A) A transfer function model was fit to the average of all stimulus- evoked artefacts. **B)** A Kalman filter was used to generate an artefact free signal (red) using the raw signal (black) and a model of the average artefact (blue). **C)** Voltage trace showing the artefact free signal (arrows indicate stimulus pulses).

2.4.3. Beta frequency stimulation does not corrupt the oscillatory profile or the baseline firing properties of the STN.

While several studies have investigated the behavioral effects of continuous beta-frequency stimulation, to our knowledge there has been little exploration of how such stimulation affects ongoing beta oscillations (Kühn et al., 2009). Therefore, we first evaluated whether beta frequency stimulation led to any gross changes in the beta frequency power over the entire local field potential recordings (> 15 s). Following stimulus artefact removal, the spectral content of the recovered LFP for individual patients was similar to that observed without stimulation (**Fig. 2.5 A**). This lack of difference in spectral features between stimulated and unstimulated segments of the LFP was observed across all patients (**Fig. 2.5B**). In line with this observation, stimulation did not result in a significant difference in either the peak beta power (± 3 Hz) (**Fig. 2.5C**) or wide band beta activity (8-35 Hz) (**Fig.**

2.5D) relative to total power between 5 and 45 Hz in seven out of the eight patients included in the analysis. Stimulation did elevate beta power in one patient, however, as this was exception rather than the rule, it is unlikely that it significantly altered the group results. All in all, this analysis demonstrates that following stimulus artefact removal, residual artefacts did not significantly corrupt the frequency content of the signal, as this would have resulted in large spectral peaks at the stimulation frequency. Moreover, the lack of modulation of overall beta power demonstrates that beta frequency stimulation did not lead to consistent suppression or elevation of the amplitude of ongoing pathological beta oscillations over the entire recording period.

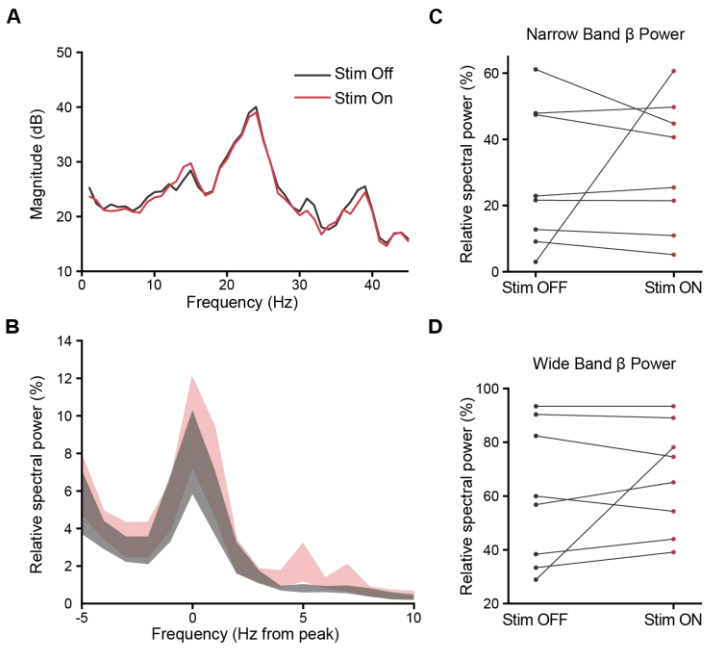


Figure 2.5. Beta frequency stimulation does not modulate overall beta activity across patients. A) In an example subject, the spectral activity did not change significantly with beta frequency stimulation (red) compared to stimulation off (black). **B)** Average ± S.E.M power spectra aligned to the peak beta frequency across eight patients. A prominent beta peak was seen in spontaneous local field potential recordings (black) as well as during beta frequency stimulation (red). **C)** There was no significant difference in peak beta power (peak beta frequency ± 3 Hz) relative to 5-45 Hz with stimulation (red) ($p = 0.6665$, Wilcoxon ranked sum test). **D)** There was no significant difference in total wide band beta frequency power (8-35 Hz) relative to 5-45 Hz with stimulation ($p = 0.4894$, Wilcoxon ranked sum test).

2.4.4. Recovery of action potentials and firing rate changes of the STN neurons

The dataset presented here was exceptional in a sense that often single units could be delineated from the electrical signal recorded by the 'micro' tip, regardless of the proximity of the corruptive stimulating site. **Fig 2.6** shows two raw traces to demonstrate the difference between single and multiunits. The spike sorting was done in a semi-supervised way (details in the methods/ footnote). The main distinction between a single and a multi unit was that the former displayed a waveform that was stable in shape and amplitude over time, and sometimes the modulation could be seen on a trial-by-trial basis (**Fig 2.6 A**). On the other hand, the shape form versatility in recordings that were labelled as 'multi units' were probably the result of recording the activity of many neurons simultaneously (**Fig 2.6 B**). This was often the case, as the STN is a densely packed structure (Oorschot, 2010). Sometimes, a unit appeared to be 'single', but due to the cardiovascular/ respiratory or other movement related artefacts, it was not possible to employ reliable sorting. In those cases, the unit was labelled as 'multi unit'.

Additionally, beta frequency stimulation did not consistently alter the firing rate of the STN single or multi units (**Fig. 2.7 E** and **F**, $p = 0.9534$, Wilcoxon ranked sum test) with respect to the unstimulated baseline. This finding was consistent with all stimulation intensities used in this study ranging from 0.25 mA to 1.5 mA (**Fig. 2.7 A to B**). The lack of modulation demonstrates that beta frequency stimulation did not lead to consistent changes to firing rates of STN neurons over the entire recording period.

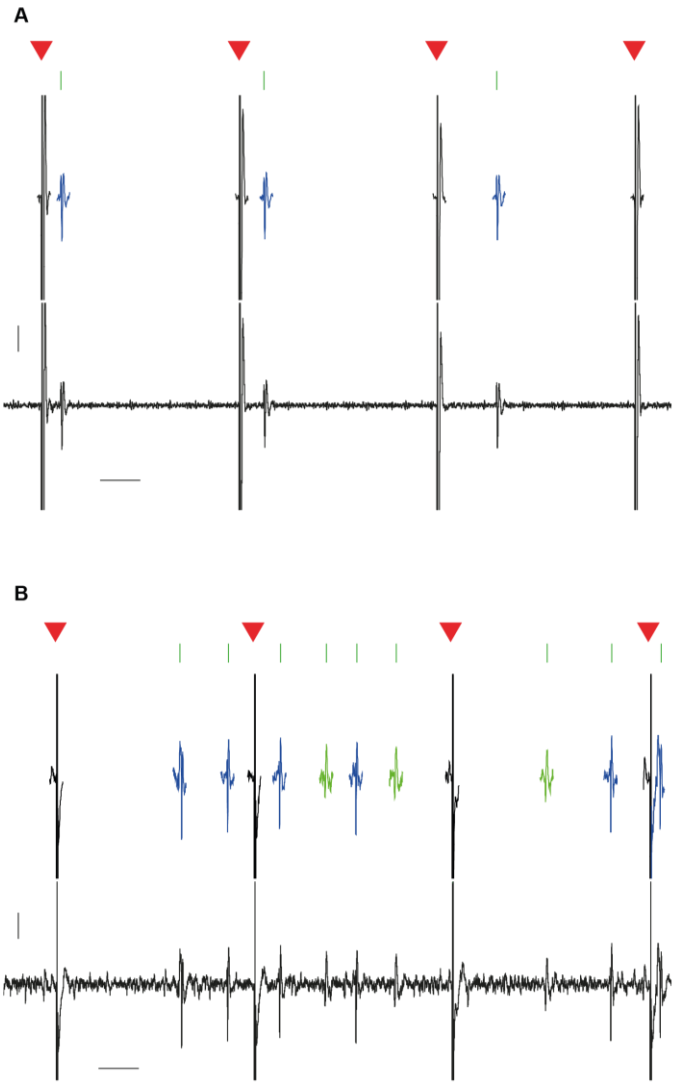


Figure 2.6. Short latency spikes trains of single- and multi-units could be isolated during continuous 20 Hz stimulation. Representative examples of raw unit data during consecutive electrical stimuli a raw STN spiking traces to illustrate the difference between single unit **(A)** and multi-unit **(B)** recording (scale bars: 0.005 mA (A) and 0.002 mA (B) and 0.01 s respectively, black: raw trace; red arrow: stimulation; green and blue waveforms: template-matched spikes, green line: detected spike).

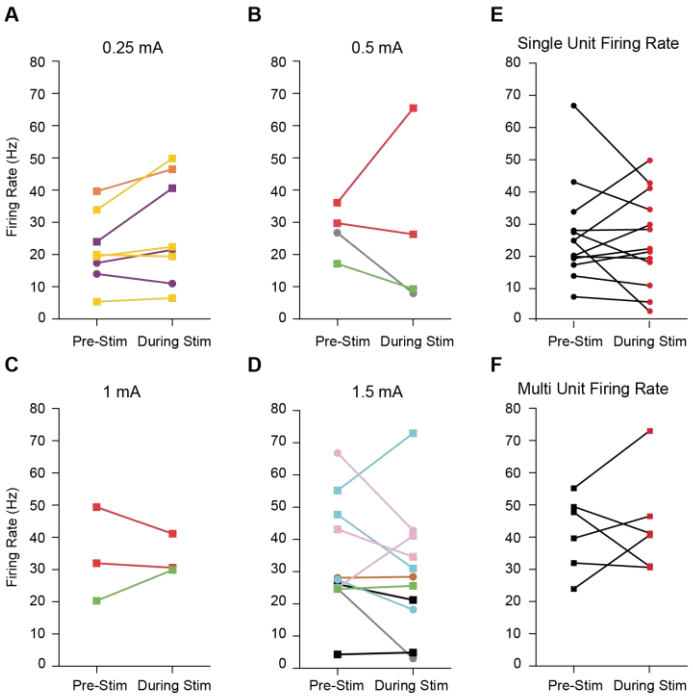


Figure 2.7. Firing rate of putative STN single- and multi-units was not altered by the 20 Hz stimulation regardless of the stimulation intensities used. (A) - **(D)** There was no significant difference in the firing rate of single and multi-units (circles indicate cells classified as single units, squares multi-units.) across patients (same colour line indicate recordings from the same patient) on different stimulation intensities compared to the pre-stimulus baseline. **(E) – (F)** There was no significant difference in firing rates of putative subthalamic units ($p = 0.9534$, Wilcoxon ranked sum test). Circles indicate cells classified as single units, squares multi-units.

2.4.5. Beta frequency stimulation is effective in modulating the spiking pattern of the STN activity.

In order to demonstrate how the phase of the stimulation affects the amplitude of the STN LFP beta oscillations by using a more refined analytical approach in the next chapter, it is essential to establish that using sub-therapeutic stimulation intensities have a physiological effect on signals related to the STN LFP. While STN neurons where not modulated on the timescale of seconds, demonstrating stimulation evoked effects on the spiking pattern regardless of the unchanged rate would imply that the modulatory effect is not due to an artefact introduced by the stimulation.

In line with previous work, we found that stimulation could lead to short-latency excitation (**Fig. 2.8 F**) or inhibition of spiking (**Fig. 2.8 A, E, I**), often followed by further multiphasic responses (**Fig. 2.8 C, G**). Furthermore, with some of the patients we were able to run the 20 Hz protocol and to record the same unit long enough to test the effect of different stimulation intensities. **Fig. 2.9** shows that in case of two STN units, the magnitude and shape of the multiphasic responses could be amplitude dependent. In the case of **Fig. 2.9 A**, the pattern of the evoked response remained similar, while the firing rate increased with higher stimulation intensity. In case of cell B on the same figure, however, the pattern of the evoked response only became apparent when the amplitude of the stimulation was high enough (1-1.5 mA). The diversity in the amplitude-dependent responses was likely due to the variability in the position of the recording electrode and the stimulation site.

As **Fig. 2.10** shows, however, there was no clear consistency based on stimulation/recording location. This figure illustrates that when keeping the same amplitude within a single patient (row A and B represents two subjects), different response patterns can be recorded as the electrode is being lowered (histograms are showing a more ventral stimulating location left to right). Lower stimulating and recording position results in a more

specific multiphasic response in Patient 4 (**Fig. 2.10.** row **A**), whereas in Patient 6 (**Fig 2.10** row **B**), the short latency spiking response that is evoked by 1.5 mA can only be observed at the first, most rostral stimulation depth. These results demonstrate that the stimulation protocol employed could alter the spike timing of individual STN neurons within individual stimulation cycles, without significantly changing in firing rate with respect to baseline.

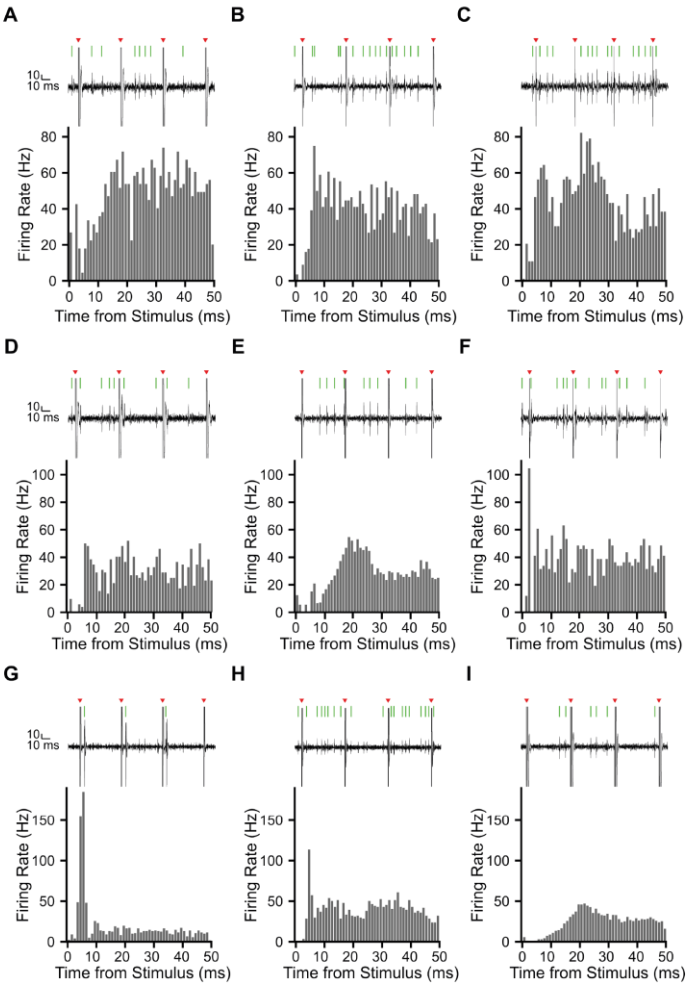


Figure 2.8. Beta frequency stimulation delivered dorsal to the subthalamic nucleus (STN) modulates STN unit activity. Peristimulus time histograms (PSTH), using 1 ms width bins, from nine example STN units (single or multi-units) across seven patients. Beta frequency stimulation was applied at 0.25 mA **(A-C)**, 1 mA **(D-F)**, and 1.5 mA **(G-I)**. Spikes were detected from microelectrode recordings in the STN; representative examples of raw unit data during 3 consecutive electrical stimuli are shown above each PSTH (black: raw trace; red arrow: stimulation; green line: detected spike). **(A-C)** 0.25 mA stimulation was delivered 0.23 mm **(A)**, 3.00 mm **(B)**, and 1.08 mm **(C)** dorsal to the STN. **(D-F)** 1 mA stimulation was delivered 2.17 mm **(D)**, 1.99 mm **(E)**, and 0.84 mm **(F)** dorsal to the STN. **(G-I)** 1.5 mA stimulation was delivered 3.00 mm **(G)**, 0.07 mm **(H)**, and 1.99 mm **(I)** dorsal to the STN. The recording electrode was fixed 3 mm below stimulation contacts.

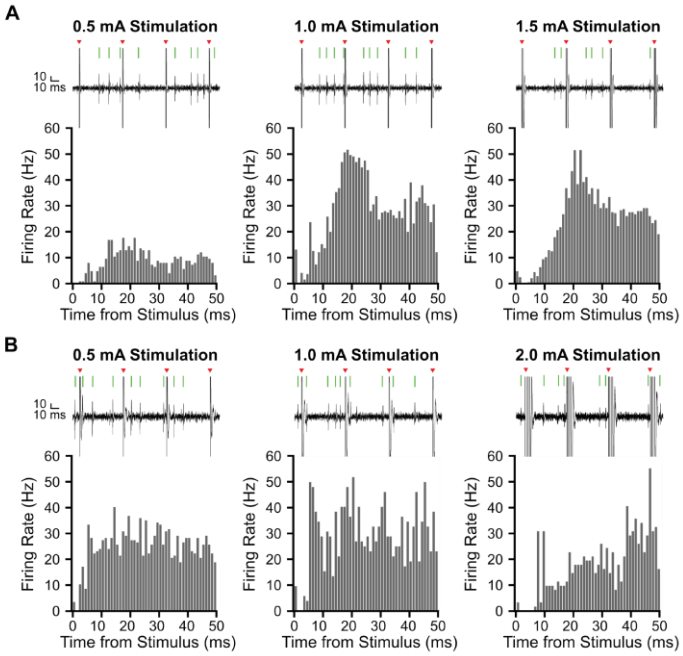


Figure 2.9. Modulation of subthalamic units by low amplitude beta frequency stimulation delivered dorsal to the STN can be amplitude dependent. Peristimulus time histograms (PSTH) (1 ms wide bins) from two example units in response to three different stimulus amplitudes. Bipolar, biphasic stimulation was delivered dorsal to the STN. Spikes were detected from microelectrode recordings shown above each PSTH (black: raw trace; red arrow: stimulation; green line: detected spike). **A)** 0.5, 1, and 1.5 mA stimulation was delivered 1.99 mm dorsal to the STN border in subject 7. **B)** 0.5, 1, and 2 mA stimulation was delivered 1.36 mm dorsal to the STN border in subject 1.

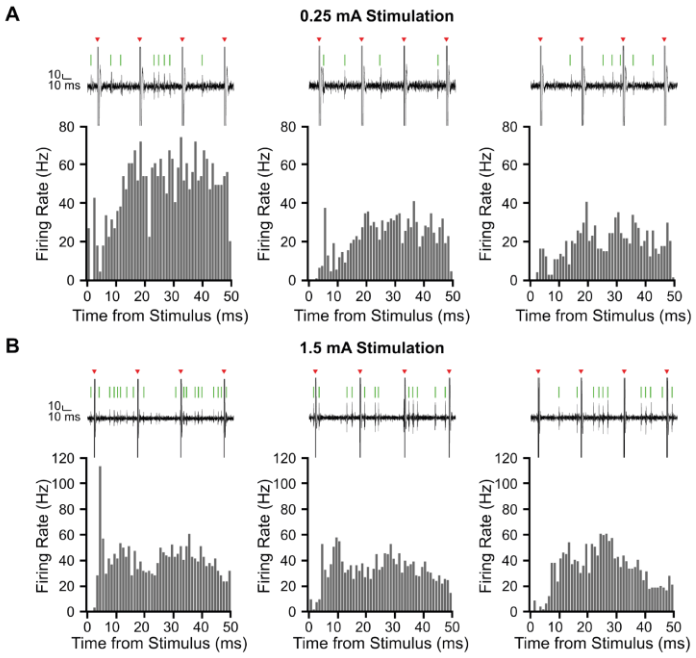


Figure 2.10. Modulation of subthalamic unit activity is seen at different stimulation/recording locations within the same subject. In two patients, peristimulus time histograms (PSTH) (1 ms bins) are shown from three stimulation/recording locations (stimulation fixed at 3 mm above recording location). 20 Hz bipolar stimulation was delivered dorsal to the STN. Spikes were detected from microelectrode recordings shown above each PSTH (black: raw trace; red arrow: stimulation; green line: detected spike). **A)** PSTHs for three STN units recorded from subject 4 during 0.25 mA stimulation. Relative to the dorsal STN border, stimulation/recording locations were: left) recording 2.77 mm ventral, stimulation 0.23 dorsal; middle) recording 2.27 mm ventral, stimulation 0.73 mm dorsal; right) recording 1.78 mm ventral, stimulation 1.22 mm dorsal. **B)** PSTHs for three STN units recorded from subject 6 during 1.5 mA stimulation. Relative to the dorsal STN border, stimulation/recording locations were: left) recording 1.39 mm ventral, stimulation 1.61 dorsal; middle) recording 1.15 mm, stimulation 1.85 mm dorsal; right) recording 0.33 mm ventral, stimulation 2.67 mm dorsal.

2.4.6. Beta frequency stimulation is effective in modulating the activity of the cortex

To evaluate the success of low-intensity stimulation on modulating the activity of the the extended network, we investigated consistent changes in the cortical activity. Using coincidental EEG recordings, we examined whether sub-threshold stimulation intensities can facilitate cortical motor evoked potentials (cMEP). In line with previous work (Ashby et al., 2001a; Eusebio et al., 2008), stimulation pulses led to evoked potentials in all midline EEG channels. Similar to Walker (2011), identifying the first, non-variable peak in our evoked signals was deployed to prove that low amplitude stimulation is similarly efficient in modulating structures other than STN (**Fig. 2.11**). The evoked potential waveforms on all central channels (Fz, Cz, Pz) appears to follow a similar waveform to what has previously been reported. The first peak (~10 ms, presumably 'antidromic' component) is especially pronounced on the Fz channel (**Fig. 2.11**). The multiphasic evoked response structure can be observed on the other two channels, but it reduces in magnitude from ventral to dorsal. Our complimentary findings to previous reports demonstrated that the low intensity stimulation parameters used here could modulate cortical activity.

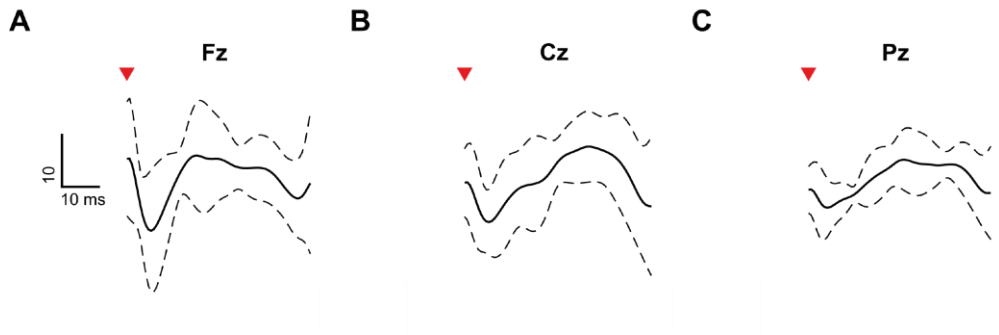


Figure 2.11. Cortical Motor Evoked Potentials recorded over the Midline EEG Channels Show the Effectiveness of Low Amplitude Stimulation in PD Patients. (A-C) Average (± standard deviation) cortical evoked responses from frontal/midline EEG (Fz, Cz, and Pz) locations) across eight patients for Fz and seven patients for Cz and Pz. EEG signals were bandpass filtered 1 – 100 Hz to remove any slow drift, and notch filtered 49 – 51 Hz to remove line noise.

2.5. Discussion

2.5.1. Stimulation does not impose adverse effect or induce gross changes in the network state or the local activity of the STN

This chapter demonstrates that an intraoperative setup can be utilised to investigate the relationship between the stimulation phase and the amplitude of the ongoing beta oscillation in awake Parkinson's disease patients undergoing DBS surgery. We aimed to study this relationship by delivering electrical current dorsal to the border of the STN. This arrangement allowed us to subtly modulate STN activity and its cortical outputs and to record with less pronounced artefacts (Godinho et al., 2006; Hamel et al., 2003; Benazzouz et al., 2004). Regardless of not applying current to the STN directly, the setup was initially not suitable for such experiments because the electrical artefact of the monopolar monophasic, relatively fast stimulation was overshadowing the signals. Similar to the study by O'suilleabhain et al. (2003), we found that implementing bipolar, biphasic stimulation and using stimulation intensities approximately ~25% of the therapeutic average enabled us to recover LFP signals and spiking activity. To perform refined phase analysis, we had to ensure that the remaining artefact is removed with a method that is flexible, but preserves the spectral and time-domain features of the original non-stationary signal. The Kalman filter approach provided a suitable solution to remove the stimulation artefact without biasing the properties of the local field potential. This was further confirmed by showing that the stimulation did not alter the average –wide and narrow band– peak of the ongoing beta oscillation. This provided evidence that following signal processing, the potential artefacts caused by large spectral peaks introduced by the electrical stimulation in the matched spectral range to the ongoing oscillation were not corrupting the signal significantly. In addition, this finding suggests that beta frequency stimulation, at least using these parameters, does not cause gross amplitude change in the scale of the entire recording,

Thus, if there is a modulatory effect, it might only be captured on a different timescale. The fact that beta stimulation did not evoke a gross change in the spectral domain also had to be addressed in light of studies showing its potential adverse effect on motor performance, especially regarding slowness of movement (Timmermann et al., 2004;Fogelson et al., 2005,Chen et al., 2007; Eusebio et al., 2008). Patients in our study did not report that beta frequency had any adverse effect, although detailed monitoring of motor performance would have been needed to verify this.

2.5.2.Stimulation is effective in modulating the local activity of the STN and its outputs

Any external stimulation of the brain, including high-frequency DBS, is expected to affect multiple neuronal elements in the vicinity of the stimulating electrode (McIntyre et al., 2004). While the novel stimulation set-up used in this study better allowed us to recover and analyse the underlying beta oscillation, the electrical current spread was likely different from conventional DBS. Due to the dorsal stimulating position together with the horizontal orientation of the electric field (as opposed to the vertical orientation with conventional DBS electrodes), current was potentially delivered to multiple neuronal populations and fiber tracts (internal capsule, zona incerta, and fields of Forel) containing excitatory cortico-subthalamic and inhibitory pallido-subthalamic axons (Hamani et al., 2004). The choice for this placement is in line with studies that found that stimulating the fiber tracts around the STN is does not only result in similar clinical effects, but also require lower stimulus intensities displaying potentially better benefit/energy ratio (Voges et al., 2002). This is especially true for alleviating symptoms that correlate with the amplitude of beta oscillation, such as rigidity (Hamel et al., 2003). Stimulation of these elements could lead to both orthodromic effects in the STN (and other targets) and antidromic effects at the source of the afferent fibers. Current may also have spread to the STN itself, but given the bipolar

configuration it was likely more concentrated in these dorsal areas. Thus, as with therapeutic DBS, modulation of STN activity in our configuration likely occurred through a variety of direct and indirect mechanisms that cannot be fully delineated.

On the other hand, using low stimulus intensities meant further evidence was necessary that the stimulation elicits a physiologically tangible effect. For this purpose, single neurons recorded with the same tips as the LFPs provided an excellent signal for testing that such an effect occurred. Even if the setup is not ideal for collecting a vast amount of single unit data, the high quality of the raw recordings allowed for reliable spike sorting and the possibility for the calculation of single-cell PSTHs. Regardless of having no consistent change in firing rate or pattern across the recorded subthalamic neurons, a modulation by sub-therapeutic amplitude stimulation in all recorded STN units could be obtained. The combination of different up- and downstream effects was the likely the cause of the variance in the multiphasic responses that the stimulation evoked in STN spiking activity, including both short latency (<10ms) excitation and inhibition. Such multiphasic responses are likely to result from a combination of excitatory and inhibitory afferents, and the integration of these inputs with the pacemaker currents that drive the spontaneous firing of STN neurons (Nambu et al., 2000;Magill et al., 2004a). These different types of evoked responses were mirrored by the variability in firing rate during the stimulation, in comparison to pre-stimulation period. Overall, while neuronal activity in the STN was markedly influenced by the stimulation, it did not show a consistent modulation of the recorded sample.

Here I also report that 20 Hz stimulation of the dorsal STN borders modulates the cortex at short and medium latencies. Cortical motor evoked potentials have similar shape to what has been documented before using electrical and transcranial magnetic stimulation (Ashby et al., 2001a; Hanajima et al., 2004; Kuriakose et al., 2010). Eusebio et al. (2009), for instance found that 14-22 ms (medium) peak latency evoked potentials are especially

enhanced following 20 Hz stimulation compared to higher or lower stimulation frequencies, and hypothesised that this is due to replaying the resonance frequency of the diseased cortico-subthalamic circuit. This comparison was utilised to test whether our stimulation setup has not only local but long-range network level modulation using considerably lower stimulation intensities. The short latency response is presumably due to the activation of the large myelinated axons of the zona incerta, which is the putative stimulation location for most of the analysed electrode locations (Ashby et al., 2001a). Even if the arrangement of the stimulation used was bipolar, hence more focal than a monopolar, it cannot be excluded that the STN was activated by the spread of the electrical current, causing antidromic activation of the motor cortex (via the hyperdirect pathway, Ashby et al., 2001a; Li et al., 2012), and ortodromic recruitment of the basal ganglia via the GP (subthalamic-pallidal-thalamo-cortical pathway, MacKinnon et al., 2005;Tisch et al., 2008). Nevertheless, the MEP data shows that the stimulation setup was sufficient to evoke network-level modulation.

To summarise, this chapter demonstrated the plausibility of modulatory but not overtly drive of the STN output and the cortex by beta frequency stimulation in awake human patients undergoing DBS surgery.

Chapter III Phase-dependent suppression of beta oscillations in Parkinson's disease patients

3.1. Introduction

The previous chapter has shown an effective method to retain information in the phase and spectral domains in the beta range from electrophysiological recordings of the cortico-subthalamic network of Parkinson's disease patients during concurrent stimulation at the same frequency. This chapter demonstrates the analysis of the dataset obtained with this experimental paradigm, focusing on how the phase relationship between the local field potential (LFP) beta oscillation and the continuous stimulation can be exploited to determine whether -in principal - phase-dependent DBS could be harnessed to modulate the amplitude of pathological activity in the STN and its outputs.

3.1.1. Role of pathological oscillation in Parkinson's disease

Here I briefly recapitulate the main thoughts introduced in the first chapter regarding the role of oscillations. Neural oscillations play a fundamental role in normal brain processing by temporally coordinating activity within and across regions (Engel et al., 2001; Buzsaki & Draguhn, 2004). Dysfunctional communication resulting from an inability to properly modulate oscillatory activity, either through hypo- or hypersynchrony, has been implicated in a number of neurological disorders (Schnitzler & Gross, 2005;Uhlhaas & Singer, 2006). In Parkinson's disease, exaggerated oscillations in the beta frequency range (12-35 Hz) are thought to be mechanistically involved in symptoms by distorting communication between brain areas needed for initiation of voluntary movement (Brown, 2007;Engel & Fries, 2010;Dorval & Grill, 2014). Beta oscillations detected in basal ganglia unit activity and LFP correlate with severity of akinetic/rigid symptoms (Sharott et al., 2014b;Neumann et al.,

2016), and importantly, magnitude reduction following pharmacological or stimulation treatment positively correlates with motor improvement (Kühn et al., 2006; Kühn et al., 2009; Ray et al., 2008).

3.1.2. Deep Brain Stimulation as an efficient but suboptimal therapeutic option

High frequency (≥ 130 Hz) deep brain stimulation (DBS) is an established treatment for Parkinson's disease, but is limited by stimulation-induced side effects (Hariz et al., 2008;Tripoliti et al., 2011;Castrioto et al., 2014) and partial efficacy (Little & Brown, 2012). While therapeutic DBS decreases exaggerated beta oscillations, it does not achieve complete suppression as is seen with dopaminergic medication (Giannicola et al., 2012). One approach to more effectively control symptoms using less electrical current is to target exaggerated beta oscillations by triggering high frequency stimulation only during periods of high amplitude (Little et al., 2013). However, applying bursts of high frequency stimulation could still disrupt physiological activity at timescales relevant for coding of movement in the STN (Amirnovin et al., 2004;Rodriguez-Oroz et al., 2005;Schrock et al., 2009; Lipski et al., 2017; Sharott et al., 2018c). To further advance DBS, it may be necessary to account for the temporal dynamics of the underlying pathophysiology (Montgomery Jr et al., 2000) to more precisely control the timing of stimulation.

3.1.3. Phase dependent approaches to stimulation

Closed-loop stimulation, where electrical impulses are delivered on-demand has been the subject of great interest in translational neuroscience (Meidahl et al., 2017). The potential for a tailored stimulation protocol, leading to a wider therapeutic window has driven investigators to infer a suitable peripheral or central signal that can be used as a biomarker for the dysfunction, and serve as a feedback signal to time stimulation. Triggering a closed

loop system off a central biomarker has been exploited before for translational purposes as well as to probe the function of oscillations. Berényi et al. (2012) showed the advantage of tracking seizures and applying on-demand transcranial magnetic stimulation in a generalized rodent model of epilepsy. In-phase auditory stimulation aligned to slow oscillations is shown to enhance spindle activity and memory consolidation (Ngo et al., 2013). High frequency adaptive DBS for Parkinson's disease, when the stimulator is only switched on in case the power of the ongoing beta oscillation surpasses a threshold, has been shown to be just as effective as conventional continuous DBS (Little et al., 2013). Thus far, adjusting the precise timing of stimulation has not been considered for closed loop algorithms targeting LFP beta oscillations in Parkinson's disease.

A phase-dependent approach, where stimulation is timed to a certain phase of the ongoing oscillation, has the potential to more selectively dampen the beta activity. A proof-of-principle study on non-human primates has suggested that applying a burst of stimulation to the GPi based on the activity of the motor cortex can alleviate symptoms (Rosin et al., 2011). This study can be regarded as the first to provide evidence for phase-related effects: in case of a stable beta oscillation (~12.5 Hz in primates), the constant 80 ms lag between the M1 activity and the GPi stimulation presumably 'canceled' the next double-frequency tremor burst in the GPi. This is further supported by the fact that shorter intervals did not achieve similar efficacy. The utility of patterning the stimulation can be seen in essential tremor patients, where symptoms are suppressed with thalamic stimulation locked to a specific phase of the tremor (Cagnan et al., 2017). Brittain et al. (2013) showed that phase cancellation using the tremor measured using the accelerometer as the biomarker, in PD tremor patients is a powerful method for adjusting stimulation parameters. Phase cancellation was achieved by delivering anti-phase alternating current stimulation to cortex in order to cancel the ongoing exaggerated peripheral activity. This method could attenuate

tremor by ~50%, which supports the importance of taking time in consideration when adjusting stimulation parameters. Cagnan et al. (2013a) and (2017) showed the utility of such approach in a series of studies on essential tremor patients. Using the assumption that DBS can be locked to the peripheral tremor with fixed time-lags, these studies provide evidence for the existence of an optimal phase alignment between the peripheral oscillation and stimulation that can achieve tremor suppression up to 87 % in some patients.

For akinesia and rigidity, where no peripheral oscillation provides a marker of symptom severity, many groups have proposed stimulation phase locked to the beta oscillation in the LFP (Rosin et al., 2011; Meidahl et al., 2017; Azodi-Avval & Gharabaghi, 2015; Holt et al., 2016). Conversely, there is a lack of experimental evidence supporting this approach for LFP beta oscillation is likely due to significant challenges that arise when using the centrally recorded oscillation, including 1) the beta oscillation is more transient and faster than tremor or slow oscillations (Tinkhauser et al., 2017a), and 2) simultaneously delivering stimulation and recording in the same location make it difficult to recover the phase without significant corruption by stimulus artifact (Carlson et al., 2010).

3.1.4. Electrophysiological Output Measures of Phase-Dependent Modulation

In this chapter we interrogate the network-level mechanisms of the phase dependent harnessing of beta oscillations. For this purpose, we aimed to investigate the modulatory effect of the stimulation phase not only on the amplitude of the local field potential, but also on local and network level oscillatory outputs of the STN.

As it has been stated in the Introduction, the background unit activity (BUA) represents the activity of a population of neurons around the recording contact, distinct from single and multiunit activity (Moran & Bar-Gad, 2010). The BUA is a useful metric to measure the

direct oscillatory output of a given structure, presumably reflecting the synchronous activity of a local neuronal ensemble surrounding the recording electrode (Moran et al., 2008b). The background unit activity resembles the local field potential being a continuous and spike-free signal that is suitable for spectral analysis, while representing a functionally distinct activity pattern to the LFP. The LFP is known to reflect the summation of sub-threshold membrane potential fluctuations of a larger neuronal group or structure, and hence it is more likely to be indicative of the 'inputs' to the recorded a structure (Mitzdorf, 1985;Buzsaki & Draguhn, 2004; Logothetis, 2002; Moran et al., 2008a). As opposed to the LFP, the high-pass filtered BUA signal presumably reflects the extracellular spiking activity of a small neuronal group (approx.. 100-micron radius from the recording contact within the STN, ~10 neurons, Moran et al., 2008), hence representing the immediate 'output' measure close to the recording contact. In PD patients and parkinsonian primates, BUA activity is coherent and phase locked to (low) beta band oscillatory activity (8-20 Hz) of individual STN neurons and multi units, and coherently locked to the LFP, with a phase shift representing an ~25 ms time lag (Moran & Bar-Gad, 2010; Moran et al., 2008a). These studies underline that BUA is an independent, but relevant measure of local oscillatory output activity of the STN.

In terms of global network connections, modulation of oscillatory connections with the cortex by STN stimulation is well documented in the literature (Ashby et al., 2001a; Baker et al., 2002; Walker et al., 2012;Hanajima et al., 2004;Kuriakose et al., 2010;). Several studies have demonstrated that beta oscillations in STN are possibly driven by the motor/premotor cortex (Fogelson et al., 2006; Shimamoto et al., 2013; Williams et al., 2002). In parkinsonian animals and PD patients, the coherence measured between the motor cortex and the STN is known to be exaggerated in beta band, and this synchronization is correlated with the severity of akinetic/rigid symptoms (Sharott et al., 2018a). It has also been shown that high frequency stimulation reduces the heightened beta-band synchrony between the

STN and motor cortex (Kühn et al., 2008). As detailed in the previous chapter, STN stimulation induced cortical evoked potentials (cEPs) are well studied in PD patients and parkinsonian animals (Ashby et al., 2001a; Magill et al., 2004a). Additionally to simple measures addressing the entraining effect of stimulation such as cEP, the time-domain impact of stimulation between oscillatory nodes of the cortico-basal ganglia loop can be captured by the phase synchrony index (PSI, Stam et al., 2007b). The PSI is a well-established measurement of functional connectivity in the spectral domain and known to reflect the time-dependent phase difference between oscillators, which can be used to assess the phase entrainment of a signal by another (Mehta et al., 2014). Cagnan et al. (2015) showed that PSI is an useful measure to assess the beta amplification-favoring phase relations between interconnected nodes of the basal ganglia (STN and GPi), and can be utilized to interrogate the effect of such time-domain interactions on the amplitude of ongoing oscillations.

3.2. Aims

Based on a novel stimulation strategy described in Chapter II, the overarching aim of this chapter was to examine whether the phase at which electrical stimulation was delivered relative to the underlying beta oscillation could produce short-latency effects on the amplitude of pathophysiological activity in the STN.

Specific objectives included examining whether the beta oscillation amplitude was modulated depending on coincident alignment of stimulation pulses to the oscillation. Additionally, this chapter probes what parameters of the beta phase at which stimuli arrive influence this modulation (phase specificity, stimulation intensity). Lastly, it is also explored whether modulating of the STN LFP extends to STN spiking output as well as to the wider network (i.e. cortex).

3.3. Methods

3.3.1. Acquiring signals for analysis

As outlined in the previous chapter, STN LFP beta oscillation was recorded from the microelectrode contact was not used for bipolar stimulation. Recordings were referenced to the uninsulated distal most part of the guide tube for that microelectrode (contact size of this macrotip ~1 mm, impedance <1 kΩ), located 3 mm above the microtip. LFPs were band pass filtered between 0.00070 and 0.4 kHz and sampled at 1.375 kHz. In order to retain the spectral properties of the signal, an off-line artefact removal approach was used (see the detailed description of Kalman filter in Chapter II).

Midline EEG signals were band pass filtered between 0.001 kHz and 0.1 kHz to remove the contribution of slow drifts and high frequency activity, and notch filtered between 0.049 and 0.051 kHz, to remove line noise (EEG-related methods are in the previous Chapter, too).

Microelectrode channel recordings were used for the calculation of Background Unit Activity (BUA). The raw signal based on which BUA was calculated was acquired by bandpass filtering between 0.6 and 6 kHz, amplified (×20,000), and sampled at 44 kHz, while LFPs were bandpass filtered between 0.00070 and 0.4 kHz and sampled at 1.375 kHz. Recordings were referenced to the uninsulated distal most part of the guide tube for that microelectrode (contact size of this macrotip ~1 mm, impedance <1 kΩ), located 3 mm above the microtip.

3.3.2. Stimulation protocol

The previous chapter has outlined that the stimulation parameters were fine-tuned to serve the dual purpose of being modulatory and allowing for the recovery of the spectral properties of the ongoing STN LFP beta oscillation. Bipolar, biphasic, stimulation pulses (total pulse

width: 200 µsec, 100 µsec initial phase negative, 100 µsec positive phase, amplitude: 0.25 – 2 mA, constant current, stimulation time: 15-115 seconds, as permitted) were delivered through the macroelectrode contacts of two electrodes immediately dorsal to the STN while the microelectrode recording contact was recording LFP within the STN.

Stimulation was applied at or near the peak beta frequency (beta frequency stimulation) to determine effects of stimulation timing on beta oscillation amplitude. When well matched, stimulus pulses occurred at the same phase of the oscillation for at least two consecutive cycles. However, due to the natural variability in frequency and burst-like nature of the oscillation (Feingold et al., 2015a; Tinkhauser et al., 2017a), pulses drifted through different phases of the oscillation over the entire recording (Brittain et al., 2013; Cagnan et al., 2013b). **Fig. 3.1** shows the filtered LFP traces from two different patients. In both patients, the oscillation was waxing-and-waning (fluctuating around it's mean frequency) as the continuous beta frequency stimulation naturally hit various different stages of the cycle, which caused a natural variability in phases the stimuli arrived at. When the oscillation frequency was very closely matched to the stimulation frequency (patient A, 1 Hz difference), the likelihood of the stimulation pulses consecutively arriving in the same phase bin increased. When the frequency of the stimulation was not perfectly matched (patient B, 4 Hz difference), the consistency of this relationship decreased. For this reason, only patients whose peak beta oscillation frequency was within 5 Hz of the stimulation frequency were included in analysis to ensure consecutive cycles of stimulation occurring at the same phase of the beta oscillation occurred.

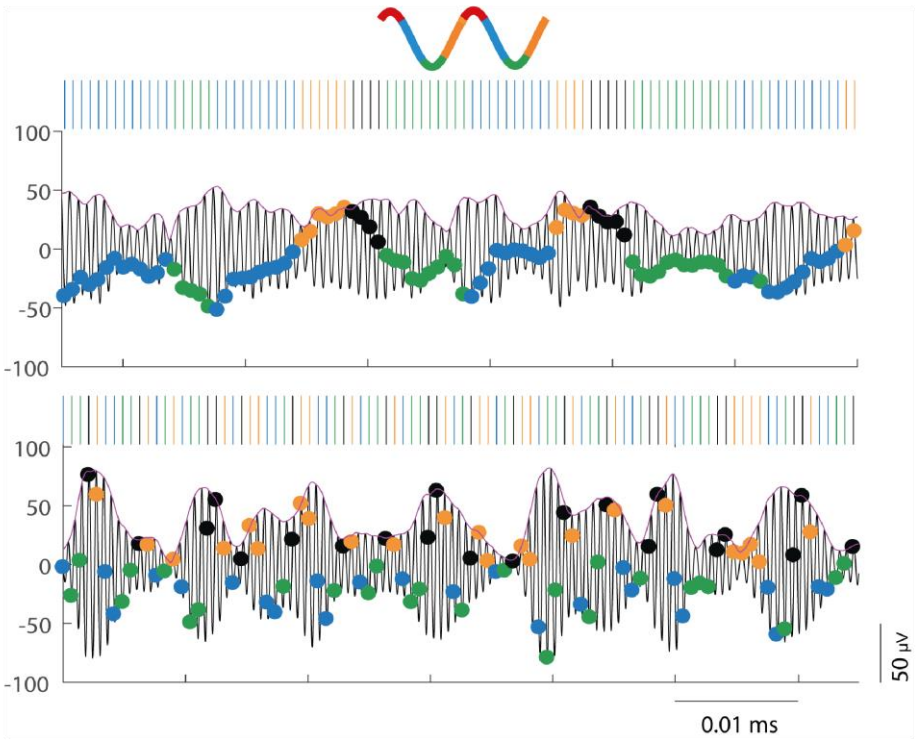


Figure 3.1. Well-Matched Stimulation Frequency Leads to Consecutive Pulses Arriving in the Same Phase Bin of the Ongoing Beta Oscillation. The figure shows STN LFP traces (black line) filtered in beta frequency range, and the corresponding Hilbert amplitude envelope (magenta line). The beta cycle was split into fourth-of-a-cycle wide bins (on the figure: trough- green, ascending-black, peak-yellow, descending: blue). The top row displays a case where the difference between the mean beta frequency (19 Hz) and the stimulation frequency (20 Hz) is minimal (1 Hz). This case naturally facilitates that the stimulation pulses arrive consecutively in the same phase bin with higher probability. The second row shows a patient with larger mismatch (mean beta frequency = 23 Hz, stimulation = 20 Hz, difference = 4 Hz). This figure depicts that less well-matched stimulation frequency causes greater variability in the timing of stimulation pulses, On the other hand, if the stimulation frequency is more tightly matched to the mean frequency of the ongoing oscillation, the probability of stimuli arriving consecutively in same phase bin is higher .

3.3.3. Instantaneous phase and amplitude estimation.

To estimate the phase and amplitude of the beta oscillation, microelectrode LFP signals were first band-pass filtered ±3 Hz around the peak beta frequency using a second order Butterworth filter with zero-phase digital filtering to preserve the true phase of the signal. The Hilbert transform was then used to estimate the instantaneous phase and envelope of the oscillation. Phase is defined as $\varphi(t) = \text{atan}(\frac{v(t)}{H(v(t))})$, where $v(t)$ is the filtered LFP signal and H(v(t))is the Hilbert transform of $v(t)$. The amplitude envelope is defined as $A(t) = \sqrt{(v(t)^2 + H(v(t))^2}$.

3.3.5. Instantaneous effects of stimulus phase.

To assess how stimulus pulses occurring at a certain phase of the beta oscillation affect the amplitude envelope, the phase of the stimulus was divided into eight overlapping phase bins ¼ of a cycle wide (as depicted on **Fig 3.1**). The percentage change in median envelope over the cycle following the stimulus pulse was compared to the median envelope of the entire signal. Surrogate results were generated by sampling an unstimulated portion of data at the stimulation frequency. The Kruskal-Wallis test was use to assess phase dependent effects on beta amplitude in both the surrogate and stimulation conditions. Stimulation effects were compared to surrogates using the Wilcoxon rank-sum test for each phase bin.

3.3.3. Cumulative effects of stimulus phase.

As discussed in the previous chapter and above, stimulating at or near the peak beta frequency results in stimuli occurring at the same phase over consecutive cycles coincidentally. Similar to the analysis of instantaneous effects, eight overlapping phase bins ¼th of a cycle wide were used to evaluate effects of consecutive stimuli occurring at the same phase over multiple cycles on beta amplitude. The percentage change in amplitude envelope

from the median was plotted as a function of the number of consecutive stimuli for each phase bin. As discussed above, phase is not being tracked in real-time, the chances of observing further stimuli occurring within the same phase bin decreased as the number of stimuli increased (i.e. five consecutive stimuli in the same phase bin occurred less often than three). If there were fewer than five occurrences of one, two, three, four, or five consecutive pulses delivered at a specific phase throughout the entire recording, this occurrence was eliminated from analysis. For each patient, suppressing and amplifying bins were defined as the phase bins leading to the maximum suppression (color coded with blue on all figures) and amplification (color coded yellow) of the oscillation envelope respectively. Results for suppressing and amplifying bins were grouped across all eight patients. The Kruskal-Wallis test was used to establish whether there was a significant effect of the number of consecutive pulses on amplitude and the multiple comparison test adjusted by the False Discovery Rate was used to assess the significance of consecutive pulses at the amplifying and suppressing phase bin for each patient as well as across the group. To determine how precision of the defined stimulus phase affected beta amplitude modulation, the width of the amplifying and suppressing phase bins were varied comparing 8^{th} , 4^{th} and half cycle length bins .

3.3.6. Surrogate data.

Cumulative effects were compared to surrogates to ensure significant phase dependent modulation of the beta amplitude is not seen in unstimulated data. Surrogate data was generated by replacing the amplitude envelope during stimulation with a segment from an unstimulated portion of data. Modulation of the unstimulated amplitude was evaluated for the defined suppressing and amplifying phases in each patient to verify that the number of consecutive stimuli seen in each bin does not simply lead to a decrease or increase in beta amplitude. To ensure effects of stimulation were larger than any natural phase dependent variability in the oscillation amplitude, new amplifying and suppressing phase bins were

calculated using the unstimulated envelope (**Fig. 3.2**). Stimulation effects were compared to surrogate effects using the Wilcoxon ranked sum test. Statistics reported in the results section of this chapter are in comparison to the first surrogate, where the defined amplifying and suppressing phase bins were preserved from the stimulated data when substituting an unstimulated portion of the data.

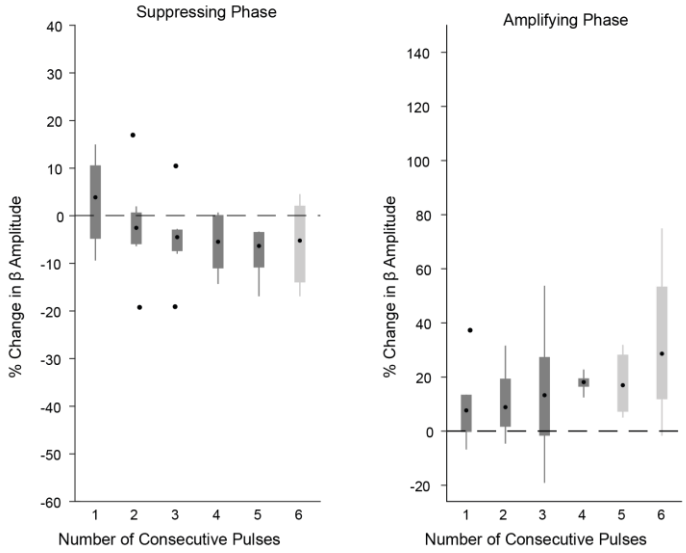


Figure 3.2. Significant Beta Amplitude Modulation is Not Seen Using Alternative Surrogates. The percent change in amplitude from the median is plotted as a function of number of consecutive stimulus pulses. The amplitude envelope from an unstimulated portion of the recording was used to replace the envelope during stimulation. Instead of preserving the amplification and suppression phases (as in **Fig. 3.4**.), new suppression and amplification phases were chosen using the same methods described to select the phases during stimulation. While **Fig. 3.4.** allowed us to determine whether the same number of cumulative pulses lead to suppression or amplification because of the consecutive structure, this control allows us to assess the maximum phase dependent modulation of the beta amplitude seen without stimulation. Neither suppression ($p = 0.3753$) nor amplification ($p = 0.6114$) was dependent on the number of consecutive cycles of stimulation (Kruskal-Wallis test, $p > 0.05$). At the suppressing phase, six consecutive pulses were not seen in five patients, while at the amplifying phase neither five nor six consecutive pulses were seen in five patients (indicated by the lighter grey).

3.3.7. Calculation of the Background Unit Activity

To generate the BUA signal, large amplitude spikes (3 standard deviations above the mean) were removed from the unit microelectrode recording by replacing a window from 1 ms before to 3 ms after each spike with a random 4 ms spike-free segment of the same recording. The signal was then low-pass filtered at 300 Hz (third-order Butterworth, zero-phase digital filtering), rectified, and downsampled to 1.375 kHz (Moran & Bar-Gad, 2010; Moran et al., 2008a; Sharott et al., 2017). The BUA was bandpass filtered and analyzed for cumulative phase dependent effects of stimulation on signal amplitude as described for the LFP.

3.3.8. Phase Synchrony Index

To evaluate the phase relationship between the STN (LFP) and cortex (EEG), instantaneous phase of the EEG signal was determined as described for the LFP (2^{nd} order Butterworth bandpass filter, Hilbert transform). The phase synchrony index (PSI) between the two signals was then calculated over periods of three consecutive stimuli occurring at the suppressing or amplifying phase (Stam et al., 2007a). The PSI is defined as:

$$PSI = \frac{1}{N}\left|\sum_{n=1}^{N} e^{i\Delta\varphi}\right|$$

where N is the length of the segment (3 cycles), and $\Delta\varphi$ is the phase difference between the cortical and LFP signal (calculated using the Circular Statistics toolbox Berens, 2009a). PSI values range from 0 to 1, with 1 representing a constant phase difference between the two signals.

3.4. Results

3.4.1. Phase-dependent modulation of beta amplitude

In the previous chapter it was discussed that beta frequency stimulation did not lead to any observable changes in beta power over the entire recording. On the other hand, single unit activity in the STN and cortical activity was modulated by the low-amplitude stimulation. These findings demonstrate that we were able to obtain non-corrupted oscillatory signals, and on the other hand, imply that if we want to capture the amplitude-modulation that did not occur on the gross scale of the recording, we would have to dissect between the ongoing oscillation and the concurrent stimulation on shorter timescales. Therefore, we investigated whether the specific phase relation between the stimulus pulse and ongoing oscillation could lead to the transient modulation in beta amplitude. When all individual stimuli were used for analysis without accounting for stimulus phase history, there was a significant trend in phase dependent modulation of the beta amplitude (**Fig. 3.3,** $p = 1.88e\text{-}4$, Kruskal-Wallis test). However, modulatory effects were not significantly different from effects seen in an unstimulated portion of the recording sampled at the stimulation frequency ($p > 0.05$, Wilcoxon ranked sum test). This suggests there were no significant phase-dependent effects of single stimuli on the amplitude of the beta oscillation beyond what is seen in the natural variability of the signal.

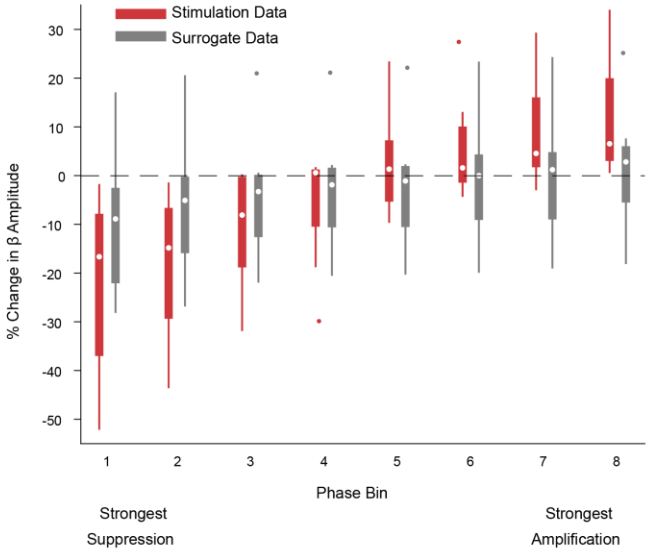


Figure 3.3. Phase Dependent Effects of Single Stimuli on Beta Amplitude Do Not Exceed Variability of the Unstimulated LFP. To evaluate the effects of stimulus phase on beta amplitude, stimulus pulses across the entire recording were grouped into eight overlapping phase bins, $^1/_4{}^{th}$ of a cycle wide. Across eight patients, bins were grouped according to median effect on beta amplitude, with bins leading to maximum suppression grouped together, etc. The percentage change in beta amplitude was dependent on stimulus phase (p = 1.88e-4, Kruskal-Wallis test) during stimulation, but not when sampling an unstimulated time-matched portion of the recording at the stimulation frequency (p = 0.3073, Kruskal-Wallis test). However, modulation from stimulation was not significantly different from that seen using the surrogate for any phase bin (p > 0.05, Wilcoxon ranked sum test). This indicates there were no significant phase dependent effects of stimulation on beta amplitude when stimulus phase history is not considered. Data is shown using a boxplot where the central dot is the median and box edges are the 25th and 75th percentiles. Outliers are plotted individually and defined as outside $q_{75} - w * (q_{75} - q_{25})$ and $q_{25} + w * (q_{75} - q_{25})$, where q_{25} and q_{75} are the 25th and 75th percentiles respectively and w is the maximum whisker length.

We hypothesized the history of past stimulus phases may influence modulatory effects. To address this, epochs where the stimulation phase was consistent within $\pi/4$ radians for multiple cycles were used to evaluate the beta amplitude following each consecutive pulse. In single subjects, 2-3 consecutive pulses at a given phase could either suppress (suppressing phase) or amplify (amplifying phase) the beta amplitude of the following cycle compared to the median (**Fig. 3.4A**). Importantly, similar numbers of consecutive stimuli delivered at alternative phases did not result in a change in the amplitude. The defined phase bins leading to suppression and amplification of the beta oscillation were specific to each individual patient (**Fig. 3.4C**), but the difference between the two were always between 90 and 180 degrees (**Fig. 3.4D**).

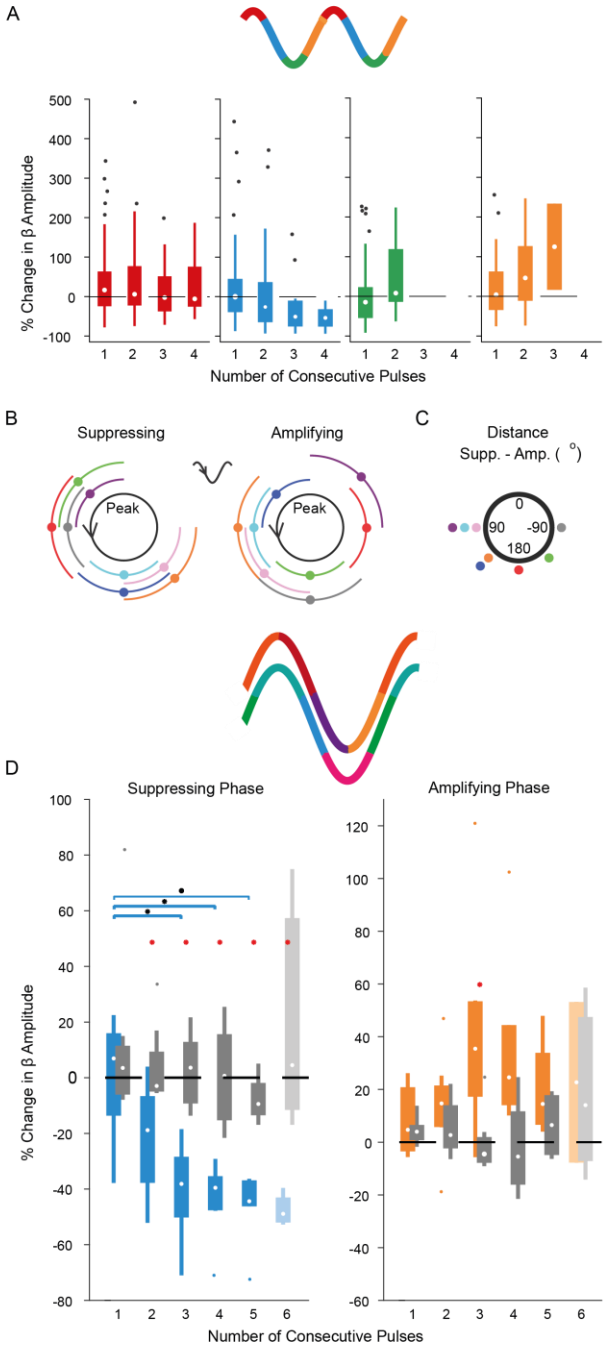

A
% Change in β Amplitude
Number of Consecutive Pulses
B
Suppressing
Amplifying
Peak
Peak
C
Distance
Supp. - Amp. (°)
0
90
-90
180
D
Suppressing Phase
Amplifying Phase
% Change in β Amplitude
Number of Consecutive Pulses

Figure 3.4. Consecutive Phase-Consistent Stimulus Pulses Modulate Beta Oscillation Amplitude. (A) Percentage change in beta oscillation amplitude from the median after consecutive cycles of stimuli occurring at a consistent phase is shown for four phase bins in an example subject. For this example patient, we used non-overlapping, four cycle-wide bins denoted by the four colors on the schematic sine wave. In this subject, amplitude suppression was seen after three consecutive cycles of stimuli delivered on the descending portion of the oscillation (blue), while amplification was seen after three consecutive cycles of stimuli delivered on the ascending phase (yellow). Stimuli delivered at alternative phases (red, green) did not result in suppression or amplification of the beta amplitude. **(B)** Suppressing and amplifying phase bins for each patient. **(C)** Phase difference between the amplifying and suppressing phase bin for each patient. **(D)** Median suppressing (blue) and amplifying (yellow) effects were grouped across eight patients. For the group calculations, four cycle-wide overlapping bins were used (8 bins total per cycle, as depicted by the 2 schematic sine waves on the top of panel **D**) The percentage change in beta amplitude was compared to surrogate effects generated by replacing the amplitude envelope during stimulation with the amplitude from an unstimulated time-matched portion of data (grey). Beta suppression was dependent on the number of consecutive stimuli delivered at the suppressing phase of the oscillation ($p = 0.0016$, Kruskal-Wallis test), while beta amplification was not ($p = 0.1902$, Kruskal-Wallis test). As six consecutive stimuli were only observed in four out of the eight patients at the suppressing phase and two out of eight patients at the amplifying phase (indicated by lighter boxes), these was not included in the Kruskal-Wallis test. Horizontal lines indicate differences between groups (corrected for multiple comparisons using the false discovery rate, $p \leq 0.05$). Red stars indicate stimulation effects significantly different from surrogates ($p \leq 0.05$, Wilcoxon ranked sum test).

Across patients, phase dependent suppression of the beta oscillation was dependent on consecutive cycles of stimulation at the suppressing phase ($p = 0.0016$, Kruskal-Wallis test). The median percentage reduction in beta oscillation magnitude went from 21.8% after two consecutive stimulus pulses to 46.8% after five consecutive pulses. As it becomes increasingly unlikely that consecutive stimuli will arrive in the same phase bin, only four patients had at least 5 occurrences of 6 consecutive stimuli at the suppressing phase. However, in these four patients, 6 consecutive stimuli led to an average 47.5% reduction in amplitude. Importantly, beta amplitude reduction seen after two through six consecutive stimulus pulses at the suppressing phase was significantly beyond what was seen using the amplitude envelope from an unstimulated portion of the recording ($p \leq 0.05$, Wilcoxon rank-sum test). This suggests suppression is not simply the result of measuring amplitude after a certain number of consecutive cycles. Furthermore, a significant suppressive trend was seen at an individual level in five out of eight patients ($p < 0.05$, Kruskal-Wallis test) during stimulation at the suppressing phase, but in no patients when using the unstimulated amplitude envelope, $p > 0.05$, Kruskal-Wallis test). The strength of suppression across patients was correlated with the relative beta power detected from the power spectral density of the entire recordings ($r^2 = 0.504$, $p = 0.049$, linear regression analysis) (**Fig. 3.5**). This suggests that while suppression was still seen in patients with high relative peak beta power, the beta amplitude was more difficult to suppress than in patients with low relative peak beta power (**Fig. 3.5**).

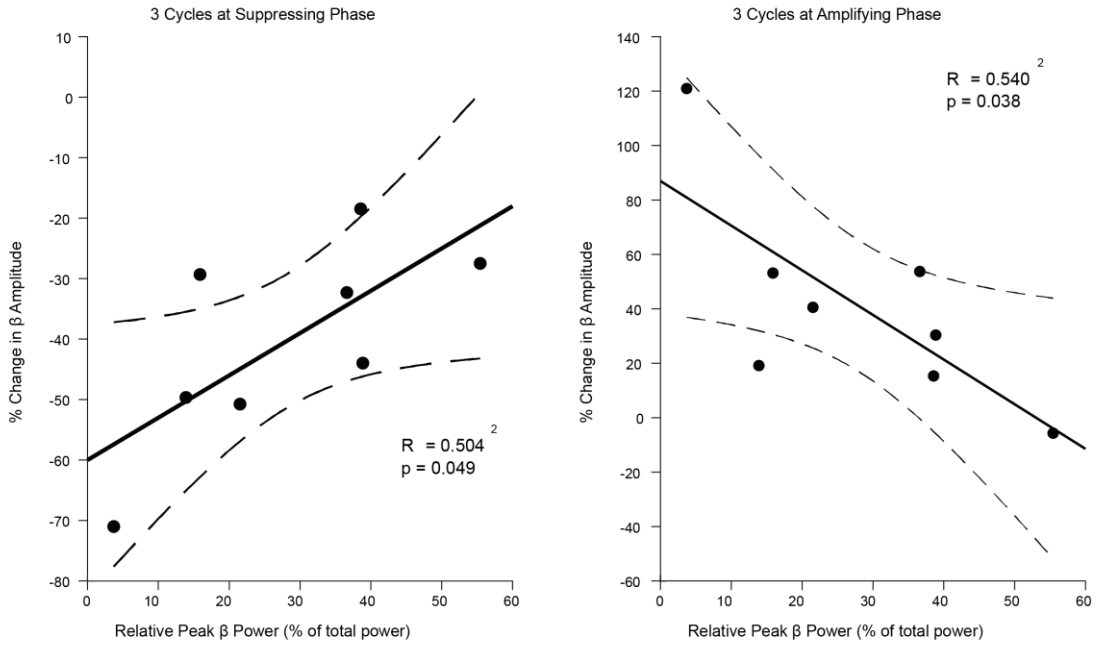


Figure 3.5. Correlation Between the Strength of Beta Amplitude Modulation and the Peak Beta Power. The percent change in beta amplitude after the third cycle of stimulation at the suppressing (left) and amplifying (right) phase is plotted as a function of the relative peak beta power (peak ± 3 Hz). The third stimulus pulse was chosen as this was the maximum suppression and amplification that could be seen in all patients (i.e. not all patients had 4 consecutive cycles of stimulation at the suppressing or amplifying phase). The peak beta power was calculated from the power spectrum of the entire recording (relative to 5 – 45 Hz), as seen in Fig. 2.5. C. Linear regression fit is shown by the black line and the 95% confidence limits are shown with the dashed lines for the suppressing phase ($R^2 = 0.504$, $p = 0.049$) and amplifying phase ($R^2 = 0.540$, $p = 0.038$). This suggests stronger suppression can be seen when beta power is lower, although suppression is still seen in the patients with high beta power. Furthermore, it is easier to amplify the beta amplitude of patients with less beta power, perhaps because it is difficult to further amplify the beta oscillation beyond a certain point.

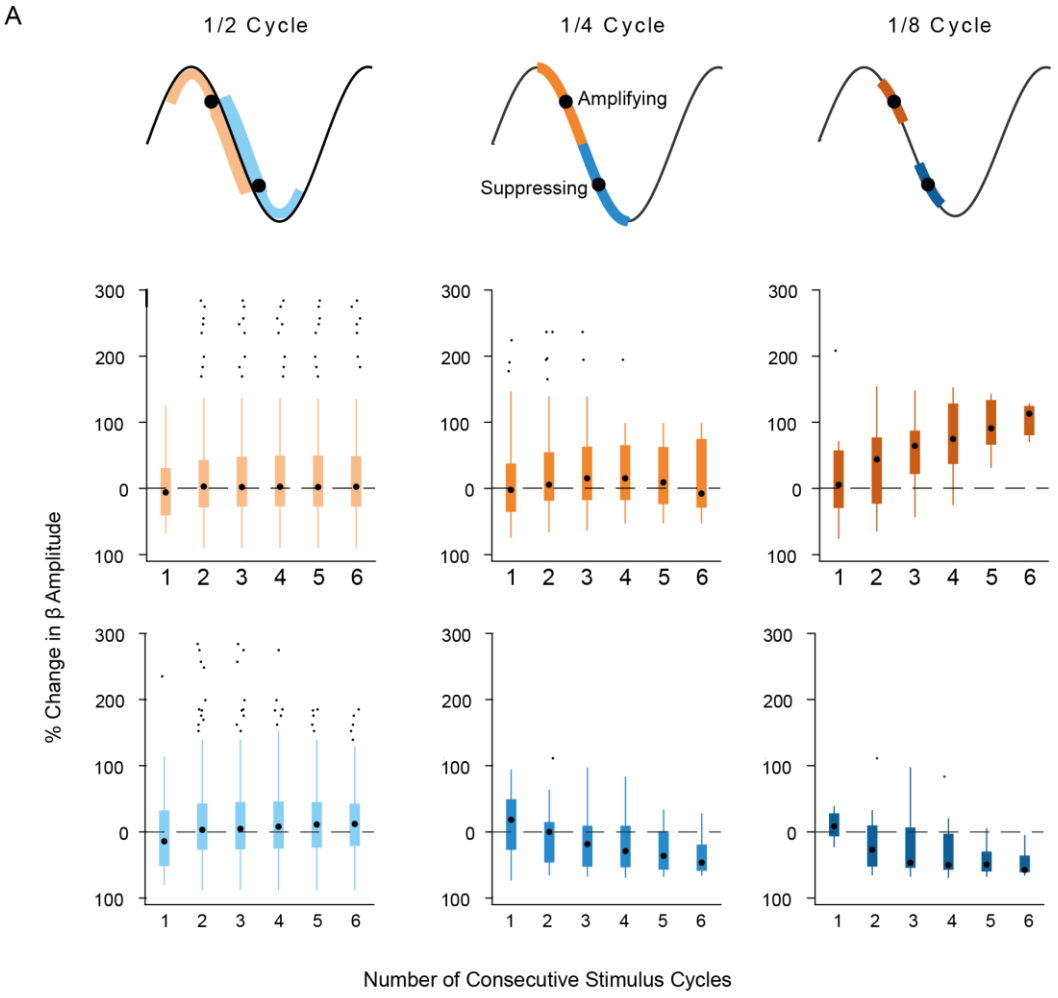
In contrast to beta suppression, there was no significant effect of consecutive stimuli delivered at the amplifying phase ($p = 0.190$, Kruskal-Wallis test) (**Fig. 3.4B**). Additionally, amplification was only greater than surrogate effects after three cycles of stimulation at the amplifying phase ($p = 0.0093$, Wilcoxon ranked-sum test). Following the third consecutive cycle, amplification returned to surrogate levels. At the individual level, only two out of eight patients showed amplification dependence on consecutive stimulus cycles ($p < 0.05$, Kruskal-Wallis). The strength of amplification across all patients was inversely correlated with the relative peak beta power of the entire recording ($r^2 = 0.540$, $p = 0.038$, linear regression analysis) (**Fig. 3.5**). Together this indicates it was more difficult to further amplify the exaggerated beta signal, however more amplification is seen when there is lower relative peak beta power. As already suggested by the spectral analysis, it was further verified that stimulation was not amplifying the entire signal by determining stimulation did not result in a significant change in the median oscillation envelope across patients ($p = 0.7344$, Wilcoxon signed rank test).

3.4.2. Increased phase-specificity enhances cumulative phase-dependent suppression of beta amplitude

In **Fig. 3.4** stimulus phase was defined for a quarter of a beta cycle. Next, we investigated how the phase precision of stimulus pulses delivered affects modulation of the beta amplitude. To achieve this, we reanalyzed the suppression and amplification effects using stimulus-phase bins of different widths. If greater effects were seen with narrower bins, this would indicate that they are dependent on the precise phase at which the stimulation arrives. In an example patient (Case 3) both enhanced suppression and amplification of the beta oscillation were seen when stimulus pulses occurred in a narrower window around the suppressing and amplifying phase (phase bins $^1/_8$th a cycle wide, amplifying bin: $p = 0.0251$,

suppressing bin: p = 0.0272, Kruskal-Wallis test) (**Fig. 3.6A**). Alternatively, when stimulus pulses occurred over a wider window around the suppressing and amplifying phase (phase bins ½ a cycle wide), neither significant amplification (p = 0.9413, Kruskal-Wallis test) nor suppression (p = 0.3882, Kruskal-Wallis test) was seen.

In order to observe cumulative effects of stimulation phase using phase bins $^1/_8$ th of a cycle wide, the stimulus frequency had to be within 1 Hz of a patient's peak beta frequency. As this was not always the case, it was not possible to provide group data using these narrower phase bins. However, bins could be widened to half a cycle for all patients (instead of a quarter of a cycle wide as in Fig. 4B). When stimulus pulses were allowed to occur over a wider window around the mean suppressing and amplifying phase, neither significant suppression nor amplification was seen across patients, even after consecutive pulses (Suppressing phase: p = 0.2755, Amplifying phase: p = 0.2502, Kruskal-Wallis test) (**Fig. 3.6B**). Overall, these results suggest that at least a quarter cycle precision is needed to see phase dependent effects of stimulation, and that narrowing the phase window for stimulation further could lead to larger effects on amplitude.


A
1/2 Cycle
1/4 Cycle
1/8 Cycle
Amplifying
Suppressing
% Change in β Amplitude
Number of Consecutive Stimulus Cycles

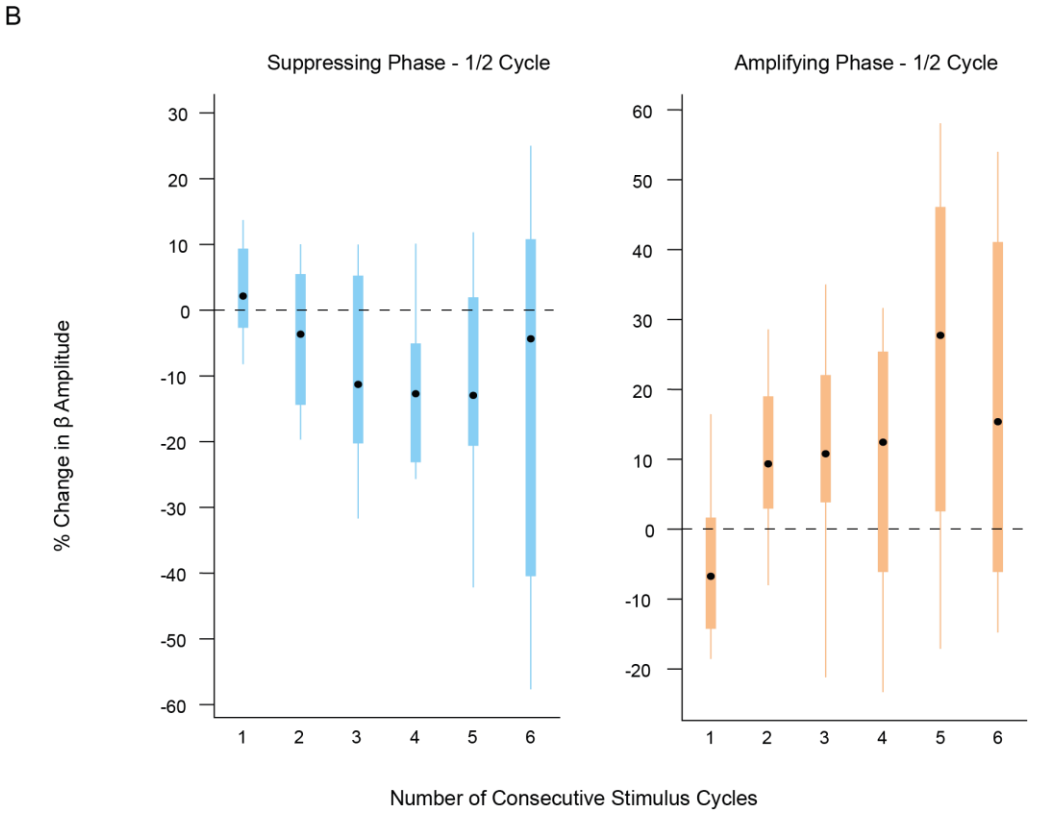

B
Suppressing Phase - 1/2 Cycle
Amplifying Phase - 1/2 Cycle
% Change in β Amplitude
Number of Consecutive Stimulus Cycles

Figure 3.6. Phase Precision of the Stimulus Pulse Affects the Strength of Beta Amplitude Modulation. **(A)** Example patient showing both enhanced suppression and amplification of beta amplitude when using narrower phase bins. Stimulation frequency (20 Hz) was 1 Hz different from peak beta frequency (19 Hz), allowing for detection of consecutive pulses despite narrower phase bins. Bins were widened or narrowed around the mean suppressing and amplifying phase (black dots). Stimulus phase was defined as: left) half the oscillation cycle; middle) $^{1}/_{4}^{th}$ the oscillation cycle; right) $^{1}/_{8}^{th}$ the oscillation cycle. Orange hues represent the suppressing phase; blue hues represent the amplifying phase. Amplitude modulation was only dependent on number of consecutive pulses when using $^{1}/_{8}^{th}$ of the oscillation cycle (amplifying phase: 2 bins, $p = 0.4594$; 4 bins, $p = 0.972$; 8 bins, $p = 0.0251$; suppressing phase, 2 bins, $p = 0.8508$; 4 bins, $p = 0.0517$; 8 bins, $p = 0.0272$, Kruskal-Wallis test) **(B)** Median suppressing and amplifying effects on the beta amplitude using phase bins half a cycle wide were grouped across eight patients. Neither beta suppression ($p = 0.2755$) nor amplification ($p = 0.2502$) was dependent on the number of consecutive stimuli (Kruskal-Wallis test).

3.4.3. Phase-dependent suppression of beta amplitude was dependent on stimulation amplitude

To test whether phase-dependent suppression of beta oscillations is dependent on stimulation amplitude, three stimulus amplitudes (0.5 mA, 1 mA, and 1.5 or 2 mA) were applied at the same recording location in three patients. As we found that suppression levels are affected by the strength of the beta power (**Fig. 3.5**), it is important to view the differences across amplitudes within each patient instead of absolute values. Consistently across patients, stronger suppression was seen after the first, second, and third pulses occurred at the suppressing phase using 1 mA stimulation compared to 0.5 mA (**Fig. 3.7**). In two of the patients (black and red), suppression seemed to plateau for each stimulation amplitude used. While in some cases, further suppression could be seen using 2 mA stimulation, results were not as consistent.

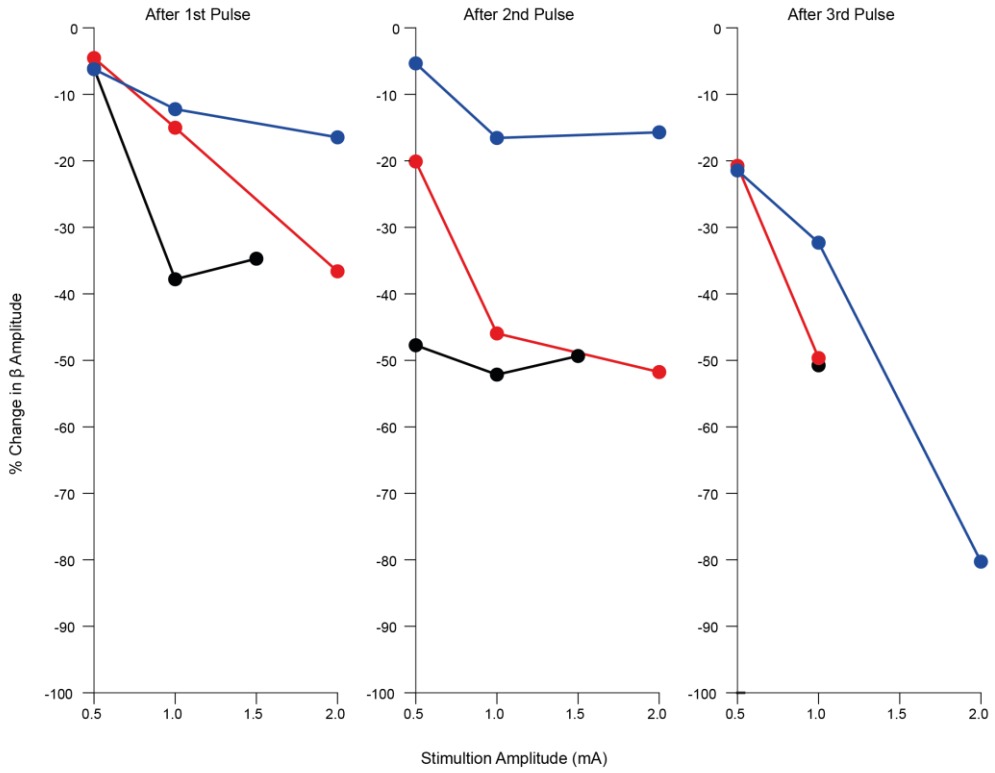


Figure 3.7. Phase Dependent Suppression of Beta Oscillations is Dependent on Stimulation Amplitude. Percentage change in beta oscillation amplitude after the 1st (left), 2nd (middle), and 3rd (right) consecutive stimulus pulse at the suppressing phase as a function of stimulus amplitude is plotted for three patients. After each stimulus, the decrease in beta amplitude was stronger when using 1 mA versus 0.5 mA. Further suppression could be seen when the stimulus amplitude was increased to 2 mA; however, effects were not as consistent.

3.4.4. Phase dependent suppression of oscillatory STN output

We next investigated whether a simultaneous change in unit activity could be seen concurrent with amplification and suppression of the LFP beta oscillation. For recordings included in the LFP analysis it was necessary to prioritize a recording location with strong beta oscillations, but units sometimes were rarely stable for long enough. Therefore, background unit activity (BUA) was used as a measure of neuronal activity, as this could be used across all patients and represents output from a local population of neurons surrounding the recording contact. When stimulus pulses occurred at the suppressing phase of the LFP over consecutive cycles, the amplitude of beta oscillatory activity in the BUA decreased across patients (Fig. 3.8, $p = 0.0046$, Kruskal-Wallis test). However, instead of seeing suppressive effects by the second or third cycle, a decrease in BUA oscillatory activity was not seen until the fourth consecutive cycle, where a median 18.7% amplitude reduction was seen. Conversely, when stimulus pulses occurred at the amplifying phase of the LFP, enhancement of oscillatory activity in the BUA signal was not seen over consecutive cycles (**Fig. 3.8**, $p = 0.7993$, Kruskal-Wallis test). These results indicate that stimulating at the suppressing phase of the LFP results in a concurrent decrease in synchronous beta frequency output of STN neurons, and could therefore modulate oscillations in downstream structures and the wider network.

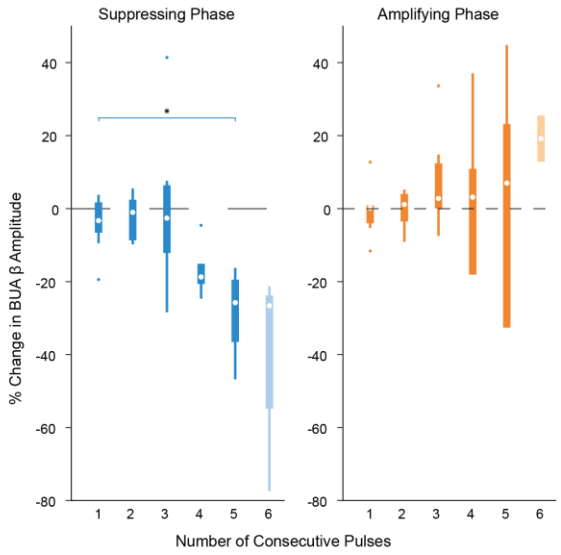


Figure 3.8. Consecutive Stimulus Pulses at the Suppressing Phase Leads to BUA Suppression of the Beta Synchronous STN Unit Activity. Background unit activity (BUA) was filtered around the peak beta frequency detected in the LFP. Median percent changes in the BUA oscillation amplitude following stimulation at the suppressing (blue) and amplifying (yellow) phase were grouped across eight patients. Suppression of beta frequency activity in the BUA was dependent on the number of consecutive stimuli delivered at the suppressing phase of the LFP oscillation ($p = 0.0046$, Kruskal-Wallis test), while amplification was not ($p = 0.7993$, Kruskal-Wallis test). As six consecutive stimuli were only observed in four out of the eight patients at the suppressing phase and two out of eight patients at the amplifying phase (indicated by lighter boxes), these was not included in the Kruskal-Wallis test. Horizontal lines indicate differences between groups (corrected for multiple comparisons using the false discovery rate, $p \leq 0.05$).

3.4.5. Phase dependent suppression led to decreased synchronization

Using coincident EEG recordings, we examined whether changes in local oscillation amplitude induced by phase-dependent stimulation extended to effects on cortico-subthalamic synchronization. One patient only had Fz EEG recordings, so was not included in Pz and Cz analysis. In line with previous work, stimulation pulses led to evoked potentials in midline EEG channels (discussed in the previous chapter, Ashby et al., 2001b; Eusebio et al., 2009; Kumaravelu et al., 2018; Walker et al., 2012). While this demonstrates cortical activity could be modulated using our stimulation protocol, consecutive stimuli occurring at the suppressing or amplifying phase of the LFP beta oscillation were not associated with simultaneous changes in cortical beta amplitude (**Fig 3.9**., Fz: amplifying: $p = 0.1269$, suppressing $p = 0.9526$; Pz: amplifying: $p = 0.7746$, suppressing $p = 0.9049$; Cz: amplifying: $p = 0.6275$, suppressing: $p = 0.9996$; Kruskal-Wallis test). However, the phase alignment between midline EEGs and the STN during stimulation at the suppressing phase was less consistent during three cycles of stimulation at the suppressing phase than at the amplifying phase (**Fig. 3.9. A-C**). This suggests phase dependent stimulation may have network-level effects on cortico-subthalamic synchrony in addition to local effects on STN beta oscillations.

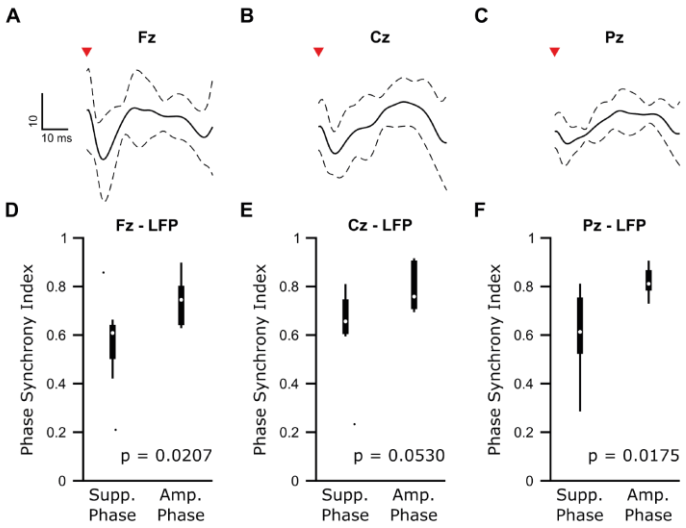


Figure 3.9. Phase dependent suppression of subthalamic beta oscillations is associated with lower cortico-subthalamic beta synchronization than phase dependent amplification. (A-C) Average (± standard deviation) cortical evoked responses from frontal/midline EEG (Fz, Cz, and Pz) locations) across eight patients for Fz and seven patients for Cz and Pz. EEG signals were bandpass filtered 1 – 100 Hz to remove any slow drift, and notch filtered 49 – 51 Hz to remove line noise. **(D-F)** Median phase synchrony index between the STN LFP and frontal/midline EEG channels over three cycles of consecutive stimuli occurring at the suppressing and amplifying phases across eight patients (Fz) or seven patients (Cz, Pz). Stimulating at the suppressing phase resulted in significantly lower cortico-subthalamic phase synchrony for Fz-LFP ($p = 0.0207$, Wilcoxon ranked sum test) and Pz-LFP ($p = 0.0175$, Wilcoxon ranked sum test, $p < 0.05$ indicated by black stars).

3.5. Discussion

This chapter shows that, in patients with Parkinson's disease, electrical stimulation delivered to a specific phase of the subthalamic beta oscillation results in suppression of local and network level pathophysiological activity. Although beta frequency stimulation did not alter the power of beta oscillations over the entire recording, transient amplification and reduction of the oscillation amplitude could be seen when the specific timing of stimulus pulses was taken into account. Remarkably, delivering stimulus pulses locked to the suppressing phase over multiple consecutive cycles reduced the beta amplitude by over 40% across patients. This provides the first evidence that a phase-dependent approach to DBS could be more efficient and effective than high-frequency stimulation at reducing pathological neural oscillations in Parkinson's disease. Moreover, our findings show that phase-dependent stimulation has the wider potential to disrupt or amplify neuronal oscillations to manipulate communication across brain areas.

3.5.1. Phase dependent amplitude suppression relies on consecutive pulses

Here we identify the existence of a critical phase of the STN beta oscillation, specific to each patient, that when stimuli occurred for multiple consecutive cycles leads to amplitude suppression of beta oscillatory activity in the LFP and BUA and a decrease in beta phase synchrony with the cortex. In parkinsonian patients and animal models of Parkinson's disease, single STN neurons lock to a specific phase of the ongoing beta oscillation in the LFP (Kuhn et al., 2005;Weinberger et al., 2006a;Mallet et al., 2008a; Sharott et al., 2018c), which leads to a correlation in the spiking across STN neurons at zero lag (Levy et al., 2002; Mallet et al., 2008a; Mallet et al., 2008b). The LFP likely reflects synchronized membrane currents of a population of neurons in the vicinity of the recording electrode. Several studies

have demonstrated that oscillations in the motor cortices precede those in the STN LFP (Fogelson et al., 2006;Lalo et al., 2008;Litvak et al., 2010a;Sharott et al., 2018c), suggesting that cortical oscillations, measured here using EEG, may drive beta in the STN LFP through monosynaptic and or polysynaptic pathways. In contrast, the BUA must predominantly reflect spiking activity due to exclusion of low (>300Hz) frequencies (Moran et al., 2008b; Siegle & Wilson, 2014). In the context of STN beta oscillations, the EEG and STN LFP signals are therefore more indicative of synaptic input to the neurons, while the BUA signal reflects the output. In line with this delineation, previous work shows the BUA output can be vastly different in conditions with similar EEG/LFP power and synchrony, demonstrating that these signals are independent (Sharott et al., 2017).

Taken together, our results show that stimulation at consecutive pulses of the suppressive phase can reduce the oscillatory input to STN (STN LFP amplitude and cortico-subthalamic synchronization) and the output (BUA amplitude). Stimulus pulses delivered to neural oscillators can result in advances or delays in the oscillator depending on the stimulus phase (Ermentrout & Chow, 2002; Farries & Wilson, 2012;Smeal et al., 2010). Within the STN, a phase shift in the beta oscillatory input may alter or reflect the reliability of the recruitment of STN neurons to the cortical oscillation, measured here using the BUA beta amplitude. Studies of beta oscillations in experimental animals have demonstrated that the synchronization observed in the STN extends across the entire cortico-basal ganglia network (Goldberg et al., 2002;Mallet et al., 2008a; Mallet et al., 2008b;Deffains et al., 2010b;Tachibana et al., 2011b;Brazhnik et al., 2012;Sharott et al., 2017). Advancing or delaying the subthalamic beta output could thus disrupt the temporal relationship between downstream brain regions, which could result in decoupling of the network as a whole.

Importantly, we only saw these effects when two or more pulses were delivered on the suppressive phase. The simplest explanation for this is that the stimulus amplitudes delivered were generally low amplitude and, indeed, stronger beta amplitude suppression with fewer pulses was seen using higher stimulation amplitudes. However, it is also possible that disrupting the temporal relationships between oscillators within and between nodes of the network may require several cycles to decouple the circuit. Regardless, one key aspect in developing improved stimulation protocols for DBS is reducing the stimulation current to prevent spread to regions outside the target. Our results suggest delivering low amplitude pulses at the suppressing phase over several cycles is sufficient to disrupt pathological network activity. Interestingly, unlike suppressing effects, phase dependent amplification did not depend on the number of consecutive cycles of stimulation and was generally weaker than suppression. This may be because oscillatory activity is already in a heightened state in Parkinson's disease, making it more difficult to enhance than suppress. The linear relationship seen between beta power and amplification resulting from stimulation supports this hypothesis. This property is potentially therapeutically useful, as enhancing ongoing beta would potentially worsen symptoms.

3.5.3. Implications for therapy

Advancements to DBS algorithms have been aimed at improving efficacy and reducing the amount of current delivered, which could limit stimulation-induced side effects and conserve battery power (Little et al., 2013;Adamchic et al., 2014;Wilson & Moehlis, 2014;Brocker et al., 2017; Cagnan et al., 2017). Closed-loop approaches to neurostimulation have already proven to be achieve some of these aims (Rosin et al., 2011;Little et al., 2013). For a closed-loop approach to be effective, an accurate biomarker of symptom severity must be used to drive stimulation. While a number of synchrony measures have been implicated

in motor symptoms of Parkinson's (Tass, 2003; Weinberger et al., 2006a; Kühn et al., 2009; de Hemptinne et al., 2013a), beta oscillations offer an appealing biomarker for the control of akinesia and rigidity for a number of reasons. First, beta oscillations can be recorded in the LFP and have proven to be an effective chronically recorded feedback signal in patients even during unimpeded movement (Little et al., 2013;Rosa et al., 2015). Second, recordings can be made from the implanted stimulation electrode, limiting the operation to a single surgical site. Finally, alternative measures implicated in motor symptoms, specifically coupling between the amplitude of high frequency activity to the phase of the beta oscillation (phase amplitude coupling) (de Hemptinne et al., 2013), would likely be disrupted with the suppression of the carrier frequency.

3.6. Conclusions

Our findings suggest that tracking the phase of ongoing beta oscillations and delivering stimulus pulses only on the suppressing phase could be an effective closed-loop strategy in Parkinson's disease. Implementing such phase tracking would allow a full evaluation of the efficacy of phase-dependent stimulation for selectively reducing beta and sparring functional activity. The increased number of consecutive stimulation cycles possible with active phase tracking could further enhance suppressive effects. Furthermore, unlike tremor, where there is an ongoing measure of motor impairment, akinetic/rigid symptoms require task-related evaluation. Phase-tracking would allow longer periods of phase-locked stimulation (compared to the 100 – 400 milliseconds seen in this study) that would enable this type of behavioral assessment. While active phase locked stimulation has been applied to low frequency neural oscillations in the hippocampus (Siegle and Wilson, 2014) and low frequency peripheral oscillations (Brittain et al., 2013; Cagnan et al., 2017), to our knowledge, this approach has not yet been successfully implemented at frequencies above 10 Hz in experimental animals or humans. Implementing active phase tracking of parkinsonian beta oscillations presents challenges not only due to the higher frequency signal, but also because oscillations tend to occur in short bursts (Tinkhauser et al., 2017) and signals are on the order of 1 μV. Such issues could be addressed by combining phase tracking with proven amplitude-based approaches to further optimize the selectivity of stimulation (Little et al., 2013). Overall, the results presented here provide strong evidence in support of exploring such an approach in the future, both for PD and other diseases where abnormal oscillations are a pathophysiological feature

Chapter IV Phase alignment dependent modulation of the amplitude of beta oscillation in Parkinson's Disease

4. 1. Introduction

4.1.1. Communication Through Coherence

Synchronised oscillations between neuronal populations are found across virtually all forebrain networks (Engel et al., 2001; Buzsaki & Draguhn, 2004). While the role of such activities remains an area of debate, the influential "communication by coherence" (CTC) hypothesis, is that they mediate communication between coupled populations (Fries, 2005, 2015). The frequency of synchronisation has been postulated to be an important parameter in determining the nature of communication (Fries et al., 2005, 2015; Michalareas et al., 2016). Much of the work in this field has focused on gamma frequency rhythms (40-80 Hz), which are thought to modulate input gain across cortical areas by providing temporally precise windows of excitability (Fries, 2005). Importantly, the increase in communication strength, measured by correlation of oscillatory amplitude, at these higher frequencies is strongest when synchronisation occurs at the most frequently occurring phase relationship between two areas (Womelsdorf et al., 2007). This phase-dependent communication within the visual cortex and corticospinal tract predicts behavioural performance (van Elswijk et al., 2010; Ni et al., 2016), supporting a function role in neuronal communication.

4.1.2. Pathological coherence in PD

Changes in the nature of these synchronised oscillations are thought to underlie the symptoms of several brain disorders. As discussed in the introduction, the most striking example of such an "oscillopathy" is Parkinson's disease (PD), where abnormally high amplitude, temporally sustained oscillations are found throughout the motor cortices, basal

ganglia and motor thalamus. Recently it was demonstrated that beta frequency oscillations recorded in the local field potentials (LFPs) of two basal ganglia nuclei, the subthalamic nucleus (STN) and globus pallidus (GP), from Parkinsonian patients display properties of synchronisation consistent with the CTC framework (Cagnan et al., 2015). The amplitude of beta oscillations in both structures was amplified during periods where the phase-relationship between the two signals was that occurring most often. As only LFPs could be recorded in these experiments, it is unclear as to whether periods of amplification were reflected in the activity of neurons in these areas. This is a crucial question, as without affecting timing of spiking activity, changes in oscillation power can have little effect on downstream motor processing and behaviour.

While these CTC relationships have been described between basal ganglia nuclei, several studies have provided evidence that the driver of these oscillations is the motor cortex (Lalo et al., 2008;Litvak et al., 2010b). Thus, if CTC is important in the propagation of pathological beta oscillations, the key properties would be expected to occur between cortical and basal ganglia signals. Of particular importance is the cortico-subthalamic pathway, which provides a short-latency route for cortical neurons to influence the basal ganglia network (Nambu et al., 2000). Population signals (ECoG, EEG) recorded from frontal cortical areas in PD patients and experimental animals are highly synchronised with LFPs and single units in the subthalamic nucleus (Williams et al., 2002; Fogelson et al., 2006; Mallet et al., 2008a; Sharott et al., 2018a). Several authors have suggested that this pathway provides the initial entrainment of basal ganglia neurons, which then spreads to other nodes in the network (Bogacz & Gurney, 2007; Mallet et al., 2008b; Deffains et al., 2016). Understanding how the phase alignment between those structures correlates with the clinically relevant increase of beta power could further our understanding about this disease phenomenon, as well as inspire applications for closed-loop deep brain stimulation.

4.2. Aims

Here we investigated whether coherent oscillations in the frontal cortex and STN displayed phase-dependent amplification in dopamine-depleted rats, and carried out complementary analyses using intraoperative recordings from PD patients. Our overarching hypothesis was that the power of pathological beta oscillations become elevated because the oscillating populations of neurons are at their preferred phase alignment.

More precisely, we aimed to test whether:

I. There is a temporal relationship between beta oscillations the STN LFP and the cortical activity in Parkinsonian rats that occurs with greater likelihood

II. There is a specific phase alignment between the two structures that correlates robustly with the elevated and sustained beta amplitude in the cortex and the STN

III. This phase alignment affects the firing properties of the STN neurons.

IV. This phase alignment can be selectively modulated by stimulation at the same frequency as the pathological oscillation

V. That findings in rodents are consistent with data from Parkinson's disease patients

4.3. Methods

4.3.1. Rat dataset

Experimental procedures were carried out on male CD rats (Charles River), and were conducted in accordance with the Animals (Scientific Procedures) Act, 1986 (United Kingdom), and with Society for Neuroscience Policies on the Use of Animals in Neuroscience Research.

4.3.2. Unilateral 6-hydroxydopamine hemi-lesion.

Unilateral lesions were carried out on 30 190 - 200g rats, as previously described (Magill et al., 2001, **Supplemental Table 4.1**). Approximately 25 mins prior the injection of 6-OHDA, all rats were given a desipramine injection (25 mg/kg, i.p.; Sigma) in order to facilitate the survival of noradrenergic neurons (Schwarting & Huston, 1996a). After the animals were placed on a stereotactic frame, anaesthesia was induced and maintained by the continuous supply of isoflurane (4% v/v isoflurane in O_2). A small hole was drilled directly over the injection site and the dura was carefully removed. Using a glass pipette (diameter: ~18 µm), animals were injected with 1 µl 6-OHDA toxin solution (final concentration of 6 mg/ml in 0.9% w/v NaCl solution containing 0.01% w/v) into the medial forebrain bundle (4.1 mm posterior, 1.4 mm lateral of bregma in 7.9 mm deep from the dura, **Fig. 4.1. Ai)** or substantia nigra pars compacta (4.1 mm posterior, 1.4 mm lateral of bregma in 7.9 mm deep from the dura**, Fig. 4.1 Bi**, Paxinos & Watson, 1986). Injections took 10 mins (~0.1 µl / min) and the pipette was left in place for an additional 5 mins. After the pipette was retracted and the wound was disinfected and closed, the wellbeing of the animal was carefully monitored until they were fully awake (Sharott et al., 2017). 0.1 ml of vetergesic solution (Ceva, 1:4 mixture of vetergesic: water for injection) was administered subcutaneously on the day of the surgery and on the following 2 days. Electrophysiological recordings took place 2 weeks or more after surgery, in line with previous studies (Mallet et al., 2008a; Sharott et al., 2017). To evaluate the success of the lesion, post mortem tyrosine hydroxylase (as described below) immunoreactions were performed on striatal sections (**Fig. 4.1 Aii, Bii**). Only those animals where a clear difference could be established in the TH fluorescence between the lesioned and the intact hemisphere were taken into analysis (**Fig. 4.1 C**).

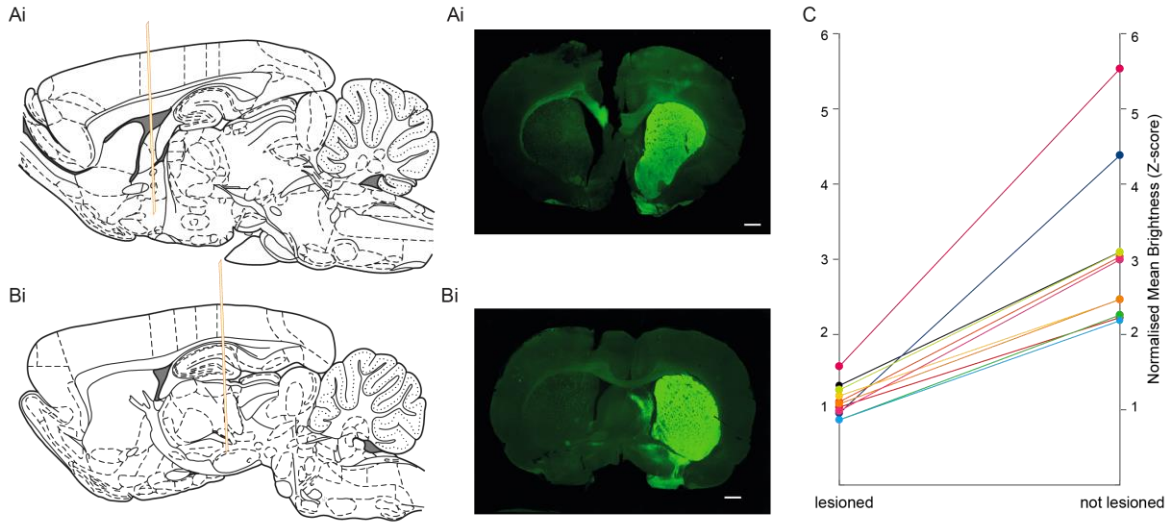


Figure 4.1. Establishing Parkinsonian phenotype in CD rats. A, B) 6-OHDA was injected to the right medial forebrain bundle (MFB, **Ai**) or to the right substantia nigra pars compacta (SNc, **Bi**) of healthy CD rats. **Bi, Bii).** The success of the lesion was assessed using *post mortem* tyrosine hydroxylase immunoreactivity (Alexa Fluofor 488). Regardless of the lesion site, a significant loss of dopaminergic terminals could be observed both for MFB (**Bi**) and SNc (**Bii**) on the ipsilateral side to the lesion in the striatum. Scale bars: 100 µm. **C)** Recordings from animals that had more than 50% difference in average brightness between the left and right striatum were included in this study. Coloured lines represent an average striatal brightness value (normalised by the corresponding cortical brightness) for the lesioned (left) and the intact (right) side for each animal (colour codes for animals stays the same through the chapter).

4.3.3. *In vivo* electrophysiological recording and juxtacellular labelling.

Altogether, experiments were performed in 10, successfully lesioned, anesthetized rats (**Supplementary Table 4.1**. provides a summary for all experiments, schematic illustration: **Fig. 4.2**.). For the anaesthesia, isoflurane was used for induction (4% v/v isoflurane in O_2) and the anaesthetised state was maintained with maintained with urethane (1.3 g/kg, i.p.; ethyl carbamate, Sigma) and supplemental doses of ketamine (30 mg/ kg, i.p.; Willows Francis) and xylazine (3 mg/kg, i.p.; Bayer) interperitoneal injections (Magill et al., 2006). After ~1 h of the induction, animals were placed in earbars on a stereotaxic frame (Kopf). Body temperature was carefully monitored and homeostatically maintained with a heating apparatus (Harvard Apparatus). The depth of the anaesthesia and the animal's wellbeing was carefully monitored during the recording by testing peripheral reflexes (with a hindpaw pinch).

The ECoG was recorded epidurally with a ~1 mm steel screw attached to the skull without breaking the dura mater above the frontal cortex (somatic sensory-motor area, 4.2 mm anterior, 2.0 mm lateral of bregma, Paxinos & Watson, 1986, **Fig. 4.2A**). The raw ECoG signal was bandpass filtered (0.3-1500 Hz, -3 dB limits) and amplified (2000´; DPA-2FS filter/amplifier; npi electronic) on-line before further analysis. Beta oscillations are known to occur during general activation (GA) state, hence only recordings in this state were utilised here (Magill et al., 2004a).

Extracellular deep recordings of the local field potential and the single neuron spike trains (or unit activity) of STN was recorded using glass electrodes (tip diameter ~1.5-2.5 µm, impedance measured *in situ* 10-30 MΩ) filled with 0.5 M NaCl solution diluted with 1.5% neurobiotin (Vector Laboratories, Magill et al., 2004a, **Fig. 4.2A**). The electrode was lowered using a motor (IVM-1000; Scientifica), which allowed the depth of the electrode to

be manipulated with micrometre precision. Electrode signals were amplified twice, first 10x with (10´) Axoprobe-1A amplifier (Molecular Devices) and then another 100´, and bandpass filtered at 300-5000 Hz (DPA-2FS filter/amplifier). The ECoG and STN LFP and unit activity were each sampled at 16.6 kHz using a Power1401 Analog-Digital converter and a PC running Spike2 acquisition and analysis software (Version 7.2, Cambridge Electronic Design).

For the purpose of precise localisation, a subset of putative STN neurons were juxtacellularly labeled (Pinault, 1996; Magill et al., 2000). Subsequent to recording the electrode was moved as close to the cell as possible and labeling with neurobiotin was attempted. Positive current pulses were applied until the cell's spike train showed entrainment by the current. Positive current pulses (2-10 nA, 200 ms, 50% duty cycle) were applied until the single-unit activity became robustly entrained by the current injections. The location of the labeled neurons were post hoc confirmed by revealing the neurobiotin filled cell bodies and the borders of the STN with standard immunohistochemical methods (**Fig. 4.3**., 'identified', see below). The unlabelled, but recorded neurons on the same path in the same animal were also included if the location, extrapolated from the position of other labelled neurons and stereotaxic measurements, indicated that the recording was also in the STN (**Fig. 4.4**, Nakamura et al., 2012) .

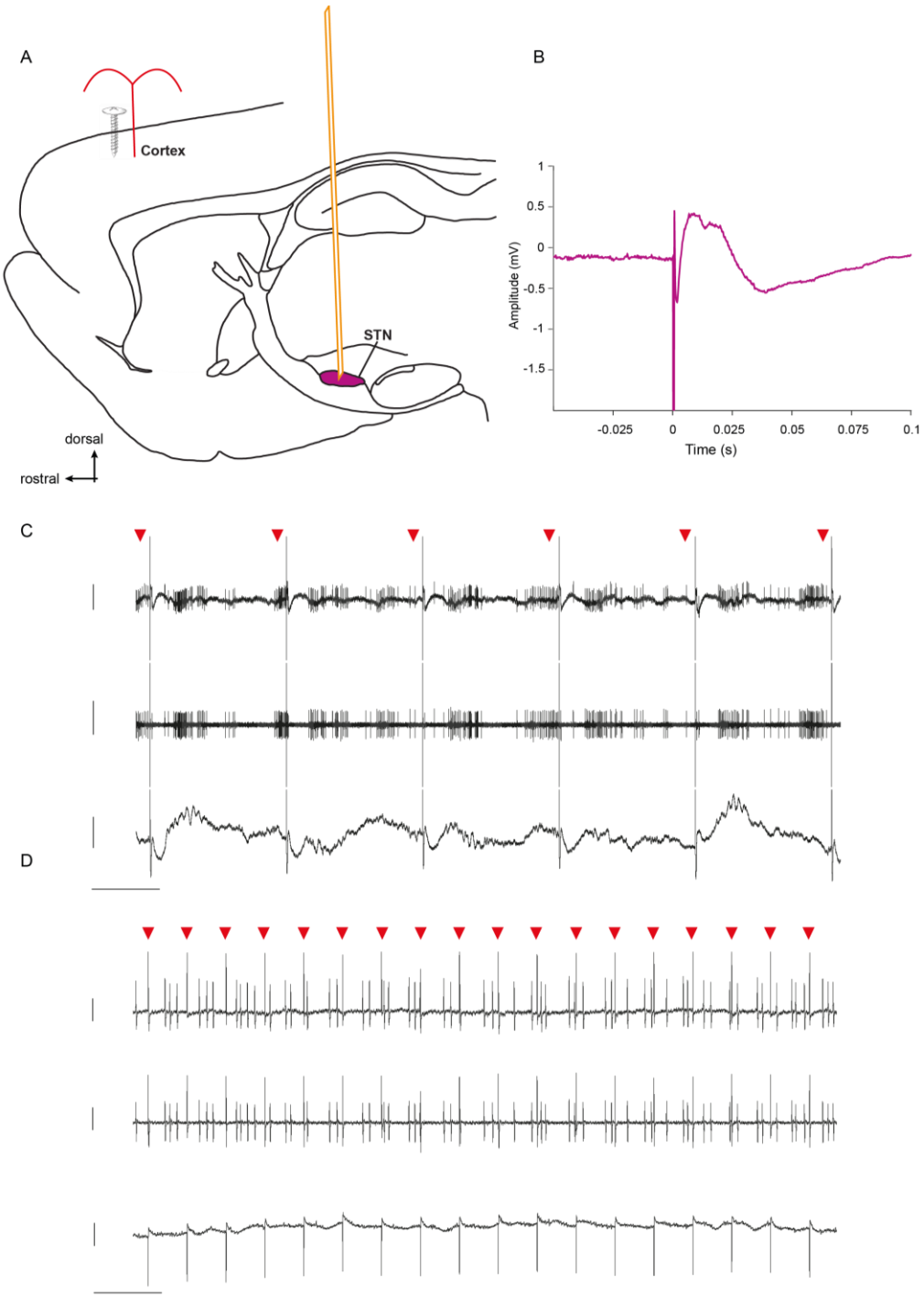

A
Cortex
STN
dorsal
rostral
B
Amplitude (mV)
1
0.5
0
-0.5
-1
-1.5
-0.025
0
0.025
0.05
0.075
0.1
Time (s)
C
D

Figure 4.2. Recording and stimulating setup in rats. A) Cortical activity was measured by using a metal screw touching the dura (ECoG). Cortical stimulation of the layer V of the M1 was achieved by using bipolar stimulating electrodes. Recording and juxtacellular labelling in the STN was attained by a glass electrode filled with neurobiotin solution. **B)** Characteristic multiphasic evoked potential was utilised for the *ad hoc* assessment of the recording electrode location. 1 Hz cortical stimulation was used (Magill (2004). **C)** 1 Hz stimulation of the M1. Top row: Wideband signal recording from the glass electrode used to extract the STN LFP (1 mV), middle row: unit activity (1 mV), Bottom row: ECoG (0.5 mV). Red triangles denote stimulation pulses (950 mA). Time: 0.5 s. **D)** 20 Hz stimulation of the M1 (50 mA) allowed for the subtraction of STN LFP (top row, 1.5 mV), spiking activity (middle row, 1.5 mV) and the cortical activity (bottom row, 0.5 mV). Time: 100 ms

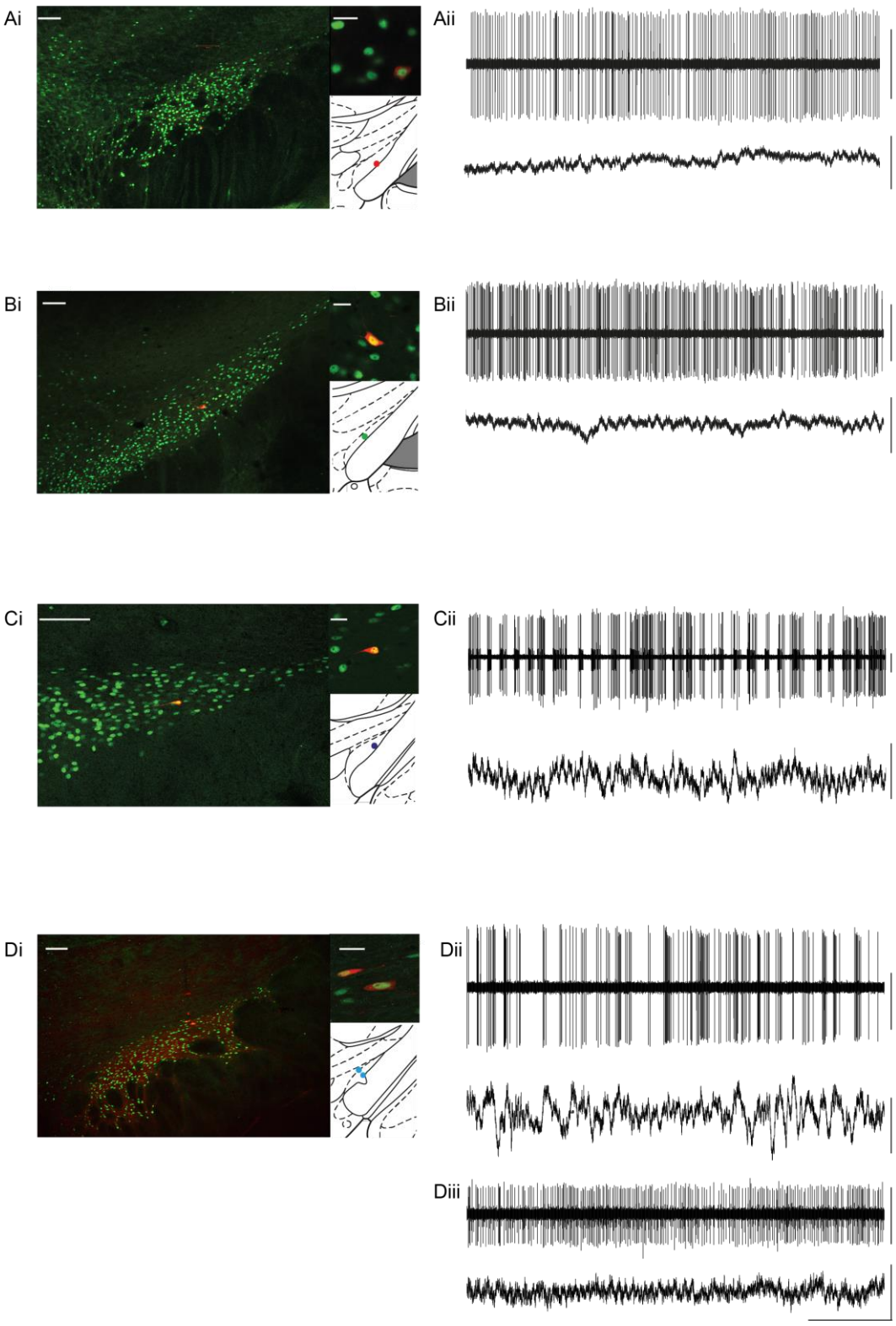

Ai
Aii
Bi
Bii
Ci
Cii
Di
Dii
Diii

Figure 4.3. *In vivo* electrophysiological properties of identified Foxp2+ STN neurons in 6-OHDA rats. A-D) Juxtacellularly labeled STN neurons and their co-localization with fluorescent neurobiotin labelling (streptavidin: red channel) and FoxP2 (Al 488: green channel). Scale bars are 100 and 20 µM. (**Ai–Di**). The traces show the spike trains of single neurons recorded by the glass pipette that was used for labelling. Coincidental cortical activity is displayed below (motor cortex ECoG). The anterior-posterior plane is displayed at the right hand corner of Ai-Di. STN neurons were recorded in rostral (**A**) and caudal (**B**) plane. In some cases, the activity of two single neurons could be isolated at a single recording position (**Cii**). Recordings from parallel tracks could be recovered (**Dii**).

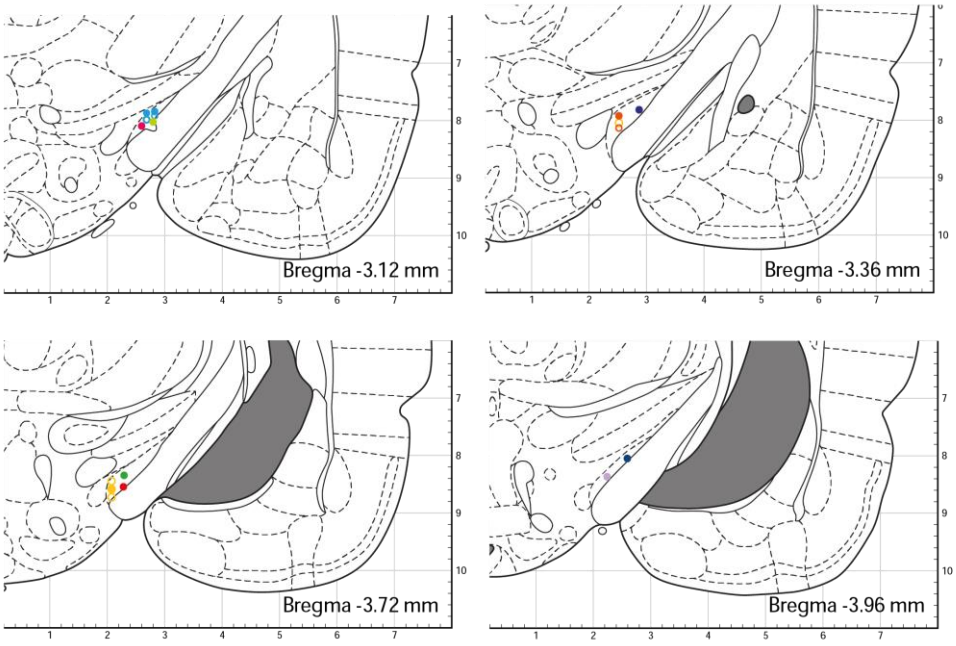


Figure 4.4. Recordings were homogenously distributed across the STN. Atlas images (Paxinos & Watson, 2013) cropped around the STN (coronal sections, clockwise from right hand corner rostral to caudal) show the locations of labeled and identified (full circle) and extrapolated (outline only) cells. Colours used for each animal stays identical throughout the legends.

4.3.4. Electrical stimulation of the motor cortex.

For the focal stimulation of the cortex, parallel, bipolar stimulating electrodes (constructed from nylon-coated stainless steel wires; California Fine Wire, **Fig. 4.2A**), with tip diameters of ~100 µm, a tip separation of ~150 µm, and an impedance of ~10 kΩ, were implanted into the ipsilateral motor cortex (Magill et al., 2004a, **Fig. 4.5A**). The coordinates of the cortical stimulation sites (4.2 mm anterior and 3.5 mm lateral of Bregma, at a depth 2.2 mm below the dura) correspond to layers 5/6 of the primary motor cortex (M1, Paxinos and Watson, 1986). Electrical stimuli, which consisted of square-wave current pulses of 0.3 ms duration and variable amplitude (50-900 µA, adjusted *in situ*, depending on the strength of the modulation), were delivered using a constant-current isolator (A360D; World Precision Instruments) that was gated by digital outputs from the Power1401 converter.

For the purpose of this study, two different frequency protocols were used (**Fig. 4.2C** and **D**). Previously it has been shown that the 1 Hz continuous stimulation of sensorimotor cortex in the anaesthetised rat experiments lead to a characteristic evoked potential in, and only in the STN (described by Magill et al., 2004a, a raw 1 Hz stimulation trace is shown on **Fig. 4.2C**, representative evoked potentials are displayed on **Fig. 4.2B** and **Fig. 4.5C**). This feature of the setup was therefore used to *ad hoc* confirm the location of the recording electrode before the main stimulating protocol was carried out. In order to see whether we could interfere the with the phase alignment between cortex and STN, we used a continuous electrical stimulation protocol at the beta frequency (20 or 25Hz) close to that of the pathological oscillation (**Fig. 4.2D**). The rationale behind using beta frequency stimulation was to test how an external drive at the same frequency to the ongoing oscillation would affect the phase alignment (McConnell et al., 2012). Both 1 and 20 Hz stimulation protocols were recorded with a minimum of 30 s before and after baseline and were applied for at least ~1 min.

4.3.5. Histology and imaging.

Standard indirect immunofluorescence protocols were used to confirm the location of neurobiotin labeled somata in the STN and the success of DA terminal depletion in the striatum (Mallet et al., 2012, Sharott et al., 2017). Animals were given a lethal dose of ketamine (150 mg/kg) and were perfused transcardially with 300 ml of 0.1% w/v glutaraldehyde and 4% w/v paraformaldehyde in 0.1 M phosphate buffer. Brains were left in the fixative solution overnight at 4°C. Perfused brains were mounted on a vibrating microtome and 50 micron-thick coronal sections were cut and collected. Free floating sections were then washed 3 x 10 min in Triton PBS (PBS containing 0.3% v/v Triton X-100 [Sigma]).

To reveal the location of the neurobiotin-labelled cells, sections from the STN region were incubated overnight with Cy3-conjugated streptavidin (1:1000 dilution; Life Technologies). The borders of the STN are known to be outlined with the expression pattern of Forkhead box protein P2 (FoxP2, Campbell et al., 2009; Hontanilla et al., 1997). To reveal FoxP2 immuno-reactivity, sections containing putative STN somata were isolated for molecular testing and were incubated in Triton PBS containing 10% v/v normal donkey serum (NDS; Jackson ImmunoResearch Laboratories) for an hour. The sections then were exposed to the solution containing the primary antibody (Triton PBS containing 1% v/v NDS with goat anti-FoxP2 antibody 1:500, Santa Cruz) and were incubated overnight at 4°C. Sections were then washed in Triton PBS and were incubated with Alexa 488 fluorophore-conjugated secondary antibody (raised in donkey, 1:1000 secondary, Life Technologies). The washed, mounted and cover-slipped (Vectashield, Vector Laboratories) sections were inspected with an epifluorescence microscope (Zeiss Axio Imager M.2) and the location of the labelled cell bodies were confirmed.

High resolution images of the confirmed STN neurons were taken using a confocal microscope (Zeiss LSM 880) equipped with 20x 0.8NA Plan-Apochromat and 40x 1.4NA Plan-Apochromat oil immersion objectives and Stereoinvestigator v11.0 software (MBF Biosciences). To capture the streptavidin labelling and the FoxP2 immuno-reactivity the following lasers and filter-sets were used: Argon 488nm laser for Alexafluor 488 (emission detection: 493-554 nm) and HeNe 543nm for Cy3 (emission detection: 554-681 nm). Imaging was performed with 10x and 40x objectives. At 40x, a series of multiple-plane z-stacked images (optical section thickness 0.8 µm) were captured in order to show the exact location of the somatodendritic structure of the well-filled STN neurons. Images were opened with Fiji software (Schindelin et al., 2012). Both channels of the low magnification (10x) image were processed using ‘Enhance contrast’ (a linear contrast adjustment that

automatically sets white and black points) set to 0.1% of pixels being saturated. The high magnification Z-stack images were flattened using standard deviation projection. This refers to the image processing method of making a composite image out of several frames taken with different focal distances (Ray, 2002). The procedure allows to display greater thickness in a 2D image compared to the single frames alone. Contrast were then enhanced with 0.8% saturation levels for the streptavidin channel. A representative streptavidin-identified STN neuron (red fluorescence) is shown on **Fig. 4.5A**, where the FoXP2 expression (green fluorescence) denotes the borders of the STN.

The extent of dopamine lesions was tested on the serially collected striatal sections using tyrosine hydroxylase immuno-reactivity (Schwarting & Huston, 1996a). Sections were chosen to be +/-0.5 mm around bregma so that the stereology was well matched between the animals. In terms of the indirect immunofluorescence, the same protocol was used as described above. Briefly, tyrosine hydroxylase (primary: Chicken anti-TH, Abcam, secondary: Alexa Fluor 488, Life Technologies) immunoreactions were performed on 3 or more striatal and at least one nigral sections. Only those brains where a clear difference in the brightness between the lesioned and intact striatum could be seen by eye were analysed further (**Fig. 4.1C**). This was done using Zeiss Axio Imager M.2, equipped with Hamamatsu Flash 4.0 LT camera and Colibri 7 LED illumination. For assessing the extent of dopamine lesion, the whole coronal section was captured (±0.5 mm bregma) using Stereoinvestigator v11.0 software (MBF Biosciences) 'Virtual Tissue' scanning mode. Images were taken on a low magnification using a Plan-Apo 5x objective (numerical aperture 0.16). To image the TH signal, the AlexaFluor-488 channel was used (LED excitation at 475 nm, filter-set: 38). Once the whole section scans were performed, images were exported to Image J software without any further image processing. Then, a grid of 1000 mm^2 squares was randomly overlaid on the image of the whole section and the most dorsolateral square (top corner of

both side's striatum) was chosen for measuring the brightness of the lesioned and non-lesioned hemispheres. In the same way, matching control areas were chosen from the cortex above each side. Mean brightness levels were measured for all four squares. Each striatal brightness measure was then subtracted by the corresponding cortical brightness measure and were compared within each animal. Animals were considered lesioned if there was more than 50% difference between the normalised brightness levels of the lesioned and non-lesioned striatum (**Fig. 4.1.C**).

4.3.6. Selection of activated state for analysis.

Neural activity was recorded during two distinct brain states in rats, slow-wave activity (SWA) and global-activation (GA). Beta oscillations in the cortical signals are enhanced following chronic dopamine lesions in rats during the activated state, but not during SWA (Magill et al., 2006; Mallet et al., 2008a). As we were interested in beta oscillations, the ECoG signal was used to differentiate the two states and remove periods of SWA. Data was divided into overlapping (50%) 10 second segments. If the ratio of power (determined using multitaper power spectral density) at alpha frequencies (0.5 - 2 Hz) to beta frequencies (15 - 30 Hz) was less than 75, the segment was removed. Only signals in which the activated state was longer than 45 seconds were included in analysis. A representative example of a slow-wave state switching to activated is shown on **Fig. 4.5B** bottom row.

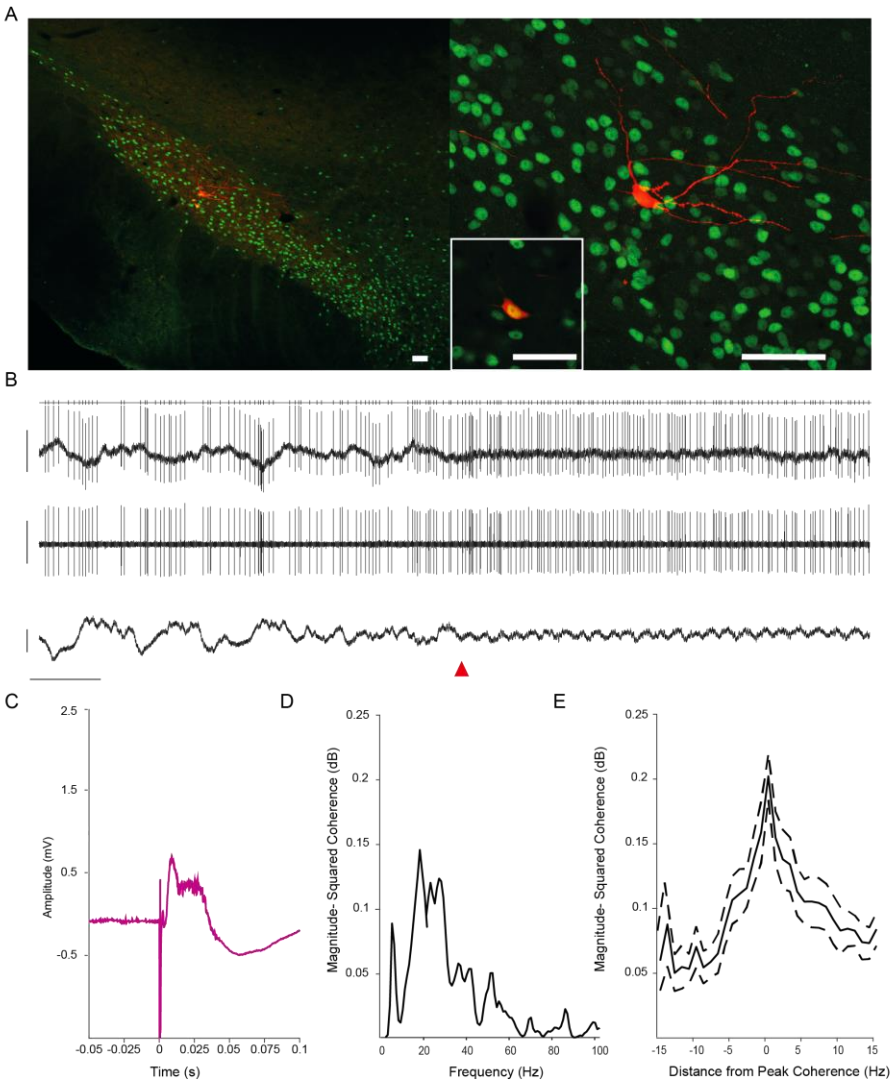

A
B
C
D
E
Amplitude (mV)
2.5
1.5
0.5
-0.5
-0.05 -0.025 0 0.025 0.05 0.075 0.1
Time (s)
Magnitude- Squared Coherence (dB)
0.25
0.2
0.15
0.1
0.05
0 20 40 60 80 100
Frequency (Hz)
Magnitude- Squared Coherence (dB)
0.25
0.2
0.15
0.1
0.05
-15 -10 -5 0 5 10 15
Distance from Peak Coherence (Hz)

Figure 4.5. Representative examples and spectral properties of STN units and LFPs in the Parkinsonian rodent. A) Immunofluorescent marker FoXP2 in green is a selective marker for STN borders (left panel, scale bar: 100 µm). On the right hand side, single plane confocal fluorescence micrographs (right panel, scale bar: 10 µm) of a subthalamic projection neuron, identified after labeling with neurobiotin (NB) expressed immunoreactivity for FoxP2 in the green channel (framed panel, scale bar: 10 µm). **B)** Spontaneously firing identified STN neuron (spike sorted binary channel: top row; row trace: middle row) and the coincidental STN local field potentials (second row) during slow wave sleep and cortical activation, as verified in ECoG recordings (bottom row). Red arrow denoted a switch in brain state from slow wave sleep to global activation. Scale bars: 1 mV and 1 s. Electrophysiological traces were recorded from the same neuron shown on (A). Note that STN neurons tend to modulate their firing rate and pattern with the cortical state. For the sake of this study, only recordings during global activation were included in the analysis. **C)** STN localisation was guided *ad hoc* the characteristic multiphasic evoked response to 1 Hz cortical stimulation. **D** 6-OHDA hemi-lesioned rodents displayed a robust peak in the 15-25 Hz range of the STN-ECoG coherence. **E** ECoG and STN LFP recordings (n= 10 animals) displayed a robust coherence in the 15-25 Hz range. To account for the variability in peak beta frequency across animals, the magnitude of power is shown as the function of the frequency distance from peak coherence, which was aligned to 0 degrees (peak).

4.3.7. Human dataset

In addition to the dataset presented in Chapter II, another set of intraoperative recordings were combine with those patients for the preferred phase analysis (16 patients from the surgical setting described in Chapter II, 7 patients from the setup described here). These recordings were made using similar experimental procedures to that described in Chapter II were carried out (Sharott et al., 2018a; includes a different analytical approach applied on the same dataset). For the sake of this chapter, I include the experimental procedure for the second dataset, as details of the first dataset are identical to Chapter II.

PD patients (characteristics described for all patients – Chapter II and Chapter IV, included in the present analysis **Supplementary Table 4.2**) undergoing DBS surgery agreed to participate recording and stimulation of STN region under local anaesthesia before the chronic DBS leads got implanted. CT-scans fused with *in situ* MRI images were used to bilaterally target the STN (11–13 mm lateral to the midline, 1–3 mm inferior and 1–3 mm posterior to the mid-commissural point on both sides). The recording setup in these patients consisted of 5 electrodes with a proximal 'micro' and a distal 'macro' tip, and the electrode bundle was lowered as a concentric array (impedance = 0.7 ± 0.2 (range, 0.2–1.25) megaOhm at 1000 Hz; FHC Inc., Bowdoinham, ME, USA) using MicroGuide targeting system by Alpha-Omega, Nazareth, Israel (Zaghloul et al., 2012).

LFP signals were recorded from both the macro- and microtip contacts that were judged to be in the STN based on physiological parameters and recording depth (Sharott et al., 2018a). The location of the recording tip was confirmed by the online assessment of a neuro-physician based on standard procedures (described in Chapter II, Moran et al., 2006). Single and multi units were also acquired from the 'microtip' contacts (see Chapter II for spike isolation and spike sorting methods).

Cortical signals were collected as part of a 32 channel system (AlphaLab, Alpha Omega Inc., Nazareth, Israel) which was used to amplify and record electroencephalographic (EEG) and electrocorticogram signals (ECoG, amplification × 4.000; band pass, 0–400 Hz for both) at a sampling rate of 3005 Hz during the microrecording and stimulation periods (Moll et al., 2015). ECoG was collected from a ball electrode, from the dura above the craniotomy, approximately over the dorsolateral prefrontal cortex and referenced to the Cz channel. Out of the 4 scalp electrodes (Ag/AgCl cup electrodes filled with conductive gel; Nicolet Biomedical, Madison, WI, USA), Fz was used for the purpose of this study. And was re-referenced to Cz. If a patient had both ECoG and Fz EEG recordings, the ECoG channel was included because of higher magnitude coherence with the STN LFP.

The data was collected as part of the localisation mapping routine, which aimed to target STN for the chronic implantation of the DBS leads. Patients were only included in this study if > 45 s, were recorded from one or both hemispheres (Sharott et al., 2014b). Only fully awake and co-operative patients were included in this study. In some recordings, patients were also performing various brief movements (flexion/extension of wrist or ankle) which served the assessment of the localisation accuracy, as part of the implementation procedure.

4.3.1. Data Analysis

Data from patient and rat recordings were analysed using similar methods. Cortical signals, either ECoG (rats) or frontocentral EEG (EEG Fz) or epidural ECoG (PD patients), and STN LFPs were used to assess how phase alignment between the two brain regions affects the amplitude of beta activity in each. Data were analysed off-line using MATLAB (Mathworks, Natick, MA). Areas of EEG or ECoG saturation were removed from the signals.

Spike removal from STN signal.

In order to analyse the influence of phase alignment on both LFP and single unit activity, these signals were extracted from the wideband signal recorded from the glass electrode. To remove spikes, a linear interpolation from 1.5 ms before to 2.5 ms following the detected spike was used. Spikes were detected as peaks at least 3.5 standard deviations above the mean of the signal (for a representative example of spike sorting, see **Fig. 4.5. B** top row).

Coherence analysis and filtering

To investigate how coherence between the STN and cortex affects beta amplitude, the peak beta coherence was defined for each recording and used to filter each signal. Coherence between the cortical (EEG or ECoG) and STN LFP was used to evaluate consistent phase differences at a range of frequencies (representative example of coherence is shown on **Fig. 4.5 D**, where peak is ~19 Hz). All signals were resampled to 500 Hz for analysis. The magnitude squared coherence between the two signals, MSCxy, was calculated by normalizing the cross-spectral density, Sxy, by the power spectra of each: MSCxy(f) = Sxy(f)2sxx(f)Syy(f). Values range from 0 to 1, with 1 representing signals that have a constant phase difference at the same frequency. The maximum coherence value between 12 and 30 Hz was defined as the peak beta coherence. Recordings with no coherence were excluded from analysis (calculation of the coherence was obtained like in Sharott et al., 2005). Signals were band-pass filtered forwards and backwards ± 5 Hz around the peak coherence frequency using a 3rd order Butterworth filter (zero-phase lag).

Analysis of the phase alignment-amplitude relationship and the cumulative effects of the phase alignment.

To investigate how beta amplitude is affected by the phase alignment between the STN and cortex, the instantaneous phase and envelope for each signal was derived using the Hilbert Transform of the filtered signals. The CircStats toolbox (Berens, 2009b) was used to calculate the instantaneous phase distance between the signals and 20 bins were used for the histograms denoting the probability of the average phase distance (**Fig. 4.6. Bi**). Next, we looked at how staying in a given phase alignment over 1-8 consecutive cycles affected the instantaneous beta amplitude. To do this, two alignments were defined, 1) the preferred phase alignment, defined as ± 90˚ from the average circular distance between the cortical and STN signal, and 2) the non-preferred phase alignment, defined as any phase distance greater than 90˚ from the average circular distance. For comparison, amplitude was also investigated for one cycle before entering a given phase alignment for epochs with consistent phase alignment for at least one cycle.

Unit analysis.

Measures of unit activity were compared during epochs when the STN LFP and cortical signals were in the preferred or non-preferred phase alignment for at least 5 cycles. Firing rate, percentage of interspike-intervals (ISI) less than 10 ms, and phase locking of units to the cortical and STN signal were analysed. Phase locking was reported as a z-score, where vector lengths were compared to 100 ISI shuffled surrogates. Wilcoxon's signed rank test was used to compare values in the non-preferred and preferred state. Post stimulus time histograms (PSTH) were calculated by averaging all trials over 20 bins (0.12 ms wide for 20 Hz and 0.15 ms wide for 25 Hz stimulation) for each representative neuron.

4. 4. Results

4.4.1. Characterizing preferred phase alignment between cortex and STN in rats.

The overall objective of this chapter was to define how the communication through coherence (CTC) theory can be applied to understand the pathological amplitude increase during coherent beta oscillations in the cortex and the STN. Our aim was to establish the likely phase alignment, and provide evidence that it can be related to the pattern of sustained power increase often correlated with symptoms in PD. To address this, we investigated the probability of certain phase alignments and described the progression of the amplitude in prevalent versus non-prevalent phase relations. To this end, we applied the same analytical framework to 6-OHDA hemi-lesioned rats as well as PD patients. To attain better insight into the local effects of certain phase alignments, we also examined the firing properties and the phase –locking (to the STN LFP and ECoG) of identified STN neurons. To provide further evidence for the relevance of the specific timing between the two oscillators, we probed these effects by delivering a low-frequency stimulation in rodents. This allowed us to interrogate the effect of an external modulatory input on the phase-specific coupling.

Periods of corticosubthalamic coherence in 6-OHDA-lesioned rats can be divided into preferred phase and non-preferred phase alignment

To test the applicability of the CTC theory on the electrophysiological features of PD, we first used 6-OHDA hemi-lesioned rats. Each animal had a prevalent phase alignment between the beta oscillation detected in the STN and cortex. In nine out of the ten rats, the most prevalent phase alignment was around 0 degrees, where the beta oscillations were in phase, while in one rat, the signals showed anti-phase relationship (180 degrees offset, **Fig. 4.6. Ai**). To account for the recordings that were dispersed from the otherwise homogeneous distribution, all calculations were aligned to the most frequently observed circular distance

for that ECoG/LFP pair (0 degrees, **Fig. 4.6. Aii**). In line with the CTC framework, we hypothesised that the most prevalent phase difference would result in elevated power of the oscillations. In line with this hypothesis, the median power of cortical and STN LFP beta oscillation was highest when the circular distance was the closest to the most likely phase alignment. This is shown by the histograms of the normalised power envelope for the distribution of possible circular distances. Both the STN LFP (**Fig. 4.6. Bi**) and the cortical (**Fig. 4.6. Bii**) amplitude were highest when the signals were aligned at their most prevalent phase lag (0 circular distance).

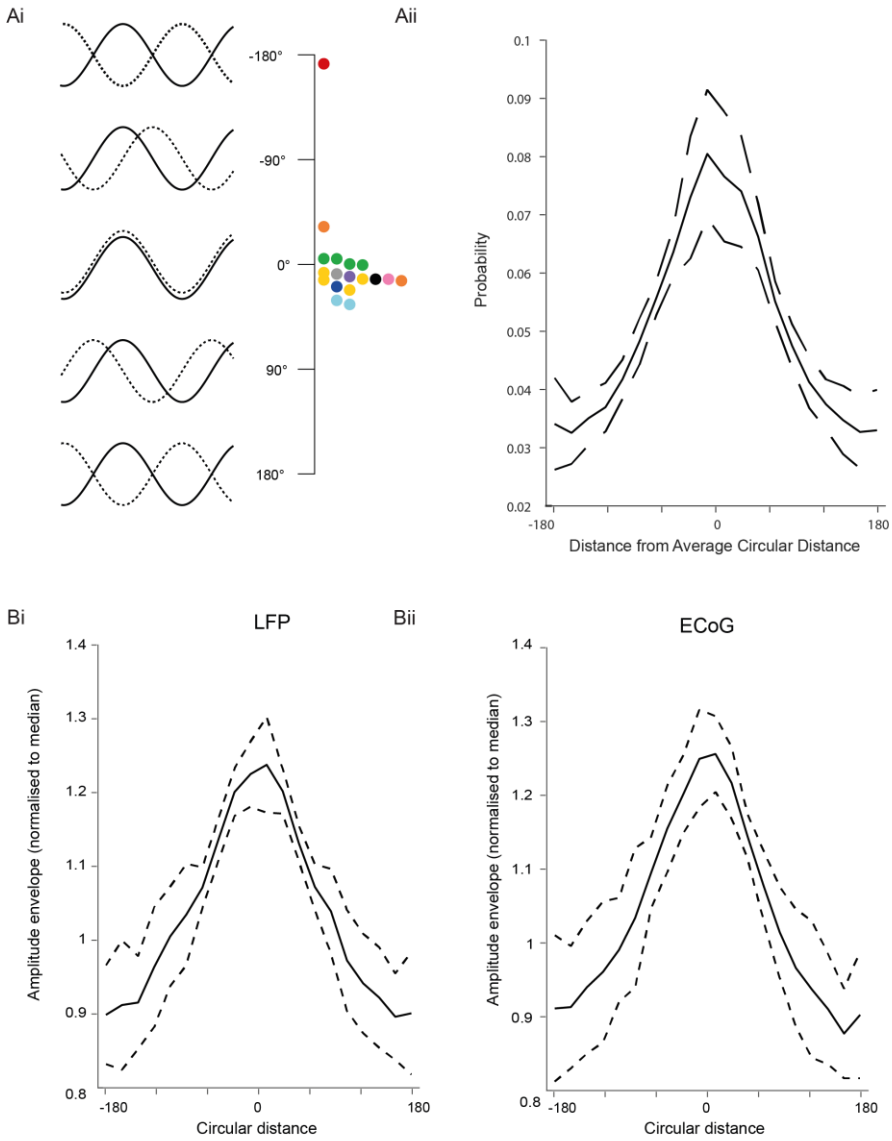


Figure 4.6. There is a prevalent phase alignment between the STN and the cortex of the 6-OHDA hemi-lesioned rodent. Ai) Schematic sine waves showing different alignment possibilities between the cortical (dotted lines) and the subthalamic LFP (solid lines) signal. Coloured dots denote the most prevalent phase alignment for each rat of the recorded sample (each recorded animal is assigned a different colour). For most of the recordings, the phase difference that occurred most frequently was around 0 degrees (aligned at the peak). **Aii**) The probability of occurrence of different phase alignments, with respect to the most common alignment (0 distance , n=10). **B**) The normalised amplitude envelope of the STN LFP (**Bi**) and the ECoG (**Bii**) for the distribution over the circular distances shown in **Aii**. Both of the signals show the highest at the most common phase alignment (n = 10, number of animals).

Ultimately, sustained periods of likely phase alignment are characterised by high beta power for both structures in the 6-OHDA hemi-lesioned rats. When the cortical and subthalamic signals were aligned at their most likely phase difference for a sustained period of time, we assigned the term '**preferred phase alignment**' (± 90 degrees from most likely alignment, denoted by pink shading throughout the chapter). Conversely, the phase differences occurring on the other 180 degrees of the circle were classified as '**non-preferred phase alignment**' (denoted by grey shading). In a characteristic example depicted on **Fig. 4.7 Ai**, the most prevalent phase alignment is at the peak (0 degrees). The filtered LFP and ECoG trace show how recordings could be split into preferred (pink) and non-preferred alignment (**Fig. 4.7 Aii**).

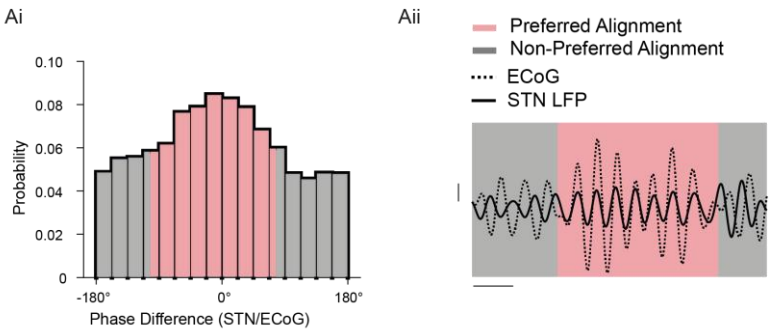


Figure 4.7. Dividing corticosubthalamic recordings according to preferred and non-preferred phase alignment Ai) Phase difference was obtained by calculating the circular distance between the two signals. The probability of the occurrence of a certain alignment is shown on a probability histogram over 20 bins. In case of this example, the most likely phase alignment occurred at the peak (in-phase, 0 phase lag) **Aii)** Example traces of ECoG (dashed line) and STN LFP (solid line), filtered around the peak beta coherence of the two signals. Different coloured epochs are showing frequently occurring (denoted by pink highlight) and less frequently occurring (grey highlight) phase alignment epochs. Scale bars: 10 mV and 100 ms

To test the assumption that the cortico-subthalamic pathway is modulated by the parameters of synchronisation we first defined the amplitude progression of epochs of sustained preferred and non-preferred phase alignment.

The amplitude of beta oscillations increases and stays elevated during sustained epochs of preferred phase alignment

In the rat dataset, cortico-subthalamic coupling at preferred phase lasted for longer and was sustained over larger number of beta cycles (**Fig. 4.8. Ai** and **Aii**). The cortical and subthalamic signals spent significantly more time at the preferred phase alignment (68.01% ± 4.72% of the entire recording, Wilcoxon signed rank test $p>0.001$). Furthermore, the preferred phase alignment epochs tend to last for more cycles (preferred cycle length: 3.68 ± 1.01; non-preferred cycle length 1.73 ± 0.42, Wilcoxon signed rank test $p > 0.001$). This provides further evidence that there are sustained periods of non-likely as well as likely phase alignment in lesioned rats. To investigate whether the beta amplitude changed throughout sustained preferred and non-preferred phase alignment periods, we compared the normalised amplitude of the cortical and STN LFP during consecutive cycles of both (**Fig. 4.8 B** panels). Group results of the progression of the amplitude changes are shown on **Fig. 4.8 Bi** for STN and **Fig. 4. 8 Bi,ii** for ECoG beta amplitude. Regardless of starting from a lower baseline, both cortical and STN LFP median beta amplitude increased robustly when the two signals were at their preferred beta phase (**Fig. 4.8.,** pink line, Kruskal-Wallis test, $H(5) = 46.57$ $p < 0.001$ for Bii (LFP) and $H(5) = 44.31$ $p < 0.001$ for Bii (ECoG)). Compared to baseline (–1 cycle), the amplitude of the cortical beta increased by 34.52% (Wilcoxon matched pair test, $p< 0.001$), whereas the amplitude of the STN LFP increased by 32.93 % (Wilcoxon matched pair test, $p< 0.001$) by the 2^{nd} , already locked cycle of the given phase alignment. The timecourse during the preferred phase alignment was identical for ECoG and LFP power: the biggest increase was seen from 1^{st} to 2^{nd} cycle, but the effect plateaued after the 3^{rd} consecutive cycle the signals spent at the preferred alignment. Additionally, this finding supports the rationale for choosing a minimum of 3 cycles as an inclusion criterion.

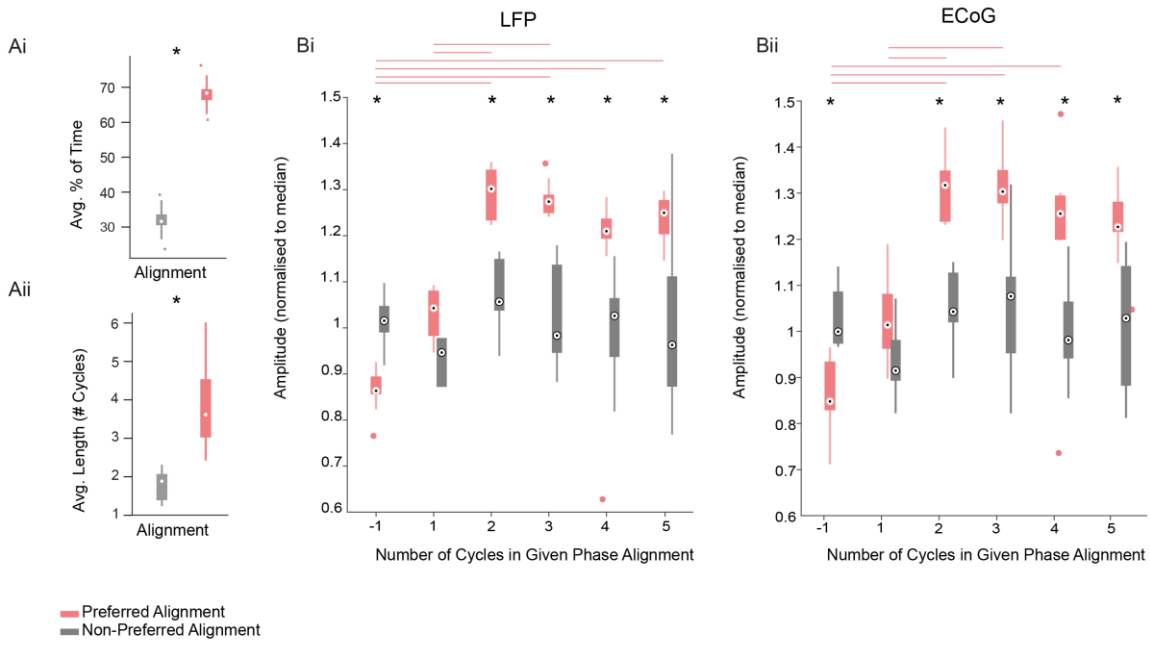


Figure 4.8. Preferred phase alignment correlates with longer, elevated and sustained beta power in 6-OHDA hemilesioned rats. A) Over the whole recordings, STN LFP/ECoG synchronisation at the preferred phase occurs for more than twice as long as non-preferred phase (Ai) and preferred phase last significantly more cycles than non-preferred phase synchronisation. Stars denote $p< 0.01$ on Wilcoxon rank sum test for n= 14 (number of recording positions) **B)** Progression of beta amplitude envelope during preferred and non-preferred phase alignment from one cycle before entering a given phase alignment for the first five cycles of the give alignment for 6-OHDA hemi-lesioned rodents (n=10, number of rats). Following two cycles of preferred phase alignment, the amplitude of the beta oscillation ramps up (from -1 cycle to 2nd cycle) and stays elevated (2nd to 5th cycle) for both the ECoG power (**Bi**) and the LFP power (**Bii**). Statistics for multiple comparison within the phase alignment was tested by Kruskal Wallis test ($H(5) = 44.31$ $p < 0.001$ for Bi (ECoG) and $H(5) = 46.57$ $p < 0.001$ for Bii (LFP). Non-preferred phase alignment does not correlate with such change in the beta amplitude (Kruskal Wallis test $H(5) = 9.29$ $p = 0.0982$ for Bi (ECoG) and $H(5) = 8.47$ $p = 0.1321$ for Bii (LFP). Horizontal lines in the colour of the corresponding phase alignment indicate differences between the cycles (corrected for multiple comparisons using the false discovery rate, $p \leq 0.05$). Black stars denote $p< 0.01$ between the phase alignment cases for each cycle (False Discovery Rate (FDR) -adjusted Wilcoxon signed rank test). Statistical comparisons are summarised in **Supplementary Table 4.3.**

On the other hand, no such pattern was observed during the non-preferred phase alignment, in which the power of the 2nd cycle only increased by less than 5% compared to baseline for both recorded signals (Kruskal Wallis test, $p > 0.05$). The power during the non-preferred phase alignment decreased slightly after the signals locked at their non-preferred phase alignment (-1 cycle compared to the 1st cycle spent in the non-preferred alignment: -9.8 % in the ECoG power, Wilcoxon rank sum test $p = 0.0173$; -8.8 % in the LFP power, Wilcoxon rank sum test $p = 0.0257$), and stayed low for the rest of the cycles. In summary, non-preferred phase alignment was associated with an initial decrease in beta amplitude, which then returned to baseline and remained constant for subsequent cycles.

There was a clear difference in the progression of the amplitude envelope between the two signals during preferred and non-preferred alignment. Statistical comparisons between the two phase alignments confirmed that the beta amplitude was robustly higher in the preferred phase alignment (Wilcoxon signed rank test, FDR adjusted, **Supplementary Table 4.3**). Normalised amplitude of the non-preferred alignment's was significantly higher than the baseline amplitude (-1th cycle) for the preferred-phase (Wilcoxon signed rank test, FDR adjusted , $p = 0.0004$ for ECoG and $p = 0.0004$for LFP). Regardless of starting on a lower baseline, amplitudes measured over the 2nd through to the 5th cycle were significantly lower for the non-preferred phase alignment than for the preferred alignment for both the STN LFP (**Fig. 4.8 Bii**) and the ECoG power (**Fig. 4.8Bi**, summary of statistics in **Supplementary Table 3**.). In particular, the highest value of beta amplitude was more than threefold higher in the preferred phase alignment than the highest power measured at the non-preferred alignment.

Preferred phase alignment affects the phase locking but not the firing rate of identified STN neurons

To investigate the effect of phase alignment on the firing properties of the identified STN neurons, we first looked at the firing rate (FR). There was no significant change between preferred and non-preferred alignment for n=14 neurons (FR during preferred phase 17.93 ± 16.47; FR during non-preferred phase = 17.72 ± 5.49, **Fig. 4.9. A** Wilcoxon signed rank test, p = 0.98167). Next, we looked into whether there was a change in how the timing of action potentials was locked to a specific phase of the ongoing oscillations. During sustained (>= 4 cycles) of preferred alignment, the locking of STN units to the STN LFP was significantly stronger compared to the non-preferred alignment (**Fig. 4.9 C**, Wilcoxon signed rank test p = 0.0017). The relationship was weaker in relation to the cortical signal. (**Fig. 4.9 B**, Wilcoxon signed rank test p = 0.03).

Phase-dependent effect of 20 Hz cortical stimulation on oscillatory power and identified single unit activity in STN

Next we used 20/25 Hz stimulation was to test whether the amplitude during a specific phase alignment can be selectively perturbed or modulated by an external oscillatory input. Beta frequency stimulation of the cortex provided a uniform source of input to the STN, allowing us to test how amplitude is affected when one oscillation is selectively driven away from the naturally occurring phase alignments. To address this, we first had to establish whether the 20 Hz cortical stimulation is sufficient for eliciting a modulatory effect on the local population in the STN without prominent silencing.

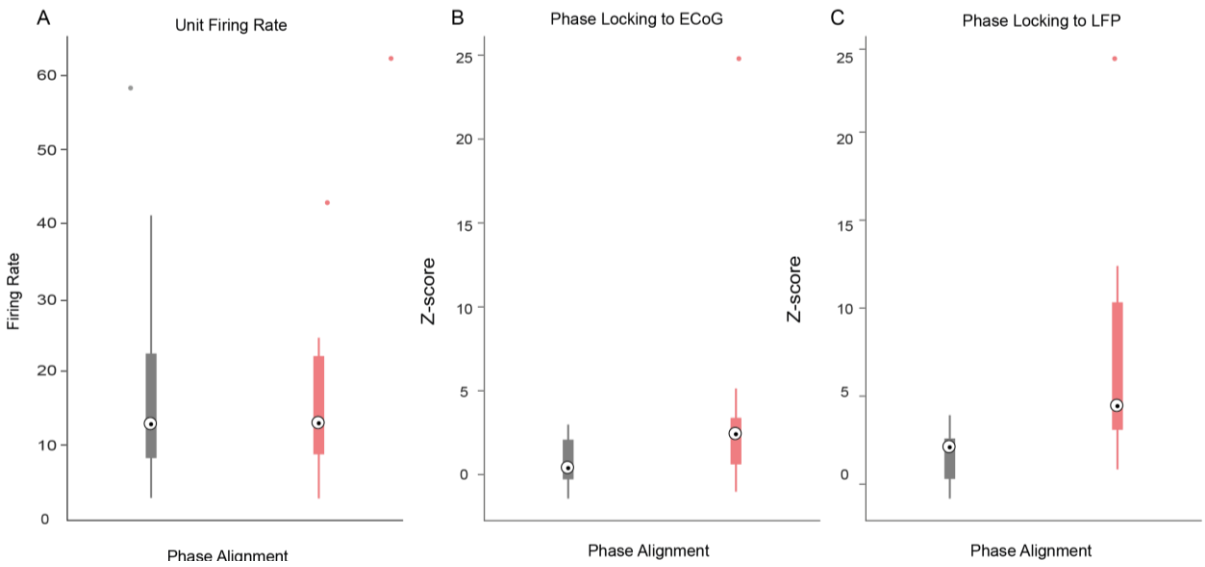


Figure 4.9. Changes in firing properties of identified single STN neurons during preferred and non-preferred alignment. A) There was no significant change in the firing rate of identified single neurons between preferred (pink box) and non-preferred (grey box) alignment (Wilcoxon signed rank test p = 0.98167). However, during periods of preferred alignment (pink box), phase locking of STN units to the STN LFP was significantly stronger than during non-preferred alignment (Wilcoxon signed rank test p = 0.0017) (**C**) but not to the cortex (Wilcoxon signed rank test, p = 0.030818) (**B**). Phase locking is shown as a Z-score calculated by comparing the locking to 100 times shuffled inter stimulus interval surrogates at the given alignment. Stars denote significant p-values on the Wilcoxon signed rank test.

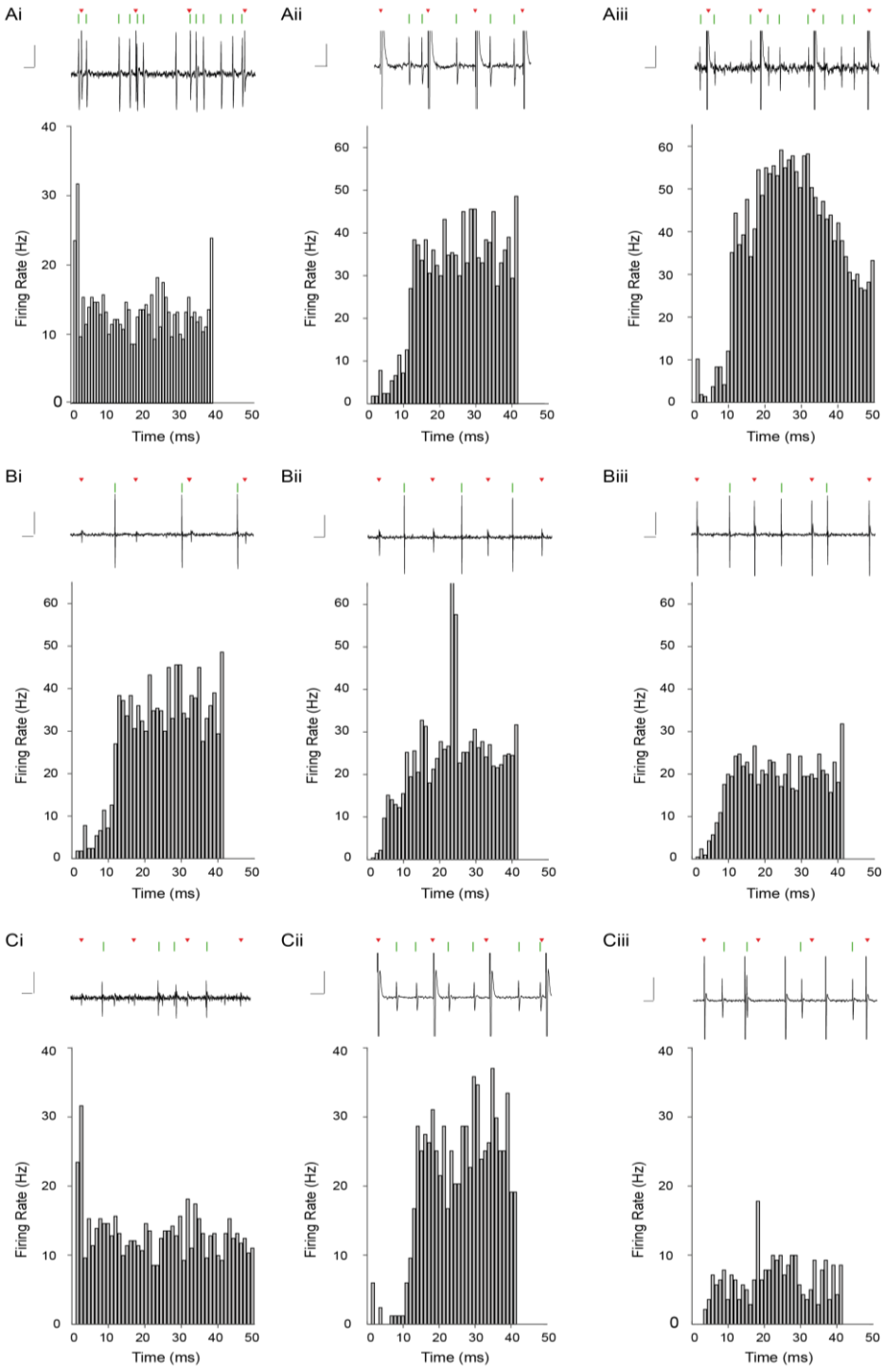

Ai
Aii
Aiii
Bi
Bii
Biii
Ci
Cii
Ciii
Firing Rate (Hz)
Time (ms)

Figure 4.10. Post Stimulus Time Histograms (PSTH) of identified STN neurons responding to matched beta frequency beta-frequency stimulation of the motor cortex in rodents. Each subplot shows the averaged and binned (1 ms wide bins) firing rate (Hz) of identified single neuron. Above the PSTHs, a representative raw trace from the same neuron is shown. The green lines denote the spike times and the red arrows represent the squared stimulation pulse. 20 Hz stimulation was delivered for **Aiii** and **Ci**, the rest of the traces is of 25 Hz stimulation. The frequency was chosen to try and match that of the ongoing beta oscillation. The first row displays the three most commonly observed pattern of response to 20/25 Hz stimulation: initial excitation (**Ai**), inhibition (**Aii**) and multiphasic response (**Aiii**). Scalebars: 1 ms and 0.5 mV. The second row shows amplitude dependent responses of the same neuron responding to 50 (**Bi**), 100 (**Bii**) and 250 (**Biii**) µA stimulation (scale bars: 1 ms and 0.5 mV). Finally, the third row shows responses from different recording position: **Ci** is the most rostral (scale bar: 1 ms and 0.5 mV), **Cii** is centre and **Ciii** is from the most caudal recording position (scale bars for both 1 ms and 1 mV)

4.4.2.Effect of beta frequency stimulation in 6-OHDA hemilesioned rodents

Firing properties during 20 Hz cortical stimulation without the phase alignment

To establish the downstream effects of the cortical beta frequency stimulation, we calculated the post stimulus time histograms (PSTH) for all recorded and juxtacellularly labelled STN neurons. **Fig. 14.10** is showing the representative examples. Firstly, we found that 20 Hz continuous cortical stimulation did not silence the neurons, neither did it cause a significant change in the mean firing rate over (full length of stimulation versus spontaneous periods, Wilcoxon signed rank test, p= 0.8968). Instead, most of the units were modulated by the cortical stimulation by showing a pattern of initial, short latency excitation (**Fig. 4.10 Ai**), initial inhibition (**Fig. 4.10 Aii**) or multiphasic responses (**Fig. 4.10 Aiii**). These categories closely resemble our observations in human patients (discussed in Chapter II). Secondly, for most recordings, neurons modulated their responses in an amplitude dependent manner (**Fig. 4.10 Bi-Biii**). Generally speaking, stimulation-evoked responses could be observed at the minimum of 50 µA stimulation (**Fig. 4.10 Bi**), elicited high entrainment around ~100 µA (**Fig. 4.10 Bii**) and reduced the firing rate for 250 µA and above (**Fig. 4.10 Biii**). Therefore, 50-250 µA stimulation range was implemented in this study. A major advantage of the juxtacellular recoding method that it allowed for the precise localisation of the recording electrode, hence we could exclude the possibility of sampling from only one region of the STN. Mapping of all recording positions clearly demonstrated that units and LFPs were sampled over a wide range of positions throughout the rostro-caudal axis of the STN (**Fig. 4.4.**). Accordingly, modulation each type of response could be observed in the rostral (**Fig. 4.10 Ci**), central (**Fig. 4.10 Cii**) and caudal recording positions (**Fig. 4.10 Ciii**).

In summary, PSTH results revealed that 20 Hz cortical stimulation is adequate to elicit modulatory responses that are amplitude and location dependent in the STN. The setup established is hence suitable to investigating the effect of an external modulation on the specific phase-alignment.

There is preferred and non-preferred phase alignment during low frequency stimulation of the cortex.

Next, we defined the characteristics of corticosubthalamic phase alignment in the presence of cortical beta frequency stimulation. Due to the smaller sample size of the stimulated recordings, we had to ensure that the stimulation sample was sufficiently matched to the control data. Hence, we recalculated the analysis of spontaneous data, only including recordings that were collected from the same site as recordings with stimulation. We plotted the coherence and the probability distribution of the phase differences between the two signals during the continuous beta frequency stimulation of cortex (**Fig. 4.11 A**). The magnitude of coherence during 20 Hz stimulation was significantly higher than in the spontaneous cases (Wilcoxon rank sum test $p = 0.0286$; **Fig. 4.11 A**). Additionally, the probability distribution was similar to that observed in spontaneous recordings: some circular differences were more prevalent than others during 20 Hz stimulation (**Fig. 4.11 B**). However, in comparison to the spontaneous cases, both the cortical power (**Fig. 4.11 Ci**) and the STN LFP (**Fig. 4.11 Cii**) showed a less peaked distribution over the most probable alignment (0 degree difference). In other words, we failed to find similarly prominent distribution of power increase at likely phase alignment during external stimulation. These results indicate that during periods of high coherence, there is preferred and non-preferred phase alignment during beta-frequency stimulation.

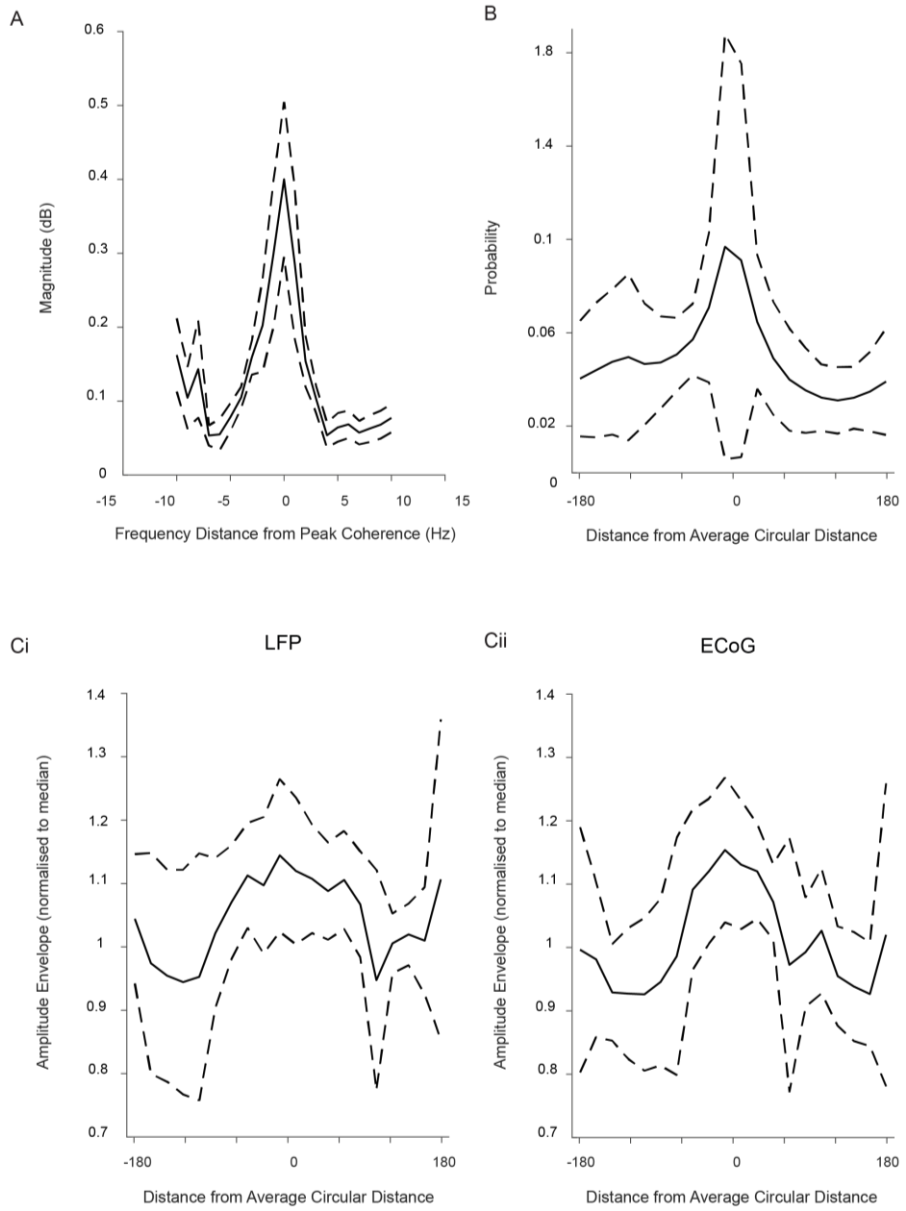


Figure 4.11. Beta coherence and more prevalent phase alignment are maintained in the cortex and STN during beta frequency stimulation of cortex. A Spectral properties of the rodent dataset during beta frequency stimulation. Increased coherence values at beta frequency were displayed between the STN and the cortical ECoG during continuous, matched-frequency cortical stimulation. Magnitude of power is shown as the function of the frequency distance from peak coherence, which was aligned to 0 degrees (peak). **B** The probability of the all phase alignments in relation to the preferred phase alignment is plotted for recordings with 20/25 Hz continuous stimulation (n=10). Panel **C** shows the normalised amplitude envelope of the ECoG (**Ci**) and the STN LFP (**Cii**) for the distribution over the average circular distances during stimulation. Both of the signals show the highest amplitude during 0 phase lag, albeit the distribution is more even than that observed in the spontaneous data (both signals are aligned at their peak, n=10).

Amplitude progression during 20/25 Hz stimulation shows marked differences to matched spontaneous recordings

Next we compared the cycle-by-cycle differences in amplitude for the two phase alignments during stimulation to those of the location matched spontaneous data. The analysis on 'matched' spontaneous data were very similar to those observed with the complete spontaneous dataset (**Fig. 4.12**). Preferred phase alignment was significantly longer (**Fig. 4. 12 Ai**), lasted over more cycles (**Fig. 4.12 Aii**), and showed a progressive amplitude increase for both recorded signals (**Fig 4.12 Bi and Bii**, pink boxes, Wilcoxon signed rank test $p < 0.05$ for both comparisons). On the other hand, non-preferred alignment lasted shorter and even over many cycles of alignment did not result in significant power increase for neither of the signals (**Fig 4.12 Bi and Bii**, grey boxes).

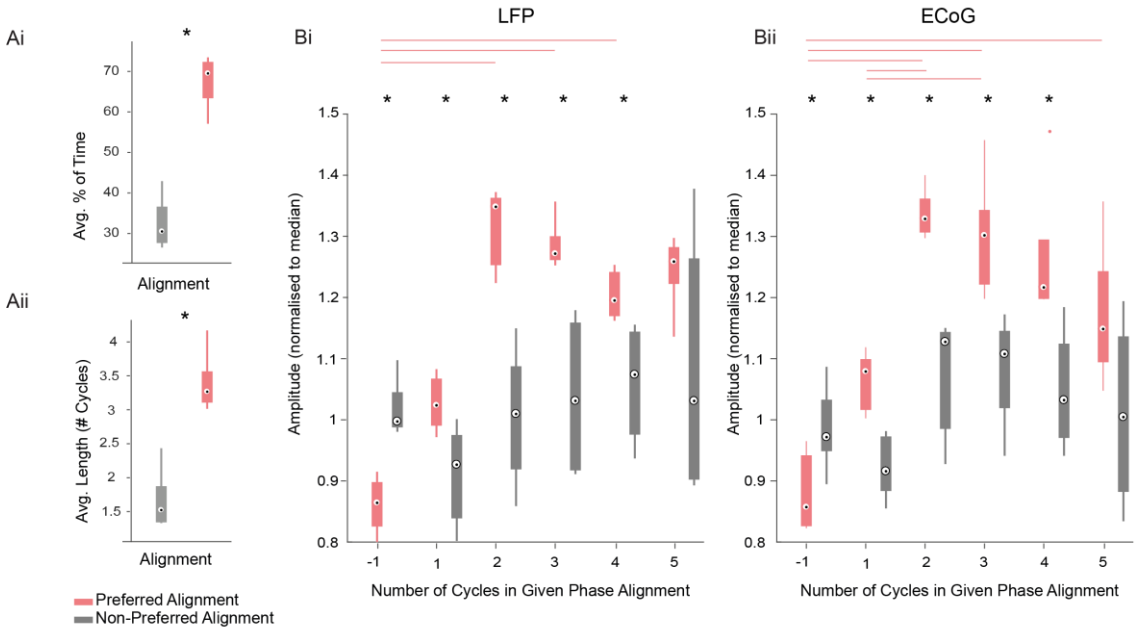


Figure 4.12. Characteristics of preferred and non-preferred phase alignment during the 'matched' spontaneous recordings from the same exact location of the stimulated data. A) Description of the basic characteristics of preferred (pink boxes) and non-preferred (grey boxes) phase alignment. There is a significant difference between the percentage of the average time (**Ai**) and the number of cycles (**Aii**) spent at preferred versus non-preferred phase alignment. Stars denote $p < 0.01$ on Wilcoxon rank sum test for n= 10 (number of recording positions). **B)** Following two cycles of preferred phase alignment, the amplitude of the beta oscillation increases from -1th cycle to 3rd cycle for both the LFP power (**Bi**) and the ECoG power (**Bii**, n= 5, number of rats). Non-preferred phase alignment does not correlate with such change in the beta amplitude. At preferred phase alignment, both ECoG and LFP signal increase steeply after the 3rd cycle in comparison to the non-preferred phase alignment. Horizontal lines in the colour of the corresponding phase alignment indicate differences between the cycles (probed with Kruskal Wallis test, corrected for multiple comparisons using the false discovery rate, $p \leq 0.05$). Black stars denote $p < 0.01$ between the phase alignment cases for each cycle (False Discovery Rate (FDR) -adjusted Wilcoxon signed rank test). Statistical comparisons are summarised in **Supplemental Table 4.3.**

After having established a matched control, it was possible to investigate the temporal features of the phase alignments and the amplitude progression displayed by the STN and the cortex during externally driven input. We first investigated whether beta-frequency cortical stimulation could alter for how long the two signals couple at their preferred phase (**Fig. 4.13 A**). During beta stimulation neither the average time (**Fig. 4.13. Ai**), nor the number of cycles spent at the certain alignment (**Fig. 4.13Aii**) were significantly different between preferred and non-preferred phase alignments compared to the spontaneous matched recordings (Wilcoxon signed rank test n=10, recording positions). Next, we probed the progression of the amplitude envelope for both signals during stimulation. To gain a better insight into whether the modulation external input lead to changes in beta amplification, we plotted the progression of the on the amplitude for both the preferred and the non-preferred phase alignment (n= 5, number of rats, **Fig. 4.13. Bi,ii**). The ECoG power envelope progression retained almost identical pattern during stimulation (**Fig. 4.13 Bii** Kruskal Wallis test $H(5)= 16.13$, $p = 0.0065$ for preferred phase and $H(5)= 2.14$, $p = 0.83$ for non-preferred phase). Importantly, power was lower for all cycles during non-preferred alignment compared to the preferred alignment.

Per contra, none of the power comparisons between the phase alignment cases were significantly different with regards to the STN LFP (**Fig. 4.13 Bi**, Wilcoxon signed rank test are all n.s.). Phase-alignment specific power progression in the STN LFP was not modulated significantly by the beta frequency stimulation (preferred phase alignment: Kruskal Wallis test $H(5)=10. 16$, $p= 0.0708$; non-preferred phase alignment: $H(5)=9.35$, $p= 0.0958$). The subthalamic power, as opposed to the controls, did show a pattern of increase over consecutive cycles during cortical stimulation for both alignment cases, but this effect was not significant. However, we did see change in the pattern of the LFP power progression during stimulation in comparison to the controls. On the spontaneous matched recordings,

we could see that the power is significantly higher at the preferred phase from the 1st to the 4th cycle of alignment (Wilcoxon signed rank test corrected with FDR, $p>0.05$). By comparison, the cycle-by-cycle power between preferred and non-preferred phase alignment during beta frequency stimulation was not significantly different (Wilcoxon signed rank test corrected with FDR, all n.s.). This indicated that externally patterned input diminished the phase-alignment inflicted power differences over many cycles of concomitant phase alignment (**Supplementary Table 4.3**).

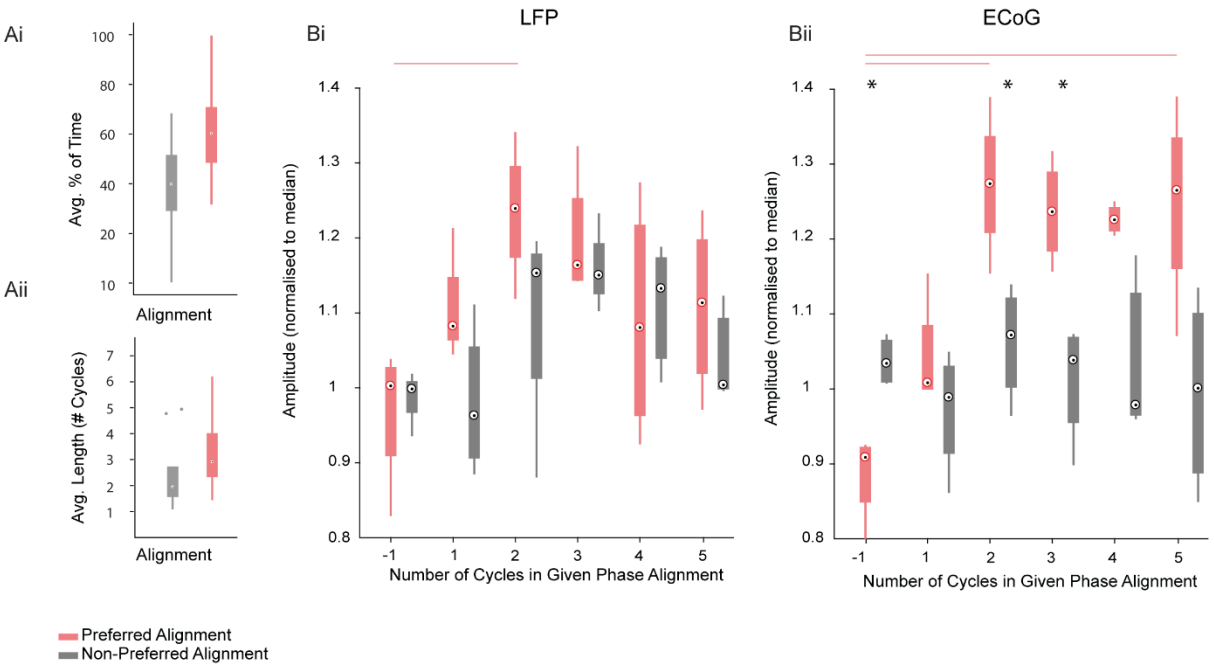


Figure 4.13. Characteristics of preferred and non-preferred phase alignment during continuous low-frequency cortical stimulation in 6-OHDA hemi-lesioned rats. A) Description of the basic characteristics of preferred (pink boxes) and non-preferred (grey boxes) phase alignment during 20/25 Hz stimulation. There is no significant difference between the percentage of the average time (Ai) nor the number of cycles (Aii) spent at preferred versus non-preferred phase alignment, n= 10 (number of recordings). **B)** Progression of beta amplitude envelope during preferred and non-preferred phase alignment from one cycle before entering a given phase alignment through the first five cycles of the give alignment during low-frequency stimulation n=5 (number of rats). **Bi**) The power of the STN LFP for both preferred and non-preferred alignment show progressive power- increase by the 3rd cycle, however these effects are not significant, with the exception of the power comparison between the -1 to the 2nd cycle during preferred phase alignment. Note that there are also no significant differences between the power of preferred and non-preferred cycles **Bii)** Following two cycles of preferred phase alignment, the amplitude increases and stays elevated for the cortex (**Bii**). Non-preferred phase alignment in the cortex does not show similar pattern. Horizontal lines in the colour of the corresponding phase alignment indicate differences between the cycles (corrected for multiple comparisons using the false discovery rate, $p \leq 0.05$). Black stars denote $p < 0.01$ between the phase alignment cases for each cycle (False Discovery Rate (FDR) -adjusted Wilcoxon signed rank test, summarised by **Supplementary Table 4.3**).

4.4.3. Establishing the effect of preferred and non-preferred phase alignment in PD patients

In order to study whether the findings described above translated to human PD, we derived the same analysis on signals acquire from patients undergoing chronic implantation of DBS electrodes (**Supplementary Table 4.2.**).

Characterisation of the preferred phase in PD patients.

Despite greater heterogeneity in the recoding positions in intraoperative recordings, as compared to experimental animals, the distribution of the most likely phase alignments was fairly consistent across recording positions and patients (**Fig. 4.14. A** panels). To capture the homogeneity within the sample, the mode of all recording position was plotted for each patient (**Fig. 4.14 Aii**). The angle of the most prevalent phase alignment was characteristic to each individual. The most prevalent alignment between the cortex and the STN signal occurred around 200 degrees. Thus, the probability distribution of the phase differences occurring between the cortical and subthalamic signals in human PD patients showed similar within-sample distribution, but at a different angle to the rat sample (**Fig. 4.14 B**). This formed the foundation for further investigating the relationship between the phase differences and the power of beta oscillations in those structures. Human recordings also displayed the highest power envelope over the most probable phase differences for both the STN (**Fig. 4.14 Ci**) and the cortical signal (Fig**. 4.14 Cii**). This allowed us to split the human DBS recordings into preferred and non-preferred phase alignment using the same methods established using the rat dataset.

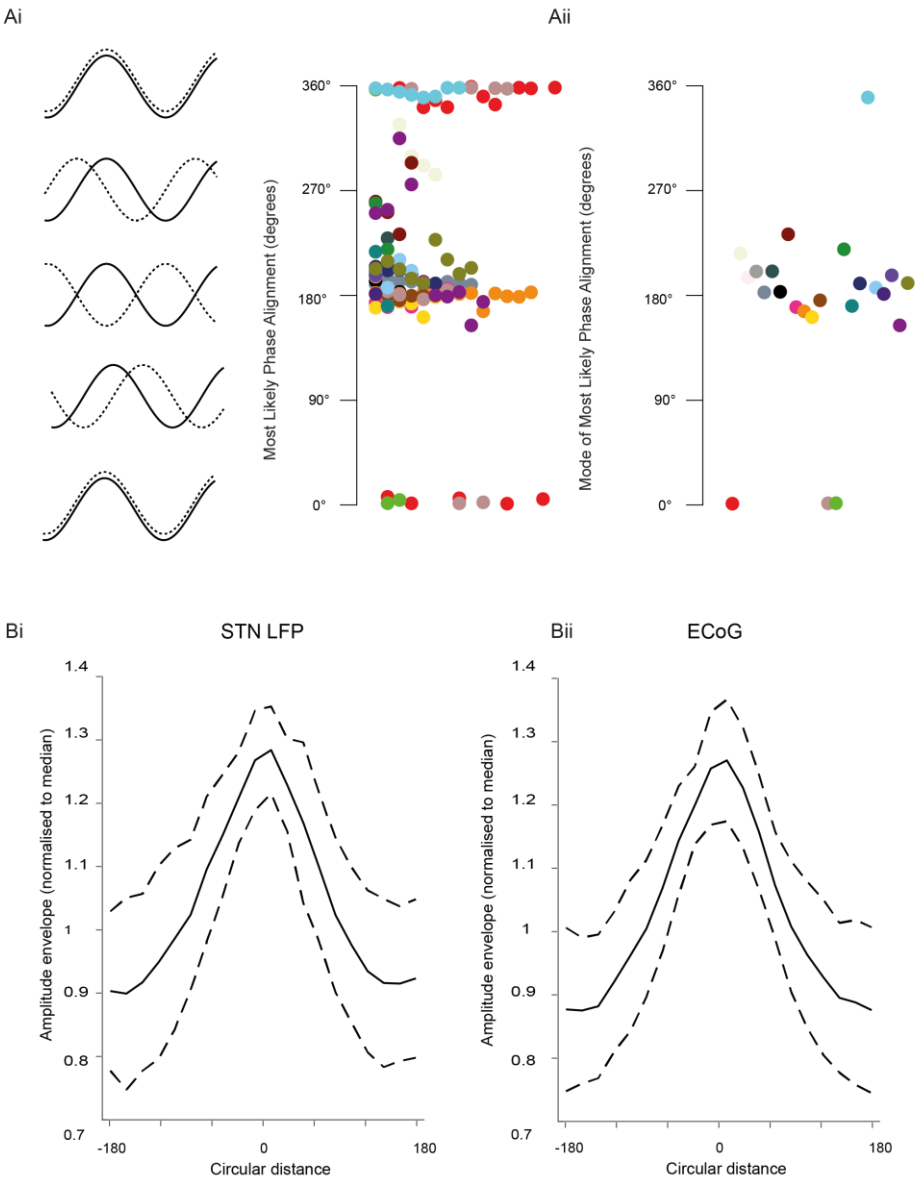


Figure 4.14. Probability of phase alignment and associated amplitude envelope across the distribution of circular distances in the PD patients. **Ai)** The most common alignment between the cortex and the STN in human patients. The colourful dots denote all recording positions (n = 131, number of recordings) **Aii)** The mode of the most common alignment per patients. The most likely alignment across the sample occurred around 200 degrees (n=23, number of patients). Circular distance values were shifted to zero phase difference for all recordings before averaging. Panel **B** shows the normalised amplitude envelope of the STN LFP (**Bi**) and the ECoG/EEG Fz (**Bii**) for the distribution over the average circular distances (n=23, number of patients).

Progressive changes in beta power during preferred and non-preferred phase alignment in PD patients

After defining the periods of preferred and non-preferred phase alignment for the human patients, we investigated whether there is a difference in overall time spent at a given alignment (**Fig. 4.15 A**). For the human patients (n=23), the STN LFP and cortical activity tend to be at their preferred phase for longer (**Fig. 15 Ai**) and for more cycles (**Fig. 15Aii**). The two signals engage in preferred phase alignment for 71.1 ± 0.1 % of the time for 2.6 cycles longer, which is significantly higher than time spent at the non-preferred alignment (for both, Wilcoxon signed rank test $p > 0.001$). This result tallies with what has been observed on the 6-OHDA hemi-lesioned rats.

The amplitude progression in patients was remarkably similar to that observed with the 6-OHDA hemi-lesioned rats. Both in case of the STN LFP and the cortical (ECoG or EEG Fz), a different pattern of amplitude progression could be observed in respect to the preferred versus non-preferred alignment (**Fig. 4.15 Bi,ii** cortical activity). During preferred phase alignment, the power of both signals 1) significantly increased compared to the cycle preceding, 2) increased steeply by the 3rd cycle, and 3) this increase remained unchanged between the 3rd and the 5th cycle (Kruskal Wallis test for the preferred phase alignment Bi, $H(5) = 83.3$ $p < 0.001$ and for Bii $H(5) = 94.88$ $p< 0.001$ for the non-preferred phase alignment, for multiple comparisons, see **Supplementary Table 4.3.**). Conversely, the power decreased during the first cycle spent at non-preferred phase alignment (grey box), returned to baseline by the second cycle and did not increase further between the 3rd and the 5th cycle. This effect could be observed for both the STN LFP and the cortical signal (**Fig. 4.15.**, Kruskal Wallis test for the non-preferred phase alignment Bi (STN LFP), $H(5) = 14.92$ $p = 0.0107$ for Bii (ECoG) $H(5) = 22.79$ $p= 0.0004$). Post-hoc comparisons showed that this was caused by the slight decrease in power as the two oscillators entered non-preferred

phase alignment (comparison between the -1 cycle to the 1st cycle spent in non-preferred alignment was $p = 0.015$ for the STN LFP and $p = 0.003$ for the cortical power, **Supplementary Table 4.3**.). The normalised power, however, remained close to baseline throughout all cycles of the non-preferred phase alignment. The maximum power difference between the two phase alignments could be observed during the second cycle of preferred alignment of the ECoG power (27.64 %) and during the third cycle of the STN LFP power (48.72% difference). The power was consistently dissimilar between the two phase alignment periods, and was significantly higher in the preferred versus non preferred phase alignment for both the STN LFP and the cortical power (summary of FDR corrected Wilcoxon signed rank tests, **Supplementary Table 4.3**.).

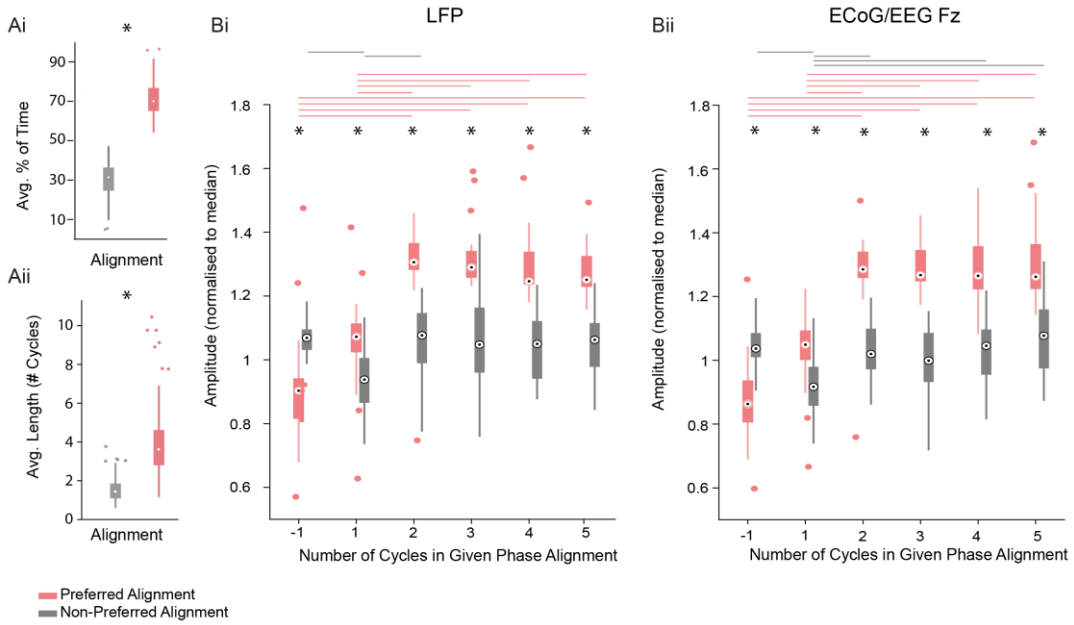


Figure 4.15. Preferred phase alignment correlates with longer, elevated and sustained beta power in PD patients. A) Description of the basic characteristics of preferred (pink boxes) and non-preferred (grey boxes) phase alignment in human patients. STN LFP and the cortical signal tend to spend longer (**Aii**, depicted as the function of the percentage of the time spent in the given alignment in respect to the length of the whole recording) and more cycles (**Aii**) at the preferred alignment compared to the non-preferred alignment. Stars denote $p < 0.01$ on Wilcoxon rank sum test for n= 23 (number of recordings). **B)** Progression of beta amplitude envelope during preferred and non-preferred phase alignment from one cycle before entering a given phase alignment for the first five cycles of the give alignment for PD patients (n=23, number of patients). Following two cycles of preferred phase alignment, the amplitude of the beta oscillation rises and stays elevated for both the cortical (**Bi**) and the LFP (**Bii**) power. Statistics for multiple comparison within the phase alignment was tested by Kruskal Wallis test and were $p < 0.001$ for all comparisons. Non-preferred phase alignment does not correlate with such change in the power envelope. Albeit starting on a lower baseline, both ECoG and LFP signal increase steeply after the 2nd, and stay elevated after the 3rd cycle in comparison to the non-preferred phase alignment. Horizontal lines in the colour of the corresponding phase alignment indicate differences between the cycles (corrected for multiple comparisons using the false discovery rate, $p \leq 0.05$). Black stars denote $p < 0.01$ between the phase alignment cases for each cycle (False Discovery Rate (FDR) -adjusted Wilcoxon signed rank test, summarised by **Supplementary Table 4.3**.).

4.5 Discussion

4.5.1. There is preferred phase alignment between the cortex and the subthalamic nucleus of parkinsonian animals and PD patients

Many studies have demonstrated that dopamine depletion increases corticosubthalamic beta coherence (Williams et al., 2002; Fogelson et al., 2006; Lalo et al. 2007 Mallet et al., 2008). Here we used two data sets, in parkinsonian animals and PD patients, with strong beta frequency coherence. The detection of significant coherence, which increases with phase consistency between two signals, already indicates that there is a "preferred" phase alignment at beta frequency. These preferred phase alignment epochs occur for longer and more frequently that the non-preferred relationship. Importantly, however, we demonstrate that there are sustained epochs where the non-preferred alignment occurs. As predicted by the communication by coherence framework, the epochs where the preferred phase alignment occurs are associated with modulation of the oscillation amplitude, whereas non-preferred phase alignment is not. These results demonstrate that pathological cortico-subthalamic coupling in PD follows the same principals as cortico-cortical (Fries, 2005; Womelsdorf et al., 2012) and cortico-spinal (Schoffelen et al., 2005) coupling in the healthy brain.

4.5.2. Defining the time course of amplitude and synchronisation of pathological beta oscillations

Here we provide a description of the progression of the beta amplitude during epochs of preferred and non-preferred phase synchrony. In both 6-OHDA lesioned rats and human PD patients, there was an abrupt increase in power during the second cycle of preferred phase alignment, and this amplification was then sustained over subsequent cycles. This is temporal evolution of phase synchronisation and power is important, because it indicates that the former precedes the latter. While this analysis does not prove causation, it is

suggestive that a specific alignment of cortical and subcortical oscillators that can leads to more powerful and sustained oscillatory epochs in both structures. Such a relationship has previously been observed between STN and GP LFPs in PD patients (Cagnan et al., 2015). Given that STN and GP are reciprocally connected (Carpenter et al., 1981), it is not surprising that phase-dependent amplification occurs at both sites. The anatomical relationship between cortex and STN, however, is very different. Cortical neurons project monosynaptically to STN, whereas STN can only influence cortex through polysynaptic circuits involving the motor thalamus (Introduction, **Fig 1.1**.). Moreover, the number of cortical neurons that project to STN is likely orders of magnitude higher than that of their targets (Wilson, 2013). Thus it is interesting that the preferred phase alignment of cortex and STN is associated with an increase in the amplitude of oscillations in the cortex. Rather than indicating that STN is in some way driving the amplification of beta oscillations in cortex, it is more likely that the cortico-subthalamic phase alignment is providing a window into network synchronisation, which would predict increased amplitude across the extended basal ganglia network. Whether or not this is the case, synchronisation at the preferred phase between cortex and STN could provide a useful biomarker of upcoming increases in beta amplitude for closed-loop applications.

4.5.3. Relevance of preferred phase and non-preferred phase to amplitude modulation of beta oscillations.

A key finding here is that there are sustained periods of non-preferred phase synchronisation. If any sustained synchronisation *per se* increases the amplitude of a given oscillation, non-preferred phase epochs would also be expected to result in increased amplitude, but this does not occur in experimental animals or patients. This result is in agreement with the many studies by Fries and colleagues demonstrating that, for gamma frequency oscillations in cortex, there are “good” phase alignments (similar to the preferred phase used here) that

increase the correlation of power in the synchronised structures more than "bad" phase alignments (similar to non-preferred phase here: Womelsdorf et al., 2014). There is evidence that the same mechanism is present for beta oscillations in the motor system in the cortico-spinal tract (Fries et al., 2002; Fries, 2005) and between motor cortical areas (Zanos et al., 2018). To our knowledge, our experiments provide the first evidence that this framework also applies to cortico-basal ganglia coherence. Although we focused on changes in amplitude (because of its importance in PD), rather than amplitude correlation (as in many of the papers by Fries and colleagues), the fact that preferred phase synchronised epochs were associated with increased amplitude in both structures suggests that we are essentially observing the same phenomenon. Many studies into communication by coherence have focused on changes in the LFPs of the two structures. In the hemi-lesioned rats, we had the opportunity to investigate how the direct output activity of the subthalamic nucleus relates to the specific phase alignment between the STN and the cortex. Given that it has been proposed that preferred or good phase alignment results in optimal windows of excitability, it might have been expected that the firing rate would increase during these epochs, as has been shown for gamma oscillations in cortex (Womelsdorf et al., 2012). In contrast, we found no phase-dependent changes in firing rate, but locking of STN units to a specific phase of the LFP got more pronounced during preferred phase alignment. This finding may be specific to STN neurons (and other non-striatal basal ganglia neurons), where many spikes are driven by intrinsically generated currents and synaptic inputs mostly alter the timing of these intrinsically generated spikes (Wilson, 2015, McIver et al., 2018). Performing the same analysis on striatum, where indirect pathway spiny neurons lock to cortical beta oscillations and also receive direct cortical input (Sharott et al., 2017), could yield a different result as these neurons require coordinated synaptic input to fire action potentials. Such a comparison

could give important insight as to how cortical oscillations are propagated through the circuit.

4.5.4. Beta frequency stimulation of cortex disrupts the distribution of preferred and non-preferred phase synchronized periods.

The physiological and behavioural effects of stimulating the cortex or basal ganglia at beta frequency have led to contradictory findings. Stimulation applied to the STN in experimental animals does not lead to clear behavioural effects, despite entraining local neurons (Syed et al., 2016). In patients, however, 20 Hz stimulation delivered through therapeutic electrodes leads to modest impairments in reaction time (Chen et al., 2007). Similarly, beta frequency stimulation of motor cortex using transcranial alternating current stimulation in healthy subjects leads to small, but significant impairment of motor performance (Pogosyan et al., 2009). We hypothesised that, in the presence of pathological beta oscillations, continuous cortical stimulation at beta frequency would interfere in the cortico-subthalamic synchronisation in a phase-alignment specific way. While the results were not clear cut, we found that introducing an external oscillation at the pathological frequency actually diminished the alignment-dependent differences in the amount of time that the cortex and STN spent at the amplifying alignment. For the cortical power, we saw the same pattern of amplification during preferred phase, and no significant no change in power during consecutive cycles of non-preferred phase alignment. This is exactly the same pattern as we observed on the location matched control sample. As shown for the amplifying phase results in Chapter III, beta frequency stimulation may have to be applied in a precise, phase dependent manner to amplify the existing pathological oscillation. This may explain why beta stimulation has previously has limited or no effect on motor performance. In regard to closed-loop stimulation, these findings provide further evidence that using beta frequency stimulation will not necessarily enhance pathological activity, unless it is precisely timed.

Chapter V Discussion

5.1. General summary of the results

In this thesis, using a novel human intraoperative electrophysiological stimulating and recording approach presented in Chapter II, we demonstrated that in each parkinsonian patient there is a specific phase of the subthalamic LFP beta oscillation at which consecutive pulses of local electrical stimulation can suppress its amplitude without changes to overall excitability (Chapter III). Furthermore, this modulation extends to the output of STN neurons and to corticosubthalamic synchrony. These results provide the first evidence in humans for using the phase of a subcortical oscillation to more selectively control its amplitude, and opens up the possibility of using such an approach for neurological disorders with oscillatory pathologies and to test the mechanistic role of these activities in functional processes.

We also investigated whether coherent oscillations in the frontal cortex and STN displayed phase-dependent amplification dopamine-depleted rats, and carried out complementary analyses using intraoperative recordings from PD patients (Chapter IV). We found that the corticosubthalamic pathway has a strong preferred phase relationship, which predicts amplification of the ongoing beta oscillation in both cortex and STN and increases the beta-entrainment of the spiking activity of single units. These results suggest that sustained beta oscillations in PD are underlain by specific temporal relationships between cortical and subcortical neuronal populations.

5.2. Similarities and differences in recording from parkinsonian animals versus Parkinson's disease patients

A unique feature of this thesis is that it utilises complimentary recording and stimulating setup (throughout the thesis), furthermore, identical analyses (Chapter IV) of

human PD patients and 6-OHDA hemilesioned rats with a Parkinsonian phenotype. Providing this comparison has the potential to be useful for several reasons. Firstly, while the importance of showing pathophysiological mechanisms directly in the clinical setting is clear, PD patients are extremely heterogeneous in terms of their symptom profile, medication history and disease duration. One example of the inter-sample diversity in PD patients is how we failed to find a consistent angle that was efficient in supressing or amplifying the power of the beta oscillation for all the patients (Chapter III, **Fig 3.4**.). Instead, suppressive or amplifying phase was a characteristic of the individual recording for each patient. Contrarily, examples of the homogeneity in the sample, could also be found with humans: preferred, beta-amplifying phase alignment was strikingly consistent (Chapter IV **Fig 4.14 A**). This was surprising given the manifold uncontrolled factors that had to be accounted for recording the patient sample (cortical signal collection, STN recording position, history of patients, and alertness of the patients during surgery). Even though experiments were considerably more controlled, there are also examples of heterogeneity in data from 6-OHDA lesioned rodents (Chapter IV, **Fig 4.10**). Interestingly, beta-frequency stimulation resulted short-latency responses of single neurons that were far more heterogeneous that those see with 1Hz stimulation in the same set-up (Magill et al., 2004a), not dissimilar to those observed in Chapter II with the human STN neurons. Thus, it may be the continuous nature of the stimulation in patients, in addition to the differences in stimulation/recording position that leads to variable multiphasic responses (human setup, Chapter II, **Fig 2.1** Rat recording locations, Chapter IV, **Fig. 4.4.**). Nevertheless, rodent experiments enabled us to stimulate a specific set of input neurons to the STN, and using the ECoG, record a signal related to the activity of these neurons. This level of specificity is currently not possible in intraoperative recordings. On the top of the effect of different recording positions within the STN (Chapter IV, **Fig. 2.1**.), the diversity in PSTH responses

could also indicate the possibility that STN neurons do not form the homogenous population that has been previously assumed (Oorschot, 2010).

Nevertheless, using animal models, such as the parkinsonian rat, allows pathophysiological activities to be investigated under relatively consistent conditions of dopamine depletion. By using histological methods to quantify the lesion, we were able to avoid giving any dopamine replacement, which is often used in hemi-lesioned rodent for the rotation test. While electrode position can be estimated with a good degree of accuracy in intraoperative recordings (Sharott et al., 2014a), juxtacellular labelling allowed unambiguous, precise verification of the position of LFP and unit recordings in the STN. A significant disadvantage of being able to obtain juxtacellular labelling is the necessity for anaesthesia. Human patients, however, were awake during the surgical procedures, albeit to a different extent, because anaesthesia was obviously not controlled for the sake of the experiment, but for the sake of the wellbeing and safety of the patients. This also makes it possible to record data with behaviour to test the application of the stimulation. Although not presented here, the findings in this thesis will provide a test-bed to try out the effects of phase-specific stimulation during simple movements, such as a manual grip task (Tan et al., 2016). The utility of the 6-OHDA rat set-up for studying beta oscillations and other pathophysiological activities has already been well established (Mallet et al., 2008a; Mallet et al., 2008b; Mallet et al., 2012; Sharott et al., 2017). The small size of the rat STN, however, makes in challenging to record large data sets, in comparison to other basal ganglia structures, whereas using the traditional "Ben's Gun" set up in PD patients, it is possible to record 10 or more units in a hemisphere (Sharott et al., 2018c; Sharott et al., 2014a). Given the relative pros and cons of the two approaches, we hypothesised that any phenomenon that could be observed in both set-ups, as with phase-dependent amplification here, may well represent a robust feature of pathophysiology in PD.

Another important advantage of the anaesthetised rodent is the opportunity to perform well defined perturbations of specific points in the network. As discussed in Chapter II, the stimulation of the area to dorsal to the STN in patients could result in modulation of various cell populations and white matter tracts. In the 6-OHDA lesioned rodents, we were able to apply beta frequency stimulation to the deep layers of an area of cortex with dense projections to STN. The possibility for a less invasive cortical stimulation is an attractive, however not yet feasible option in human patients. Implementing transcranial alternating current stimulation (TACs) was trialled in patients with essential tremor before and has proven to be successful, but the externalised nature of such device and the low precision regarding the localisation is still holding the generalised clinical application behind (Lefaucheur, 2009; Zanos et al., 2018). On the other end of the spectrum, genetically engineered rodent lines provide an excellent framework for anatomically precise stimulation of specific pathways, even cell types within the cortico-basal ganglia loop (Vazey & Aston-Jones, 2013). Optogenetics is a powerful tool in addressing multiple key questions regarding the basal ganglia, such as the functional role of the direct and the indirect pathway in movement initiation (Kravitz et al., 2010). An important question that can be addressed with optogenetics, for example, is what specific pathways are contributing to the mechanism of deep brain stimulation. Gradinaru et al. (2009) demonstrated example for a pathway-specific targeting in understanding the mechanisms for deep brain stimulation. This study made a case not only for the efficacy of optogenetic stimulation for symptomatic relief in PD, but also highlighted the importance of the inputs to the STN (cortical afferents) by showing the superiority of targeting the fiber inputs to the STN. Clinical observations already suggested the efficacy of peri-STN stimulation for PD, but this is the first study to provide experimental evidence, albeit in rodents (Chapter IV). The translational potential of these findings are

complex in the light of studies showing the variety and power of antidromic responses in the cortex of freely moving parkinsonian rats (Li et al., 2012; Li et al., 2007).

For the sake of the experiments presented in this thesis, however, we did not implement optogenetic tools due to the following considerations. First and foremost, mice lines are more readily available for optogentical experimentation to this date. Additionally, beta oscillations have not been reliably established in Parkinsonian mice models (however see Chen et al., 2018). Genetically modified rat lines are under development and hopefully will provide a good test bed for dissecting the cortico-subthalamic network in the future. Additionally, *in situ* localisation of the extremely small STN is well established using cortical 1 Hz stimulation (Magill et al., 2004a), which necessitated relying on electrical stimulation protocols. Last, but not least, even though optogenetic control of BG circuits were proven successful in rodents and non-human primates, optogentic manipulations are not yet available on human patients (Gradinaru et al., 2009; Han et al., 2009; Galvan et al., 2012). Some of the limitations regarding the implementation of optogenetics in humans include the inability to deal with heat generated by the light stimulation; not knowing the chronic effects of the delivery of viral vectors, and not being able to predict the extra energy demand imposed by the potential leak currents of the transfected neurons (Rossi et al., 2015). Finally, DBS targets some of the smallest structures in the brain, it is currently unclear how precise viral vector delivery can be done, and, what amount of opsin expression is sufficient for eliciting symptomatic relief in patients. In summary, in order to capitalise on the value of matching the two experimental dataset and draw conclusions of the translational value of our results, we had to implement electrical stimulation.

5.3. General implications to pathological and healthy oscillations

The general results of this thesis centres around the time-dependent description and manipulation of oscillatory activity in the cortical-basal ganglia network. Both studies presented here addresses the question: what criterions have to be met to amplify (Chapter IV) or modulate (Chapter III) a network of coupled oscillators (Winfree, 1967, Tass & Majtanik, 2006, Cagnan et al., 2015).

Timing, besides vigour, is unequivocally one of the most important feature of motor control. Even according to the most minimalistic views of the basal ganglia function, specific timing between the composite stations of this network will decide whether the movement is carried out at all, if so, when exactly is it initiated and terminated and with the activation of which muscle groups, following what precise sequence. Oscillations might provide a one-stop-shop for tying all these mechanisms together. According to a theory laid out by Pascal Fries (2002, 2005, 2015), oscillations provide common inertial frame of reference, by which areas connected over long distances can synchronise their activity, so that the net output of the system reflects the unison action of many nodes, regardless of the different time lags.

Several lines of evidence presented here support that this theory can be applied to beta oscillations. First and foremost, some phase alignments between an external structure (cortex) and the basal ganglia (STN) are better than others in causing beta amplification. It has already been shown that high coherence correlates with higher firing rate (Womelsdorf et al., 2012; Womelsdorf et al., 2014). The existence of intermittent and sustained periods of high coherence that *do not* favour elevated power, nor increased firing rate, is the key result to emphasise the importance of timing (non-preferred phase alignment). This result provides evidence for the necessity of taking the internal temporal dynamics of oscillatory

coupling into consideration in understanding beta amplification. In this thesis I was also able to provide evidence that single, identified STN neurons increase their phase locking to the STN LFP oscillations when the cortical input is in the right phase alignment. The fact that this happens without firing rate changes highlights the complexity of network related electrophysiological changes in the context of a pathological network (Fischer et al., 2018; Tai et al., 2011, but see Leblois et al., 2007).

Secondly, some stimulation phases are better in supressing pathological oscillations than others. Implicit evidence for the role of specific timing was provided by Chapter III, where I demonstrated that continuous, same frequency stimulation does not cause mere amplification of the pathological signal as it was hypothesised before (Chen et al., 2007; Hassler et al., 1960, Constantoyannis et al., 2004). Matched frequency stimulation, in fact will cause periods of high and low amplitude, which will be defined by the specific phase of the stimulation. Furthermore, phase-dependent modulation by beta frequency stimulation supports not only local fluctuations in power, but inflict network-level changes on the cortico-subthalamic network. In Chapter III we show that stimulation resulting in amplification also correlates with higher cortico-subthalamic beta synchronisation (Chapter III **Fig. 3.9.**).

A common feature of both studies is that amplification and modulation by stimulation requires consecutive cycles. This is not surprising, since beta oscillations themselves are not an instantaneous feature of the parkinsonian network, rather the emergence of beta oscillations relies on chronic dopamine depletion in parkinsonian animals (Sharott et al., 2005). Based on the studies presented here, it is also likely that modulating the amplitude by continuous beta-frequency stimulation relies on subsequence instances of phase relations between 1) the pathological oscillation and the stimulation (Chapter III) and 2) the oscillators involved (Chapter IV). Previous studies have provided evidence for similar

findings before. Cagnan et al. (2013a), for example, has shown similar effects on tremor patients with matched frequency stimulation. The authors hypothesised that the optimal tremor suppression will be heavily influenced by the history of the stimulation, either because the spike-timing dependent plasticity or the entrainment / decoupling of the oscillators will take time to settle in or disengage. This line of reasoning fits very well with our observations and the CTC theory. It is hypothesised that 'good' phase alignment is advantageous in promoting efficient communication, because it assists two distant structures in achieving spike timing dependent plasticity. The other study that is providing implicit evidence that tallies with our findings, particularly regarding the stimulation data, was carried out by Rosin et al. (2011). The authors used feedback signal triggered closed-loop stimulation algorithm, which was triggered off the unit activity (bursting) of the cortex and the GP. The units were used for phase dependence, as well as a time delay. This study used fixed time lags between the stimulation and the occurrence of bursting (oscillatory component), that served as a biomarker. This implies that the authors did not need phase tracking, because the dynamics of the system were settled enough that the effects could be elicited only relying on the phase readout, without varying time windows (further insights on this study below). This study highlights a very important addition to the applicability of the CTC theory. The system performance during beta oscillations is supposedly low because the most common (in our study: preferred) phase relation dominates (Brittain & Brown, 2014). One might speculate, that the persistent 'unleashed' nature of beta oscillations is in fact what makes them a pathological feature. Various studies have demonstrated that intermittent periods of beta can be captured during healthy motor control, and in hypothesised its role in signalling the 'edges' of the movement (pre-movement beta desynchronization and post movement beta rebound); it is sensitive to change of sensorimotor scenario of any kind, but sustained and elevated during maintained posture

(Toma et al., 2000; van Wijk et al., 2012; Lee et al., 2003;Kühn et al., 2006;Feingold et al., 2015b; Courtemanche et al., 2003). Supporting the above, a line of studies carried out by Tinkhauser (Tinkhauser et al., 2017a; Tinkhauser et al., 2017b) demonstrated that the less transient (longer) beta bursts could be correlated with higher degrees of symptom severity. Similar effects were found by Deffains et al., 2018 using MPTP-treated monkeys. The authors reported that beta oscillations were present in several nodes of the BG in healthy moneys, whereas prolonged epochs were characteristic to the Parkinsonian state.

Finally, one could argue that placing beta oscillations into the CTC framework is counterintuitive given that 'good phase alignment' in the case of beta oscillation actually correlates with symptom severity. Higher synchrony, in the case of the cortex, correlates with higher system performance, and more optimised behavioural output (Fries, 2005). Based on converging evidence and the supposed role of beta oscillations in healthy motor control it seems that the prolonged and sustained nature of the phase alignments resulting in adverse effects might distinguish this mechanism from what has been observed with inter-areal gamma coherence recorded in the cortex (Bastos et al., 2015; but see Buzsaki & Schomburg, 2015).

This addition also expands the view that beta oscillation is a mechanism maintaining the 'status quo' of the sensory-motor set (Engel & Fries, 2010). One might speculate that certain phase alignments during the ongoing beta oscillation will be promoting low expectations for a change in the sensory-motor milieu, while others will correlate with a lower threshold for forming responses to novel stimuli. This information processing dichotomy has previously been applied to the seesaw balance between gamma and beta oscillations (Little et al., 2014). Here I propose that different network excitability states - defined by the phase alignment between structures or stimulation - might exist within the ongoing beta oscillation. In fact, a novel version of the CTC theory that has been proposed recently, emphasises that the

behavioural outcome of the 'good phase alignment' is that "selective coherence implements selective communication". In the case of PD, exaggerated coherence exists, but the selectiveness is lost.

Beta oscillations are indeed a ubiquitous feature of the parkinsonian network without an obvious source of initiation (Brazhnik et al., 2016;Deffains et al., 2010a; Goldberg et al., 2002;Mallet et al., 2008a; Mallet et al., 2008b; Sharott et al., 2017; Tachibana et al., 2011a). Data promoting the origin of beta oscillation can be found for almost all nodes of the cortico-basal ganglia-thalamocortical loop. So far, the motor cortex (Kato et al., 2015;Litvak et al., 2011; Sharott et al., 2018b), the STN and the GPe loop (Cagnan et al., 2015; Mallet et al., 2008a; Nevado-Holgado et al., 2014; Tachibana et al., 2011a); the striatum and the GPe (Blenkinsop et al., 2017; Corbit et al., 2016) have been suspected of being the instigator. However, if its speculated that not an individual oscillator, but the specific timing within the system is crucial, this question can be resolved by a cutting the Gordian knot: the origin is not the issue, but instead the internal temporal dynamics that ramp up and sustain beta oscillations should be focused on.

5.4. Limitations

As I have pointed out earlier, our studies are not without limitations or pitfalls, which mostly affect the extent of conclusions that can be drawn regarding clinical assumptions. Firstly, we were not in a position to record behaviour, neither from patients, nor from the rodents. In order to be able to make reliable assumptions for clinical applications this would be required. Secondly, not only did our studies lack behavioural data, but the effects were not correlated to severity of Parkinson's disease. Furthermore, we did not have a chance to record long epochs of phase dependent stimulation or specific phase alignments. The rat dataset was collected during anaesthesia, which made the interpretation of the brain state difficult. Finally, electrical stimulation is not a pitfall *per se*, but implementing optogenetic

manipulation would have allowed us to draw more precise conclusions on the pathways involved in the phase dependent effects. Finally, the sample size for the rat stimulation data is somewhat small, though recording and juxtacellularly labelling in a 6-OHDA hemilesioned rat's STN during cortical stimulation is a challenging and long experiment to conduct.

5.5. Suggestions for closed-loop applications

My final discussion point is regarding the therapeutic implications of my findings. As it was presented in the introduction, advancements in current DBS protocols are geared towards the implementation of closed loop approaches. Implementing tailored and responsive systems, in theory, would result in several advantages, including reducing the net amount of stimulation delivered, limit therapeutic side-effects and provide longer battery life (Beuter et al., 2014). Closed-loop systems have already been trialled in rodents, MPTP-treated monkeys and humans, but have not yet been implemented in the routine clinical settings of the stimulating apparatus in PD patients (Gradinaru et al., 2009; Rosin et al., 2011; Little et al., 2013). To recapitulate some of the challenges I covered in the introduction, a good DBS closed-loop system has to meet the following criteria to be successfully implemented: 1) high accuracy, 2) highly responsive, low latency system, 3) able to operate in the presence of stimulation artefacts, 4) and – if the biomarker is based on neuronal synchrony- it has to be able to adapt to frequency shifts.

As it was discussed in the introduction, a central biomarker is favourable over a peripheral, because of its convenience for the patients, and the fact that it is presumably tackling the some of the aetiological causes rather than the symptoms only. Here I provide a brief summary of three of the most relevant studies that complement our findings that have emphasised the importance of timing albeit implementing different biomarkers. Brittain et al. (2013), for example, trialled a similar approach to my experimental setup to promote the

idea of phase cancellation for neurostimulation. Even though this study, like ours, was not using actual phase tracking, the authors have implemented same frequency stimulation to provide evidence for tremor suppression by phase specific modulation. Another similarity to our findings is that this approach as well implemented a larger scale stimulation focusing on the inputs of the theoretical target (cortex), rather than the target itself. However, a major difference is that this study used a peripheral biomarker (tremor), that is not only easier to record, but also a slower paced oscillation and less transient than beta oscillations. A slower oscillation is obviously easier to phase-track, because it requires a less responsive system in terms of the latency. The difficulties of phase tracking were neglected by the first landmark study implementing a central oscillation as a biomarker on PD patients by Little and Brown (2013). This paper demonstrated that tracking only the power changes in the exaggerated beta oscillation is sufficient for symptomatic release. However, a recent paper on the *post-hoc* analysis of these findings revealed that the amplitude-responsive stimulation might also be effective because of timing-related effects. Tinkhauser et al., 2017a showed that during amplitude responsive DBS, the length of beta bursts gets trimmed by the adaptive stimulation. This result is in agreement with our findings on the requirement for having a phase-related (amplification or stimulation induced suppression) effect displayed for consecutive cycles. Putatively, the preferred (amplification favouring) phase alignment that persists over many cycles might be what these authors refer to as long beta burst. The third and final study was the already mentioned one by Rosin et al. (2011), that is a good example of implementing pseudo-phase aligned stimulation using two sites. As I previously discussed, this approach was pseudo-phase dependent, because it utilised a constant, 80 ms time lag, that corresponds to one, low-frequency beta cycle that is characteristic to MPTP-treated monkeys. This study resolved the problems of artefacts and phase tracking of a fast

and transient oscillation by using an external biomarker site and single unit activity for a feedback signal.

Our research has implications for both phase-locked (using one signal) or phase-coupled (two signals) closed-loop adaptive stimulation. Firstly, in the second chapter, we presented an elegant and effective way to deal with artefacts that occur during the continuous, same site phase-locked stimulation implementing the Kalman filter. Secondly, the third chapter presented the viability of the phase-dependent amplitude modulation during same site stimulation and recording, implementing low frequency stimulation. Finally, the results of beta -frequency stimulation presented in the fourth chapter are somewhat challenging to interpret in the light of implementing a closed loop DBS algorithm. This experiment was intended to show that an external stimulation, serving as a patterned 'noise', will alter the amplitude progression during specific phase alignments. We did, in fact, see phase-alignment specific modulation, but was not significant in both of the recorded structures. Respectively, the cortical power, which was recorded from the vicinity of the stimulation, was not modulated in a phase-alignment sensitive way. In other words, the analysis of the stimulated portion of the data has shown the same exact pattern of amplification as it has been observed with the spontaneous data. One could speculate that this negative result is particularly telling of the importance of the timing: an external oscillation without specific timing will not drive any modulatory effects. This might explain the controversy of not being able to find adverse parkinsonian symptoms when stimulating with beta frequency in healthy animals (Syed et al., 2012). On the other hand, beta frequency stimulation of the cortex did not cause a pattern of progressive amplification of the STN LFP power. However, the 20 Hz stimulation did diminish the differences between the power of the preferred and non-preferred phase alignments. This might be due to a putative entrainment of the STN LFP during the non-preferred phase alignment. This appears to be the case, because in our data,

the cortical oscillation is more robust and originates from many areas, whereas the STN beta oscillations in 6-OHDA rats can be measured prominently as cortico-subthalamic coherence. Our results suggest that beta frequency and low amplitude stimulation was sufficient to drive a power increase in the STN (that is known to be hyper-sensitive to cortical input in PD, Magill et al., 2001), but it wasn't adequate to alter the more resilient cortical oscillation.

All in all, here we provide a proof-of-principle framework making a case for implementing a closed loop approach that takes the specific phase of the stimulation or the specific phase alignments between two oscillators into consideration. Elements of these implications have already been proposed on the basis of the successful phase-dependent modulation of low frequency oscillations (Cagnan et al., 2013a). Furthermore, a beta phase dependent closed-loop stimulation was proven successful in modulating of cortical synaptic plasticity in MPTP-treated monkeys (Zanos et al., 2018). As it has been demonstrated that phase tracking is feasible for stable oscillations (Van Zaen et al., 2010), our findings might provide an appealing framework and a reassuring addition towards the evidence supporting the implementation phase-dependent closed-loop approaches in the treatment of PD.

Supplementary Tables

Case	Age (years), gender	Disease duration (years)	Motor UPDRS OFF	Motor UPDRS ON	Preoperative anti-parkinson drugs	Hoehn/Yahr Score	Dominant Side	Mattis Dementia Rating Scale	Major Symptoms	Included in analysis
1	72, M	6	33	13	Levodopa 650 g	3	Right	143	Akinetic, Rigid	Yes
2	64, M	7	50	19	Levodopa 250 mg Budipin,Piribedil, Rasagilin	3	Left	127	Akinetic, Rigid	Yes
3	70, F	9	30	12	Levodopa 1350 mg	3/4	Left	137	Rigid, Tremor	Yes
4	60, M	12	31	17	Levodopa 1000 mg	2	Right	141	Akinetic, Rigid Tremor	Yes
5	68, F	8	18	13	Levodopa 500 mg	3	Right	139	Akinetic Rigid	Yes
6	56, F	10	34	16	Levodopa 450 mg	2	Right	139	Akinetic	Yes

									Rigid	
7	57, M	17	33	16	Levodopa 1600 mg	3	Right	143	Akinetic, Rigid, Tremor	Yes
8	62, F	17	60	33	Levodopa 1400 mg Apomorphine Pramippexol	4	Left	137	Akinetic, Rigid, Tremor	Yes
9	53, M	22	63	9	Levodopa 600 mg Benserazide 25 mg Rasagiline 1 mg	3	Right	137	Akinetic, Rigid, Tremor	No
10	49, M	10	21	8	Levodopa 600 mg Benserazide 25 mg Ropinirole 32 mg Safinamide 100 mg	2	Right	142	Akinetic Rigid	No

Table 2.1 Characteristics of the PD Patient Sample included in Chapter III analysis

	Rat Spontaneous LFP					Rat Spontaneous ECoG				
Comparison	**n**	**p**	**z**	**ranksum**	**FDR - p**	**n**	**p**	**z**	**ranksum**	**FDR - p**
-1th	10	0.0002	-3.6663	56	**0.0004**	10	0.0002	-3.7418	55	**0.0004**
1st	10	0.0046	2.8347	143	**0.0055**	10	0.0211	2.3056	136	**0.0211**
2nd	10	0.0002	3.7418	155	**0.0004**	10	0.0002	3.7418	155	**0.0004**
3rd	10	0.0002	3.7418	155	**0.0004**	10	0.0010	3.2883	149	**0.0015**
4th	10	0.0002	3.7418	155	**0.0004**	10	0.0002	3.7418	155	**0.0004**
5th	10	0.0117	na	123	**0.0117**	10	0.0014		129	**0.0017**
	Rat Spontaneous Matched LFP					**Rat Spontaneous Matched ECoG**				
Comparison	**n**	**p**	**z**	**ranksum**	**FDR - p**	**n**	**p**	**z**	**ranksum**	**FDR - p**
-1th	5	0.0079	na	15	**0.0238**	5	0.0317	na	17	**0.0381**
1st	5	0.0317	na	38	**0.0381**	5	0.0079	na	40	**0.0238**
2nd	5	0.0079	na	40	**0.0238**	5	0.0079	na	40	**0.0238**
3rd	5	0.0159	na	35	**0.0238**	5	0.0159	na	35	**0.0238**
4th	5	0.0159	na	35	**0.0238**	5	0.0159	na	35	**0.0238**
5th	5	0.4127	na	29	0.4127	5	0.1905	na	31	0.1905
	Rat Stimulation LFP					**Rat Stimulation ECoG**				
Comparison	**n**	**p**	**z**	**ranksum**	**FDR - p**	**n**	**p**	**z**	**ranksum**	**FDR - p**
-1th	5	1.0000	na	18	1.0000	5	0.0286	na	10	0.0571
1st	5	0.2000	na	23	0.6000	5	0.4857	na	21	**0.4857**
2nd	5	0.2000	na	23	0.6000	5	0.0286	na	26	0.0571
3rd	5	0.8857	na	19	1.0000	5	0.0286	na	26	0.0571
4th	5	0.8571	na	15	1.0000	5	0.0571	na	22	0.0857
5th	5	0.6286	na	18	1.0000	5	0.1143	na	21	0.1371
	Human Spontaneous LFP					**Human Spontaneous ECoG**				
Comparison	**n**	**p**	**z**	**ranksum**	**FDR - p**	**n**	**p**	**z**	**ranksum**	**FDR - p**
-1th	23	9.74E-06	-4.42292	373	**1.17E-05**	23	0.0000	-5.0621	342	**6.23E-07**
1st	23	3.21E-04	3.598129	763	**0.00032**	23	0.0001	3.9280	779	**8.56E-05**
2nd	23	4.46E-09	5.866291	873	**2.68E-08**	23	0.0000	5.9075	875	**1.36E-08**
3rd	23	6.09E-08	5.41612	831	**1.83E-07**	23	0.0000	5.8630	852	**1.36E-08**
4th	23	4.95E-07	5.028339	732	**9.90E-07**	23	0.0000	5.2868	743	**2.48E-07**
5th	23	1.05E-06	4.882022	707	**1.58E-06**	23	0.0000	4.1759	678	**3.56E-05**

Table 4.3.1. Cycle-By-Cycle Statistical Comparison of the Average Power at Preferred Versus Non-Preferred Phase Alignment

Rat Spontaneous LFP n= 10							
	non-pref	5	4	3	2	1	-1
non-pref	pref	-1	1	2	3	4	5
5	-1	NaN	1	1	0.8136	0.9943	1
4	1	**0.962**	NaN	1	0.9417	0.8988	1
3	2	**0**	**0.0008**	NaN	0.9795	0.8054	1
2	3	**0**	**0.0013**	1	NaN	0.0668	0.9941
1	4	**0.0156**	0.5157	0.4517	0.5595	NaN	0.6945
-1	5	**0.0007**	0.0759	0.9706	0.989	0.9997	NaN

Rat Spontaneous ECoG n = 10							
	non-pref	5	4	3	2	1	-1
non-pref	pref	-1	1	2	3	4	5
5	-1	NaN	1	1	0.9999	0.7309	1
4	1	**0.9777**	NaN	0.97	0.9167	0.9795	0.9999
3	2	**0**	**0.0018**	NaN	1	0.1879	1
2	3	**0**	**0.001**	1	NaN	0.119	0.9999
1	4	**0.0017**	0.1182	0.9797	0.9439	NaN	0.5824
-1	5	**0.0074**	0.2993	0.8408	0.7314	1	NaN

Rat Spontaneous Matched LFP n= 5							
	non-pref	5	4	3	2	1	-1
non-pref	pref	-1	1	2	3	4	5
5	-1	NaN	1	1	1	0.8966	1
4	1	0.999	NaN	1	0.9999	0.5105	1
3	2	**0.0018**	**0.0473**	NaN	1	0.9178	1
2	3	**0.0043**	0.0909	1	NaN	0.9447	1
1	4	0.4054	0.9768	0.7347	0.8791	NaN	0.8288
-1	5	**0.0422**	0.4338	0.9994	1	0.9994	NaN

Rat Spontaneous Matched ECoG n = 5							
	non-pref	5	4	3	2	1	-1
non-pref	pref	-1	1	2	3	4	5
5	-1	NaN	1	0.9974	0.9991	0.9785	1
4	1	0.995	NaN	1	1	0.6941	0.9999
3	2	**0.0014**	0.0592	NaN	1	0.314	0.9753
2	3	**0.0125**	0.2783	1	NaN	0.323	0.9861
1	4	**0.0422**	0.554	0.9984	1	NaN	0.9931
-1	5	0.3513	0.9867	0.7347	0.9867	0.9998	NaN

Rat Stimulation LFP n = 5							
	non-pref	5	4	3	2	1	-1
non-pref	pref	-1	1	2	3	4	5
5	-1	NaN	0.9935	0.8271	0.997	1	1
4	1	0.908	NaN	1	1	0.7428	0.816
3	2	0.0545	0.908	NaN	1	0.2526	0.3222
2	3	0.1941	0.9967	1	NaN	0.7627	0.8382
1	4	0.9462	1	0.8559	0.9913	NaN	1
-1	5	0.908	1	0.908	0.9967	1	NaN

Rat Stimulation ECoG n = 5							
	non-pref	5	4	3	2	1	-1
non-pref	pref	-1	1	2	3	4	5
5	-1	NaN	1	1	0.9975	1	1
4	1	0.9995	NaN	1	0.9999	1	1
3	2	**0.0286**	0.3102	NaN	1	0.9999	1
2	3	0.0858	0.5882	1	NaN	0.9586	1
1	4	0.2196	0.8559	1	1	NaN	0.9986
-1	5	0.0545	0.461	1	1	1	NaN

Table 4.3.2. Statistical Comparison between Different Cycles within Preferred Versus Non-Preferred Phase Alignment

Human Spontaneous LFP n= 23								Human Spontaneous ECoG n = 23							
	non-pref	5	4	3	2	1	-1		non-pref	5	4	3	2	1	-1
non-pref	pref	-1	1	2	3	4	5	non-pref	pref	-1	1	2	3	4	5
5	-1	NaN	1	1	1	0.0625	1	**5**	-1	NaN	1	0.5147	0.9937	**0.0007**	1
4	1	**0.7192**	NaN	1	1	0.1484	1	**4**	1	**0.6408**	NaN	0.9633	1	**0.0106**	1
3	2	**0**	**0**	NaN	1	0.1059	1	**3**	2	**0**	**0**	NaN	0.9975	0.3942	0.857
2	3	**0**	**0**	1	NaN	0.0294	1	**2**	3	**0**	**0**	1	NaN	0.0248	1
1	4	**0**	**0.002**	0.9065	0.9919	NaN	0.015	**1**	4	**0**	**0.0001**	0.9997	1	NaN	0.003
-1	5	**0**	**0.0021**	0.9032	0.9914	1	NaN	**-1**	5	**0**	**0**	1	1	1	NaN

Table 4.3.2. Statistical Comparison between Different Cycles within Preferred Versus Non-Preferred Phase Alignment

	Lesion Target	Animal Died	Behaviour	Lesion (TH)	STN label	20 Hz	1 Hz	20 Hz Analysis Inclusion
ECL007	mfb	0	rotation	1	0	1	1	0
ECL008	mfb	0	rotation	1	1	1	1	**1**
ECL009	mfb	0	rotation	1	1	0	1	**1**
ECL010	mfb	0	rotation	1	0	1	1	0
ECL011	mfb	1	rotation	0	0	0	0	0
ECL012	mfb	0	rotation	1	0	1	1	0
ECL033	snc	0	corridor test	1	0	1	1	0
ECL038	snc	0	corridor test	1	1	1	1	**1**
ECL040	snc	0	corridor test	1	1	1	1	**1**
ECL041	snc	0	corridor test	1	0	1	1	0
ECL042	snc	0	corridor test	1	0	1	1	0
ECL046	snc	0	corridor test	1	1	1	1	**1**
ECL047	snc	0	corridor test	1	1	1	1	**1**
ECL049	snc	0	corridor test	0	0	1	1	0
ECL050	snc	0	corridor test	1	0	1	1	0
ECL055	snc	1	stepping test	0	0	0	0	0

ECL057	snc	0	stepping test	1	1	1	1	**1**
ECL058	snc	0	stepping test	1	0	1	1	0
ECL059	snc	1	stepping test	0	0	0	0	0
ECL060	snc	0	stepping test	1	1	1	1	**1**
ECL061	snc	0	stepping test	1	1	1	1	**1**
ECL066	snc	0	stepping test	1	1	1	1	**1**
ECL067	snc	0	stepping test	0	1	1	1	0
ECL070	snc	0	stepping test	1	1	0	1	0
ELC072	snc	0	stepping test	0	0	1	1	0
ECL073	snc	0	stepping test	1	0	1	1	0
ECL074	snc	0	stepping test	1	1	1	1	0
ECL075	snc	0	stepping test	0	1	0	1	0
ECL076	snc	0	stepping test	1	0	1	1	0
ECL079	snc	0	stepping test	1	1	1	1	0

Table 4.1. Summary of the 6-OHDA Experiments

Case	Age (years) gender	Disease duration (years)	Motor UPDRS OFF	Motor UPDRS ON	Preoperative antiparkinson drugs	Hoehn/Yahr Score	Dominant Side	Mattis Dementia Rating Scale	Major Symptoms
1	72,M	6	33	13	650	3	right	143	akinetic, rigid
2	64,M	7	50	19	N.A.	3	left	127	akinetic, rigid
3	53,M	32	63	9	1412	3	right	137	akinetik, rigid
4	68,F	8	18	13	500	3	right	139	akinetic, rigid
5	56,F	10	34	16	450	2	right	139	akinetic, rigid
6	49,M	10	21	8	1726 + 100 mg Safinamid	2	right	142	akinetic rigid
7	62,F	17	60	33	1400	4	left	137	akinetic rigid

8	51,M	11	36	22	1676	2	left	144	akinetic, rigid
9	57,F	13	36	15	916	2	left	140	akinetic, rigid
10	68,F	9	28	19	1503	4	right	142	akinetic, rigid
11	52,M	6	24	15	1340	2	right	143	Tremor
12	58,M	15	25	17	1479	2	left	140	bradykinesia, end-of dose akinesia, dysarthrophonia
13	66,M	6	26	15	456	2	right	142	bradykinesia, fluctuations, camptocormia
14	54,M	10	46	11	1514	2, 3	right	144	tremor right hand, end-of-dose akinesia
15	58,M	7	38	25	1088	2	right	142	equivalence type, tremor, rigor

16	74,F	13	32	22	1459	2.5	left	136	bradykinesia, dyskinesia, camptocormia
17	70,F	26	45	24	1215	4	Left	N.A	Tremor, Akinesia/rigidity
18	72,F	18	41	19	831	4	Left	N.A	Equivalence type Fluctuations, Dyskensia
19	70,F	8	38	21	1203 + 40 mg alpha-dihzdroergo-cryptine	3	Left	N.A	Bradykinesia, Fluctuations, Dyskinesia
20	66,M	17	49	20	1478	4	Left	N.A	Dyskinesias, Rigidity
21	64,M	15	53	39	1535	4	Left	N.A	Akinesia/rigidity, Camptocormia
22	69,F	9	21.5	7	960	3	Right	N.A	Equivalence type Fluctuations Dyskinesia
23	66,M	11	28	14	2022	4	Right	N.A	Akinesia/rigidity Fluctuations

Table 4.2. Properties of PD Patient Sample Involved in Chapter IV Analysis

References

Abdi, A., Mallet, N., Mohamed, F. Y., Sharott, A., Dodson, P. D., Nakamura, K. C., Suri, S., Avery, S. V., Larvin, J. T., Garas, F. N., Garas, S. N., Vinciati, F., Morin, S., Bezard, E., Baufreton, J., & Magill, P. J. (2015). Prototypic and arkypallidal neurons in the dopamine-intact external globus pallidus. *J Neurosci, 35*(17), 6667-6688. doi:10.1523/JNEUROSCI.4662-14.2015

Accolla, E. A., Aust, S., Merkl, A., Schneider, G. H., Kuhn, A. A., Bajbouj, M., & Draganski, B. (2016a). Deep brain stimulation of the posterior gyrus rectus region for treatment resistant depression. *J Affect Disord, 194*, 33-37. doi:10.1016/j.jad.2016.01.022

Accolla, E. A., Herrojo Ruiz, M., Horn, A., Schneider, G. H., Schmitz-Hubsch, T., Draganski, B., & Kuhn, A. A. (2016b). Brain networks modulated by subthalamic nucleus deep brain stimulation. *Brain, 139*(Pt 9), 2503-2515. doi:10.1093/brain/aww182

Adamchic, I., Hauptmann, C., Barnikol, U. B., Pawelczyk, N., Popovych, O., Barnikol, T. T., Silchenko, A., Volkmann, J., Deuschl, G., Meissner, W. G., Maarouf, M., Sturm, V., Freund, H. J., & Tass, P. A. (2014). Coordinated reset neuromodulation for Parkinson's disease: proof-of-concept study. *Mov Disord, 29*(13), 1679-1684. doi:10.1002/mds.25923

Afsharpour, S. (1985a). Light microscopic analysis of Golgi-impregnated rat subthalamic neurons. *J Comp Neurol, 236*(1), 1-13. doi:10.1002/cne.902360102

Afsharpour, S. (1985b). Topographical projections of the cerebral cortex to the subthalamic nucleus. *J Comp Neurol, 236*(1), 14-28. doi:10.1002/cne.902360103

Agnesi, F., Connolly, A. T., Baker, K. B., Vitek, J. L., & Johnson, M. D. J. P. o. (2013). Deep brain stimulation imposes complex informational lesions. *8*(8), e74462.

Albin, R. L., Young, A. B., & Penney, J. B. (1989). The functional anatomy of basal ganglia disorders. *Trends Neurosci, 12*(10), 366-375.

Aleksandrova, L. R., Creed, M. C., Fletcher, P. J., Lobo, D. S., Hamani, C., & Nobrega, J. N. (2013). Deep brain stimulation of the subthalamic nucleus increases premature responding in a rat gambling task. *Behav Brain Res, 245*, 76-82. doi:10.1016/j.bbr.2013.02.011

Alexander, G. E., Crutcher, M. D., & DeLong, M. R. (1990). Basal ganglia-thalamocortical circuits: parallel substrates for motor, oculomotor, "prefrontal" and "limbic" functions. *Prog Brain Res, 85*, 119-146.

Alexander, G. E., DeLong, M. R., & Strick, P. L. (1986). Parallel organization of functionally segregated circuits linking basal ganglia and cortex. *Annu Rev Neurosci, 9*, 357-381. doi:10.1146/annurev.ne.09.030186.002041

Alkemade, A., Schnitzler, A., & Forstmann, B. U. (2015). Topographic organization of the human and non-human primate subthalamic nucleus. *Brain Struct Funct, 220*(6), 3075-3086. doi:10.1007/s00429-015-1047-2

Alvarez, L., Macias, R., Guridi, J., Lopez, G., Alvarez, E., Maragoto, C., Teijeiro, J., Torres, A., Pavon, N., & Rodriguez-Oroz, M. J. (2001). Dorsal subthalamotomy for Parkinson's disease. *Mov Disord, 16*(1), 72-78.

Amirnovin, R., Williams, Z. M., Cosgrove, G. R., & Eskandar, E. N. J. (2004). Visually guided movements suppress subthalamic oscillations in Parkinson's disease patients. *J Neurosci, 24*(50), 11302-11306.

Anderson, T. R., Hu, B., Iremonger, K., & Kiss, Z. H. J. (2006). Selective attenuation of afferent synaptic transmission as a mechanism of thalamic deep brain stimulation-induced tremor arrest. *J Neurosci, 26*(3), 841-850.

Aron, A. R. (2007). The neural basis of inhibition in cognitive control. *Neuroscientist, 13*(3), 214-228. doi:10.1177/1073858407299288

Aron, A. R., & Poldrack, R. A. J. (2006). Cortical and subcortical contributions to stop signal response inhibition: role of the subthalamic nucleus. *J Neurosci, 26*(9), 2424-2433.

Ashby, P., Paradiso, G., Saint-Cyr, J., Chen, R., Lang, A., & Lozano, A. J. (2001a). Potentials recorded at the scalp by stimulation near the human subthalamic nucleus. *Clin Neurophysiol, 112*(3), 431-437.

Ashby, P., Paradiso, G., Saint-Cyr, J. A., Chen, R., Lang, A. E., & Lozano, A. M. (2001b). Potentials recorded at the scalp by stimulation near the human subthalamic nucleus. *Clin Neurophysiol, 112*(3), 431-437.

Atherton, J. F., & Bevan, M. D. J. (2005). Ionic mechanisms underlying autonomous action potential generation in the somata and dendrites of GABAergic substantia nigra pars reticulata neurons in vitro. *J Neurosci, 25*(36), 8272-8281.

Atherton, J. F., Menard, A., Urbain, N., & Bevan, M. D. (2013). Short-term depression of external globus pallidus-subthalamic nucleus synaptic transmission and

implications for patterning subthalamic activity. *J Neurosci, 33*(17), 7130-7144. doi:10.1523/JNEUROSCI.3576-12.2013

Augood, S. J., Waldvogel, H. J., Munkle, M. C., Faull, R. L., & Emson, P. C. (1999). Localization of calcium-binding proteins and GABA transporter (GAT-1) messenger RNA in the human subthalamic nucleus. *Neuroscience, 88*(2), 521-534.

Aziz, T. Z., Peggs, D., Sambrook, M. A., & Crossman, A. R. (1991). Lesion of the subthalamic nucleus for the alleviation of 1-methyl-4-phenyl-1,2,3,6-tetrahydropyridine (MPTP)-induced parkinsonism in the primate. *Mov Disord, 6*(4), 288-292. doi:10.1002/mds.870060404

Azodi-Avval, R., & Gharabaghi, A. J. (2015). Phase-dependent modulation as a novel approach for therapeutic brain stimulation. *Front Comput Neurosci, 9*, 26.

Baizabal-Carvallo, J. F., Kagnoff, M. N., Jimenez-Shahed, J., Fekete, R., & Jankovic, J. (2014). The safety and efficacy of thalamic deep brain stimulation in essential tremor: 10 years and beyond. *J Neurol Neurosurg Psychiatry, 85*(5), 567-572. doi:10.1136/jnnp-2013-304943

Baker, K. B., Montgomery Jr, E. B., Rezai, A. R., Burgess, R., & Lüders, H. O. (2002). Subthalamic nucleus deep brain stimulus evoked potentials: physiological and therapeutic implications. *Mov Disord, 17*(5), 969-983.

Baker, S., Spinks, R., Jackson, A., & Lemon, R. J. (2001). Synchronization in monkey motor cortex during a precision grip task. I. Task-dependent modulation in single-unit synchrony. *J Neurophysiol, 85*(2), 869-885.

Baker, S. N., Olivier, E., & Lemon, R. N. (1997). Coherent oscillations in monkey motor cortex and hand muscle EMG show task-dependent modulation. *J Physiol, 501 (Pt 1)*, 225-241.

Bar-Gad, I., & Bergman, H. (2001). Stepping out of the box: information processing in the neural networks of the basal ganglia. *Curr Opin Neurobiol, 11*(6), 689-695.

Bar-Gad, I., Havazelet-Heimer, G., Goldberg, J. A., Ruppin, E., & Bergman, H. (2000). Reinforcement-driven dimensionality reduction--a model for information processing in the basal ganglia. *J Basic Clin Physiol Pharmacol, 11*(4), 305-320.

Bar-Gad, I., Heimer, G., Ritov, Y., & Bergman, H. (2003a). Functional correlations between neighboring neurons in the primate globus pallidus are weak or nonexistent. *J Neurosci, 23*(10), 4012-4016.

Bar-Gad, I., Morris, G., & Bergman, H. (2003b). Information processing, dimensionality reduction and reinforcement learning in the basal ganglia. *Prog Neurobiol, 71*(6), 439-473. doi:10.1016/j.pneurobio.2003.12.001

Bar-Gad, I., Ritov, Y. a., Vaadia, E., & Bergman, H. (2001). Failure in identification of overlapping spikes from multiple neuron activity causes artificial correlations. *J Neurosci Methods, 107*(1-2), 1-13.

Baram, Y. (2013). Virtual sensory feedback for gait improvement in neurological patients. *Front Neurol, 4*, 138. doi:10.3389/fneur.2013.00138

Barlow, H. B. (1961). *Journal of current problems in animal behaviour.* The coding of sensory messages.

Baron, M. S., Vitek, J. L., Green, J., Kaneoke, Y., Hashimoto, T., Turner, R. S., Woodard, J. L., Delong, M. R., Bakay, R. A., Cole, S. A. (1996). Treatment of advanced Parkinson's disease by posterior GPi pallidotomy: 1-year results of a pilot study. *Ann Neurol,40*(3), 355-366.

Bartho, P., Hirase, H., Monconduit, L., Zugaro, M., Harris, K. D., & Buzsaki, G. (2004). Characterization of neocortical principal cells and interneurons by network interactions and extracellular features. *J Neurophysiol, 92*(1), 600-608. doi:10.1152/jn.01170.2003

Bastos, A. M., Vezoli, J., & Fries, P. (2015). Communication through coherence with inter-areal delays. *Curr Opin Neurobiol, 31*, 173-180. doi:10.1016/j.conb.2014.11.001

Baufreton, J., Atherton, J. F., Surmeier, D. J., & Bevan, M. D. (2005). Enhancement of excitatory synaptic integration by GABAergic inhibition in the subthalamic nucleus. *J Neurosci, 25*(37), 8505-8517. doi:10.1523/JNEUROSCI.1163-05.2005

Baufreton, J., & Bevan, M. D. (2008). D2-like dopamine receptor-mediated modulation of activity-dependent plasticity at GABAergic synapses in the subthalamic nucleus. *J Physiol, 586*(8), 2121-2142. doi:10.1113/jphysiol.2008.151118

Baufreton, J., Kirkham, E., Atherton, J. F., Menard, A., Magill, P. J., Bolam, J. P., & Bevan, M. D. (2009). Sparse but selective and potent synaptic transmission from the globus pallidus to the subthalamic nucleus. *J Neurophysiol, 102*(1), 532-545. doi:10.1152/jn.00305.2009

Baunez, C., Amalric, M., & Robbins, T. W. (2002). Enhanced food-related motivation after bilateral lesions of the subthalamic nucleus. *J Neurosci, 22*(2), 562-568.

Baunez, C., Dias, C., Cador, M., & Amalric, M. (2005). The subthalamic nucleus exerts opposite control on cocaine and 'natural' rewards. *Nat Neurosci, 8*(4), 484-489. doi:10.1038/nn1429

Baunez, C., Nieoullon, A., & Amalric, M. (1995). In a rat model of parkinsonism, lesions of the subthalamic nucleus reverse increases of reaction time but induce a dramatic premature responding deficit. *J Neurosci, 15*(10), 6531-6541.

Benabid, A.-L., Krack, P., Benazzouz, A., Limousin, P., Koudsie, A., & Pollak, P. (2000). Deep brain stimulation of the subthalamic nucleus for Parkinson's disease: methodologic aspects and clinical criteria. *J Neurol, 55*(12 Suppl 6), S40-44.

Benabid, A. L., Chabardes, S., Mitrofanis, J., & Pollak, P. (2009). Deep brain stimulation of the subthalamic nucleus for the treatment of Parkinson's disease. *Lancet Neurol, 8*(1), 67-81. doi:10.1016/S1474-4422(08)70291-6

Benabid, A. L., Pollak, P., Gervason, C., Hoffmann, D., Gao, D. M., Hommel, M., Perret, J. E., & de Rougemont, J. (1991). Long-term suppression of tremor by chronic stimulation of the ventral intermediate thalamic nucleus. *Lancet, 337*(8738), 403-406.

Benabid, A. L., Pollak, P., Louveau, A., Henry, S., & de Rougemont, J. (1987). Combined (thalamotomy and stimulation) stereotactic surgery of the VIM thalamic nucleus for bilateral Parkinson disease. *Appl Neurophysiol, 50*(1-6), 344-346.

Benarroch, E. E. (2013). Monoamine transporters: structure, regulation, and clinical implications. *Neurology, 81*(8), 761-768. doi:10.1212/WNL.0b013e3182a1ab4a

Benazzouz, A., Breit, S., Koudsie, A., Pollak, P., Krack, P., & Benabid, A. L. (2002). Intraoperative microrecordings of the subthalamic nucleus in Parkinson's disease. *Mov Disord, 17 Suppl 3*, S145-149.

Benazzouz, A., Gao, D., Ni, Z., Piallat, B., Bouali-Benazzouz, R., & Benabid, A. (2000). Effect of high-frequency stimulation of the subthalamic nucleus on the neuronal activities of the substantia nigra pars reticulata and ventrolateral nucleus of the thalamus in the rat. *J Neurol, 99*(2), 289-295.

Benazzouz, A., Tai, C. H., Meissner, W., Bioulac, B., Bezard, E., & Gross, C. (2004). High-frequency stimulation of both zona incerta and subthalamic nucleus induces a similar normalization of basal ganglia metabolic activity in experimental parkinsonism. *FASEB J, 18*(3), 528-530. doi:10.1096/fj.03-0576fje

Berens, P. (2009a). CircStat: A MATLAB Toolbox for Circular Statistics. *Journal of Statistical Software, 31*(10).

Berens, P. (2009b). CircStat: A MATLAB Toolbox for Circular Statistics. *Journal of Statistical Software, 31*(10), 1-21.

Berényi, A., Belluscio, M., Mao, D., & Buzsáki, G. (2012). Closed-loop control of epilepsy by transcranial electrical stimulation. *J Science 337*(6095), 735-737.

Berger, H. J. (1929). *Archiv für psychiatrie und nervenkrankheiten*, Über das elektrenkephalogramm des menschen. *87*(1), 527-570.

Bergman, H., Wichmann, T., & DeLong, M. R. (1990). Reversal of experimental parkinsonism by lesions of the subthalamic nucleus. *J Science, 249*(4975), 1436-1438.

Bergman, H., Wichmann, T., Karmon, B., & DeLong, M. R. (1994). The primate subthalamic nucleus. II. Neuronal activity in the MPTP model of parkinsonism. *J Neurophysiol, 72*(2), 507-520. doi:10.1152/jn.1994.72.2.507

Berke, J. J. E. (2009). Fast oscillations in cortical-striatal networks switch frequency following rewarding events and stimulant drugs. *J Neurosci, 30*(5), 848-859.

Beurrier, C., Bioulac, B., Audin, J., & Hammond, C. J. (2001). High-frequency stimulation produces a transient blockade of voltage-gated currents in subthalamic neurons. *J Neurosci, 85*(4), 1351-1356.

Beurrier, C., Bioulac, B., & Hammond, C. J. (2000). Slowly inactivating sodium current (I NaP) underlies single-spike activity in rat subthalamic neurons. *J Neurosci, 83*(4), 1951-1957.

Beurrier, C., Congar, P., Bioulac, B., & Hammond, C. (1999). Subthalamic nucleus neurons switch from single-spike activity to burst-firing mode. *J Neurosci, 19*(2), 599-609.

Beuter, A., Lefaucheur, J. P., & Modolo, J. (2014). Closed-loop cortical neuromodulation in Parkinson's disease: An alternative to deep brain stimulation? *Clin Neurophysiol, 125*(5), 874-885. doi:10.1016/j.clinph.2014.01.006

Bevan, M. D. (2017). Chapter 14 - The Subthalamic Nucleus. In H. Steiner & K. Y. Tseng (Eds.), *Handbook of Behavioral Neuroscience* (Vol. 24, pp. 277-291): Elsevier.

Bevan, M. D., Atherton, J. F., & Baufreton, J. (2006). Cellular principles underlying normal and pathological activity in the subthalamic nucleus. *Curr Opin Neurobiol, 16*(6), 621-628. doi:10.1016/j.conb.2006.10.003

Bevan, M. D., & Bolam, J. P. (1995). Cholinergic, GABAergic, and glutamate-enriched inputs from the mesopontine tegmentum to the subthalamic nucleus in the rat. *J Neurosci, 15*(11), 7105-7120.

Bevan, M. D., Booth, P. A., Eaton, S. A., & Bolam, J. P. J. (1998). Selective innervation of neostriatal interneurons by a subclass of neuron in the globus pallidus of the rat. *J Neurosci, 18*(22), 9438-9452.

Bevan, M. D., Crossman, A. R., & Bolam, J. P. (1994). Neurons projecting from the entopeduncular nucleus to the thalamus receive convergent synaptic inputs from the subthalamic nucleus and the neostriatum in the rat. *Brain Res, 659*(1-2), 99-109.

Bevan, M. D., Francis, C. M., & Bolam, J. P. (1995). The glutamate-enriched cortical and thalamic input to neurons in the subthalamic nucleus of the rat: convergence with GABA-positive terminals. *J Comp Neurol, 361*(3), 491-511. doi:10.1002/cne.903610312

Bevan, M. D., Magill, P. J., Terman, D., Bolam, J. P., & Wilson, C. J. (2002). Move to the rhythm: oscillations in the subthalamic nucleus-external globus pallidus network. *Trends Neurosci, 25*(10), 525-531.

Bevan, M. D., & Wilson, C. J. (1999). Mechanisms underlying spontaneous oscillation and rhythmic firing in rat subthalamic neurons. *J Neurosci, 19*(17), 7617-7628.

Blandini, F., & Armentero, M. T. (2012). Animal models of Parkinson's disease. *FEBS J, 279*(7), 1156-1166. doi:10.1111/j.1742-4658.2012.08491.x

Blenkinsop, A., Anderson, S., & Gurney, K. (2017). Frequency and function in the basal ganglia: the origins of beta and gamma band activity. *J Physiol, 595*(13), 4525-4548. doi:10.1113/JP273760

Bogacz, R., & Gurney, K. (2007). The basal ganglia and cortex implement optimal decision making between alternative actions. *Neural Comput, 19*(2), 442-477. doi:10.1162/neco.2007.19.2.442

Bogacz, R., Martin Moraud, E., Abdi, A., Magill, P. J., & Baufreton, J. (2016). Properties of Neurons in External Globus Pallidus Can Support Optimal Action Selection. *PLoS Comput Biol, 12*(7), e1005004. doi:10.1371/journal.pcbi.1005004

Boraud, T., Bezard, E., Bioulac, B., & Gross, C. E. (2000). Ratio of inhibited-to-activated pallidal neurons decreases dramatically during passive limb movement in the MPTP-treated monkey. *J Neurophysiol, 83*(3), 1760-1763. doi:10.1152/jn.2000.83.3.1760

Boraud, T., Bezard, E., Guehl, D., Bioulac, B., & Gross, C. (1998). Effects of L-DOPA on neuronal activity of the globus pallidus externalis (GPe) and globus pallidus internalis (GPi) in the MPTP-treated monkey. *Brain Res, 787*(1), 157-160.

Bostan, A. C., & Strick, P. L. (2010). The cerebellum and basal ganglia are interconnected. *Neuropsychol Rev, 20*(3), 261-270. doi:10.1007/s11065-010-9143-9

Brazhnik, E., Cruz, A. V., Avila, I., Wahba, M. I., Novikov, N., Ilieva, N. M., McCoy, A. J., Gerber, C., & Walters, J. R. J. (2012). State-dependent spike and local field synchronization between motor cortex and substantia nigra in hemiparkinsonian rats. *J Neurosci, 32*(23), 7869-7880.

Brazhnik, E., McCoy, A. J., Novikov, N., Hatch, C. E., & Walters, J. R. (2016). Ventral Medial Thalamic Nucleus Promotes Synchronization of Increased High Beta Oscillatory Activity in the Basal Ganglia-Thalamocortical Network of the Hemiparkinsonian Rat. *J Neurosci, 36*(15), 4196-4208. doi:10.1523/JNEUROSCI.3582-15.2016

Brillinger, D. R. (1981). *Time series: data analysis and theory* (Vol. 36): Siam.

Brittain, J.-S., Watkins, K. E., Joundi, R. A., Ray, N. J., Holland, P., Green, A. L., Aziz, T. Z., & Jenkinson, N. J. (2012). A role for the subthalamic nucleus in response inhibition during conflict. *J Neurosci, 32*(39), 13396-13401.

Brittain, J. S., & Brown, P. (2014). Oscillations and the basal ganglia: motor control and beyond. *Neuroimage, 85 Pt 2*, 637-647. doi:10.1016/j.neuroimage.2013.05.084

Brittain, J. S., Probert-Smith, P., Aziz, T. Z., & Brown, P. (2013). Tremor suppression by rhythmic transcranial current stimulation. *Curr Biol, 23*(5), 436-440. doi:10.1016/j.cub.2013.01.068

Brocker, D. T., Swan, B. D., So, R. Q., Turner, D. A., Gross, R. E., & Grill, W. M. (2017). Optimized temporal pattern of brain stimulation designed by computational evolution. *Sci Transl Med, 9*(371). doi:10.1126/scitranslmed.aah3532

Bronte-Stewart, H., Barberini, C., Koop, M. M., Hill, B. C., Henderson, J. M., & Wingeier, B. J. E. n. (2009). The STN beta-band profile in Parkinson's disease is stationary and shows prolonged attenuation after deep brain stimulation. *Exp Neurol,215*(1), 20-28.

Brooks, D. J. (2004). Neuroimaging in Parkinson's disease. *NeuroRx, 1*(2), 243-254. doi:10.1602/neurorx.1.2.243

Brown, P., & Marsden, C. D. (1999). Bradykinesia and impairment of EEG desynchronization in Parkinson's disease. *Mov Disord,14*(3), 423-429.

Brown, P., & Williams, D. (2005). Basal ganglia local field potential activity: character and functional significance in the human. *Clin Neurophysiol, 116*(11), 2510-2519. doi:10.1016/j.clinph.2005.05.009

Brown, P. (2007). Abnormal oscillatory synchronisation in the motor system leads to impaired movement. *Curr Opin Neurobiol,17*(6), 656-664.

Brunenberg, E. J., Moeskops, P., Backes, W. H., Pollo, C., Cammoun, L., Vilanova, A., Janssen, M. L., Visser-Vandewalle, V. E., ter Haar Romeny, B. M., Thiran, J. P., & Platel, B. (2012). Structural and resting state functional connectivity of the subthalamic nucleus: identification of motor STN parts and the hyperdirect pathway. *PLoS One, 7*(6), e39061. doi:10.1371/journal.pone.0039061

Bunney, B. S., Walters, J. R., Roth, R. H., & Aghajanian, G. K. (1973). Dopaminergic neurons: effect of antipsychotic drugs and amphetamine on single cell activity. *J Pharmacol Exp Ther, 185*(3), 560-571.

Buzsaki, G., Anastassiou, C. A., & Koch, C. (2012). The origin of extracellular fields and currents--EEG, ECoG, LFP and spikes. *Nat Rev Neurosci, 13*(6), 407-420. doi:10.1038/nrn3241

Buzsaki, G., & Draguhn, A. (2004). Neuronal oscillations in cortical networks. *Science, 304*(5679), 1926-1929. doi:10.1126/science.1099745

Buzsaki, G., & Schomburg, E. W. (2015). What does gamma coherence tell us about inter-regional neural communication? *Nat Neurosci, 18*(4), 484-489. doi:10.1038/nn.3952

Cagnan, H., Brittain, J. S., Little, S., Foltynie, T., Limousin, P., Zrinzo, L., Hariz, M., Joint, C., Fitzgerald, J., Green, A. L., Aziz, T., & Brown, P. (2013a). Phase dependent modulation of tremor amplitude in essential tremor through thalamic stimulation. *Brain, 136*(Pt 10), 3062-3075. doi:10.1093/brain/awt239

Cagnan, H., Brittain, J. S., Little, S., Foltynie, T., Limousin, P., Zrinzo, L., Hariz, M., Joint, C., Fitzgerald, J., Green, A. L., Aziz, T., & Brown, P. (2013b). Phase dependent modulation of tremor amplitude in essential tremor through thalamic stimulation. *Brain, 136*(10), 3062-3075. doi:10.1093/brain/awt239

Cagnan, H., Duff, E. P., & Brown, P. (2015). The relative phases of basal ganglia activities dynamically shape effective connectivity in Parkinson's disease. *Brain, 138*(Pt 6), 1667-1678. doi:10.1093/brain/awv093

Cagnan, H., Kuhn, A. A., & Brown, P. (2014). Co-modulation of finely tuned high-gamma band activity across hemispheres in Parkinson's disease. *Clin Neurophysiol, 125*(4), 777-785. doi:10.1016/j.clinph.2013.10.001

Cagnan, H., Pedrosa, D., Little, S., Pogosyan, A., Cheeran, B., Aziz, T., Green, A., Fitzgerald, J., Foltynie, T., Limousin, P., Zrinzo, L., Hariz, M., Friston, K. J.,

Denison, T., & Brown, P. (2017). Stimulating at the right time: phase-specific deep brain stimulation. *Brain, 140*(1), 132-145. doi:10.1093/brain/aww286

Campbell, P., Reep, R. L., Stoll, M. L., Ophir, A. G., & Phelps, S. M. (2009). Conservation and diversity of Foxp2 expression in muroid rodents: functional implications. *J Comp Neurol, 512*(1), 84-100. doi:10.1002/cne.21881

Cannon, J., McCarthy, M. M., Lee, S., Lee, J., Borgers, C., Whittington, M. A., & Kopell, N. (2014). Neurosystems: brain rhythms and cognitive processing. *Eur J Neurosci, 39*(5), 705-719. doi:10.1111/ejn.12453

Canteras, N. S., Shammah-Lagnado, S. J., Silva, B. A., & Ricardo, J. A. (1990). Afferent connections of the subthalamic nucleus: a combined retrograde and anterograde horseradish peroxidase study in the rat. *Brain Res, 513*(1), 43-59.

Carlson, J. D., Cleary, D. R., Cetas, J. S., Heinricher, M. M., & Burchiel, K. J. (2010). Deep brain stimulation does not silence neurons in subthalamic nucleus in Parkinson's patients. *J Neurophysiol, 103*(2), 962-967. doi:10.1152/jn.00363.2009

Carpenter, M. B. (1955). Ballism associated with partial destruction of the subthalamic nucleus of luys. *Neurology, 5*(7), 479-489.

Carpenter, M. B., Baton, R. R., 3rd, Carleton, S. C., & Keller, J. T. (1981). Interconnections and organization of pallidal and subthalamic nucleus neurons in the monkey. *J Comp Neurol, 197*(4), 579-603. doi:10.1002/cne.901970404

Castrioto, A., Lhommée, E., Moro, E., & Krack, P. (2014). Mood and behavioural effects of subthalamic stimulation in Parkinson's disease. *Lancet Neurol, 13*(3), 287-305.

Chan, C. S., Shigemoto, R., Mercer, J. N., & Surmeier, D. J. J. J. o. N. (2004). HCN2 and HCN1 channels govern the regularity of autonomous pacemaking and synaptic resetting in globus pallidus neurons. *24*(44), 9921-9932.

Chang, H. T., Wilson, C. J., & Kitai, S. T. (1981). Single neostriatal efferent axons in the globus pallidus: a light and electron microscopic study. *Science, 213*(4510), 915-918.

Chen, C. C., Hsu, Y. T., Chan, H. L., Chiou, S. M., Tu, P. H., Lee, S. T., Tsai, C. H., Lu, C. S., & Brown, P. (2010). Complexity of subthalamic 13-35 Hz oscillatory activity directly correlates with clinical impairment in patients with Parkinson's disease. *Exp Neurol, 224*(1), 234-240. doi:10.1016/j.expneurol.2010.03.015

Chen, C. C., Litvak, V., Gilbertson, T., KŘhn, A., Lu, C. S., Lee, S. T., Tsai, C. H., Tisch, S., Limousin, P., & Hariz, M. (2007). Excessive synchronization of basal ganglia

neurons at 20áHz slows movement in Parkinson's disease. *Exp Neurol, 205*(1), 214-221.

Chen, H., Lei, H., & Xu, Q. J. B. b. r. (2018). Neuronal activity pattern defects in the striatum in awake mouse model of Parkinson's disease. *Behav brain res, 3 41*, 135-145.

Chesselet, M. F., Fleming, S., Mortazavi, F., & Meurers, B. (2008). Strengths and limitations of genetic mouse models of Parkinson's disease. *Parkinsonism Relat Disord, 14 Suppl 2*, S84-87. doi:10.1016/j.parkreldis.2008.04.004

Cheyne, D., Bells, S., Ferrari, P., Gaetz, W., & Bostan, A. C. (2008). Self-paced movements induce high-frequency gamma oscillations in primary motor cortex. *J Neuroimage, 42*(1), 332-342.

Chiken, S., & Nambu, A. (2016). Mechanism of deep brain stimulation: inhibition, excitation, or disruption? *The Neuroscientist, 22*(3), 313-322.

Chu, H.-Y., Atherton, J. F., Wokosin, D., Surmeier, D. J., & Bevan, M. D. (2015). Heterosynaptic regulation of external globus pallidus inputs to the subthalamic nucleus by the motor cortex. *Neuron, 85*(2), 364-376.

Clarke, N., Bevan, M., Cozzari, C., Hartman, B., & Bolam, J. (1997). Glutamate-enriched cholinergic synaptic terminals in the entopeduncular nucleus and subthalamic nucleus of the rat. *J Neurosci, 81*(2), 371-385.

Connolly, B. S., & Lang, A. E. (2014). Pharmacological treatment of Parkinson disease: a review. *JAMA, 311*(16), 1670-1683. doi:10.1001/jama.2014.3654

Constantoyannis, C., Kumar, A., Stoessl, A. J., & Honey, C. R. (2004). Tremor induced by thalamic deep brain stimulation in patients with complex regional facial pain. *Mov Disord, 19*(8), 933-936. doi:10.1002/mds.20047

Corbit, V. L., Whalen, T. C., Zitelli, K. T., Crilly, S. Y., Rubin, J. E., & Gittis, A. H. (2016). Pallidostriatal Projections Promote beta Oscillations in a Dopamine-Depleted Biophysical Network Model. *J Neurosci, 36*(20), 5556-5571. doi:10.1523/JNEUROSCI.0339-16.2016

Courtemanche, R., Fujii, N., & Graybiel, A. M. (2003). Synchronous, focally modulated beta-band oscillations characterize local field potential activity in the striatum of awake behaving monkeys. *J Neurosci, 23*(37), 11741-11752.

Cragg, S. J., Baufreton, J., Xue, Y., Bolam, J. P., & Bevan, M. D. (2004). Synaptic release of dopamine in the subthalamic nucleus. *Eur J Neurosci, 20*(7), 1788-1802.

Creutzfeldt, O. D., Watanabe, S., & Lux, H. D. (1966). Relations between EEG phenomena and potentials of single cortical cells. I. Evoked responses after thalamic and erpicortical stimulation. *Electroencephalogr Clin Neurophysiol, 20*(1), 1-18.

Crone, N. E., Miglioretti, D. L., Gordon, B., Sieracki, J. M., Wilson, M. T., Uematsu, S., & Lesser, R. P. (1998). Functional mapping of human sensorimotor cortex with electrocorticographic spectral analysis. I. Alpha and beta event-related desynchronization. *Brain, 121*(12), 2271-2299.

Cui, G., Jun, S. B., Jin, X., Pham, M. D., Vogel, S. S., Lovinger, D. M., & Costa, R. M. (2013). Concurrent activation of striatal direct and indirect pathways during action initiation. *Nature, 494*(7436), 238-242. doi:10.1038/nature11846

de Hemptinne, C., Ryapolova-Webb, E. S., Air, E. L., Garcia, P. A., Miller, K. J., Ojemann, J. G., Ostrem, J. L., Galifianakis, N. B., & Starr, P. A. (2013a). Exaggerated phase-amplitude coupling in the primary motor cortex in Parkinson disease. *Proc Natl Acad Sci U S A, 110*(12), 4780-4785. doi:10.1073/pnas.1214546110

De Hemptinne, C., Ryapolova-Webb, E. S., Air, E. L., Garcia, P. A., Miller, K. J., Ojemann, J. G., Ostrem, J. L., Galifianakis, N. B., & Starr, P. A. (2013b). Exaggerated phase–amplitude coupling in the primary motor cortex in Parkinson disease. *PNAS*, 201214546.

De Hemptinne, C., Swann, N. C., Ostrem, J. L., Ryapolova-Webb, E. S., San Luciano, M., Galifianakis, N. B., & Starr, P. A. (2015). Therapeutic deep brain stimulation reduces cortical phase-amplitude coupling in Parkinson's disease. *Nat Neurosci,18*(5), 779.

de Solages, C., Hill, B. C., Koop, M. M., Henderson, J. M., & Bronte-Stewart, H. (2010). Bilateral symmetry and coherence of subthalamic nuclei beta band activity in Parkinson's disease. *Exp Neurol,221*(1), 260-266.

Deffains, M., Iskhakova, L., Katabi, S., Haber, S. N., Israel, Z., & Bergman, H. (2016). Subthalamic, not striatal, activity correlates with basal ganglia downstream activity in normal and parkinsonian monkeys. *Elife, 5*. doi:10.7554/eLife.16443

Deffains, M., Iskhakova, L., Katabi, S., Israel, Z., & Bergman, H. (2018). Longer β oscillatory episodes reliably identify pathological subthalamic activity in Parkinsonism. *Mov Disord, 33*(10), 1609-1618.

Deffains, M., Legallet, E., & Apicella, P. (2010a). Modulation of neuronal activity in the monkey putamen associated with changes in the habitual order of sequential movements. *J Neurophysiol, 104*(3), 1355-1369. doi:10.1152/jn.00355.2010

Deffains, M., Legallet, E., & Apicella, P. J. (2010b). Modulation of neuronal activity in the monkey putamen associated with changes in the habitual order of sequential movements. *J Neurophysiol,104*(3), 1355-1369.

Degos, B., Deniau, J. M., Le Cam, J., Mailly, P., & Maurice, N. (2008). Evidence for a direct subthalamo-cortical loop circuit in the rat. *Eur J Neurosci, 27*(10), 2599-2610. doi:10.1111/j.1460-9568.2008.06229.x

DeLong, M. R. (1990). Primate models of movement disorders of basal ganglia origin. *Trends Neurosci, 13*(7), 281-285.

DeLong, M. R., Crutcher, M. D., & Georgopoulos, A. P. (1985). Primate globus pallidus and subthalamic nucleus: functional organization. *J Neurophysiol, 53*(2), 530-543. doi:10.1152/jn.1985.53.2.530

Deschenes, M., Bourassa, J., & Parent, A. (1996). Striatal and cortical projections of single neurons from the central lateral thalamic nucleus in the rat. *Neuroscience, 72*(3), 679-687.

Deuschl, G., & Elble, R. J. (2000). The pathophysiology of essential tremor. *Neurology, 54*(11 Suppl 4), S14-20.

Devergnas, A., & Wichmann, T. (2011). Cortical potentials evoked by deep brain stimulation in the subthalamic area. *Front Sys Neurosci, 5*, 30.

Devos, D., Szurhaj, W., Reyns, N., Labyt, E., Houdayer, E., Bourriez, J., Cassim, F., Krystkowiak, P., Blond, S., & Destée, A. (2006). Predominance of the contralateral movement-related activity in the subthalamo-cortical loop. *Clin Neurophys, 117*(10), 2315-2327.

Do, M. T., & Bean, B. P. (2003). Subthreshold sodium currents and pacemaking of subthalamic neurons: modulation by slow inactivation. *Neuron, 39*(1), 109-120.

Do, M. T., & Bean, B. P. (2004). Sodium currents in subthalamic nucleus neurons from Nav1.6-null mice. *J Neurophysiol, 92*(2), 726-733. doi:10.1152/jn.00186.2004

Donoghue, J. P., Sanes, J. N., Hatsopoulos, N. G., & Gaal, G. (1998). Neural discharge and local field potential oscillations in primate motor cortex during voluntary movements. *J Neurophysiol, 79*(1), 159-173. doi:10.1152/jn.1998.79.1.159

Dorval, A. D., & Grill, W. M. (2014). Deep brain stimulation of the subthalamic nucleus reestablishes neuronal information transmission in the 6-OHDA rat model of parkinsonism. *J Neurosci, 111*(10), 1949-1959.

Dorval, A. D., Kuncel, A. M., Birdno, M. J., Turner, D. A., & Grill, W. M. (2010). Deep brain stimulation alleviates parkinsonian bradykinesia by regularizing pallidal activity. *104*(2), 911-921.

Dorval, A. D., Russo, G. S., Hashimoto, T., Xu, W., Grill, W. M., & Vitek, J. L. (2008). Deep brain stimulation reduces neuronal entropy in the MPTP-primate model of Parkinson's disease. *J Neurophys, 100*(5), 2807-2818.

Dostrovsky, J., Levy, R., Wu, J., Hutchison, W., Tasker, R., & Lozano, A. J. J. o. n. (2000). Microstimulation-induced inhibition of neuronal firing in human globus pallidus. *84*(1), 570-574.

Doyle, L., Kühn, A., Hariz, M., Kupsch, A., Schneider, G. H., & Brown, P. (2005). Levodopa-induced modulation of subthalamic beta oscillations during self-paced movements in patients with Parkinson's disease. *Eur J Neurosci,21*(5), 1403-1412.

Drago, J., Padungchaichot, P., Wong, J. Y., Lawrence, A. J., McManus, J. F., Sumarsono, S. H., Natoli, A. L., Lakso, M., Wreford, N., Westphal, H., Kola, I., & Finkelstein, D. I. (1998). Targeted expression of a toxin gene to D1 dopamine receptor neurons by cre-mediated site-specific recombination. *J Neurosci, 18*(23), 9845-9857.

Durieux, P. F., Bearzatto, B., Guiducci, S., Buch, T., Waisman, A., Zoli, M., Schiffmann, S. N., & de Kerchove d'Exaerde, A. (2009). D2R striatopallidal neurons inhibit both locomotor and drug reward processes. *Nat Neurosci, 12*(4), 393-395. doi:10.1038/nn.2286

Durieux, P. F., Schiffmann, S. N., & de Kerchove d'Exaerde, A. (2012). Differential regulation of motor control and response to dopaminergic drugs by D1R and D2R neurons in distinct dorsal striatum subregions. *EMBO J, 31*(3), 640-653. doi:10.1038/emboj.2011.400

Eagle, D. M., Baunez, C., Hutcheson, D. M., Lehmann, O., Shah, A. P., & Robbins, T. W. (2008). Stop-signal reaction-time task performance: role of prefrontal cortex and subthalamic nucleus. *Cereb Cortex, 18*(1), 178-188. doi:10.1093/cercor/bhm044

Eberle, W., Penders, J., & Yazicioglu, R. F. (2011). Closing the loop for Deep Brain Stimulation implants enables personalized healthcare for Parkinson's disease patients. *Conf Proc IEEE Eng Med Biol Soc, 2011*, 1556-1558. doi:10.1109/IEMBS.2011.6090453

Eccles, J. C. (1951). Interpretation of action potentials evoked in the cerebral cortex. *Electroencephalogr Clin Neurophysiol, 3*(4), 449-464.

Edley, S. M., & Graybiel, A. M. (1983). The afferent and efferent connections of the feline nucleus tegmenti pedunculopontinus, pars compacta. *J Comp Neurol, 217*(2), 187-215. doi:10.1002/cne.902170207

Ehringer, H., & Hornykiewicz, O. (1960). [Distribution of noradrenaline and dopamine (3-hydroxytyramine) in the human brain and their behavior in diseases of the extrapyramidal system]. *Klin Wochenschr, 38*, 1236-1239.

Engel, A. K., & Fries, P. (2010). Beta-band oscillations--signalling the status quo? *Curr Opin Neurobiol, 20*(2), 156-165. doi:10.1016/j.conb.2010.02.015

Engel, A. K., Fries, P., & Singer, W. (2001). Dynamic predictions: oscillations and synchrony in top-down processing. *Nat Rev Neurosci, 2*(10), 704-716. doi:10.1038/35094565

Engel, A. K., Konig, P., Kreiter, A. K., & Singer, W. (1991). Interhemispheric synchronization of oscillatory neuronal responses in cat visual cortex. *Science, 252*(5009), 1177-1179.

Engel, A. K., Moll, C. K., Fried, I., & Ojemann, G. A. (2005). Invasive recordings from the human brain: clinical insights and beyond. *Nat Rev Neurosci, 6*(1), 35-47. doi:10.1038/nrn1585

Ermentrout, G. B., & Chow, C. C. (2002). Modeling neural oscillations. *Physiol Behav, 77*(4-5), 629-633.

Escola, L., Michelet, T., Macia, F., Guehl, D., Bioulac, B., & Burbaud, P. (2003). Disruption of information processing in the supplementary motor area of the MPTP-treated monkey: a clue to the pathophysiology of akinesia? *Brain, 126*(Pt 1), 95-114.

Eusebio, A., Chen, C. C., Lu, C. S., Lee, S. T., Tsai, C. H., Limousin, P., Hariz, M., & Brown, P. (2008). Effects of low-frequency stimulation of the subthalamic nucleus on movement in Parkinson's disease. *Exp Neurol, 209*(1), 125-130. doi:10.1016/j.expneurol.2007.09.007

Eusebio, A., Pogosyan, A., Wang, S., Averbeck, B., Gaynor, L. D., Cantiniaux, S., Witjas, T., Limousin, P., Azulay, J. P., & Brown, P. (2009). Resonance in subthalamo-cortical circuits in Parkinson's disease. *Brain, 132*(Pt 8), 2139-2150. doi:10.1093/brain/awp079

Eusebio, A., Thevathasan, W., Gaynor, L. D., Pogosyan, A., Bye, E., Foltynie, T., Zrinzo, L., Ashkan, K., Aziz, T., Brown, P. J. (2010). Deep brain stimulation can suppress pathological synchronisation in parkinsonian patients. *J Neurol Neurosurg Psychiat,* 2010.217489.

Fahn, S. (1987). Drug treatment of hyperkinetic movement disorders. *Semin Neurol, 7*(2), 192-208. doi:10.1055/s-2008-1041419

Fahn, S., & Sulzer, D. (2004). Neurodegeneration and neuroprotection in Parkinson disease. *NeuroRx, 1*(1), 139-154. doi:10.1602/neurorx.1.1.139

Farries, M. A., Kita, H., & Wilson, C. J. J. (2010). Dynamic spike threshold and zero membrane slope conductance shape the response of subthalamic neurons to cortical input. *J Neurosci, 30*(39), 13180-13191.

Farries, M. A., & Wilson, C. J. J. (2012). Phase response curves of subthalamic neurons measured with synaptic input and current injection. *J Neurophysiol,108*(7), 1822-1837.

Fasano, A., & Lozano, A. M. (2015). Deep brain stimulation for movement disorders: 2015 and beyond. *Curr Opin Neurol, 28*(4), 423-436. doi:10.1097/WCO.0000000000000226

Feingold, J., Gibson, D. J., DePasquale, B., & Graybiel, A. M. (2015a). Bursts of beta oscillation differentiate postperformance activity in the striatum and motor cortex of monkeys performing movement tasks. *Proc Natl Acad Sci U S A, 112*(44), 13687-13692. doi:10.1073/pnas.1517629112

Fife, K. H., Gutierrez-Reed, N. A., Zell, V., Bailly, J., Lewis, C. M., Aron, A. R., & Hnasko, T. S. (2017). Causal role for the subthalamic nucleus in interrupting behavior. *Elife, 6*. doi:10.7554/eLife.27689

Filali, M., Hutchison, W. D., Palter, V. N., Lozano, A. M., & Dostrovsky, J. O. (2004). Stimulation-induced inhibition of neuronal firing in human subthalamic nucleus. *Exp Brain Res, 156*(3), 274-281. doi:10.1007/s00221-003-1784-y

Filion, M., Tremblay, L., & Bedard, P. J. (1991). Effects of dopamine agonists on the spontaneous activity of globus pallidus neurons in monkeys with MPTP-induced parkinsonism. *Brain Res, 547*(1), 152-161.

Fischer, P., Lipski, W., Neumann, W. J., Turner, R. S., Fries, P., Brown, P., & Richardson, R. M. (2018). Cortico-basal-ganglia communication: Temporally structured activity for selective motor control. *bioRxiv*, 413286.

Flaherty, A. W., & Graybiel, A. M. (1991). Corticostriatal transformations in the primate somatosensory system. Projections from physiologically mapped body-part representations. *J Neurophysiol, 66*(4), 1249-1263. doi:10.1152/jn.1991.66.4.1249

Flores, G., Hernandez, S., Rosales, M. G., Sierra, A., Martines-Fong, D., Flores-Hernandez, J., & Aceves, J. J. N. l. (1996). M3 muscarinic receptors mediate cholinergic excitation of the spontaneous activity of subthalamic neurons in the rat. *203*(3), 203-206.

Foffani, G., Ardolino, G., Egidi, M., Caputo, E., Bossi, B., & Priori, A. (2006). Subthalamic oscillatory activities at beta or higher frequency do not change after high-frequency DBS in Parkinson's disease. *Brain Res, 69*(2), 123-130.

Fogelson, N., Kühn, A. A., Silberstein, P., Limousin, P. D., Hariz, M., Trottenberg, T., Kupsch, A., & Brown, P. J. (2005). Frequency dependent effects of subthalamic nucleus stimulation in Parkinson's disease. *J Neuroscience letters, 382*(1-2), 5-9.

Fogelson, N., Williams, D., Tijssen, M., van Bruggen, G., Speelman, H., & Brown, P. (2006). Different functional loops between cerebral cortex and the subthalmic area in Parkinson's disease. *Cereb Cortex, 16*(1), 64-75. doi:10.1093/cercor/bhi084

Fonnum, F., Gottesfeld, Z., & Grofova, I. (1978). Distribution of glutamate decarboxylase, choline acetyl-transferase and aromatic amino acid decarboxylase in the basal ganglia of normal and operated rats. Evidence for striatopallidal, striatoentopeduncular and striatonigral GABAergic fibres. *Brain Res, 143*(1), 125-138.

Fortin, M., & Parent, A. (1996). Calretinin as a marker of specific neuronal subsets in primate substantia nigra and subthalamic nucleus. *Brain Res, 708*(1-2), 201-204.

François, C., Savy, C., Jan, C., Tande, D., Hirsch, E. C., & Yelnik, J. (2000). Dopaminergic innervation of the subthalamic nucleus in the normal state, in MPTP-treated monkeys, and in Parkinson's disease patients. *J Comp Neuro, 425*(1), 121-129.

Frank, M. J. (2006). Hold your horses: a dynamic computational role for the subthalamic nucleus in decision making. *Neural Netw, 19*(8), 1120-1136. doi:10.1016/j.neunet.2006.03.006

Frank, M. J., Samanta, J., Moustafa, A. A., & Sherman, S. J. (2007). Hold your horses: impulsivity, deep brain stimulation, and medication in parkinsonism. *Science, 318*(5854), 1309-1312. doi:10.1126/science.1146157

Fries, P. (2005). A mechanism for cognitive dynamics: neuronal communication through neuronal coherence. *Trends Cogn Sci, 9*(10), 474-480. doi:10.1016/j.tics.2005.08.011

Fries, P. (2015). Rhythms for Cognition: Communication through Coherence. *Neuron, 88*(1), 220-235. doi:10.1016/j.neuron.2015.09.034

Fries, P., Roelfsema, P. R., Engel, A. K., Konig, P., & Singer, W. (1997). Synchronization of oscillatory responses in visual cortex correlates with perception in interocular rivalry. *Proc Natl Acad Sci U S A, 94*(23), 12699-12704.

Fries, P., Schroder, J. H., Roelfsema, P. R., Singer, W., & Engel, A. K. (2002). Oscillatory neuronal synchronization in primary visual cortex as a correlate of stimulus selection. *J Neurosci, 22*(9), 3739-3754. doi:20026318

Fries, P., Womelsdorf, T., Oostenveld, R., & Desimone, R. (2008). The effects of visual stimulation and selective visual attention on rhythmic neuronal synchronization in macaque area V4. *J Neurosci, 28*(18), 4823-4835. doi:10.1523/JNEUROSCI.4499-07.2008

Frost, J. D., Jr. (1968). EEG-intracellular potential relationships in isolated cerebral cortex. *Electroencephalogr Clin Neurophysiol, 24*(5), 434-443.

Fujimoto, K., & Kita, H. (1993). Response characteristics of subthalamic neurons to the stimulation of the sensorimotor cortex in the rat. *Brain Res, 609*(1-2), 185-192.

Fujiyama, F., Nakano, T., Matsuda, W., Furuta, T., Udagawa, J., Kaneko, T. J. B. S., & Function. (2016). A single-neuron tracing study of arkypallidal and prototypic neurons in healthy rats. *221*(9), 4733-4740.

Gale, J. T., Shields, D. C., Jain, F. A., Amirnovin, R., & Eskandar, E. N. (2009). Subthalamic nucleus discharge patterns during movement in the normal monkey and Parkinsonian patient. *Brain Res, 1260*, 15-23.

Galvan, A., Hu, X., Smith, Y., & Wichmann, T. (2012). In vivo optogenetic control of striatal and thalamic neurons in non-human primates. *PLoS One, 7*(11), e50808.

Garcia, L., Audin, J., D'Alessandro, G., Bioulac, B., & Hammond, C. J. (2003). Dual effect of high-frequency stimulation on subthalamic neuron activity. *J Neurosci, 23*(25), 8743-8751.

Garcia, L., D'Alessandro, G., Bioulac, B., & Hammond, C. (2005). High-frequency stimulation in Parkinson's disease: more or less? *Trends Neurosci, 28*(4), 209-216. doi:10.1016/j.tins.2005.02.005

Gatev, P., Darbin, O., & Wichmann, T. (2006). Oscillations in the basal ganglia under normal conditions and in movement disorders. *Mov Disord, 21*(10), 1566-1577. doi:10.1002/mds.21033

Georgopoulos, A. P., DeLong, M. R., & Crutcher, M. D. (1983). Relations between parameters of step-tracking movements and single cell discharge in the globus pallidus and subthalamic nucleus of the behaving monkey. *J Neurosci, 3*(8), 1586-1598.

Giannicola, G., Rosa, M., Servello, D., Menghetti, C., Carrabba, G., Pacchetti, C., Zangaglia, R., Cogiamanian, F., Scelzo, E., Marceglia, S., Rossi, L., & Priori, A. (2012). Subthalamic local field potentials after seven-year deep brain stimulation in Parkinson's disease. *Exp Neurol, 237*(2), 312-317. doi:10.1016/j.expneurol.2012.06.012

Gispert, S., Ricciardi, F., Kurz, A., Azizov, M., Hoepken, H. H., Becker, D., Voos, W., Leuner, K., Muller, W. E., Kudin, A. P., Kunz, W. S., Zimmermann, A., Roeper, J., Wenzel, D., Jendrach, M., Garcia-Arencibia, M., Fernandez-Ruiz, J., Huber, L., Rohrer, H., Barrera, M., Reichert, A. S., Rub, U., Chen, A., Nussbaum, R. L., & Auburger, G. (2009). Parkinson phenotype in aged PINK1-deficient mice is accompanied by progressive mitochondrial dysfunction in absence of neurodegeneration. *PLoS One, 4*(6), e5777. doi:10.1371/journal.pone.0005777

Godinho, F., Thobois, S., Magnin, M., Guenot, M., Polo, G., Benatru, I., Xie, J., Salvetti, A., Garcia-Larrea, L., Broussolle, E., & Mertens, P. (2006). Subthalamic nucleus stimulation in Parkinson's disease : anatomical and electrophysiological localization of active contacts. *J Neurol, 253*(10), 1347-1355. doi:10.1007/s00415-006-0222-z

Gold, C., Henze, D. A., Koch, C., & Buzsaki, G. (2006). On the origin of the extracellular action potential waveform: A modeling study. *J Neurophysiol, 95*(5), 3113-3128. doi:10.1152/jn.00979.2005

Goldberg, J. A., Boraud, T., Maraton, S., Haber, S. N., Vaadia, E., & Bergman, H. (2002). Enhanced synchrony among primary motor cortex neurons in the 1-methyl-4-phenyl-1,2,3,6-tetrahydropyridine primate model of Parkinson's disease. *J Neurosci, 22*(11), 4639-4653. doi:20026424

Goldberg, J. A., Rokni, U., Boraud, T., Vaadia, E., & Bergman, H. (2004). Spike synchronization in the cortex/basal-ganglia networks of Parkinsonian primates reflects global dynamics of the local field potentials. *J Neurosci, 24*(26), 6003-6010. doi:10.1523/JNEUROSCI.4848-03.2004

Goldberg, J. A., Teagarden, M. A., Foehring, R. C., & Wilson, C. J. (2009). Nonequilibrium calcium dynamics regulate the autonomous firing pattern of rat striatal cholinergic interneurons. *J Neurosci, 29*(26), 8396-8407.

Goldberg, M. E., & Bruce, C. J. (1985). Cerebral cortical activity associated with the orientation of visual attention in the rhesus monkey. *J Vis Res, 25*(3), 471-481.

Goto, Y., & O'Donnell, P. (2001). Network synchrony in the nucleus accumbens in vivo.*J Neurosci, 21*(12), 4498-4504.

Gradinaru, V., Mogri, M., Thompson, K. R., Henderson, J. M., & Deisseroth, K. (2009). Optical deconstruction of parkinsonian neural circuitry. *Science, 324*(5925), 354-359. doi:10.1126/science.1167093

Grill, W. M., Snyder, A. N., & Miocinovic, S. (2004). Deep brain stimulation creates an informational lesion of the stimulated nucleus. *J Neuroreport, 15*(7), 1137-1140.

Guehl, D., Pessiglione, M., Francois, C., Yelnik, J., Hirsch, E., Feger, J., & Tremblay, L. (2003). Tremor-related activity of neurons in the ‘motor’thalamus: changes in firing rate and pattern in the MPTP vervet model of parkinsonism. *Eur J Neurosci,17*(11), 2388-2400.

Guridi, J., & Lozano, A. M. (1997). A brief history of pallidotomy. *J Neurosurg, 41*(5), 1169-1183.

Guridi, J., Rodriguez-Oroz, M. C., Lozano, A. M., Moro, E., Albanese, A., Nuttin, B., Gybels, J., Ramos, E., & Obeso, J. A. (2000). Targeting the basal ganglia for deep brain stimulation in Parkinson's disease. *Neurology, 55*(12 Suppl 6), S21-28.

Hahn, P. J., Russo, G. S., Hashimoto, T., Miocinovic, S., Xu, W., McIntyre, C. C., & Vitek, J. (2008). Pallidal burst activity during therapeutic deep brain stimulation. *J Exp Neurol, 211*(1), 243-251.

Hallworth, N. E., Wilson, C. J., & Bevan, M. D. (2003). Apamin-sensitive small conductance calcium-activated potassium channels, through their selective coupling to voltage-gated calcium channels, are critical determinants of the precision, pace, and pattern of action potential generation in rat subthalamic nucleus neurons in vitro. *J Neurosci, 23*(20), 7525-7542.

Hamada, I., & DeLong, M. R. (1992). Excitotoxic acid lesions of the primate subthalamic nucleus result in transient dyskinesias of the contralateral limbs. *J Neurophysiol, 68*(5), 1850-1858. doi:10.1152/jn.1992.68.5.1850

Hamani, C., Saint-Cyr, J. A., Fraser, J., Kaplitt, M., & Lozano, A. M. (2004). The subthalamic nucleus in the context of movement disorders. *Brain, 127*(Pt 1), 4-20. doi:10.1093/brain/awh029

Hamel, W., Fietzek, U., Morsnowski, A., Schrader, B., Herzog, J., Weinert, D., Pfister, G., Muller, D., Volkmann, J., Deuschl, G., & Mehdorn, H. M. (2003). Deep brain stimulation of the subthalamic nucleus in Parkinson's disease: evaluation of active electrode contacts. *J Neurol Neurosurg Psychiatry, 74*(8), 1036-1046.

Han, X., Qian, X., Bernstein, J. G., Zhou, H.-h., Franzesi, G. T., Stern, P., Bronson, R. T., Graybiel, A. M., Desimone, R., & Boyden, E. S. J. N. (2009). Millisecond-timescale optical control of neural dynamics in the nonhuman primate brain. *Exp Neurol,62*(2), 191-198.

Hanajima, R., Ashby, P., Lozano, A. M., Lang, A. E., & Chen, R. (2004). Single pulse stimulation of the human subthalamic nucleus facilitates the motor cortex at short intervals. *J Neurophysiol, 92*(3), 1937-1943.

Hanslmayr, S., Spitzer, B., & Bauml, K. H. (2009). Brain oscillations dissociate between semantic and nonsemantic encoding of episodic memories. *Cereb Cortex, 19*(7), 1631-1640. doi:10.1093/cercor/bhn197

Hanslmayr, S., Staudigl, T., & Fellner, M. C. (2012). Oscillatory power decreases and long-term memory: the information via desynchronization hypothesis. *Front Hum Neurosci, 6*, 74. doi:10.3389/fnhum.2012.00074

Hao, C., Duan, H., Li, H., Wang, s., Zhang, C., & Pan, L. (2017). The Changes of the Learning and Memory Ability after Stimulation by STN-DBS in Parkinson's Disease Rats. *The FASEB Journal, 31*(1_supplement), lb511-lb511.

Hariz, M., Blomstedt, P., & Zrinzo, L. (2013). Future of brain stimulation: new targets, new indications, new technology. *Mov Disord, 28*(13), 1784-1792.

Hariz, M. I., Rehncrona, S., Quinn, N. P., Speelman, J. D., & Wensing, C. (2008). Multicenter study on deep brain stimulation in Parkinson's disease: an independent assessment of reported adverse events at 4 years. *Mov Disord, 2, 3*(3), 416-421.

Hariz, M. I. (2002). Complications of deep brain stimulation surgery. *Mov Disord, 17*(S3), S162-S166.

Hashimoto, T., Elder, C. M., Okun, M. S., Patrick, S. K., & Vitek, J. L. (2003). Stimulation of the subthalamic nucleus changes the firing pattern of pallidal neurons. *J Neurosci, 23*(5), 1916-1923.

Hassani, O. K., Mouroux, M., & Feger, J. (1996). Increased subthalamic neuronal activity after nigral dopaminergic lesion independent of disinhibition via the globus pallidus. *Neuroscience, 72*(1), 105-115.

Hassler, R. (1979). Striatal regulation of adverting and attention directing induced by pallidal stimulation. *Appl Neurophysiol, 42*(1-2), 98-102.

Hassler, R., Riechert, T., Mundinger, F., Umbach, W., & Ganglberger, J. A. (1960). Physiological observations in stereotaxic operations in extrapyramidal motor disturbances. *Brain, 83*, 337-350.

Heimer, G., Bar-Gad, I., Goldberg, J. A., & Bergman, H. (2002). Dopamine replacement therapy reverses abnormal synchronization of pallidal neurons in the 1-methyl-4-phenyl-1,2,3,6-tetrahydropyridine primate model of parkinsonism. *J Neurosci, 22*(18), 7850-7855.

Henze, D. A., Borhegyi, Z., Csicsvari, J., Mamiya, A., Harris, K. D., & Buzsaki, G. (2000). Intracellular features predicted by extracellular recordings in the hippocampus in vivo. *J Neurophysiol, 84*(1), 390-400. doi:10.1152/jn.2000.84.1.390

Hikida, T., Kimura, K., Wada, N., Funabiki, K., & Nakanishi, S. (2010). Distinct roles of synaptic transmission in direct and indirect striatal pathways to reward and aversive behavior. *Neuron, 66*(6), 896-907. doi:10.1016/j.neuron.2010.05.011

Hikosaka, O. (2007). GABAergic output of the basal ganglia. *Prog Brain Res, 160*, 209-226. doi:10.1016/S0079-6123(06)60012-5

Hirschmann, J., Hartmann, C. J., Butz, M., Hoogenboom, N., Özkurt, T. E., Elben, S., Vesper, J., Wojtecki, L., & Schnitzler, A. (2013). A direct relationship between oscillatory subthalamic nucleus–cortex coupling and rest tremor in Parkinson's disease. *Brain, 136*(12), 3659-3670.

Holt, A. B., Wilson, D., Shinn, M., Moehlis, J., & Netoff, T. I. (2016). Phasic Burst Stimulation: A Closed-Loop Approach to Tuning Deep Brain Stimulation Parameters for Parkinson's Disease. *PLoS Comput Biol, 12*(7), e1005011. doi:10.1371/journal.pcbi.1005011

Hontanilla, B., Parent, A., & Gimenez-Amaya, J. M. (1997). Parvalbumin and calbindin D-28k in the entopeduncular nucleus, subthalamic nucleus, and substantia nigra of

the rat as revealed by double-immunohistochemical methods. *Synapse, 25*(4), 359-367. doi:10.1002/(SICI)1098-2396(199704)25:4<359::AID-SYN7>3.0.CO;2-9

Horn, A., Neumann, W. J., Degen, K., Schneider, G. H., & Kuhn, A. A. (2017). Toward an electrophysiological "sweet spot" for deep brain stimulation in the subthalamic nucleus. *Hum Brain Mapp*. doi:10.1002/hbm.23594

Huerta, M. F., & Kaas, J. H. (1990). Supplementary eye field as defined by intracortical microstimulation: connections in macaques. *J Comp Neurol, 293*(2), 299-330.

Hyam, J. A., Akram, H., Foltynie, T., Limousin, P., Hariz, M., & Zrinzo, L. (2015). What you see is what you get: lead location within deep brain structures is accurately depicted by stereotactic magnetic resonance imaging. *J Operative Neurosurgery, 11*(3), 412-419.

Inase, M., Tokuno, H., Nambu, A., Akazawa, T., & Takada, M. (1999). Corticostriatal and corticosubthalamic input zones from the presupplementary motor area in the macaque monkey: comparison with the input zones from the supplementary motor area. *Brain Res, 833*(2), 191-201.

Isoda, M., & Hikosaka, O. (2008). Role for subthalamic nucleus neurons in switching from automatic to controlled eye movement. *J Neurosci, 28*(28), 7209-7218. doi:10.1523/JNEUROSCI.0487-08.2008

Jaeger, D., Kita, H., & Wilson, C. J. (1994). Surround inhibition among projection neurons is weak or nonexistent in the rat neostriatum. *J Neurophysiol, 72*(5), 2555-2558. doi:10.1152/jn.1994.72.5.2555

Jahanshahi, M. (2013). Effects of deep brain stimulation of the subthalamic nucleus on inhibitory and executive control over prepotent responses in Parkinson's disease. *Front Syst Neurosci, 7*, 118. doi:10.3389/fnsys.2013.00118

Jasper, H. H., & Andrews, H. L. (1938). Brain potentials and voluntary muscle activity in man. *J Neurophysiol, 1*(2), 87-100.

Jenkinson, N., & Brown, P. (2011). New insights into the relationship between dopamine, beta oscillations and motor function. *Trends in Neurosci, 34*(12), 611-618.

Johnson, L. A., Nebeck, S. D., Muralidharan, A., Johnson, M. D., Baker, K. B., & Vitek, J. L. (2016). Closed-Loop Deep Brain Stimulation Effects on Parkinsonian Motor Symptoms in a Non-Human Primate - Is Beta Enough? *Brain Stimul, 9*(6), 892-896. doi:10.1016/j.brs.2016.06.051

Johnson, M. D., Vitek, J. L., & McIntyre, C. C. (2009). Pallidal stimulation that improves parkinsonian motor symptoms also modulates neuronal firing patterns in primary motor cortex in the MPTP-treated monkey. *Exp Neurol, 219*(1), 359-362.

Joundi, R. A., Jenkinson, N., Brittain, J.-S., Aziz, T. Z., & Brown, P. J. C. B. (2012). Driving oscillatory activity in the human cortex enhances motor performance. *J Curr Biol, 22*(5), 403-407.

Kandel, E., Schwarz, J., & Jessell, T. J. M. (2000). Principals ofneural science.

Kato, K., Yokochi, F., Taniguchi, M., Okiyama, R., Kawasaki, T., Kimura, K., & Ushiba, J. (2015). Bilateral coherence between motor cortices and subthalamic nuclei in patients with Parkinson's disease. *Clin Neurophysiol, 126*(10), 1941-1950. doi:10.1016/j.clinph.2014.12.007

Kimura, M., Rajkowski, J., & Evarts, E. (1984). Tonically discharging putamen neurons exhibit set-dependent responses. *Proc Natl Acad Sci U S A, 81*(15), 4998-5001.

Kita, H., Chang, H. T., & Kitai, S. T. (1983). The morphology of intracellularly labeled rat subthalamic neurons: a light microscopic analysis. *J Comp Neurol, 215*(3), 245-257. doi:10.1002/cne.902150302

Kita, H., & Kitai, S. J. B. r. (1991). Intracellular study of rat globus pallidus neurons: membrane properties and responses to neostriatal, subthalamic and nigral stimulation. *564*(2), 296-305.

Kita, T., & Kita, H. (2012). The subthalamic nucleus is one of multiple innervation sites for long-range corticofugal axons: a single-axon tracing study in the rat. *J Neurosci, 32*(17), 5990-5999. doi:10.1523/JNEUROSCI.5717-11.2012

Kitai, S., & Deniau, J. (1981). Cortical inputs to the subthalamus: intracellular analysis. *Brain Res, 214*(2), 411-415.

Kitai, S., & Kita, H. (1987). Anatomy and physiology of the subthalamic nucleus: a driving force of the basal ganglia. In *The Basal Ganglia II* (pp. 357-373): Springer.

Koós, T., & Tepper, J. M. (1999). Inhibitory control of neostriatal projection neurons by GABAergic interneurons. *Nature neurosci*, 2(5), 467.

Krause, V., Wach, C., Südmeyer, M., Ferrea, S., Schnitzler, A., & Pollok, B. J. F. i. h. n. (2014). Cortico-muscular coupling and motor performance are modulated by 20 Hz transcranial alternating current stimulation (tACS) in Parkinson's disease. *Front in human neurosci, 7*, 928.

Kravitz, A. V., Freeze, B. S., Parker, P. R., Kay, K., Thwin, M. T., Deisseroth, K., & Kreitzer, A. C. (2010). Regulation of parkinsonian motor behaviours by

optogenetic control of basal ganglia circuitry. *Nature, 466*(7306), 622-626. doi:10.1038/nature09159

Kreitzer, A. C., & Malenka, R. C. (2008). Striatal plasticity and basal ganglia circuit function. *Neuron, 60*(4), 543-554. doi:10.1016/j.neuron.2008.11.005

Kringelbach, M. L., Jenkinson, N., Owen, S. L., & Aziz, T. Z. (2007). Translational principles of deep brain stimulation. *Nat Rev Neurosci, 8*(8), 623-635. doi:10.1038/nrn2196

Kühn, A. A., Kempf, F., Brücke, C., Doyle, L. G., Martinez-Torres, I., Pogosyan, A., Trottenberg, T., Kupsch, A., Schneider, G.-H., & Hariz, M. I. J. J. o. N. (2008). High-frequency stimulation of the subthalamic nucleus suppresses oscillatory β activity in patients with Parkinson's disease in parallel with improvement in motor performance. *28*(24), 6165-6173.

Kühn, A. A., Kupsch, A., Schneider, G. H., & Brown, P. (2006). Reduction in subthalamic 8–35 Hz oscillatory activity correlates with clinical improvement in Parkinson's disease. *Eur J Neurosci, 23*(7), 1956-1960.

Kuhn, A. A., Trottenberg, T., Kivi, A., Kupsch, A., Schneider, G. H., & Brown, P. (2005). The relationship between local field potential and neuronal discharge in the subthalamic nucleus of patients with Parkinson's disease. *Exp Neurol, 194*(1), 212-220. doi:10.1016/j.expneurol.2005.02.010

Kühn, A. A., Tsui, A., Aziz, T., Ray, N., Brücke, C., Kupsch, A., Schneider, G.-H., & Brown, P. (2009). Pathological synchronisation in the subthalamic nucleus of patients with Parkinson's disease relates to both bradykinesia and rigidity. *Exp Neurosci, 215*(2), 380-387.

Kuhn, A. A., Williams, D., Kupsch, A., Limousin, P., Hariz, M., Schneider, G. H., Yarrow, K., & Brown, P. (2004). Event-related beta desynchronization in human subthalamic nucleus correlates with motor performance. *Brain, 127*(Pt 4), 735-746. doi:10.1093/brain/awh106

Kumaravelu, K., Oza, C. S., Behrend, C. E., & Grill, W. M. (2018). Model-based Deconstruction of Cortical Evoked Potentials Generated by Subthalamic Nucleus Deep Brain Stimulation. *J Neurophysiol*. doi:10.1152/jn.00862.2017

Kuncel, A. M., & Grill, W. M. (2004). Selection of stimulus parameters for deep brain stimulation. *Clin Neurophysiol, 115*(11), 2431-2441. doi:10.1016/j.clinph.2004.05.031

Kuriakose, R., Saha, U., Castillo, G., Udupa, K., Ni, Z., Gunraj, C., Mazzella, F., Hamani, C., Lang, A. E., Moro, E., Lozano, A. M., Hodaie, M., & Chen, R. (2010). The nature and time course of cortical activation following subthalamic stimulation in Parkinson's disease. *Cereb Cortex, 20*(8), 1926-1936. doi:10.1093/cercor/bhp269

Lalo, E., Gilbertson, T., Doyle, L., Di Lazzaro, V., Cioni, B., & Brown, P. (2007). Phasic increases in cortical beta activity are associated with alterations in sensory processing in the human. *Exp Brain Res, 177*(1), 137-145.

Lalo, E., Thobois, S., Sharott, A., Polo, G., Mertens, P., Pogosyan, A., & Brown, P. (2008). Patterns of bidirectional communication between cortex and basal ganglia during movement in patients with Parkinson disease. *J Neurosci, 28*(12), 3008-3016. doi:10.1523/JNEUROSCI.5295-07.2008

Lanciego, J. L., Luquin, N., & Obeso, J. A. (2012). Functional neuroanatomy of the basal ganglia. *Cold Spring Harb Perspect Med, 2*(12), a009621. doi:10.1101/cshperspect.a009621

Lang, A. E., Lozano, A. M., Montgomery, E., Duff, J., Tasker, R., & Hutchinson, W. (1997). Posteroventral medial pallidotomy in advanced Parkinson's disease. *New England Journal of Medicine, 337*(15), 1036-1043.

Lardeux, S., & Baunez, C. (2008). Alcohol preference influences the subthalamic nucleus control on motivation for alcohol in rats. *Neuropsychopharmacology, 33*(3), 634-642. doi:10.1038/sj.npp.1301432

Lardeux, S., Pernaud, R., Paleressompoulle, D., & Baunez, C. (2009). Beyond the reward pathway: coding reward magnitude and error in the rat subthalamic nucleus. *J Neurophysiol, 102*(4), 2526-2537. doi:10.1152/jn.91009.2008

Lavoie, B., & Parent, A. (1990). Immunohistochemical study of the serotoninergic innervation of the basal ganglia in the squirrel monkey. *J Comp Neurol, 299*(1), 1-16.

Leblois, A., Meissner, W., Bioulac, B., Gross, C. E., Hansel, D., & Boraud, T. (2007). Late emergence of synchronized oscillatory activity in the pallidum during progressive Parkinsonism. *Eur J Neurosci, 26*(6), 1701-1713.

Lee, H.-M., Park, H., & Ghovanloo, M. (2013). A power-efficient wireless system with adaptive supply control for deep brain stimulation. *J IEEE journal of solid-state circuits, 48*(9), 2203-2216.

Lee, M. S., & Marsden, C. D. (1994). Movement disorders following lesions of the thalamus or subthalamic region. *Mov Disord, 9*(5), 493-507. doi:10.1002/mds.870090502

Lee, P.-L., Wu, Y.-T., Chen, L.-F., Chen, Y.-S., Cheng, C.-M., Yeh, T.-C., Ho, L.-T., Chang, M.-S., & Hsieh, J.-C. (2003). ICA-based spatiotemporal approach for single-trial analysis of postmovement MEG beta synchronization. *J Neuroimage 20*(4), 2010-2030.

Lefaucheur, J. P. (2009). Treatment of Parkinson's disease by cortical stimulation. *Expert Rev Neurother, 9*(12), 1755-1771. doi:10.1586/ern.09.132

Leventhal, D. K., Gage, G. J., Schmidt, R., Pettibone, J. R., Case, A. C., & Berke, J. D. (2012). Basal ganglia beta oscillations accompany cue utilization. *Neuron, 73*(3), 523-536.

Levy, R., Ashby, P., Hutchison, W. D., Lang, A. E., Lozano, A. M., & Dostrovsky, J. O. (2002). Dependence of subthalamic nucleus oscillations on movement and dopamine in Parkinson's disease. *Brain, 125*(Pt 6), 1196-1209.

Levy, R., Dostrovsky, J. O., Lang, A. E., Sime, E., Hutchison, W. D., & Lozano, A. M. (2001). Effects of apomorphine on subthalamic nucleus and globus pallidus internus neurons in patients with Parkinson's disease. *J Neurophysiol, 86*(1), 249-260. doi:10.1152/jn.2001.86.1.249

Lewicki, M. S. (1998). A review of methods for spike sorting: the detection and classification of neural action potentials. *Network, 9*(4), R53-78.

Li, Q., Ke, Y., Chan, D. C., Qian, Z. M., Yung, K. K., Ko, H., Arbuthnott, G. W., & Yung, W. H. (2012). Therapeutic deep brain stimulation in Parkinsonian rats directly influences motor cortex. *Neuron, 76*(5), 1030-1041. doi:10.1016/j.neuron.2012.09.032

Li, S., Arbuthnott, G. W., Jutras, M. J., Goldberg, J. A., & Jaeger, D. (2007). Resonant antidromic cortical circuit activation as a consequence of high-frequency subthalamic deep-brain stimulation. *J Neurophysiol, 98*(6), 3525-3537.

Lipski, W. J., Wozny, T. A., Alhourani, A., Kondylis, E. D., Turner, R. S., Crammond, D. J., & Richardson, R. M. (2017). Dynamics of human subthalamic neuron phase-locking to motor and sensory cortical oscillations during movement. *J Neurophysiol, 118*(3), 1472-1487. doi:10.1152/jn.00964.2016

Little, S., & Brown, P. (2012). What brain signals are suitable for feedback control of deep brain stimulation in Parkinson's disease?, *Annals of the New York Academy of Sciences, 1265*(1), 9-24.

Little, S., Brown, P. (2014). The functional role of beta oscillations in Parkinson's disease. *J Parkinsonism related disorders, 20*, S44-S48.

Little, S., Pogosyan, A., Kuhn, A. A., & Brown, P. (2012). Beta band stability over time correlates with Parkinsonian rigidity and bradykinesia. *Exp Neurol, 236*(2), 383-388. doi:S0014-4886(12)00196-3 [pii]

10.1016/j.expneurol.2012.04.024

Little, S., Pogosyan, A., Neal, S., Zavala, B., Zrinzo, L., Hariz, M., Foltynie, T., Limousin, P., Ashkan, K., FitzGerald, J., Green, A. L., Aziz, T. Z., & Brown, P. (2013). Adaptive deep brain stimulation in advanced Parkinson disease. *Ann Neurol, 74*(3), 449-457. doi:10.1002/ana.23951

Little, S., Tripoliti, E., Beudel, M., Pogosyan, A., Cagnan, H., Herz, D., Bestmann, S., Aziz, T., Cheeran, B., Zrinzo, L., Hariz, M., Hyam, J., Limousin, P., Foltynie, T., & Brown, P. (2016). Adaptive deep brain stimulation for Parkinson's disease demonstrates reduced speech side effects compared to conventional stimulation in the acute setting. *J Neurol Neurosurg Psychiatry, 87*(12), 1388-1389. doi:10.1136/jnnp-2016-313518

Litvak, V., Eusebio, A., Jha, A., Oostenveld, R., Barnes, G. R., Penny, W. D., Zrinzo, L., Hariz, M. I., Limousin, P., Friston, K. J., & Brown, P. (2010a). Optimized beamforming for simultaneous MEG and intracranial local field potential recordings in deep brain stimulation patients. *Neuroimage, 50*(4), 1578-1588. doi:10.1016/j.neuroimage.2009.12.115

Litvak, V., Jha, A., Eusebio, A., Oostenveld, R., Foltynie, T., Limousin, P., Zrinzo, L., Hariz, M. I., Friston, K., & Brown, P. (2010b). Resting oscillatory cortico-subthalamic connectivity in patients with Parkinson's disease. *Brain, 134*(Pt 2), 359-374. doi:awq33210.1093/brain/awq332

Litvak, V., Jha, A., Eusebio, A., Oostenveld, R., Foltynie, T., Limousin, P., Zrinzo, L., Hariz, M. I., Friston, K., & Brown, P. (2011). Resting oscillatory cortico-subthalamic connectivity in patients with Parkinson's disease. *Brain, 134*(Pt 2), 359-374. doi:10.1093/brain/awq332

Llinás, R. R., Leznik, E., & Urbano, F. (2002). Temporal binding via cortical coincidence detection of specific and nonspecific thalamocortical inputs: a voltage-dependent dye-imaging study in mouse brain slices. *Proc Natl Acad Sci U S A, 99*(1), 449-454.

Logan, G. D., Cowan, W. B., & Davis, K. A. (1984). On the ability to inhibit simple and choice reaction time responses: a model and a method. *J Exp Psychol Hum Percept Perform, 10*(2), 276-291.

Logothetis, N. K. (2002). The neural basis of the blood-oxygen-level-dependent functional magnetic resonance imaging signal. *Philos Trans R Soc Lond B Biol Sci, 357*(1424), 1003-1037. doi:10.1098/rstb.2002.1114

Lopez-Azcarate, J., Tainta, M., Rodriguez-Oroz, M. C., Valencia, M., Gonzalez, R., Guridi, J., Iriarte, J., Obeso, J. A., Artieda, J., & Alegre, M. (2010). Coupling between beta and high-frequency activity in the human subthalamic nucleus may be a pathophysiological mechanism in Parkinson's disease. *J Neurosci, 30*(19), 6667-6677. doi:10.1523/JNEUROSCI.5459-09.2010

Loucif, K., Wilson, C., Baig, R., Lacey, M., & Stanford, I. M. (2005). Functional interconnectivity between the globus pallidus and the subthalamic nucleus in the mouse brain slice. *J Phys, 5 67*(3), 977-987.

Machado, A., Rezai, A. R., Kopell, B. H., Gross, R. E., Sharan, A. D., & Benabid, A. L. (2006). Deep brain stimulation for Parkinson's disease: surgical technique and perioperative management. *Mov Disord, 21 Suppl 14*, S247-258. doi:10.1002/mds.20959

MacKinnon, C. D., Webb, R. M., Silberstein, P., Tisch, S., Asselman, P., Limousin, P., & Rothwell, J. C. (2005). Stimulation through electrodes implanted near the subthalamic nucleus activates projections to motor areas of cerebral cortex in patients with Parkinson's disease. *Eur J Neurosci, 21*(5), 1394-1402.

Magill, P. J., Bolam, J. P., & Bevan, M. D. (2000). Relationship of activity in the subthalamic nucleus-globus pallidus network to cortical electroencephalogram. *J Neurosci, 20*(2), 820-833.

Magill, P. J., Bolam, J. P., & Bevan, M. D. (2001). Dopamine regulates the impact of the cerebral cortex on the subthalamic nucleus-globus pallidus network. *Neuroscience, 106*(2), 313-330.

Magill, P. J., Pogosyan, A., Sharott, A., Csicsvari, J., Bolam, J. P., & Brown, P. (2006). Changes in functional connectivity within the rat striatopallidal axis during global

brain activation in vivo. *J Neurosci, 26*(23), 6318-6329. doi:10.1523/JNEUROSCI.0620-06.2006

Magill, P. J., Sharott, A., Bevan, M. D., Brown, P., & Bolam, J. P. (2004a). Synchronous unit activity and local field potentials evoked in the subthalamic nucleus by cortical stimulation. *J Neurophysiol, 92*(2), 700-714. doi:10.1152/jn.00134.2004

Magill, P. J., Sharott, A., Bolam, J. P., & Brown, P. (2004b). Brain state-dependency of coherent oscillatory activity in the cerebral cortex and basal ganglia of the rat. *J Neurophysiol, 92*(4), 2122-2136. doi:10.1152/jn.00333.2004

Mallet, N., Ballion, B., Le Moine, C., & Gonon, F. (2006). Cortical inputs and GABA interneurons imbalance projection neurons in the striatum of parkinsonian rats. *J Neurosci, 26*(14), 3875-3884. doi:10.1523/JNEUROSCI.4439-05.2006

Mallet, N., Micklem, B. R., Henny, P., Brown, M. T., Williams, C., Bolam, J. P., Nakamura, K. C., & Magill, P. J. (2012). Dichotomous organization of the external globus pallidus. *Neuron, 74*(6), 1075-1086. doi:10.1016/j.neuron.2012.04.027

Mallet, N., Pogosyan, A., Marton, L. F., Bolam, J. P., Brown, P., & Magill, P. J. (2008a). Parkinsonian beta oscillations in the external globus pallidus and their relationship with subthalamic nucleus activity. *J Neurosci, 28*(52), 14245-14258. doi:28/52/1424510.1523/JNEUROSCI.4199-08.2008

Mallet, N., Pogosyan, A., Sharott, A., Csicsvari, J., Bolam, J. P., Brown, P., & Magill, P. J. (2008b). Disrupted dopamine transmission and the emergence of exaggerated beta oscillations in subthalamic nucleus and cerebral cortex. *J Neurosci, 28*(18), 4795-4806. doi:10.1523/JNEUROSCI.0123-08.2008

Marsden, J., Limousin-Dowsey, P., Ashby, P., Pollak, P., & Brown, P. (2001). Subthalamic nucleus, sensorimotor cortex and muscle interrelationships in Parkinson's disease. *Brain, 124*(2), 378-388.

Martinez-Gonzalez, C., Bolam, J. P., & Mena-Segovia, J. (2011). Topographical organization of the pedunculopontine nucleus. *Front Neuroanat, 5*, 22. doi:10.3389/fnana.2011.00022

Mastro, K. J., Bouchard, R. S., Holt, H. A., & Gittis, A. H. (2014). Transgenic mouse lines subdivide external segment of the globus pallidus (GPe) neurons and reveal distinct GPe output pathways. *J Neurosci, 34*(6), 2087-2099. doi:10.1523/JNEUROSCI.4646-13.2014

Mathai, A., & Smith, Y. (2011). The corticostriatal and corticosubthalamic pathways: two entries, one target. So what? *Front Syst Neurosci, 5*, 64.

Matsumura, M., Kojima, J., Gardiner, T. W., & Hikosaka, O. (1992). Visual and oculomotor functions of monkey subthalamic nucleus. *J Neurophysiol, 67*(6), 1615-1632. doi:10.1152/jn.1992.67.6.1615

Maurice, N., Mercer, J., Chan, C. S., Hernandez-Lopez, S., Held, J., Tkatch, T., & Surmeier, D. J. (2004). D2 dopamine receptor-mediated modulation of voltage-dependent Na+ channels reduces autonomous activity in striatal cholinergic interneurons. *J Neurosci, 24*(46), 10289-10301.

McCairn, K. W., & Turner, R. S. (2009). Deep brain stimulation of the globus pallidus internus in the parkinsonian primate: local entrainment and suppression of low-frequency oscillations. *J Neurophysiol,101*(4), 1941-1960.

McConnell, G. C., So, R. Q., Hilliard, J. D., Lopomo, P., & Grill, W. M. (2012). Effective deep brain stimulation suppresses low-frequency network oscillations in the basal ganglia by regularizing neural firing patterns. *J Neurosci, 32*(45), 15657-15668. doi:10.1523/JNEUROSCI.2824-12.2012

McIntyre, C. C., & Grill, W. M. (2000). Selective microstimulation of central nervous system neurons. *Ann biomed eng, 28*(3), 219-233.

McIntyre, C. C., Savasta, M., Kerkerian-Le Goff, L., & Vitek, J. L. (2004). Uncovering the mechanism (s) of action of deep brain stimulation: activation, inhibition, or both. *J Clin Neurophys, 1 15*(6), 1239-1248.

McIver, E. L., Chu, H.-Y., Atherton, J. F., Cosgrove, K. E., Kondapalli, J., Wokosin, D., Surmeier, D. J., & Bevan, M. D. (2018). Chemogenetic restoration of autonomous subthalamic nucleus activity ameliorates Parkinsonian motor dysfunction. doi:10.1101/385443 %J bioRxiv

Mehta, A. R., Brittain, J.-S., & Brown, P. (2014). The selective influence of rhythmic cortical versus cerebellar transcranial stimulation on human physiological tremor. *J Neurosci, 34*(22), 7501-7508.

Meidahl, A. C., Tinkhauser, G., Herz, D. M., Cagnan, H., Debarros, J., & Brown, P. (2017). Adaptive Deep Brain Stimulation for Movement Disorders: The Long Road to Clinical Therapy. *Mov Disord, 32*(6), 810-819. doi:10.1002/mds.27022

Meissner, W., Leblois, A., Hansel, D., Bioulac, B., Gross, C. E., Benazzouz, A., & Boraud, T. (2005). Subthalamic high frequency stimulation resets subthalamic

firing and reduces abnormal oscillations. *Brain, 128*(Pt 10), 2372-2382. doi:10.1093/brain/awh616

Mercer, J. N., Chan, C. S., Tkatch, T., Held, J., & Surmeier, D. J. (2007). Nav1.6 sodium channels are critical to pacemaking and fast spiking in globus pallidus neurons. *J Neurosci, 27*(49), 13552-13566. doi:10.1523/JNEUROSCI.3430-07.2007

Michalareas, G., Vezoli, J., van Pelt, S., Schoffelen, J. M., Kennedy, H., & Fries, P. (2016). Alpha-Beta and Gamma Rhythms Subserve Feedback and Feedforward Influences among Human Visual Cortical Areas. *Neuron, 89*(2), 384-397. doi:10.1016/j.neuron.2015.12.018

Millecchia, R., McIntyre, T. J. C., & Research, B. (1978). Automatic nerve impulse identification and separation. *J Comp Biomed Res, 11*(5), 459-468.

Milosevic, L., Kalia, S. K., Hodaie, M., Lozano, A. M., Fasano, A., Popovic, M. R., & Hutchison, W. D. (2018). Neuronal inhibition and synaptic plasticity of basal ganglia neurons in Parkinson's disease. *Brain, 141*(1), 177-190. doi:10.1093/brain/awx296

Mink, J. W. (1996). The basal ganglia: focused selection and inhibition of competing motor programs. *Prog Neurobiol, 50*(4), 381-425.

Mink, J. W. (2003). The Basal Ganglia and involuntary movements: impaired inhibition of competing motor patterns. *Arch Neurol, 60*(10), 1365-1368. doi:10.1001/archneur.60.10.1365

Miocinovic, S., Somayajula, S., Chitnis, S., & Vitek, J. L. (2013). History, applications, and mechanisms of deep brain stimulation. *JAMA Neurol, 70*(2), 163-171. doi:10.1001/2013.jamaneurol.45

Mitzdorf, U. (1985). Current source-density method and application in cat cerebral cortex: investigation of evoked potentials and EEG phenomena. *Physiol Rev, 65*(1), 37-100. doi:10.1152/physrev.1985.65.1.37

Moll, C. K., Buhmann, C., Gulberti, A., Fickel, U., Poetter-Nerger, M., Westphal, M., Gerloff, C., Hamel, W., & Engel, A. K. (2015). Synchronized cortico-subthalamic beta oscillations in Parkin-associated Parkinson's disease. *Clin Neurophysiol, 126*(11), 2241-2243. doi:10.1016/j.clinph.2015.02.008

Monakow, K. H., Akert, K., & Kunzle, H. (1978). Projections of the precentral motor cortex and other cortical areas of the frontal lobe to the subthalamic nucleus in the monkey. *Exp Brain Res, 33*(3-4), 395-403.

Montgomery Jr, E. B., Baker, K. B., Lyons, K., & Koller, W. C. J (2000). Motor initiation and execution in essential tremor and Parkinson's disease. *Mov Disord, 15*(3), 511-515.

Moran, A., & Bar-Gad, I. (2010). Revealing neuronal functional organization through the relation between multi-scale oscillatory extracellular signals. *J Neurosci Methods, 186*(1), 116-129. doi:10.1016/j.jneumeth.2009.10.024

Moran, A., Bar-Gad, I., Bergman, H., & Israel, Z. (2006). Real-time refinement of subthalamic nucleus targeting using Bayesian decision-making on the root mean square measure. *Mov Disord, 21*(9), 1425-1431. doi:10.1002/mds.20995

Moran, A., Bergman, H., Israel, Z., & Bar-Gad, I. (2008a). Subthalamic nucleus functional organization revealed by parkinsonian neuronal oscillations and synchrony. *Brain, 131*(Pt 12), 3395-3409. doi:10.1093/brain/awn270

Moran, A., Bergman, H., Israel, Z., & Bar-Gad, I. (2008b). Subthalamic nucleus functional organization revealed by parkinsonian neuronal oscillations and synchrony. *Brain, 131*(12), 3395-3409.

Moran, A., Stein, E., Tischler, H., & Bar-Gad, I. (2012). Decoupling neuronal oscillations during subthalamic nucleus stimulation in the parkinsonian primate. *Neurobiol Dis, 45*(1), 583-590. doi:10.1016/j.nbd.2011.09.016

Morbidi, F., Garulli, A., Prattichizzo, D., Rizzo, C., Manganotti, P., & Rossi, S. (2007). Off-line removal of TMS-induced artifacts on human electroencephalography by Kalman filter. *J Neurosci Methods, 162*(1-2), 293-302. doi:10.1016/j.jneumeth.2006.12.013

Moreau, C., Defebvre, L., Destee, A., Bleuse, S., Clement, F., Blatt, J. L., Krystkowiak, P., & Devos, D. (2008). STN-DBS frequency effects on freezing of gait in advanced Parkinson disease. *Neurology, 71*(2), 80-84. doi:10.1212/01.wnl.0000303972.16279.46

Moro, E., Esselink, R., Xie, J., Hommel, M., Benabid, A., & Pollak, P. (2002). The impact on Parkinson's disease of electrical parameter settings in STN stimulation. *J Neurol, 59*(5), 706-713.

Mouroux, M., Hassani, O.-K., & Feger, J. (1995). Electrophysiological study of the excitatory parafascicular projection to the subthalamic nucleus and evidence for ipsi-and contralateral controls. *J Neurosci, 67*(2), 399-407.

Mure, H., Tang, C. C., Argyelan, M., Ghilardi, M.-F., Kaplitt, M. G., Dhawan, V., & Eidelberg, D. J. (2012). Improved sequence learning with subthalamic nucleus

deep brain stimulation: evidence for treatment-specific network modulation. *J Neurosci, 32*(8), 2804-2813.

Nakamura, K. C., Sharott, A., & Magill, P. J. (2012). Temporal coupling with cortex distinguishes spontaneous neuronal activities in identified basal ganglia-recipient and cerebellar-recipient zones of the motor thalamus. *Cerebr Cortex, 24*(1), 81-97.

Nakanishi, H., Kita, H., & Kitai, S. T. (1987). Intracellular study of rat substantia nigra pars reticulata neurons in an in vitro slice preparation: electrical membrane properties and response characteristics to subthalamic stimulation. *Brain Res, 437*(1), 45-55.

Nambu, A. (2008). Seven problems on the basal ganglia. *Curr Opin Neurobiol, 18*(6), 595-604. doi:10.1016/j.conb.2008.11.001

Nambu, A., Takada, M., Inase, M., & Tokuno, H. (1996). Dual somatotopical representations in the primate subthalamic nucleus: evidence for ordered but reversed body-map transformations from the primary motor cortex and the supplementary motor area. *J Neurosci, 16*(8), 2671-2683.

Nambu, A., Tokuno, H., Hamada, I., Kita, H., Imanishi, M., Akazawa, T., Ikeuchi, Y., & Hasegawa, N. (2000). Excitatory cortical inputs to pallidal neurons via the subthalamic nucleus in the monkey. *J Neurophysiol, 84*(1), 289-300. doi:10.1152/jn.2000.84.1.289

Nambu, A., Tokuno, H., Inase, M., & Takada, M. (1997). Corticosubthalamic input zones from forelimb representations of the dorsal and ventral divisions of the premotor cortex in the macaque monkey: comparison with the input zones from the primary motor cortex and the supplementary motor area. *Neurosci Lett, 239*(1), 13-16.

Nambu, A., Tokuno, H., & Takada, M. (2002). Functional significance of the cortico-subthalamo-pallidal 'hyperdirect' pathway. *Neurosci Res, 43*(2), 111-117.

Nelson, A. B., Hammack, N., Yang, C. F., Shah, N. M., Seal, R. P., & Kreitzer, A. C. (2014). Striatal cholinergic interneurons Drive GABA release from dopamine terminals. *Neuron, 82*(1), 63-70. doi:10.1016/j.neuron.2014.01.023

Nelson, A. B., & Kreitzer, A. C. (2014). Reassessing models of basal ganglia function and dysfunction. *Annu Rev Neurosci, 37*, 117-135. doi:10.1146/annurev-neuro-071013-013916

Neumann, W. J., Degen, K., Schneider, G. H., Brücke, C., Huebl, J., Brown, P., & Kühn, A. A. (2016). Subthalamic synchronized oscillatory activity correlates with motor impairment in patients with Parkinson's disease. *Mov Disord, 31*(11), 1748-1751.

Nevado-Holgado, A. J., Mallet, N., Magill, P. J., & Bogacz, R. (2014). Effective connectivity of the subthalamic nucleus-globus pallidus network during Parkinsonian oscillations. *J Physiol, 592*(7), 1429-1455. doi:10.1113/jphysiol.2013.259721

Ngo, H. V., Martinetz, T., Born, J., & Molle, M. (2013). Auditory closed-loop stimulation of the sleep slow oscillation enhances memory. *Neuron, 78*(3), 545-553. doi:10.1016/j.neuron.2013.03.006

Ni, J., Wunderle, T., Lewis, C. M., Desimone, R., Diester, I., & Fries, P. (2016). Gamma-Rhythmic Gain Modulation. *Neuron, 92*(1), 240-251. doi:10.1016/j.neuron.2016.09.003

Nolden, L. F., Tartavoulle, T., & Porche, D. J. (2014). Parkinson's Disease: Assessment, Diagnosis, and Management. *The Journal for Nurse Practitioners, 10*(7), 500-506. doi:10.1016/j.nurpra.2014.04.019

O'Hare, J. K., Ade, K. K., Sukharnikova, T., Van Hooser, S. D., Palmeri, M. L., Yin, H. H., & Calakos, N. (2016). Pathway-Specific Striatal Substrates for Habitual Behavior. *Neuron, 89*(3), 472-479. doi:10.1016/j.neuron.2015.12.032

O'suilleabhain, P. E., Frawley, W., Giller, C., & Dewey, R. B. (2003). Tremor response to polarity, voltage, pulsewidth and frequency of thalamic stimulation. *J Neurol ,60*(5), 786-790.

Obeso, J. A., Rodriguez-Oroz, M. C., Rodriguez, M., Macias, R., Alvarez, L., Guridi, J., Vitek, J., & DeLong, M. R. (2000). Pathophysiologic basis of surgery for Parkinson's disease. *Neurology, 55*(12 Suppl 6), S7-12.

Odekerken, V. J., van Laar, T., Staal, M. J., Mosch, A., Hoffmann, C. F., Nijssen, P. C., Beute, G. N., van Vugt, J. P., Lenders, M. W., & Contarino, M. F. (2013). Subthalamic nucleus versus globus pallidus bilateral deep brain stimulation for advanced Parkinson's disease (NSTAPS study): a randomised controlled trial. *The Lancet Neurology,1 2*(1), 37-44.

Oertel, W. H., & Mugnaini, E. (1984). Immunocytochemical studies of GABAergic neurons in rat basal ganglia and their relations to other neuronal systems. *Neurosci Lett, 47*(3), 233-238.

Okun, M. S., Tagliati, M., Pourfar, M., Fernandez, H. H., Rodriguez, R. L., Alterman, R. L., & Foote, K. D. (2005). Management of referred deep brain stimulation failures: a retrospective analysis from 2 movement disorders centers. *Arch Neurol, 62*(8), 1250-1255. doi:10.1001/archneur.62.8.noc40425

Oldenburg, I. A., & Sabatini, B. L. (2015a). Antagonistic but Not Symmetric Regulation of Primary Motor Cortex by Basal Ganglia Direct and Indirect Pathways. *Neuron, 86*(5), 1174-1181. doi:10.1016/j.neuron.2015.05.008

Oldenburg, I. A., & Sabatini, B. L. (2015b). Antagonistic but not symmetric regulation of primary motor cortex by basal ganglia direct and indirect pathways. *Neuron, 86*(5), 1174-1181.

Olsson, M., Nikkhah, G., Bentlage, C., & Bjorklund, A. (1995). Forelimb akinesia in the rat Parkinson model: differential effects of dopamine agonists and nigral transplants as assessed by a new stepping test. *J Neurosci, 15*(5), 3863-3875.

Oorschot, D. E. (1996). Total number of neurons in the neostriatal, pallidal, subthalamic, and substantia nigral nuclei of the rat basal ganglia: a stereological study using the cavalieri and optical disector methods. *J Comp Neurol, 366*(4), 580-599. doi:10.1002/(SICI)1096-9861(19960318)366:4<580::AID-CNE3>3.0.CO;2-0

Oorschot, D. E. (2010). Cell types in the different nuclei of the basal ganglia. In *Handbook of Behavioral Neuroscience* (Vol. 20, pp. 63-74): Elsevier.

Ostrem, J. L., Markun, L. C., Glass, G. A., Racine, C. A., Volz, M. M., Heath, S. L., de Hemptinne, C., & Starr, P. A. (2014). Effect of frequency on subthalamic nucleus deep brain stimulation in primary dystonia. *Parkinsonism Relat Disord, 20*(4), 432-438. doi:10.1016/j.parkreldis.2013.12.012

Oswal, A., Beudel, M., Zrinzo, L., Limousin, P., Hariz, M., Foltynie, T., Litvak, V., & Brown, P. (2016). Deep brain stimulation modulates synchrony within spatially and spectrally distinct resting state networks in Parkinson's disease. *Brain, 139*(5), 1482-1496.

Oswal, A., Brown, P., & Litvak, V. (2013). Synchronized neural oscillations and the pathophysiology of Parkinson's disease. *Curr Opin Neurol, 26*(6), 662-670. doi:10.1097/WCO.0000000000000034

Oswal, A., Litvak, V., Sauleau, P., & Brown, P. (2012). Beta reactivity, prospective facilitation of executive processing, and its dependence on dopaminergic therapy in Parkinson's disease. *J Neurosci, 32*(29), 9909-9916.

Overton, P. G., & Greenfield, S. A. (1995). Determinants of neuronal firing pattern in the guinea-pig subthalamic nucleus: an in vivo and in vitro comparison. *J Neural Transm Park Dis Dement Sect, 10*(1), 41-54.

Parent, A., & Hazrati, L. N. (1995a). Functional anatomy of the basal ganglia. I. The cortico-basal ganglia-thalamo-cortical loop. *Brain Res Brain Res Rev, 20*(1), 91-127.

Parent, A., & Hazrati, L. N. (1995b). Functional anatomy of the basal ganglia. II. The place of subthalamic nucleus and external pallidum in basal ganglia circuitry. *Brain Res Brain Res Rev, 20*(1), 128-154.

Parent, A., Sato, F., Wu, Y., Gauthier, J., Levesque, M., & Parent, M. (2000). Organization of the basal ganglia: the importance of axonal collateralization. *Trends Neurosci, 23*(10 Suppl), S20-27.

Parent, M., Wallman, M. J., & Descarries, L. J. E. J. o. N. (2010). Distribution and ultrastructural features of the serotonin innervation in rat and squirrel monkey subthalamic nucleus. *Eur J Neurosci, 31*(7), 1233-1242.

Parkes, L. M., Bastiaansen, M. C., & Norris, D. G. (2006). Combining EEG and fMRI to investigate the post-movement beta rebound. *J Neuroimage, 29*(3), 685-696.

Patil, P. G., Carmena, J. M., Nicolelis, M. A., & Turner, D. A. (2004). Ensemble recordings of human subcortical neurons as a source of motor control signals for a brain-machine interface. *Neurosurgery, 55*(1), 27-35; discussion 35-28.

Paxinos, G., & Watson, C. (1986). *The rat brain in stereotaxic coordinates* (Ed 2 ed.). Sydney: Academic.

Pedemonte, M., Barrenechea, C., Nunez, A., Gambini, J. P., & Garcia-Austt, E. (1998). Membrane and circuit properties of lateral septum neurons: relationships with hippocampal rhythms. *Brain Res, 800*(1), 145-153.

Pedrosa, D. J., Auth, M., Pauls, K. A. M., Runge, M., Maarouf, M., Fink, G. R., & Timmermann, L. (2014). Verbal fluency in essential tremor patients: the effects of deep brain stimulation. *Brain stim, 7*(3), 359-364.

Perestelo-Pérez, L., Rivero-Santana, A., Pérez-Ramos, J., Serrano-Pérez, P., Panetta, J., & Hilarion, P. (2014). Deep brain stimulation in Parkinson's disease: meta-analysis of randomized controlled trials. *J Neurosci, 261*(11), 2051-2060.

Pessiglione, M., Guehl, D., Rolland, A.-S., François, C., Hirsch, E. C., Féger, J., & Tremblay, L. (2005). Thalamic neuronal activity in dopamine-depleted primates: evidence for a loss of functional segregation within basal ganglia circuits. *J Neurosci, 25*(6), 1523-1531.

Pfurtscheller, G., Graimann, B., Huggins, J. E., Levine, S. P., & Schuh, L. A. (2003). Spatiotemporal patterns of beta desynchronization and gamma synchronization in

corticographic data during self-paced movement. *Clinical Neurophysi, 114*(7), 1226-1236.

Pinault, D. (1996). A novel single-cell staining procedure performed in vivo under electrophysiological control: morpho-functional features of juxtacellularly labeled thalamic cells and other central neurons with biocytin or Neurobiotin. *J Neurosci Methods, 65*(2), 113-136.

Plenz, D., & Kital, S. T. (1999). A basal ganglia pacemaker formed by the subthalamic nucleus and external globus pallidus. *J Neurosci, 400*(6745), 677.

Pogosyan, A., Gaynor, L. D., Eusebio, A., & Brown, P. (2009). Boosting cortical activity at Beta-band frequencies slows movement in humans. *Curr Biol, 19*(19), 1637-1641. doi:10.1016/j.cub.2009.07.074

Pogosyan, A., Yoshida, F., Chen, C., Martinez-Torres, I., Foltynie, T., Limousin, P., Zrinzo, L., Hariz, M., & Brown, P. J. N. (2010). Parkinsonian impairment correlates with spatially extensive subthalamic oscillatory synchronization. *171*(1), 245-257.

Priori, A., Ardolino, G., Marceglia, S., Mrakic-Sposta, S., Locatelli, M., Tamma, F., Rossi, L., & Foffani, G. (2006). Low-frequency subthalamic oscillations increase after deep brain stimulation in Parkinson's disease. *Brain Res Bull, 71*(1-3), 149-154. doi:10.1016/j.brainresbull.2006.08.015

Priori, A., Foffani, G., Rossi, L., & Marceglia, S. (2013). Adaptive deep brain stimulation (aDBS) controlled by local field potential oscillations. *Exp Neurol, 245*, 77-86. doi:10.1016/j.expneurol.2012.09.013

Przedborski, S., & Vila, M. (2001). The last decade in Parkinson's disease research. Basic sciences. *Adv Neurol, 86*, 177-186.

Pudenz, R. H., Bullara, L. A., & Talalla, A. (1975). Electrical stimulation of the brain. I. Electrodes and electrode arrays. *Surg Neurol, 4*(1), 37-42.

Quiroga, R. Q., Nadasdy, Z., & Ben-Shaul, Y.. (2004). Unsupervised spike detection and sorting with wavelets and superparamagnetic clustering. *J Neural comp, 16*(8), 1661-1687.

Quiroga, R. Q. (2007). Spike sorting. *2*(12), 3583.

Rafols, J. A., & Fox, C. A. (1976). The neurons in the primate subthalamic nucleus: a Golgi and electron microscopic study. *J Comp Neurol, 168*(1), 75-111. doi:10.1002/cne.901680105

Ranck, J. B., Jr. (1975). Which elements are excited in electrical stimulation of mammalian central nervous system: a review. *Brain Res, 98*(3), 417-440.

Ray, N., Jenkinson, N., Wang, S., Holland, P., Brittain, J., Joint, C., Stein, J., & Aziz, T. J (2008). Local field potential beta activity in the subthalamic nucleus of patients with Parkinson's disease is associated with improvements in bradykinesia after dopamine and deep brain stimulation. *J Exp Neurol,213*(1), 108-113.

Ray, S. F. Applied Photographic Optics, 3rd Edition; Focal Press:Oxford, 2002, 231-232.

Raz, A., Frechter-Mazar, V., Feingold, A., Abeles, M., Vaadia, E., & Bergman, H. J. J. o. N. (2001). Activity of pallidal and striatal tonically active neurons is correlated in MPTP-treated monkeys but not in normal monkeys. *21*(3), RC128-RC128.

Raz, A., Vaadia, E., & Bergman, H. (2000). Firing patterns and correlations of spontaneous discharge of pallidal neurons in the normal and the tremulous 1-methyl-4-phenyl-1,2,3,6-tetrahydropyridine vervet model of parkinsonism. *J Neurosci, 20*(22), 8559-8571.

Redgrave, P., Rodriguez, M., Smith, Y., Rodriguez-Oroz, M. C., Lehericy, S., Bergman, H., Agid, Y., DeLong, M. R., & Obeso, J. A. (2010). Goal-directed and habitual control in the basal ganglia: implications for Parkinson's disease. *Nat Rev Neurosci, 11*(11), 760-772. doi:10.1038/nrn2915

Rodriguez-Oroz, M. C., Obeso, J. A., Lang, A. E., Houeto, J. L., Pollak, P., Rehncrona, S., Kulisevsky, J., Albanese, A., Volkmann, J., Hariz, M. I., Quinn, N. P., Speelman, J. D., Guridi, J., Zamarbide, I., Gironell, A., Molet, J., Pascual-Sedano, B., Pidoux, B., Bonnet, A. M., Agid, Y., Xie, J., Benabid, A. L., Lozano, A. M., Saint-Cyr, J., Romito, L., Contarino, M. F., Scerrati, M., Fraix, V., & Van Blercom, N. (2005). Bilateral deep brain stimulation in Parkinson's disease: a multicentre study with 4 years follow-up. *Brain, 128*(Pt 10), 2240-2249. doi:10.1093/brain/awh571

Rodriguez-Oroz, M. C., Rodriguez, M., Guridi, J., Mewes, K., Chockkman, V., Vitek, J., DeLong, M. R., & Obeso, J. A. (2001). The subthalamic nucleus in Parkinson's disease: somatotopic organization and physiological characteristics. *Brain, 124*(Pt 9), 1777-1790.

Romanelli, P., Esposito, V., Schaal, D. W., & Heit, G. (2005). Somatotopy in the basal ganglia: experimental and clinical evidence for segregated sensorimotor channels. *Brain Res Brain Res Rev, 48*(1), 112-128. doi:10.1016/j.brainresrev.2004.09.008

Romanelli, P., Heit, G., Hill, B. C., Kraus, A., Hastie, T., & Bronte-Stewart, H. M. (2004). Microelectrode recording revealing a somatotopic body map in the subthalamic

nucleus in humans with Parkinson disease. *J Neurosurg, 100*(4), 611-618. doi:10.3171/jns.2004.100.4.0611

Rosa, M., Arlotti, M., Ardolino, G., Cogiamanian, F., Marceglia, S., Di Fonzo, A., Cortese, F., Rampini, P. M., & Priori, A. (2015). Adaptive deep brain stimulation in a freely moving Parkinsonian patient. *Mov Disord, 30*(7), 1003-1005.

Rosa, M., Arlotti, M., Marceglia, S., Cogiamanian, F., Ardolino, G., Fonzo, A. D., Lopiano, L., Scelzo, E., Merola, A., & Locatelli, M. (2017). A daptive deep brain stimulation controls levodopa-induced side effects in P arkinsonian patients. *Mov Disord, 32*(4), 628-629.

Rosa, M., Fumagalli, M., Giannicola, G., Marceglia, S., Lucchiari, C., Servello, D., Franzini, A., Pacchetti, C., Romito, L., Albanese, A., Porta, M., Pravettoni, G., & Priori, A. (2013). Pathological gambling in Parkinson's disease: subthalamic oscillations during economics decisions. *Mov Disord, 28*(12), 1644-1652. doi:10.1002/mds.25427

Rosin, B., Slovik, M., Mitelman, R., Rivlin-Etzion, M., Haber, S. N., Israel, Z., Vaadia, E., & Bergman, H. (2011). Closed-loop deep brain stimulation is superior in ameliorating parkinsonism. *Neuron, 72*(2), 370-384.

Rossi, A., Garre, M. L., Ravegnani, M., Nozza, P., Abbruzzese, A., Giangaspero, F., Tortori-Donati, P. (2008). Bilateral germinoma of the basal ganglia. *J Pediatric blood cancer, 50*(1), 177-179.

Rossi, M. A., Calakos, N., & Yin, H. H. (2015). Spotlight on movement disorders: what optogenetics has to offer. *Mov Disord, 30*(5), 624-631.

Ruskin, D. N., Bergstrom, D. A., Kaneoke, Y., Patel, B. N., Twery, M. J., & Walters, J. R. J. J. o. N. (1999). Multisecond oscillations in firing rate in the basal ganglia: robust modulation by dopamine receptor activation and anesthesia. *81*(5), 2046-2055.

Sako, W., Miyazaki, Y., Izumi, Y., & Kaji, R. (2014). Which target is best for patients with Parkinson's disease? A meta-analysis of pallidal and subthalamic stimulation. *J Neurol Neurosurg Psychiatry, 85*(9), 982-986.

Sato, F., Lavallee, P., Levesque, M., & Parent, A. (2000). Single-axon tracing study of neurons of the external segment of the globus pallidus in primate. *J Comp Neurol, 417*(1), 17-31.

Sauleau, P., Raoul, S., Lallement, F., Rivier, I., Drapier, S., Lajat, Y., & Verin, M. (2005). Motor and non motor effects during intraoperative subthalamic stimulation for Parkinson's disease. *J Neurol, 252*(4), 457-464. doi:10.1007/s00415-005-0675-5

Schindelin, J., Arganda-Carreras, I., Frise, E., Kaynig, V., Longair, M., Pietzsch, T., Preibisch, S., Rueden, C., Saalfeld, S., Schmid, B., Tinevez, J. Y., White, D. J., Hartenstein, V., Eliceiri, K., Tomancak, P., & Cardona, A. (2012). Fiji: an open-source platform for biological-image analysis. *Nat Methods, 9*(7), 676-682. doi:10.1038/nmeth.2019

Schlag, J., & Schlag-Rey, M. J. J. o. N. (1987). Evidence for a supplementary eye field. *J Neurophysiol, 57*(1), 179-200.

Schneider, J. S., & Rothblat, D. S. (1996). Alterations in intralaminar and motor thalamic physiology following nigrostriatal dopamine depletion. *Brain Res, 742*(1-2), 25-33.

Schnitzler, A., & Gross, J. (2005). Normal and pathological oscillatory communication in the brain. *Nat Review Neurosci, 6*(4), 285.

Schober, A. (2004). Classic toxin-induced animal models of Parkinson's disease: 6-OHDA and MPTP. *Cell Tissue Res, 318*(1), 215-224. doi:10.1007/s00441-004-0938-y

Schoffelen, J. M., Oostenveld, R., & Fries, P. (2005). Neuronal coherence as a mechanism of effective corticospinal interaction. *Science, 308*(5718), 111-113. doi:10.1126/science.1107027

Schrock, L. E., Ostrem, J. L., Turner, R. S., Shimamoto, S. A., & Starr, P. A. (2009). The subthalamic nucleus in primary dystonia: single-unit discharge characteristics. *J Neurophysiol,102*(6), 3740-3752.

Schuepbach, W. M., Rau, J., Knudsen, K., Volkmann, J., Krack, P., Timmermann, L., Hälbig, T., Hesekamp, H., Navarro, S., & Meier, N. (2013). Neurostimulation for Parkinson's disease with early motor complications. *J New England Journal of Medicine, 368*(7), 610-622.

Schwarting, R. K., & Huston, J. P. (1996b). The unilateral 6-hydroxydopamine lesion model in behavioral brain research. Analysis of functional deficits, recovery and treatments. *Prog Neurobiol, 50*(2-3), 275-331.

Seifried, C., Weise, L., Hartmann, R., Gasser, T., Baudrexel, S., Szelenyi, A., van de Loo, S., Steinmetz, H., Seifert, V., Roeper, J., & Hilker, R. (2012). Intraoperative microelectrode recording for the delineation of subthalamic nucleus topography in Parkinson's disease. *Brain Stimul, 5*(3), 378-387. doi:10.1016/j.brs.2011.06.002

Sharott, A., Gulberti, A., Hamel, W., Koppen, J. A., Munchau, A., Buhmann, C., Potter-Nerger, M., Westphal, M., Gerloff, C., Moll, C. K., & Engel, A. K. (2018a). Spatio-temporal dynamics of cortical drive to human subthalamic nucleus neurons in Parkinson’s disease. *Neurobiol Dis., In Press*.

Sharott, A., Gulberti, A., Hamel, W., Koppen, J. A., Munchau, A., Buhmann, C., Potter-Nerger, M., Westphal, M., Gerloff, C., Moll, C. K. E., & Engel, A. K. (2018b). Spatio-temporal dynamics of cortical drive to human subthalamic nucleus neurons in Parkinson's disease. *Neurobiol Dis, 112*, 49-62. doi:10.1016/j.nbd.2018.01.001

Sharott, A., Gulberti, A., Zittel, S., Jones, A. A. T., Fickel, U., Münchau, A., Köppen, J. A., Gerloff, C., Westphal, M., & Buhmann, C. (2014a). Activity parameters of subthalamic nucleus neurons selectively predict motor symptom severity in Parkinson's disease. *J Neurosci, 34*(18), 6273-6285.

Sharott, A., Magill, P. J., Harnack, D., Kupsch, A., Meissner, W., & Brown, P. (2005). Dopamine depletion increases the power and coherence of beta-oscillations in the cerebral cortex and subthalamic nucleus of the awake rat. *Eur J Neurosci, 21*(5), 1413-1422. doi:10.1111/j.1460-9568.2005.03973.x

Sharott, A., Vinciati, F., Nakamura, K. C., & Magill, P. J. (2017). A Population of Indirect Pathway Striatal Projection Neurons Is Selectively Entrained to Parkinsonian Beta Oscillations. *J Neurosci, 37*(41), 9977-9998. doi:10.1523/JNEUROSCI.0658-17.2017

Shen, K. Z., & Johnson, S. W. J. T. (2000). Presynaptic dopamine D2 and muscarine M3 receptors inhibit excitatory and inhibitory transmission to rat subthalamic neurones in vitro. *J Phys, 525*(2), 331-341.

Shimamoto, S. A., Ryapolova-Webb, E. S., Ostrem, J. L., Galifianakis, N. B., Miller, K. J., & Starr, P. A. (2013). Subthalamic nucleus neurons are synchronized to primary motor cortex local field potentials in Parkinson's disease. *J Neurosci, 33*(17), 7220-7233. doi:10.1523/JNEUROSCI.4676-12.2013

Siegle, J. H., & Wilson, M. A. (2014). Enhancement of encoding and retrieval functions through theta phase-specific manipulation of hippocampus. *Elife, 3*, e03061. doi:10.7554/eLife.03061

Silberstein, P., Oliviero, A., Di Lazzaro, V., Insola, A., Mazzone, P., & Brown, P. J. E. n. (2005). Oscillatory pallidal local field potential activity inversely correlates with limb dyskinesias in Parkinson's disease. *J Exp Neurol, 194*(2), 523-529.

Singer, W., & Gray, C. M. (1995). Visual feature integration and the temporal correlation hypothesis. *Annu Rev Neurosci, 18*, 555-586. doi:10.1146/annurev.ne.18.030195.003011

Smeal, R. M., Ermentrout, G. B., & White, J. A. (2010). Phase-response curves and synchronized neural networks. *Philos Trans R Soc Lond B Biol Sci, 365*(1551), 2407-2422. doi:10.1098/rstb.2009.0292

Smith, Y., Bevan, M. D., Shink, E., & Bolam, J. P. (1998). Microcircuitry of the direct and indirect pathways of the basal ganglia. *Neuroscience, 86*(2), 353-387.

Soares, J., Kliem, M. A., Betarbet, R., Greenamyre, J. T., Yamamoto, B., & Wichmann, T. (2004). Role of external pallidal segment in primate parkinsonism: comparison of the effects of 1-methyl-4-phenyl-1,2,3,6-tetrahydropyridine-induced parkinsonism and lesions of the external pallidal segment. *J Neurosci, 24*(29), 6417-6426. doi:10.1523/JNEUROSCI.0836-04.2004

Spinks, R. L., Kraskov, A., Brochier, T., Umilta, M. A., & Lemon, R. (2008). Selectivity for grasp in local field potential and single neuron activity recorded simultaneously from M1 and F5 in the awake macaque monkey. *28*(43), 10961-10971.

Spraker, M. B., Prodoehl, J., Corcos, D. M., Comella, C. L., & Vaillancourt, D. E(2010). Basal ganglia hypoactivity during grip force in drug naive Parkinson's disease. *J Neurosci, 31*(12), 1928-1941.

Stam, C. J., Nolte, G., & Daffertshofer, A. (2007a). Phase lag index: assessment of functional connectivity from multi channel EEG and MEG with diminished bias from common sources. *Hum Brain Mapp, 28*(11), 1178-1193. doi:10.1002/hbm.20346

Stam, C. J., Nolte, G., & Daffertshofer, A. J. H. b. m. (2007b). Phase lag index: assessment of functional connectivity from multi channel EEG and MEG with diminished bias from common sources. *28*(11), 1178-1193.

Stein, E., & Bar-Gad, I. (2013). beta oscillations in the cortico-basal ganglia loop during parkinsonism. *Exp Neurol, 245*, 52-59. doi:10.1016/j.expneurol.2012.07.023

Steriade, M. (2000). Corticothalamic resonance, states of vigilance and mentation. *Neuroscience, 101*(2), 243-276.

Steriade, M., McCormick, D. A., & Sejnowski, T. (1993). Thalamocortical oscillations in the sleeping and aroused brain. *Neurosci, 262*(5134), 679-685.

Stuber, G. D., Hnasko, T. S., Britt, J. P., Edwards, R. H., & Bonci, A. (2010). Dopaminergic terminals in the nucleus accumbens but not the dorsal striatum corelease glutamate. *J Neurosci, 30*(24), 8229-8233. doi:10.1523/JNEUROSCI.1754-10.2010

Surmeier, D. J., Mercer, J. N., & Chan, C. S. (2005). Autonomous pacemakers in the basal ganglia: who needs excitatory synapses anyway? *Curr Opin Neurobiol, 15*(3), 312-318. doi:10.1016/j.conb.2005.05.007

Syed, E. C., Benazzouz, A., Taillade, M., Baufreton, J., Champeaux, K., Falgairolle, M., Bioulac, B., Gross, C. E., & Boraud, T. (2012). Oscillatory entrainment of subthalamic nucleus neurons and behavioural consequences in rodents and primates. *Eur J Neurosci, 36*(9), 3246-3257. doi:10.1111/j.1460-9568.2012.08246.x

Syed, E. C., Grima, L. L., Magill, P. J., Bogacz, R., Brown, P., & Walton, M. E. (2016). Action initiation shapes mesolimbic dopamine encoding of future rewards. *Nat Neurosci, 19*(1), 34-36. doi:10.1038/nn.4187

Tachibana, Y., Iwamuro, H., Kita, H., Takada, M., & Nambu, A. (2011a). Subthalamo-pallidal interactions underlying parkinsonian neuronal oscillations in the primate basal ganglia. *Eur J Neurosci, 34*(9), 1470-1484. doi:10.1111/j.1460-9568.2011.07865.x

Tachibana, Y., Iwamuro, H., Kita, H., Takada, M., & Nambu, A. (2011b). Subthalamo-pallidal interactions underlying parkinsonian neuronal oscillations in the primate basal ganglia. *Eur J Neurosci, 34*(9), 1470-1484.

Tai, C.-h., Boraud, T., Bezard, E., Bioulac, B., Gross, C., & Benazzouz, A. (2003). Electrophysiological and metabolic evidence that high-frequency stimulation of the subthalamic nucleus bridles neuronal activity in the subthalamic nucleus and the substantia nigra reticulata. *The FASEB Journal, 1 7*(13), 1820-1830.

Tai, C. H., Yang, Y. C., Pan, M. K., Huang, C. S., & Kuo, C. C. (2011). Modulation of subthalamic T-type Ca(2+) channels remedies locomotor deficits in a rat model of Parkinson disease. *J Clin Invest, 121*(8), 3289-3305. doi:10.1172/JCI46482

Tan, H., Pogosyan, A., Anzak, A., Ashkan, K., Bogdanovic, M., Green, A. L., Aziz, T., Foltynie, T., Limousin, P., & Zrinzo, L. (2013). Complementary roles of different oscillatory activities in the subthalamic nucleus in coding motor effort in Parkinsonism. *Elife, 248*, 187-195.

Tan, H., Pogosyan, A., Ashkan, K., Green, A. L., Aziz, T., Foltynie, T., Limousin, P., Zrinzo, L., Hariz, M., & Brown, P. (2016). Decoding gripping force based on local field potentials recorded from subthalamic nucleus in humans. *J Exp Neurosci, 5*, e19089.

Tankus, A., Yeshurun, Y., & Fried, I. (2009). An automatic measure for classifying clusters of suspected spikes into single cells versus multiunits. *J Neur Eng*, *6*(5), 056001.

Tasker, R. R. (1990). Thalamotomy. *1*(4), 841-864.

Tass, P. A. (2003). A model of desynchronizing deep brain stimulation with a demand-controlled coordinated reset of neural subpopulations. *Biol Cybern, 89*(2), 81-88. doi:10.1007/s00422-003-0425-7

Tass, P. A., Adamchic, I., Freund, H. J., von Stackelberg, T., & Hauptmann, C. (2012). Counteracting tinnitus by acoustic coordinated reset neuromodulation. *Restor Neurol Neurosci, 30*(2), 137-159. doi:10.3233/RNN-2012-110218

Tass, P. A., & Majtanik, M. (2006). Long-term anti-kindling effects of desynchronizing brain stimulation: a theoretical study. *J Biol Cyber,94*(1), 58-66.

Tecuapetla, F., Jin, X., Lima, S. Q., & Costa, R. M. (2016). Complementary Contributions of Striatal Projection Pathways to Action Initiation and Execution. *Cell, 166*(3), 703-715. doi:10.1016/j.cell.2016.06.032

Tecuapetla, F., Patel, J. C., Xenias, H., English, D., Tadros, I., Shah, F., Berlin, J., Deisseroth, K., Rice, M. E., Tepper, J. M., & Koos, T. (2010). Glutamatergic signaling by mesolimbic dopamine neurons in the nucleus accumbens. *J Neurosci, 30*(20), 7105-7110. doi:10.1523/JNEUROSCI.0265-10.2010

Temel, Y., Blokland, A., Steinbusch, H. W., & Visser-Vandewalle, V. (2005). The functional role of the subthalamic nucleus in cognitive and limbic circuits. *Prog Neurobiol, 76*(6), 393-413. doi:10.1016/j.pneurobio.2005.09.005

Terman, D., Rubin, J. E., Yew, A., & Wilson, C. (2002). Activity patterns in a model for the subthalamopallidal network of the basal ganglia. *J Neuroci, 22*(7), 2963-2976.

Thut, G., Ives, J. R., Kampmann, F., Pastor, M. A., & Pascual-Leone, A. (2005). A new device and protocol for combining TMS and online recordings of EEG and evoked potentials. *J Neurosci Methods, 141*(2), 207-217. doi:10.1016/j.jneumeth.2004.06.016

Timmermann, L., Wojtecki, L., Gross, J., Lehrke, R., Voges, J., Maarouf, M., Treuer, H., Sturm, V., & Schnitzler, A. (2004). Ten-Hertz stimulation of subthalamic nucleus deteriorates motor symptoms in Parkinson's disease. *Mov Disord, 19*(11), 1328-1333.

Tinkhauser, G., Pogosyan, A., Little, S., Beudel, M., Herz, D. M., Tan, H., & Brown, P. (2017a). The modulatory effect of adaptive deep brain stimulation on beta bursts in Parkinson's disease. *Brain, 140*(4), 1053-1067. doi:10.1093/brain/awx010

Tinkhauser, G., Pogosyan, A., Tan, H., Herz, D. M., Kuhn, A. A., & Brown, P. (2017b). Beta burst dynamics in Parkinson's disease OFF and ON dopaminergic medication. *Brain, 140*(11), 2968-2981. doi:10.1093/brain/awx252

Tisch, S., Rothwell, J. C., Zrinzo, L., Bhatia, K. P., Hariz, M., & Limousin, P. (2008). Cortical evoked potentials from pallidal stimulation in patients with primary generalized dystonia. *Mov Disord, 23*(2), 265-273.

Toma, K., Nagamine, T., Yazawa, S., Terada, K., Ikeda, A., Honda, M., Oga, T., & Shibasaki, H. (2000). Desynchronization and synchronization of central 20-Hz rhythms associated with voluntary muscle relaxation: a magnetoencephalographic study. *J Exp Brain Res, 134*(4), 417-425.

Trager, M. H., Koop, M. M., Velisar, A., Blumenfeld, Z., Nikolau, J. S., Quinn, E. J., Martin, T., & Bronte-Stewart, H. (2016). Subthalamic beta oscillations are attenuated after withdrawal of chronic high frequency neurostimulation in Parkinson's disease. *96*, 22-30.

Tripoliti, E., Strong, L., Hickey, F., Foltynie, T., Zrinzo, L., Candelario, J., Hariz, M., & Limousin, P. (2011). Treatment of dysarthria following subthalamic nucleus deep brain stimulation for Parkinson's disease. *J Neurobiol Dis, 26*(13), 2434-2436.

Tritsch, N. X., & Sabatini, B. L. (2012). Dopaminergic modulation of synaptic transmission in cortex and striatum. *Neuron, 76*(1), 33-50. doi:10.1016/j.neuron.2012.09.023

Uhlhaas, P. J., & Singer, W. J. N. (2006). Neural synchrony in brain disorders: relevance for cognitive dysfunctions and pathophysiology. *52*(1), 155-168.

Urbain, N., Gervasoni, D., Souliere, F., Lobo, L., Rentero, N., Windels, F., Astier, B., Savasta, M., Fort, P., Renaud, B., Luppi, P. H., & Chouvet, G. (2000). Unrelated course of subthalamic nucleus and globus pallidus neuronal activities across vigilance states in the rat. *Eur J Neurosci, 12*(9), 3361-3374.

Urbain, N., Rentéro, N., Gervasoni, D., Renaud, B., & Chouvet, G. (2002). The switch of subthalamic neurons from an irregular to a bursting pattern does not solely depend on their GABAergic inputs in the anesthetic-free rat. *J Neurosci, 22*(19), 8665-8675.

Vaillancourt, D. E., Yu, H., Mayka, M. A., & Corcos, D. M. J. N. (2007). Role of the basal ganglia and frontal cortex in selecting and producing internally guided force pulses. *36*(3), 793-803.

van Elswijk, G., Maij, F., Schoffelen, J. M., Overeem, S., Stegeman, D. F., & Fries, P. (2010). Corticospinal beta-band synchronization entails rhythmic gain modulation. *J Neurosci, 30*(12), 4481-4488. doi:10.1523/JNEUROSCI.2794-09.2010

van Wijk, B. C., Beek, P. J., & Daffertshofer, A. (2012). Neural synchrony within the motor system: what have we learned so far? *Front Hum Neurosci, 6*, 252. doi:10.3389/fnhum.2012.00252

van Wijk, B. C., Beudel, M., Jha, A., Oswal, A., Foltynie, T., Hariz, M. I., Limousin, P., Zrinzo, L., Aziz, T. Z., & Green, A. (2016). Subthalamic nucleus phase–amplitude coupling correlates with motor impairment in Parkinson's disease. *Clin Neurophysiol, 127*(4), 2010-2019.

Van Wouwe, N. C., Wylie, S. A., Van Den Wildenberg, W. P., Band, G. P., Abisogun, A. A., Elias, W. J., Frysinger, R. C., & Ridderinkhof, R. (2011). Deep brain stimulation of the subthalamic nucleus improves reward-based decision-learning in Parkinson's disease. *Front Hum Neurosci, 5*, 30.

Van Zaen, J., Uldry, L., Duchêne, C., Prudat, Y., Meuli, R. A., Murray, M. M., & Vesin, J.-M. J. J. o. n. m. (2010). Adaptive tracking of EEG oscillations. *186*(1), 97-106.

Vazey, E. M., & Aston-Jones, G. (2013). New tricks for old dogmas: optogenetic and designer receptor insights for Parkinson's disease. *Brain Res, 1511*, 153-163. doi:10.1016/j.brainres.2013.01.021

Vidaković, A., Dragasević, N., Kostić, V. J. J. o. N., Neurosurgery, & Psychiatry. (1994). Hemiballism: report of 25 cases. *57*(8), 945-949.

Vitek, J. L. (2002). Mechanisms of deep brain stimulation: excitation or inhibition. *Mov Disord, 17*(S3), S69-S72.

Voges, J., Volkmann, J., Allert, N., Lehrke, R., Koulousakis, A., Freund, H. J., & Sturm, V. (2002). Bilateral high-frequency stimulation in the subthalamic nucleus for the treatment of Parkinson disease: correlation of therapeutic effect with anatomical electrode position. *J Neurosurg, 96*(2), 269-279. doi:10.3171/jns.2002.96.2.0269

Volkmann, J., Herzog, J., Kopper, F., & Deuschl, G. (2002). Introduction to the programming of deep brain stimulators. *Mov Disord, 17 Suppl 3*, S181-187.

Voytek, B., & Knight, R. T. J. B. p. (2015). Dynamic network communication as a unifying neural basis for cognition, development, aging, and disease. *77*(12), 1089-1097.

Wach, C., Krause, V., Moliadze, V., Paulus, W., Schnitzler, A., & Pollok, B. J. F. i. h. n. (2013). The effect of 10 Hz transcranial alternating current stimulation (tACS) on corticomuscular coherence. *7*, 511.

Walker, H. C., Huang, H., Gonzalez, C. L., Bryant, J. E., Killen, J., Cutter, G. R., Knowlton, R. C., Montgomery, E. B., Guthrie, B. L., & Watts, R. L. (2012). Short latency activation of cortex during clinically effective subthalamic deep brain stimulation for Parkinson's disease. *Mov Disord, 27*(7), 864-873. doi:10.1002/mds.25025

Walter, B. L., & Vitek, J. L. (2004). Surgical treatment for Parkinson's disease. *Lancet Neurol, 3*(12), 719-728. doi:10.1016/S1474-4422(04)00934-2

Watabe-Uchida, M., Zhu, L., Ogawa, S. K., Vamanrao, A., & Uchida, N. (2012). Whole-brain mapping of direct inputs to midbrain dopamine neurons. *Neuron, 74*(5), 858-873. doi:10.1016/j.neuron.2012.03.017

Weinberger, M., Mahant, N., Hutchison, W. D., Lozano, A. M., Moro, E., Hodaie, M., Lang, A. E., & Dostrovsky, J. O. (2006a). Beta oscillatory activity in the subthalamic nucleus and its relation to dopaminergic response in Parkinson's disease. *J Neurophysiol, 96*(6), 3248-3256. doi:10.1152/jn.00697.2006

Weintraub, D., Duda, J. E., Carlson, K., Luo, P., Sagher, O., Stern, M., Follett, K. A., Reda, D., Weaver, F. M., (2013). Suicide ideation and behaviours after STN and GPi DBS surgery for Parkinson’s disease: results from a randomised, controlled trial. *Psychiatry, 84*(10), 1113-1118.

Welter, M. L., Houeto, J. L., Bonnet, A. M., Bejjani, P. B., Mesnage, V., Dormont, D., Navarro, S., Cornu, P., Agid, Y., & Pidoux, B. (2004). Effects of high-frequency stimulation on subthalamic neuronal activity in parkinsonian patients. *Arch Neurol, 61*(1), 89-96. doi:10.1001/archneur.61.1.89

Whitmer, D., De Solages, C., Hill, B. C., Yu, H., Henderson, J. M., & Bronte-Stewart, H. J. F. i. h. n. (2012). High frequency deep brain stimulation attenuates subthalamic and cortical rhythms in Parkinson's disease. *6*, 155.

Wichmann, T., Bergman, H., & DeLong, M. R. (1994a). The primate subthalamic nucleus. I. Functional properties in intact animals. *J Neurophysiol, 72*(2), 494-506. doi:10.1152/jn.1994.72.2.494

Wichmann, T., Bergman, H., & DeLong, M. R. (1994b). The primate subthalamic nucleus. III. Changes in motor behavior and neuronal activity in the internal pallidum induced by subthalamic inactivation in the MPTP model of parkinsonism. *J Neurophysiol, 72*(2), 521-530. doi:10.1152/jn.1994.72.2.521

Wichmann, T., & DeLong, M. R. (1999). Oscillations in the basal ganglia. *Nature, 400*(6745), 621-622. doi:10.1038/23148

Wichmann, T., & DeLong, M. R. (2016). Deep Brain Stimulation for Movement Disorders of Basal Ganglia Origin: Restoring Function or Functionality? *Neurotherapeutics, 13*(2), 264-283. doi:10.1007/s13311-016-0426-6

Wickens, J. R., & Arbuthnott, G. W. (1993). The corticostriatal system on computer simulation: an intermediate mechanism for sequencing of actions. *Prog Brain Res, 99*, 325-339.

Wickens J.R., & Oorshcot D. E. (2000) Neuronal dynamics and surround inhibition in the neostriatum: a possible connection. In Miller, R., Wickens, J.R. (Eds.), *Brain Dynamics and the Striatal Complex* (141-150): Australia: Harwood Academic Publishers.Wigmore, M. A., & Lacey, M. G. (2000). A Kv3-like persistent, outwardly rectifying, Cs+-permeable, K+ current in rat subthalamic nucleus neurones. *J Physiol, 527 Pt 3*, 493-506.

Wilkinson, L., Beigi, M., Lagnado, D. A., & Jahanshahi, M. (2011). Deep brain stimulation of the subthalamic nucleus selectively improves learning of weakly associated cue combinations during probabilistic classification learning in Parkinson's disease. *J Neuropsych, 25*(3), 286.

Williams, D., Tijssen, M., Van Bruggen, G., Bosch, A., Insola, A., Di Lazzaro, V., Mazzone, P., Oliviero, A., Quartarone, A., Speelman, H., & Brown, P. (2002). Dopamine-dependent changes in the functional connectivity between basal ganglia and cerebral cortex in humans. *Brain, 125*(Pt 7), 1558-1569.

Wilson, C. J. (2015). Oscillators and Oscillations in the Basal Ganglia. *Neuroscientist, 21*(5), 530-539. doi:10.1177/1073858414560826

Wilson, C. J., & Groves, P. M. (1981). Spontaneous firing patterns of identified spiny neurons in the rat neostriatum. *Brain Res, 220*(1), 67-80.

Wilson, C. J. J. N. (2013). Active decorrelation in the basal ganglia. *250*, 467-482.

Wilson, D., & Moehlis, J. (2014). Locally optimal extracellular stimulation for chaotic desynchronization of neural populations. *J Comput Neurosci, 37*(2), 243-257. doi:10.1007/s10827-014-0499-3

Windels, F., Bruet, N., Poupard, A., Urbain, N., Chouvet, G., Feuerstein, C., & Savasta, M. (2000). Effects of high frequency stimulation of subthalamic nucleus on extracellular glutamate and GABA in substantia nigra and globus pallidus in the normal rat. *Eur J Neurosci, 12*(11), 4141-4146.

Winfree, A. T. (1967). Biological rhythms and the behavior of populations of coupled oscillators. *J Theor Biol, 16*(1), 15-42.

Wingeier, B., Tcheng, T., Koop, M. M., Hill, B. C., Heit, G., & Bronte-Stewart, H. M. (2006). Intra-operative STN DBS attenuates the prominent beta rhythm in the STN in Parkinson's disease. *J Exp Neurol, 197*(1), 244-251.

Womelsdorf, T., Ardid, S., Everling, S., & Valiante, T. A. (2014). Burst firing synchronizes prefrontal and anterior cingulate cortex during attentional control. *Curr Biol, 24*(22), 2613-2621. doi:10.1016/j.cub.2014.09.046

Womelsdorf, T., Lima, B., Vinck, M., Oostenveld, R., Singer, W., Neuenschwander, S., & Fries, P. (2012). Orientation selectivity and noise correlation in awake monkey area V1 are modulated by the gamma cycle. *Proc Natl Acad Sci U S A, 109*(11), 4302-4307. doi:10.1073/pnas.1114223109

Womelsdorf, T., Schoffelen, J. M., Oostenveld, R., Singer, W., Desimone, R., Engel, A. K., & Fries, P. (2007). Modulation of neuronal interactions through neuronal synchronization. *Science, 316*(5831), 1609-1612. doi:10.1126/science.1139597

Wood, F., Black, M. J., Vargas-Irwin, C., Fellows, M., & Donoghue, J. (2004). On the variability of manual spike sorting. *J IEEE Transact Biomed, 51*(6), 912-918.

Wu, A. D., Fregni, F., Simon, D. K., Deblieck, C., & Pascual-Leone, A. (2008). Noninvasive brain stimulation for Parkinson's disease and dystonia. *Neurotherapeutics, 5*(2), 345-361. doi:10.1016/j.nurt.2008.02.002

Xiao, C., Miwa, J. M., Henderson, B. J., Wang, Y., Deshpande, P., McKinney, S. L., & Lester, H. A. (2015). Nicotinic receptor subtype-selective circuit patterns in the subthalamic nucleus. *J Neurosci, 35*(9), 3734-3746. oi:10.1523/JNEUROSCI.3528-14.2015

Xu, W., Russo, G. S., Hashimoto, T., Zhang, J., & Vitek, J. (2008). Subthalamic nucleus stimulation modulates thalamic neuronal activity. *J Neurosci, 28*(46), 11916-11924.

Yamamoto, T., Katayama, Y., Ushiba, J., Yoshino, H., Obuchi, T., Kobayashi, K., Oshima, H., & Fukaya, C. (2013). On-demand control system for deep brain

stimulation for treatment of intention tremor. *Neuromodulation, 16*(3), 230-235; discussion 235. doi:10.1111/j.1525-1403.2012.00521.x

Yelnik, J., & Percheron, G. (1979). Subthalamic neurons in primates: a quantitative and comparative analysis. *Neuroscience, 4*(11), 1717-1743.

Zaghloul, K. A., Weidemann, C. T., Lega, B. C., Jaggi, J. L., Baltuch, G. H., & Kahana, M. J. (2012). Neuronal activity in the human subthalamic nucleus encodes decision conflict during action selection. *J Neurosci, 32*(7), 2453-2460. doi:10.1523/JNEUROSCI.5815-11.2012

Zaidel, A., Spivak, A., Grieb, B., Bergman, H., & Israel, Z. (2010). Subthalamic span of β oscillations predicts deep brain stimulation efficacy for patients with Parkinson's disease. *Brain, 133*(7), 2007-2021.

Zanos, S., Rembado, I., Chen, D., & Fetz, E. E. (2018). Phase-Locked Stimulation during Cortical Beta Oscillations Produces Bidirectional Synaptic Plasticity in Awake Monkeys. *Curr Biol, 28*(16), 2515-2526 e2514. doi:10.1016/j.cub.2018.07.009

Zavala, B., Zaghloul, K., & Brown, P. (2015). The subthalamic nucleus, oscillations, and conflict. *Mov Disord, 30*(3), 328-338. doi:10.1002/mds.26072

Zheng, T., & Wilson, C. J. (2002). Corticostriatal combinatorics: the implications of corticostriatal axonal arborizations. *J Neurophysiol, 87*(2), 1007-1017. doi:10.1152/jn.00519.2001

Zhu, Z., Bartol, M., Shen, K., & Johnson, S. (2002). Excitatory effects of dopamine on subthalamic nucleus neurons: in vitro study of rats pretreated with 6-hydroxydopamine and levodopa. *Brain Res, 945*(1), 31-40.